

ADA098620

REPORT NUMBER: R-01100-7CR-47
CONTRACT NUMBER: 6014-78-C-0533



Stability/Overview of Ejector Theory and Performance

Volume I (Technical Discussion)

BY: J. W. ...
... ..

VOUGHT CORPORATION ADVANCED TECHNOLOGY CENTER—
... ..
... .. 75265

PERIOD: NOVEMBER 1978 - AUGUST 1979

FOR PUBLIC RELEASE; DISTRIBUTION UNLIMITED

... ..
... ..
... .. A 2217

... .. SCIENTIFIC RESEARCH
... ..
... ..

 **VOUGHT CORPORATION**
advanced technology center

01 5 01 141

Enclosure (1) to
R-91100/9CRL-47A

A SUMMARY/OVERVIEW OF EJECTOR AUGMENTOR
THEORY AND PERFORMANCE
PHASE II - TECHNICAL REPORT
ATC REPORT NO. R-91100/9CR-47A
VOLUME I - TECHNICAL DISCUSSION

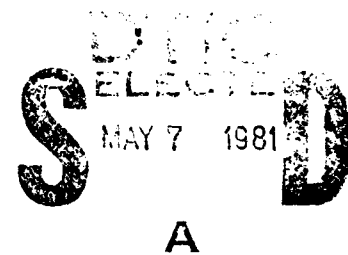
by

J. L. Porter
and
R. A. Squyers

Prepared Under

Contract No. N00014-78-C-0533

Sponsored Jointly by the
Office of Naval Research
and the
Air Force Office of Scientific Research



VOUGHT CORPORATION ADVANCED TECHNOLOGY CENTER
P. O. BOX 226144
DALLAS, TEXAS 75266

UNCLASSIFIED

Final technical report, 1 Nov 1978 - 31 Aug 1979

SECURITY CLASSIFICATION OF THIS PAGE (When Data Entered)

REPORT DOCUMENTATION PAGE

READ INSTRUCTIONS BEFORE COMPLETING FORM

1. REPORT NUMBER 16		2. GOVT ACCESSION NO. AD-A098620		3. RECIPIENT'S CATALOG NUMBER	
4. TITLE (and Subtitle) A Summary/Overview of Ejector Augmentor Theory and Performance, Phase II - Technical Report, Volume I - Technical Discussion, Volume II - Bibliography				5. TYPE OF REPORT & PERIOD COVERED Technical-Final 1 Nov. 1978 - 31 Aug. 1979	
7. AUTHOR(S) J. L. Porter and R. A. Squyers				8. PERFORMING ORG. REPORT NUMBER (14) ATC-R-91100/9CR-47A-VEU-2	
9. PERFORMING ORGANIZATION NAME AND ADDRESS Vought Advanced Technology Center P. O. Box 226144 Dallas, Texas 75266				10. PROGRAM ELEMENT, PROJECT, TASK AREA & WORK UNIT NUMBERS (15) 226	
11. CONTROLLING OFFICE NAME AND ADDRESS Office of Naval Research 800 North Quincy Street Arlington, Virginia 22217				12. REPORT DATE (17) September 1979	
14. MONITORING AGENCY NAME & ADDRESS (if different from Controlling Office) Same as Block 11 and Air Force Office of Scientific Research Bolling Air Force Base Washington, D. C. 20332				13. NUMBER OF PAGES VOL. I-205, VOL. II-120	
				15. SECURITY CLASS. (of this report) Unclassified	
				18a. DECLASSIFICATION/DOWNGRADING SCHEDULE	
16. DISTRIBUTION STATEMENT (of this Report) Approved for Public Release; Distribution Unlimited					
17. DISTRIBUTION STATEMENT (of the abstract entered in Block 20, if different from Report) Same as Block 16					
18. SUPPLEMENTARY NOTES					
19. KEY WORDS (Continue on reverse side if necessary and identify by block number) Ejectors Energy Transfer Non-Steady Thrust Augmentation Bibliography Flight Systems Mixing Components					
20. ABSTRACT (Continue on reverse side if necessary and identify by block number) The results of a "Summary/Overview of Ejector Augmentor Theory and Performance, Phase II-Technical Report" are presented. In the Volume I-Technical Discussion, the results of the study are presented first in a description of the fundamental considerations relevant to ejector augmentor design and performance and second in a discussion of experimental results for the various components comprising an ejector augmentor: primary nozzles, secondary inlet, mixing section and diffuser. In the theoretical discussion a limit value of static augmentation ratio which depends only on the ratio of primary to secondary stagnation					

DD FORM 1 JAN 73 1473

EDITION OF 1 NOV 65 IS OBSOLETE S/N 0102-014-6601

UNCLASSIFIED

SECURITY CLASSIFICATION OF THIS PAGE (When Data Entered)

31 11

UNCLASSIFIED

SECURITY CLASSIFICATION OF THIS PAGE(When Data Entered)

cont →

pressure is formulated, and it is shown that the best published experimental results approach 90% of the limit value. In the experimental section extensive data compilations are presented to provide a summary of the predominant geometric and gasdynamic parametric effects on ejector performance.

Four ejector-augmentor flight systems (XFV-12A, XV-4A, XC-8A and the JW-1), are discussed in terms of the research and development programs leading to the prototype/demonstrator vehicles, and the actual vs. predicted performance.

Conclusions regarding ejector technology based on this study are made, and recommendations for needed ejector technology research and development programs are presented. ←

Volume II - Bibliography, presents an extensive coded list of over 1600 publications relevant to ejectors.

UNCLASSIFIED

SECURITY CLASSIFICATION OF THIS PAGE(When Data Entered)

PREFACE

This technical report describes work done under Contract No. N00014-78-C-0533 with the Office of Naval Research, Arlington, Virginia, and the Air Force Office of Scientific Research, Bolling AFB, Washington, D.C. This effort represents the completion of the contract study for Phase II of a "Summary/Overview of Ejector Augmentor Theory and Performance".

The authors gratefully acknowledge the interest and advice of Dr. Robert Whitehead of the Office of Naval Research, and Dr. James Wilson of the Air Force Office of Scientific Research, who have monitored the contract. Special acknowledgement must also be made for the many contributions of Dr. K. Nagaraja of the Flight Dynamics Laboratory, Air Force Wright Aeronautical Laboratories, who provided initial impetus to the project as well as valuable technical comments in the course of the preparation of this report. Thanks are also expressed to the many contributors, too numerous to mention individually, from both private and government organizations, who provided valuable comments in response to a questionnaire sent to them in the early phase of this study; as well as, in many cases, special insight into ejector theory and performance.

Accession For	
DDIC CAA&I	<input checked="" type="checkbox"/>
DDIC TAB	<input type="checkbox"/>
Unannounced	<input type="checkbox"/>
Justification	
Distribution/	
Availability Codes	
Dist	Special
A	

TABLE OF CONTENTS

	Page No.
PREFACE	i
LIST OF FIGURES	iv
LIST OF TABLES	x
NOMENCLATURE	xi
1.0 INTRODUCTION	1
2.0 FUNDAMENTAL PHYSICS OF EJECTOR AUGMENTORS	5
2.1 FUNDAMENTALS OF OVERALL PROCESS RELATIONSHIPS	5
2.1.1 Overall Process Relationships (T-s Diagrams) ...	5
2.1.2 Maximum Augmentation Ratio Formulation	11
2.2 FUNDAMENTALS OF INDIVIDUAL PHYSICAL PROCESSES	23
2.2.1 The Interaction Phenomenon	23
2.2.2 Associated Component Phenomena	28
2.3 SUMMARY OF FUNDAMENTALS OF EJECTOR FLOWS	31
3.0 THEORIES OF OVERALL DEVICE PERFORMANCE	33
3.1 GENERAL BACKGROUND	33
3.2 CONTROL VOLUME APPROACH	35
3.3 PHYSICAL PHENOMENA APPROACH	40
3.4 SUMMARY OF APPROACHES TO THEORIES OF	44
OVERALL DEVICE PERFORMANCE	
4.0 EJECTOR COMPONENT THEORY AND EXPERIMENT.....	46
4.1 PRIMARY NOZZLES	47
4.1.1 Steady Flow Primary Nozzles	47
4.1.2 Non-Steady Primary Nozzles	56
4.2 SECONDARY INLET SECTION	73
4.3 INTERACTION SECTION	75
4.4 DIFFUSER SECTION	92
4.5 EXTERNAL FLOW AND FORWARD VELOCITY EFFECTS	102

TABLE OF CONTENTS (Cont'd)

	Page No.
5.0 EJECTOR AUGMENTOR FLIGHT SYSTEMS	111
5.1 GENERAL CONFIGURATION DESCRIPTION	111
5.2 XV-4A VTOL CONFIGURATION	111
5.3 XFV-12A VTOL CONFIGURATION	118
5.4 NASA/DITC XC-8A STOL CONFIGURATION	119
5.5 BALL-BARTOE, JW-1, AUGMENTOR WING AIRCRAFT	122
5.6 FLIGHT SYSTEM PERFORMANCE COMPARISONS	125
6.0 CONCLUSIONS AND RECOMMENDATIONS	129
6.1 GENERAL CONCLUSIONS	129
6.2 CONCLUSIONS AND RECOMMENDATIONS BASED ON THEORETICAL CONSIDERATIONS	129
6.3 CONCLUSIONS AND RECOMMENDATIONS BASED ON EXPERIMENTAL RESULTS	131
6.4 CONCLUSIONS AND RECOMMENDATIONS ARISING FROM FLIGHT SYSTEMS RESULTS	132
6.5 GENERAL RECOMMENDATIONS	132
APPENDIX A - SUMMARY OF PHASE 1 EFFORT	A-1
APPENDIX B - COMMENTS ON PREVIOUS THEORETICAL TREATMENTS	B-1
APPENDIX C - RECOMMENDED EJECTOR AUGMENTOR RESEARCH AND DEVELOPMENT AREAS	C-1

LIST OF FIGURES

Figure No.	Title	Page No.
1	Temperature-Entropy Diagram for an Isentropic Compression Process Ejector Cycle.	6
2	Temperature-Entropy Diagram for an Ejector Cycle with Heat Addition to the Primary.	8
3	Temperature-Entropy Diagram for an Ejector Cycle with Cooling of the Primary.	9
4	Temperature-Entropy Diagram for an Ejector Cycle with Heat Addition and Variable Mixing Processes.	12
5	Schematic of a Jet Nozzle.	14
6	Stationary Nozzle Unit Thrust as a Function of Exhaust Flow Conditions.	16
7	Total Energy Conversion Comparison.	18
8	Kinetic Energy Conversion for Primary Nozzle Flow with $\gamma = 1.40$.	19
9	Kinetic Energy Conversion for Primary Nozzle Flow with $\gamma = 1.13$.	21
10	Thrust Augmentation Ratio as a Function of Primary Flow Kinetic Energy Conversion Ratio, ξ .	22
11	Ejector Thrust Augmentation Relative to Complete Primary Jet Energy Conversion.	24
12	Process Description for an Ideal Ejector Augmentor.	34
13a	Constant Area Mixing Thrust Augmenting Ejector Schematic.	37
13b	Constant Pressure Mixing Thrust Augmenting Ejector Schematic.	38
14	Schematic of Finite Difference Model.	41

LIST OF FIGURES (Cont'd)

Figure No.	Title	Page No.
15	Types of Primary Nozzles.	49
16	Comparison of Augmentation Ratio Performance for Single and Multiple Nozzles as a Function of Inlet Area Ratio.	51
17	Performance Comparison between Single and Multiple Nozzles as a Function of Ejector Length.	52
18	Effect of Primary Nozzle Pressure Ratio and Nozzle Configuration on Ejector Performance.	53
19	Effect of Primary Nozzle Temperature Ratio on Augmentation Ratio.	55
20	Types of Non-Steady Flow Thrust Augmentation Ejectors.	57
21	Non-Steady Primary Ejectors.	58
22	Effect of Energy Transfer Efficiency on Static Thrust Augmentation	59
23	Rotary Jet Flow Velocity Triangles.	61
24	Experimental Set-up for a Rotary Jet Augmentor.	62
25	Comparison of Analytical and Test Results for a Rotary Jet Augmentor.	63
26	Improvement in Augmentor Entrainment Ratio with Non-Steady Primary Flow.	65
27	Augmentation Performance as a Function of Diffuser Area Ratio Employing an Oscillating Flow Nozzle.	66
28	Augmentation Performance as a Function of Diffuser Area Ratio Employing a Hypermixing Flow Nozzle.	67
29	Augmentation Performance as a Function of Diffuser Area Ratio Employing Hypermixing Nozzle and Diffuser Blockage.	69

LIST OF FIGURES (Cont'd)

Figure No.	Title	Page No.
30	Effects of Non-Steady Primary Flow for Non-Diffusing Ejectors.	70
31	Augmentation Performance as a Function of Total Length for Steady and Pulsating Jet Axisymmetric Ejectors.	71
32	Augmentation Performance as a Function of Total Length for Steady and Flapping Jet 2-D Ejectors.	72
33	Summary of Ejector Thrust Augmentation Performance.	74
34	Schematics of Various Experimental Ejector Inlet Shapes.	76
35	Effect of Primary Nozzle Position on Relative Thrust Augmentation Ratio for a 2-D Ejector.	77
36	Effect of Primary Nozzle Position on Relative Thrust Augmentation Ratio for an Axisymmetric Ejector.	78
37	General Trend of Augmentation Ratio as a Function of Inlet Area Ratio.	79
38	Typical Velocity Distributions in an Ejector Mixing Chamber.	81
39	Schematic illustrations of Basic Mixing Section Shapes.	83
40	Augmentation Performance of Constant Area Mixing Ejectors without Diffusers.	84
41	Entrainment Ratio, β , as a Function of Mixing Length to Width Ratio.	87
42	Theoretical and Empirical Limits of Ejector Performance.	88
43	Effects of Mixed Flow Entropy Increases for an Augmentor with an Initial Pressure Ratio $P_{tp}/P_{ts} = 1.05$.	89

LIST OF FIGURES (Cont'd)

Figure No.	Title	Page No.
44	Effects of Mixed Flow Entropy Increases for an Augmentor with an Initial Pressure Ratio $T_{t_p} / T_{t_s} = 1.10$.	90
45	Effects of Mixed Flow Entropy Increases for an Initial Temperature Ratio $T_{t_p} / T_{t_s} = 1.10$.	91
46	Typical Ejector Diffuser Configurations.	93
47	Influence of a Diffuser on Ejector Augmentation Ratio as a Function of Primary Total Pressure Ratio.	95
48	Effect on Augmentation Ratio of the Relationship between Diffuser Area Ratio and Inlet Area Ratio.	96
49	Results for Ejector Performance Optimization through Diffuser Area Ratio Variations.	97
50	Impact of Diffuser Flow Separation on Ejector Performance.	99
51	Effects of Different Primary Injection and Boundary Layer Control Techniques on Ejector Performance as a Function of Diffuser Area Ratio.	101
52	Ejector Augmentor Compactness Limits.	103
53	Effects of Forward Velocity on Ejector Thrust Levels and Net Augmentation Ratio.	104
54	Forward Velocity Effects on Rotary Jet Thrust Augmentation Performance.	106
55	Thrust Results for a Shielded Inlet Ejector Augmentor.	108
56	Alternate Configurations of the Ejector Blown Lift/Cruise Flap Concept.	109
57	Relative Lift Performance of Ejector-Flapped and Jet-Augmented Flapped Wings	109

LIST OF FIGURES (Cont'd)

Figure No.	Title	Page No.
58	Measured Thrust Augmentation Characteristics.	110
59	Lockheed/U.S. Army XV-4A Ejector Augmentor Aircraft.	112
60	Rockwell/U.S. Navy XFV-12A Ejector Augmentor Aircraft.	113
61	NASA/DITC XC-8A STOL Configuration.	114
62	Ball-Bartoe/University of Tennessee JW-1 Augmentor Wing Aircraft.	115
63	XV-4A Ejector Bank Schematic.	117
64	Air Distribution System for the NASA XC-8A STOL Aircraft.	121
65	Comparison of Ejector Flight Systems Entrainment-Augmentation Performance.	126
66	Comparison of Ejector Flight Systems Overall Performance for Total Exit to Primary Area Ratio.	127
67	Comparison of Ejector Flight Systems Actual Mixing Lengths (with Losses) of Optimum Lengths.	128
A-1	Chronological Summary of Reports on Fundamental Ejector Phenomena.	A-5
A-2	Chronological Summary of Published Reports on Ejector Augmentors.	A-6
A-3	Chronological Summary of Published Reports on Ejector Pumps.	A-7
A-4	Ejector Summary/Overview Information Form.	A-8
A-5	Ejector Schematic.	A-32
A-6	Effect of Diffuser Area Ratio and Secondary to Primary Inlet Area Ratio on Augmentation.	A-34

LIST OF FIGURES (Cont'd)

Figure No.	Title	Page No.
A-7	Mixing Length Effects.	A-36
A-8	State Property Effects on Augmentation Ratio.	A-37
A-9	The Effect of Mean Flow Properties on Augmentation Ratio.	A-38
A-10	Augmentation Ratio vs. A_4/A_{pex} .	A-40
A-11	Augmentation Ratio vs. Total Length.	A-41
B-1	Theoretical Non-Diffusing Ejector Performance.	B-3
B-2	Temperature-Entropy Diagram for a Supersonic Mixed Flow Augmentor, (Overexpanded, $P_{ex} < P_{amb}$).	B-7
B-3	Effects of Relative Initial Entropy Levels on Theoretical Thrust Augmentation.	B-8

LIST OF TABLES

Table No.	Title	Page No.
1	Flight Vehicle Augmentation Ratios	105
2	NASA XC-8A Air Distribution System with typical thrust losses (Medium Power Setting)	123
A-1	Examples of Primary/Secondary Relationships for Ejectors	A-19
A-2	Ejector Energy Transfer Properties of Interest	A-20
A-3	Ejector Primary/Secondary Time Dependence	A-20
A-4	Significant Operating Parameters of State	A-23
A-5	Significant Geometric Descriptions	A-25
A-6	Significant Mean Flow Operating Parameters	A-27
A-7	Significant Performance Descriptions	A-28
A-8	Significant Loss Descriptions	A-30
C-1	Ejector Technology Research and Development Topics	C-3

NOMENCLATURE

A_0	Inlet entrance area
A_{pi}	Primary inlet flow area
A_{si}	Secondary inlet flow area
A_1	Mixing Area
A_2	Throat Area, minimum area
A_3	Diffuser entrance area
A_4	Exit Area
C_{EF}	Section lift coefficient for an ejector flap
C_{JF}	Section lift coefficient for a jet flap
C_p	Specific heat
C_{p_p}, C_{v_p}	Primary fluid specific heats
C_{p_s}, C_{v_s}	Secondary fluid specific heats
D	Diameter
D_c	Correction factor for mixing length coefficient
e	Internal energy
f	Fuel flow
f/a	Fuel to air ratio
F	Thrust
h	Enthalpy
J	Jet momentum to jet kinetic energy ratio
L_M	Jet mixing length
L_t	Total length
L_o	Diffuser length
M	Mach number
\dot{m}, m	Mass flow rate
\dot{m}_{p_i}	Primary inlet mass flow rate

NOMENCLATURE (Cont'd)

\dot{m}_{s_i}	Secondary inlet mass flow rate
\dot{m}_{t_e}	Total exit mass flow rate
P	Static pressure
P_t	Total pressure
P_{p_i}	Primary inlet static pressure
P_{s_i}	Secondary inlet static pressure
P_{amb}	Ambient static pressure
P_{ex}	Exit static pressure
P_{t_p}	Primary fluid total pressure
P_{t_s}	Secondary fluid total pressure
P_{t_m}	Mixing fluid total pressure
P_{m_i}	Static fluid pressure at mixing entrance
P_{m_e}	Static fluid pressure at mixing exit
$P_{t_{me}}$	Mixed flow total pressure at the exit plane
Q	Heat flux
q	Dynamic pressure
R	Universal gas constant
S	Entropy
S_{p_i}	Primary inlet fluid entropy
S_{s_i}	Secondary inlet fluid entropy
S_m	Intermediate "mixed" flow entropy
SFC	Specific fuel consumption

NOMENCLATURE (Cont'd)

T	Static temperature
T_t	Total temperature
T_{t_p}	Primary fluid total temperature
T_{t_s}	Secondary fluid total temperature
T_{s_m}	Mixed flow total temperature
T_{p_i}	Primary inlet static temperature
T_{s_i}	Secondary inlet static temperature
T_{me}	Mixed flow static temperature at the exit plane
$T_{t_{me}}$	Mixed flow total temperature at the exit plane
T_a, T_{amb}	Ambient temperature
U, V	Velocity
U_{p_i}	Primary inlet velocity
U_{s_i}	Secondary inlet velocity
U_{p_o}	Velocity of primary fluid in the reservoir
w, w_a	Mass flow, air mass flow
W	Mixing Section width
α	Constant in Hedges and Hill finite-difference flow model
β	Entrainment ratio, $\frac{m_s}{m_p}$; Spin angle for rotary jet flow inductor, skewness factor
γ_p	Primary flow specific heat ratio
γ_s	Secondary flow specific heat ratio
δ_{ij}	Kronecker delta
ϵ	Eddy momentum diffusivity

NOMENCLATURE (Cont'd)

η_t	Energy transfer efficiency, ratio of kinetic energy gained by the secondary to kinetic energy lost by the primary.
θ	Diffuser half angle
κ_o	Jet mixing length coefficient
μ	Kinematic viscosity
ξ	Kinetic energy transfer ratio
ρ	Density
τ	Stress tensor
$\tau_{xx}, \tau_{yy}, \tau_{zz}$	Compressive stresses
$\tau_{xy}, \tau_{xz}, \tau_{yz}$	Shear stresses
ϕ	Augmentation ratio
ψ	Stream function

SUBSCRIPTS

amb, o	Ambient condition
d	downstream location
ej	ejector
ex, e	exit location
g	gross
i	inlet location
ideal	for expansion to ambient static pressure
isen	isentropic
m	mixed flow condition
max	maximum
net	net, (gross thrust minus ram drag)
p	primary flow
p_o	primary flow stagnation condition
ram	ram drag term

NOMENCLATURE (Cont'd)

s	secondary flow
t	tangential direction
u	upstream
0	freestream, inlet section
1	mixing region
2	throat
3	diffuser entrance
4	diffuser exit

SUPERSCRIPTS

o	stagnation condition
'	isentropically expanded to ambient pressure
*	sonic condition

1.0 INTRODUCTION

An ejector thrust augmentor is a device for increasing, or "augmenting", the thrust of a primary propulsive nozzle through fluid dynamic means. To those newly introduced to the concept, it may at first seem as if the ejector augmentor gets "something for nothing", but it must be remembered that the maximum thrust of a primary propulsive nozzle is limited to a value which is far less than the potential thrust which would be available if a complete conversion from internal energy to kinetic energy could be achieved. This limit is essentially set by the ambient boundary conditions, specifically the ambient pressure, into which the primary nozzle flow exhausts. The difference between the conversion of kinetic energy which occurs when a primary propulsive nozzle exhausts to a finite ambient pressure, and that which would occur if it exhausted into a vacuum (the maximum potential thrust case), represents the source for ejector thrust augmentation.

The ejector thrust augmentor utilizes the potential available in the primary propulsive nozzle fluid in the following way: The primary propulsive nozzle flow is exhausted into a larger duct, usually called the ejector "shroud", where it interacts with, and induces motion in, the ambient fluid in the shroud. The induced motion in the ambient fluid results in a local static pressure less than ambient at the primary nozzle exit plane. The primary nozzle exhaust, by virtue of this lower static pressure, thus has a higher velocity and kinetic energy than it would have if there were no shroud. The lower than ambient static pressure also results in continued entrainment of the surrounding ambient fluid into the shroud. The interaction between the two fluids, for the steady flow situation is primarily due to a viscous shear mechanism called "mixing", and results in an energy transfer from the primary flow to the ambient, or secondary, flow. The two fluids thus arrive at a nearly identical thermodynamic state intermediate between their initial conditions. This "mixed" flow, upon exhausting to the ambient back pressure, provides a greater total thrust due to the energy exchange which has taken place, than could have the primary propulsive nozzle alone. The ratio of this total device thrust to the ideal thrust of a primary propulsive nozzle exhausting to the same ambient back pressure is called the thrust augmentation ratio.

In addition to this ability to increase or augment the thrust of a primary fluid which has a given amount of energy, ejector augmentors have other inherent advantages which make them highly desirable for thrust system applications. These

are: (1) a simplicity of the basic design, (2) no moving parts, (3) ease of conformation to geometric constraints, and (4) the possibility of achieving these advantages with a lightweight, low volume system. While these advantages can be, and have been, shown both theoretically and in laboratory experiments, the ability to implement them in an effective system application is still beyond the state of the art of ejector augmentor technology. The main reason for this appears to lie in a lack of understanding, both theoretical and experimental, of the details of the flow phenomena which contribute to ejector augmentor performance and design. In this respect an ejector augmentor is directly analogous to a turbojet engine. The basic concept of compression, energy addition, and conversion of thermal energy to kinetic energy to achieve thrust, is relatively straightforward for each. The actual details of the phenomena which must take place to achieve the end result are extremely complex. The analogy between a turbojet engine and an ejector augmentor is perhaps also of interest from the historical point of view. Although Hero's recorded sketches of a steam jet-engine are dated at around 60 A.D., it was not until 1939 A.D. that von Ohain's turbojet engine first flew successfully in an airplane. Although the basic principles of turbojet propulsion were known for many years prior to the historic 1939 flight, the inertia evident then in the propulsion community in accepting an alternative to piston driven propeller propulsion may be likened to that evident now toward ejector augmentors. The similarities between the technology development of turbojets and ejector augmentors are limited, however, to the overall devices. Unlike the turbojet, for which the compressor, combustor and turbine, can be developed independently to achieve high component efficiency; in an ejector augmentor the compression, energy addition and expansion all take place concurrently during the complex interaction between secondary and primary fluids. Ejector augmentor development to date has thus been highly empirical, and theoretical design and prediction capabilities are only accurate to the extent of the applicability of the empiricisms they employ.

The experimental development of ejector augmentors in recent decades has paralleled to some extent that which occurred earlier for ejector pumps. While ejector pumps were being satisfactorily used for a variety of applications in the late 1800's^{171*} what appear to be the first exploratory tests of ejector augmentors did not take place until 1927.⁶⁶⁷ Ironically, perhaps, these tests were oriented toward showing the feasibility of jet propulsion for airplanes. The first actual application of an ejector augmentor, however, appears to have been on a Russian ambulance sled during World War II,⁶⁸⁰ and it utilized the principles of Henri Coanda (the Coanda Effect). Shortly thereafter the technical community was finally

*Superscript numerals refer to publications listed in the Part II-Bibliography.

awakened to the potential of these devices by von Karman's classical Reissner Anniversary theoretical treatment for incompressible, diffuserless ejector augmentors¹⁴⁴² (See Appendix B). This paper was oriented toward explaining the principles of the Coanda ejector. In the ensuing years, numerous theoretical and experimental variations on the basic theme have been tried. Noteworthy among these are Bertin's experiments with multiple annular nozzle configurations,¹²⁶ and Foa's invention of the non-steady rotary jet flow augmentor.⁴¹² Both of these devices were oriented toward improving the efficiency of the interaction between the ejector primary and secondary flows. While both were reasonably successful in achieving this goal, neither achieved a forceful impact on the ejector technical community. It was not until 1972 when Quinn¹⁰⁸⁹ provided a "Briefing to Industry" on the Air Force Aerospace Research Laboratory's (ARL) work on hypermixing nozzles, that significant new interest was aroused in the possible application of ejector augmentors to aircraft propulsion systems. The implications of the hypermixing nozzles, which extended the flow interaction into the ejector diffuser through the formation of vortical interaction zones, thereby reducing the required total length of the device, were discussed in their relationship to conceptual Vertical and Short Takeoff and Landing (V/STOL) aircraft at that briefing. Renewed interest in ejector augmentors occurred almost immediately, and a multimillion dollar prototype development program for a Thrust Augmentor Wing (TAW) V/STOL aircraft - the XFV-12A, was funded by the Navy. Many in the ejector community believed that while the hypermixing nozzle technology was a significant step forward, the necessary research and development (R&D) for a successful application had still not been achieved. Consequently, numerous independent R&D investigations have continued to explore the fundamentals and the potential of ejector augmentors. Perhaps the more significant of these recent investigations have been in the area of improved, more compact diffusers for ejector augmentors. Alperin has achieved notable performance with ejectors using the "Jet Flap" diffuser principle,⁴⁰ and O'Donnell and Squyers showed significant total length reductions for an ejector with hypermixing nozzles, mated to a special boundary layer control diffuser.¹⁰¹⁴

The picture which emerges, then, of the state of the art of ejector augmentor technology is one of fragmentation within the technical community. While few individuals who are knowledgeable in the area still regard ejector augmentors as only an interesting laboratory novelty, there is a diversity of opinion on whether they are yet at a stage of development which permits a viable flight system application. Those who believe that they are, have impressive experimental data (albeit primarily from controlled laboratory testing) for high performance, compact devices. Those who believe that continued research and development is required

first, cite fundamental gaps in the understanding of the interacting physical phenomena, as well as examples of premature attempts at applications which have set back technology when they failed.

In Sections 2.0 and 3.0 which follow, the fundamental physics of ejector flows as currently understood as well as the types of theoretical treatments for predicting overall ejector augmentor performance will be described. In Section 4.0, specific ejector components are discussed in terms of theoretical models which have been formulated, and the significant parameters which appear on the basis of experimental investigations. Section 5.0 describes four attempts at ejector augmentor flight systems and speculates on a possible cause for their disappointing performance. Throughout these discussions an attempt has been made to highlight those technical issues which appear to be important to achieving a viable ejector augmentor propulsion system, and which are presently unresolved. In the Conclusions and Recommendations, Section 6.0, a reiteration of these technology need areas and the relevant types of research and development programs required for their resolution, is again emphasized. In the Appendices of this Volume I some specific well-known theoretical treatments are discussed in detail, some critical R&D program objectives and approaches are identified, and a condensation of relevant results of a preliminary general study of ejectors is provided. Volume II, presents a comprehensive, coded, bibliography of over 1600 references for ejectors of all types.

2.0 FUNDAMENTAL PHYSICS OF EJECTOR AUGMENTORS

As with the theories of overall device performance, which will be discussed in Section 3.0, an understanding of the fundamental physics of ejector augmentors can be approached on two levels: (1) The overall process and what occurs in terms of bulk changes in energy and enthalpy, and (2) The individual physical processes which contribute to the overall process, in terms of the fundamental mechanisms of energy and momentum transfer.

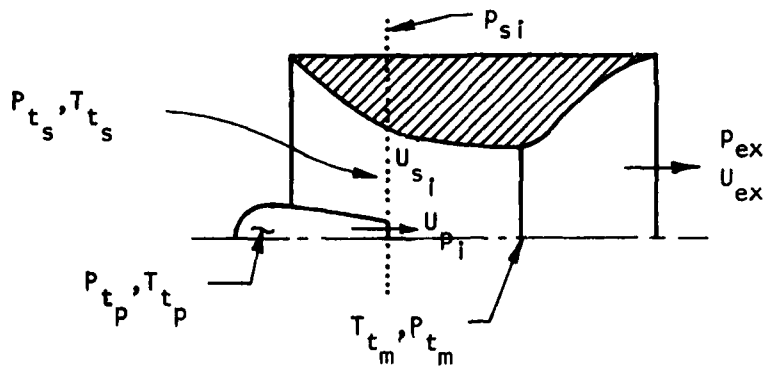
In the following sections, the overall process is first considered by means of T-s diagrams, and a relationship is established between momentum, in terms of the augmentation ratio and total energy of the primary flow. Following this general approach to ejector augmentors, the fundamental mechanisms of individual processes contributing to the overall performance are discussed. Finally, a brief summary of the current understanding of the physics of ejector augmentor flows is presented.

2.1 FUNDAMENTALS OF OVERALL PROCESS RELATIONSHIPS

2.1.1 Overall Process Relationships (T-s Diagrams)

For an ejector system with specified initial total energy and total entropy states, the thermodynamic process may be represented on a temperature-entropy (T-s) diagram. Figure 1 shows a thermodynamic path for an ejector where the primary flow is at an initial state represented by isentropic compression of the ambient air. The state conditions and the processes are shown on the figure.

In Figure 1, the (ambient) secondary and the primary are assumed to be at the same entropy level. Both the flows expand isentropically to the same inlet static pressure, $P_{s_i} = P_{p_i}$. The secondary flow entrainment is assumed isentropic as is the primary nozzle flow. The two flow streams then interact (mix), and without regard to whether it can happen physically, it has been assumed that this mixing takes place isentropically. The mixed flow resultant state is a function of the initial states A and B, the isentropic primary nozzle discharge and mixing, and the entrainment ratio, β . The mixed total temperature is defined by the energy relationship, while the mixed flow total pressure is a function of the thermodynamic process to achieve that temperature. The isentropic State D exists at the mixed total temperature, T_{tm} , and at some total pressure, P_{tm} , greater than P_{ts} , but less than P_{tp} . The thermodynamic process



STATE CONDITIONS:

- A Initial State of Both Primary and Secondary Gases
- B Initial State of Ejector Primary after Isentropic Compression
- C Static States of Expanded Primary and Secondary Flow
- D Mixed Flow State
- E Static States of Mixed Flows

PROCESSES:

- A→B Isentropic Compression of Primary Gas
- A→C Isentropic Expansion of Secondary Flow in Ejector Inlet
- B→C Isentropic Expansion of Primary Flow in Primary Nozzle
- C→D "Isentropic" Mixing of Primary and Secondary Flows
- D→E Isentropic Expansion of Mixed Flow in Ejector Exit Nozzle

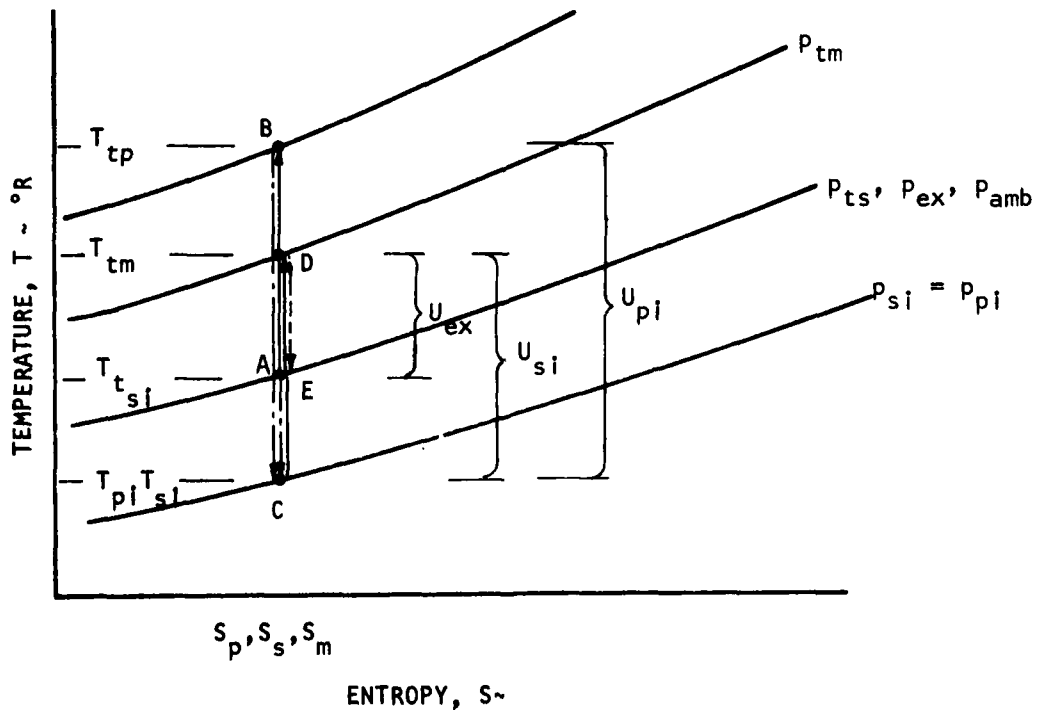


FIGURE 1. TEMPERATURE-ENTROPY DIAGRAM FOR AN ISENTROPIC COMPRESSION PROCESS EJECTOR CYCLE

for the ejector augmentor of Figure 1 is completed by the expansion of the mixed flow total pressure to the exit flow boundary condition, such as P_{amb} . With a T-s diagram such as Figure 1, the "isentropic" performance of an ejector with equal and constant specific heats may be determined. The flow properties at any location within the ejector may also be analytically described. For example, the primary flow velocity for expansion to ambient pressure is simply:

$$U_p' = \sqrt{\frac{2\gamma R}{\gamma-1} (T_{t_p} - T_p')} \quad (1)$$

and the exit velocity of the mixed flow is:

$$U_{ex} = \sqrt{\frac{2\gamma R}{\gamma-1} (T_{tm} - T_{ex})} \quad (2)$$

The thermodynamic cycle can also be used to consider ejector performance for initial primary energy states which include heat addition or cooling of the flow. The primary gas can then be at a higher or lower initial entropy state, respectively. Figures 2 and 3 illustrate the T-s diagrams for these two possible thermodynamic cycles, where the definition of states and processes is the same as for Figure 1. In these examples, with the addition of points C', D' and D'' which represent an isentropic expansion of the primary flow, the mixed flow static state after constant pressure mixing and the mixed flow static state after constant area mixing, respectively, form the two initial energy states, the primary and secondary achieve a mixed flow state as a function of the entrainment ratio and non-isentropic processes. The performance and intermediate flow properties of these two processes can be analytically evaluated as in the isentropic case.

It is perhaps worth noting that the thermodynamic interaction process is significantly different for the case of an initially cooled primary flow, than for an initially cooled primary flow. In the former case, as may be seen in Figure 2, the primary flow undergoes an increase in entropy, $\frac{dQ_p}{T} > 0$, while the secondary flow undergoes a decrease in entropy, $\frac{dQ_s}{T} < 0$. That is, although the total process may be considered adiabatic, the secondary flow loses heat to the primary during the interaction/mixing process. For the case where the initial primary flow is at a cooled state (Figure 2), these relationships are reversed. The cooled primary is typical of laboratory experiments

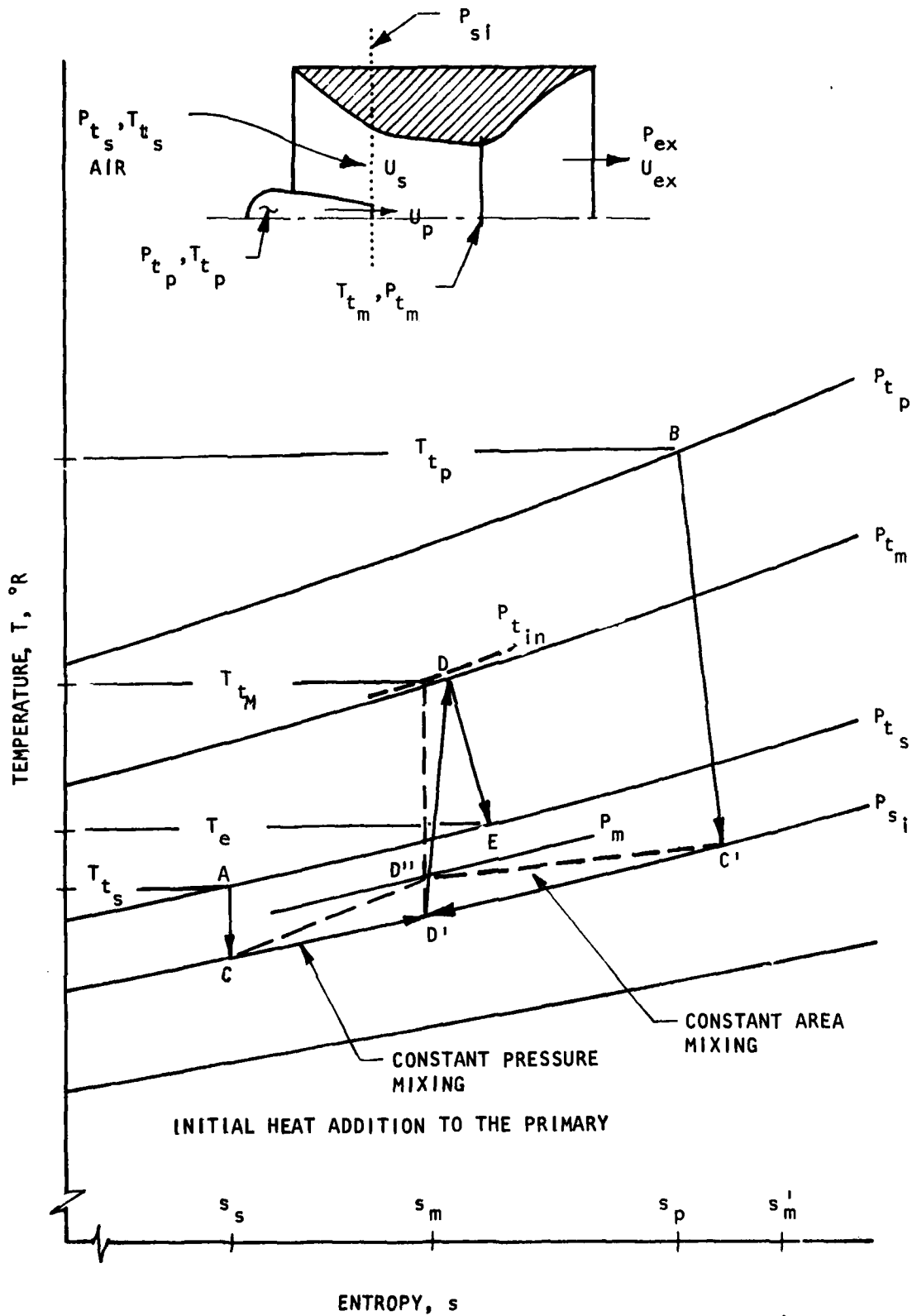


FIGURE 2. TEMPERATURE-ENTROPY DIAGRAM FOR AN EJECTOR CYCLE WITH INITIAL HEAT ADDITION TO THE PRIMARY.

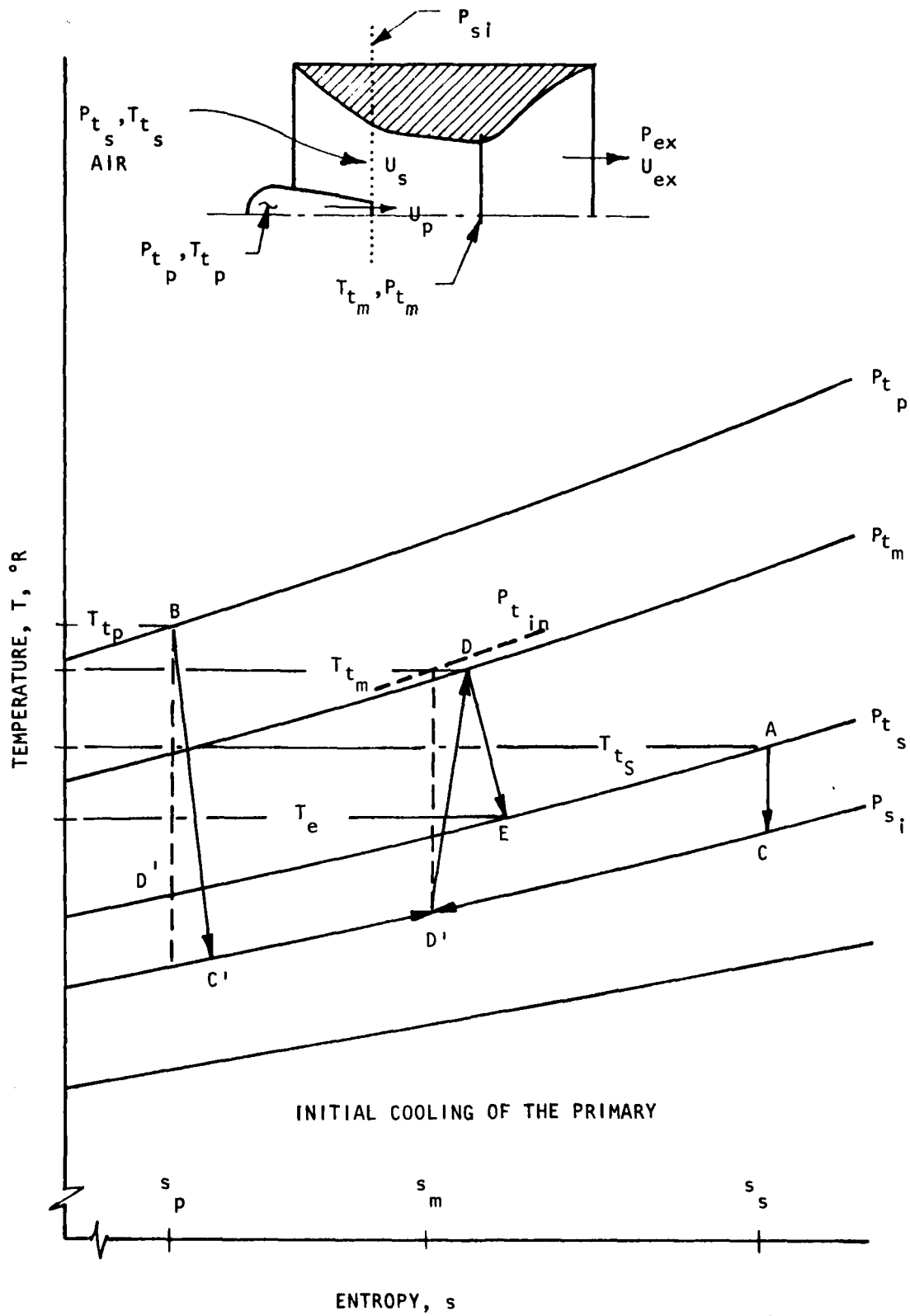


FIGURE 3. TEMPERATURE-ENTROPY DIAGRAM FOR AN EJECTOR CYCLE WITH COOLING OF THE PRIMARY.

with $T_{tp} = T_{ts}$, but $P_{tp} > P_{ts}$, whereas the heated primary is typical of jet engine/bypass flow conditions found in application of ejectors to flight systems.

Using the foregoing three types of thermodynamic cycle examples (i.e., $s_{p_i} = s_{s_i}$, $s_{p_i} > s_{s_i}$, and $s_{p_i} < s_{s_i}$), ejector system performance parameters may be determined and overall conclusions reached. For example, the mixed total temperature for any entrainment ratio for the usual condition, $T_{tp}/T_{ts} > 1.0$, is less than the primary and greater than the secondary total temperature. The final mixed temperature can be determined from the energy equation:

$$T_{tm} = \frac{T_{tp} + \beta T_{ts}}{1 + \beta} \quad (3)$$

For an adiabatic system, i.e., no heat exchanged to or through the shroud walls, regardless of whether the mixing process is isentropic or non-isentropic, this mixed total temperature is achieved. In the non-isentropic case, the mixed flow temperature is achieved at a lower mixed total pressure, as is evident in the diagrams. For maximum momentum thrust, the mixed flow is then exhausted to ambient pressure by process D→E. A discussion of maximum momentum thrust is presented in the following section.

The static thrust augmentation ratio for an ejector exhausting to ambient pressure can be determined if states A, B, D, E, and the entrainment ratio are known. For any of the three types of thermodynamic cycles, the actual static thrust augmentation ratio, ϕ , from the energy equation, written as:

$$T_{p_i} + \frac{V_{p_i}^2}{2} + \beta \left(T_{s_i} + \frac{V_{s_i}^2}{2} \right) = (1 + \beta) \left(T_e + \frac{V_e^2}{2} \right) \quad (4)$$

and the definition of ϕ :

$$\phi = (1 + \beta) \frac{V_e}{V_p} \quad (5)$$

can be expressed as:

$$\phi = \sqrt{(1 + \beta) \left[\frac{(T_{tp} - T_e) + \beta(T_{ts} - T_e)}{(T_{tp} - T_p')} \right]} \quad (6)$$

In the isentropic cycle, $T_{ts} = T_p' = T_e$ for the maximum augmentation ratio, thus

$$\phi_{max} = \sqrt{1 + \beta} \quad (7)$$

which is the analytical conclusion reached by Heiser (see Appendix B). Appendix B discusses the relationship of Eq. (6) to Heiser's general conclusions in more detail.

The T-s diagram facilitates the determination of the maximum theoretical thrust augmentation for given initial primary and secondary state conditions. Any non-isentropic process which occurs during the overall process will increase the intermediate "mixed" flow entropy above the average isentropic value given by

$$s_m = \frac{s_p + \beta s_s}{(1 + \beta)} \quad (8)$$

This increase in entropy drives the cycle performance to lower values of calculated ϕ , as shown in Figure 4. The only boundary condition which has been imposed on the thermodynamic cycle is that the energy be conserved, i.e., that the mixed flow attains the flow weighted value of T_{tm} . As can be seen in Figure 4, for a process with heat addition, the mixed flow state may occur at an entropy greater than or equal to s_m . Thus, the flow state E may be anywhere to the right of s_m but at a greater pressure than P_{ts} , such as that denoted by s_m' in Figure 4. This particular process corresponds to a large increase in entropy in the ejector. A thermodynamic process which follows this path generates an augmentation ratio greater than 1.0 but much less than the isentropic value for the same value of entrainment ratio, β . The phenomenon of decreasing thrust augmentation ratio for increasing ejector entropy can be shown for all three types of thermodynamic cycles for $\beta = \text{constant}$. However, as will be shown in Section 3.0, if β increases, ϕ can also increase even though the mass-averaged mixed flow entropy level increases.

While the T-s diagrams provide considerable insight into the overall ejector process, there remains a fundamental question of how an ejector augmentor can provide more thrust than an optimum primary flow nozzle. In the following section, the relationship of maximum ejector performance to the initial stagnation energy state of the primary flow is discussed.

2.1.2 Maximum Augmentation Ratio Formulation

In formulating an upper limit to the augmentation ratio, which can be achieved with a given primary flow, it must be remembered that an ejector augmentor works for two fundamental reasons: (1) The maximum thrust which can be achieved with a given steady primary flow, utilizing an isolated nozzle, occurs when the nozzle's exit plane static pressure is equal to the ambient static pressure, and (2) Except for the condition where the ambient static pressure is a vacuum ($P_{amb} \equiv 0$), the primary flow does not achieve a total conversion of its total energy to kinetic energy or momentum. By inducing a secondary flow and reducing the primary exit plane static pressure, the ejector augmentor causes an increased

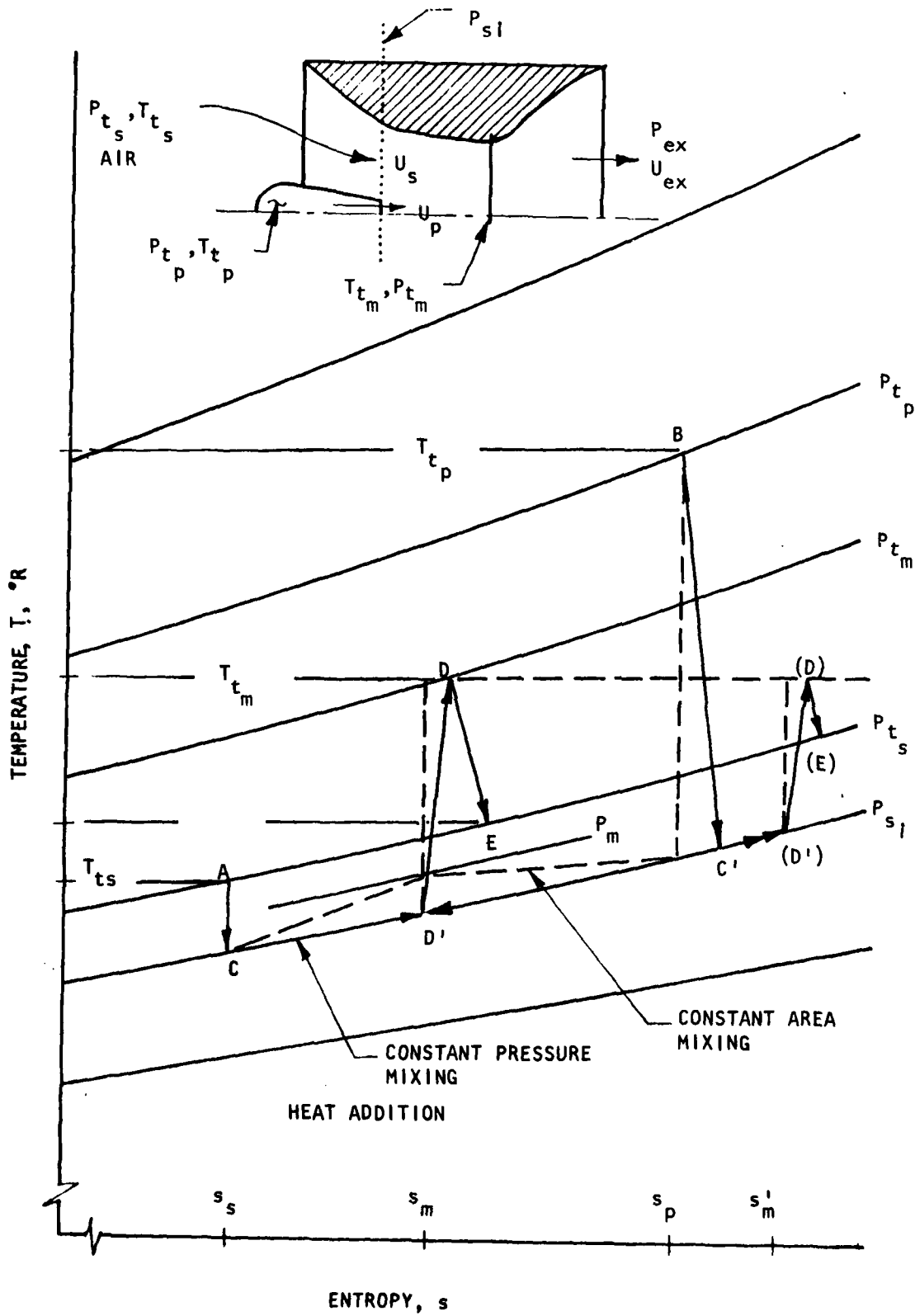


FIGURE 4. TEMPERATURE-ENTROPY DIAGRAM FOR AN EJECTOR CYCLE WITH HEAT ADDITION AND VARIABLE MIXING PROCESSES.

conversion of total to kinetic energy by the primary flow, and through the energy transfer and diffuser accomplishes a match with the ambient static pressure at its own shroud/nozzle exit plane. The above two conditions are discussed in detail in the following paragraphs.

The equation for the thrust of a steady jet can be derived from the momentum and energy laws without the need for detailed consideration of the internal mechanisms of particular nozzles. Using the flow characteristics shown in Figure 5, the net static thrust of a stationary nozzle may be expressed as:

$$F_{\text{Net}} = \int_{A_e} \rho_e U_e^2 dA_e + \int_{A_e} P_e dA_e - \int_{A_e} P_{\text{amb}} dA_e \quad (9)$$

The thrust produced by this idealized steady jet is equal to the momentum efflux through the control surface. Considering the control volume surfaces upstream, above, and below the nozzle to be at far field conditions and the density and velocity to be independent of the local area, then the momentum efflux crossing the control volume surface is $\rho_e U_e^2 A_e$. If the velocity distribution at the exit plane is nonuniform, an integral over the area is required. For an idealized analysis, the velocity and pressure may be considered uniform. The maximization of the momentum thrust occurs whenever the exit plane pressure equals the ambient pressure. This conclusion has been analytically shown by Shapiro¹²⁴⁷ for supersonic exit flows and is a necessary boundary condition for typical diffusers or nozzles with subsonic flow exhausting to ambient conditions. Thus, the actual thrust of a subsonic jet and the maximum thrust of a supersonic flow idealized nozzle is:

$$F_{\text{max}} = \rho_e U_e^2 A_e, \text{ with } P_e = P_{\text{amb}} \quad (10)$$

Equation (10) may be rearranged to show that:

$$\frac{F_{\text{max}}}{P_{\text{amb}} A^*} = \gamma M_e^2 \left(\frac{A_e}{A^*} \right) \quad (11)$$

or

$$\frac{F_{\text{max}}}{P_{\text{amb}} A^*} = \gamma M_e^{\frac{\gamma+1}{2}} \left(1 + \frac{\gamma-1}{2} M_e^2 \right)^{\frac{\gamma+1}{2(\gamma-1)}} \quad (12)$$

where

$$M_e = \left(\left[\left(\frac{P_T}{P_{\text{amb}}} \right)^{\frac{\gamma-1}{\gamma}} - 1 \right] \frac{2}{\gamma} \right)^{1/2} \quad (13)$$

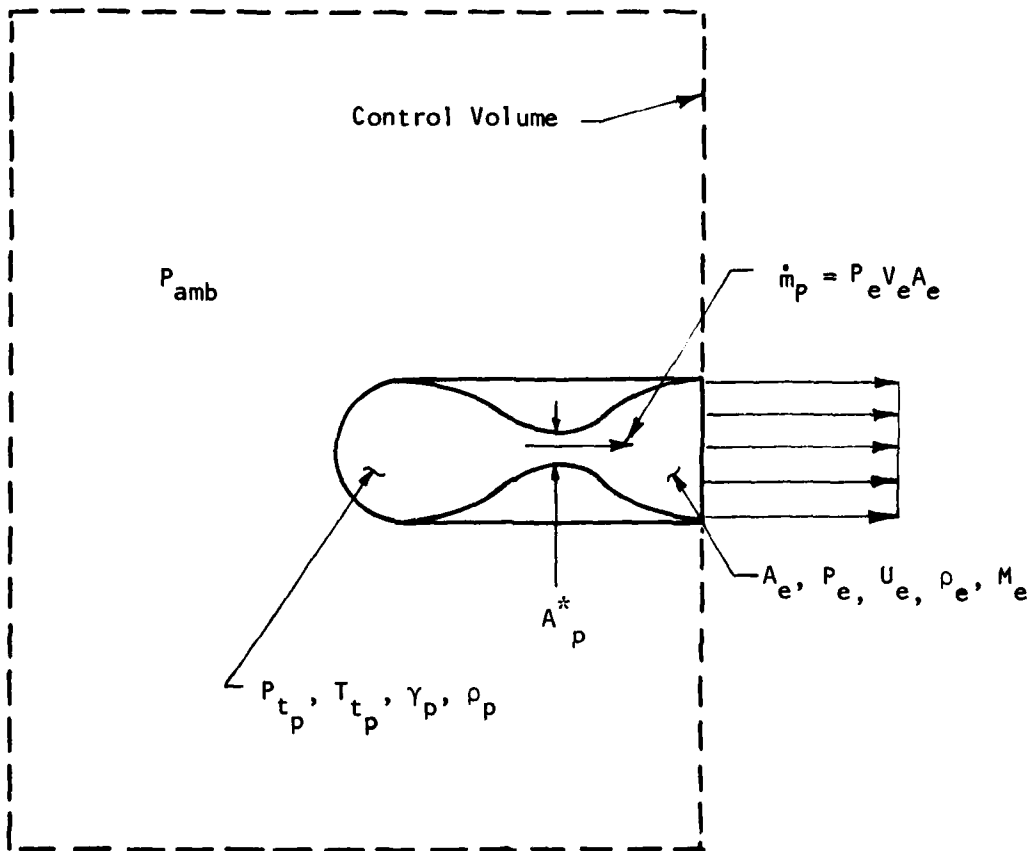


FIGURE 5. SCHEMATIC OF A THRUSTING JET NOZZLE.

Figure 6 shows that the optimum thrust per throat area parameter is achieved for expansion to ambient, $p_e/p_{amb} = 1.0$. Since the performance of a thrust augmentor is determined by the augmentation ratio, defined as:

$$\phi = \frac{F_{ej}}{F_{ideal}} = \frac{\text{Actual Thrust produced by the ejector}}{\text{Thrust generated by the primary Nozzle, isentropically expanded to ambient,}} \quad (14)$$

ϕ values greater than one necessarily imply that an improvement in total thrust was achieved for constant primary energy: $\dot{m}_p, P_{tp}, T_{tp}$. These relationships with regard to Jones, ^{678,680} are discussed further in Appendix B.

Based on the preceding discussion of the optimum thrust per throat area parameter, the utilization of the total available energy for conversion to kinetic energy can be considered. The primary flow reservoir characteristics are the basis for the total energy available with which thrust augmentation can be achieved. The total specific energy per unit mass of the primary can be written as $h_{pp} = c_{pp} T_{tp}$. The primary flow total (stagnation) temperature, T_{tp} , and the ratio of specific heat at constant pressure, c_p , are state properties, but the primary mass flow is dependent upon the geometry and pressure state of the nozzle for expansion to its static exit conditions. Energy conversion to momentum for this primary nozzle process occurs whenever the state energy is converted to kinetic energy. Using the integrated energy equation, the change in kinetic energy per unit mass for an expansion from the stagnation condition to the nozzle exit plane is:

$$\frac{\Delta K.E.}{\dot{m}_p} = c_{pp} (T_{tp} - T_e) \quad (15)$$

where

$$\frac{\Delta K.E.}{\dot{m}_p} = 1/2 (U_e^2 - U_{p0}^2) \text{ and} \quad (16)$$

where $U_{p0} = 0$ in the reservoir. Combining equations (15) and (16), the primary nozzle exit velocity becomes:

$$U_e = \left\{ \frac{2\gamma R}{\gamma - 1} (T_{tp} - T_e) \right\}^{1/2} \quad (17)$$

The requirement of exit plane ambient pressure for optimum thrust determines the required primary nozzle geometry and sets the exit flow static temperature. The exit kinetic energy is thus determined and fixed by these conditions. For

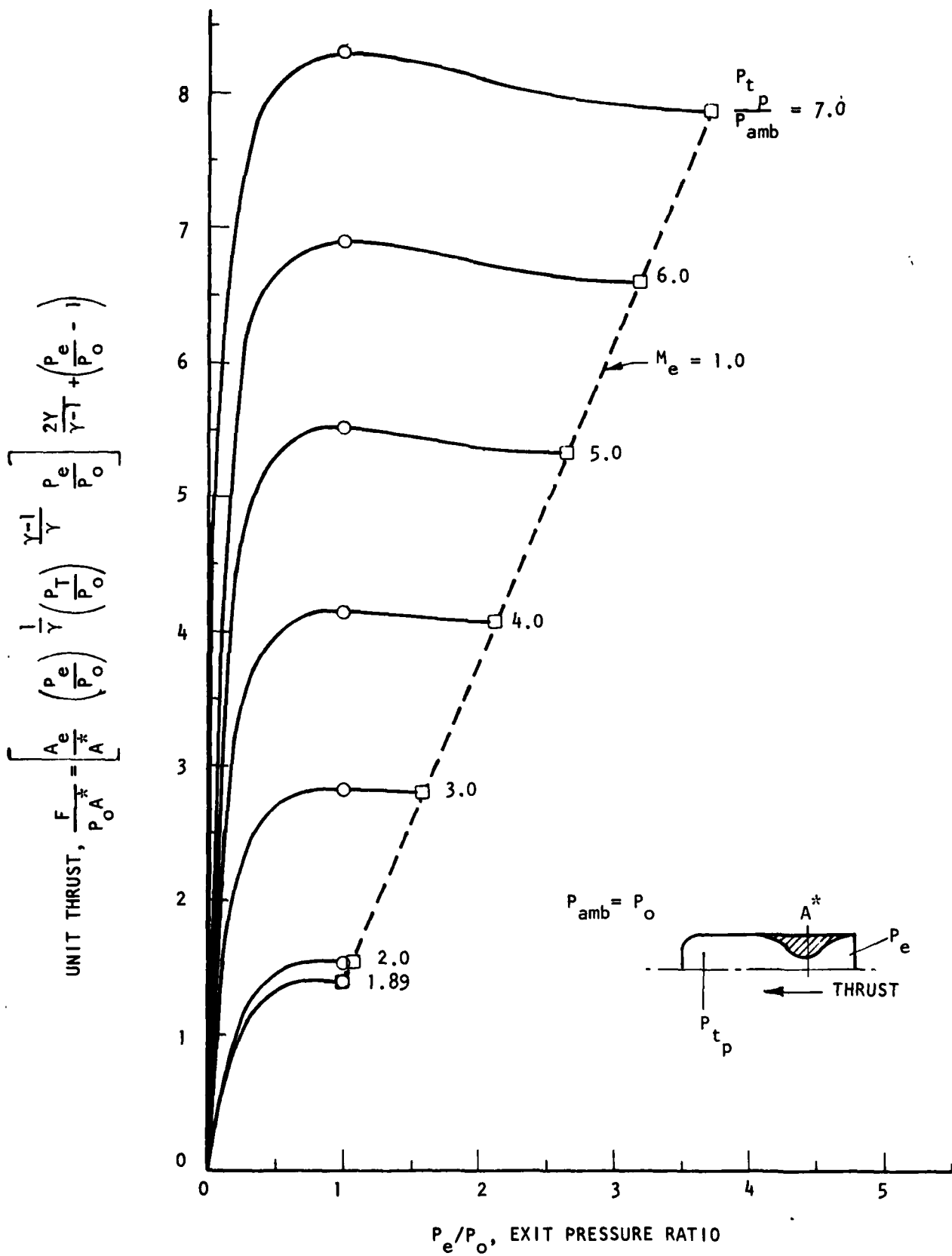


FIGURE 6. STATIONARY NOZZLE UNIT THRUST AS A FUNCTION OF EXHAUST FLOW CONDITIONS.

complete conversion of the available total energy to kinetic energy, i.e., maximum velocity, the static temperature, T_e , approaches absolute zero. The maximum velocity obtainable thus corresponds to expansion to a vacuum, and is thus defined as:

$$U_{max} = \sqrt{\frac{2\gamma R}{\gamma-1} (T_{t_p})} \quad (18)$$

For equivalent total energy primary flows, the resultant kinetic energy for expansion to finite ambient conditions ratioed to the maximum available kinetic energy is defined as ξ , as shown below:

$$\xi = \left(\frac{U_{e_{amb}}}{U_{max}} \right)^2 \quad (19)$$

or

$$\xi = \left[1 - \frac{T_e}{T_{t_e}} \right] \quad (20)$$

$$\xi = \frac{\gamma-1}{2} Me^2 / \left(1 + \frac{\gamma-1}{2} Me^2 \right) \quad (21)$$

Figure 7 illustrates the relationship of the kinetic energy conversion ratio for various total energy levels expressed by M_e , where M_e is defined by Equation (13). The exit Mach number is determined for the expansion of the primary flow to ambient conditions for the maximum thrust per throat area parameter. As may be seen in Figure 7, as the exit Mach number increases, a greater ratio of the total available energy is converted to kinetic energy. A kinetic energy ratio, ξ , of 1.0 corresponds to an isentropic expansion to an absolute zero exit temperature. For finite Mach numbers, the actual kinetic energy of the flow is a fraction of the total available energy. For moderate Mach numbers, less than 2.0, less than one-half of the total energy is converted to kinetic energy. Thus, for a jet with optimal thrust expansion to ambient, a large fraction of the total energy available is unused. Since the total temperature has been assumed to be the same for the two conditions, the relationship of actual to available kinetic energy is independent of total temperature. It is, however, a strong function of the ratio of specific heats, γ , as shown in Figure 8. The unused energy of the primary flow represents energy available to achieve thrust augmentation by transfer to a secondary fluid. Thus, the larger the exit Mach number for ideal expansion of the primary, the less the amount of unused energy that is available to be transferred to a secondary fluid.

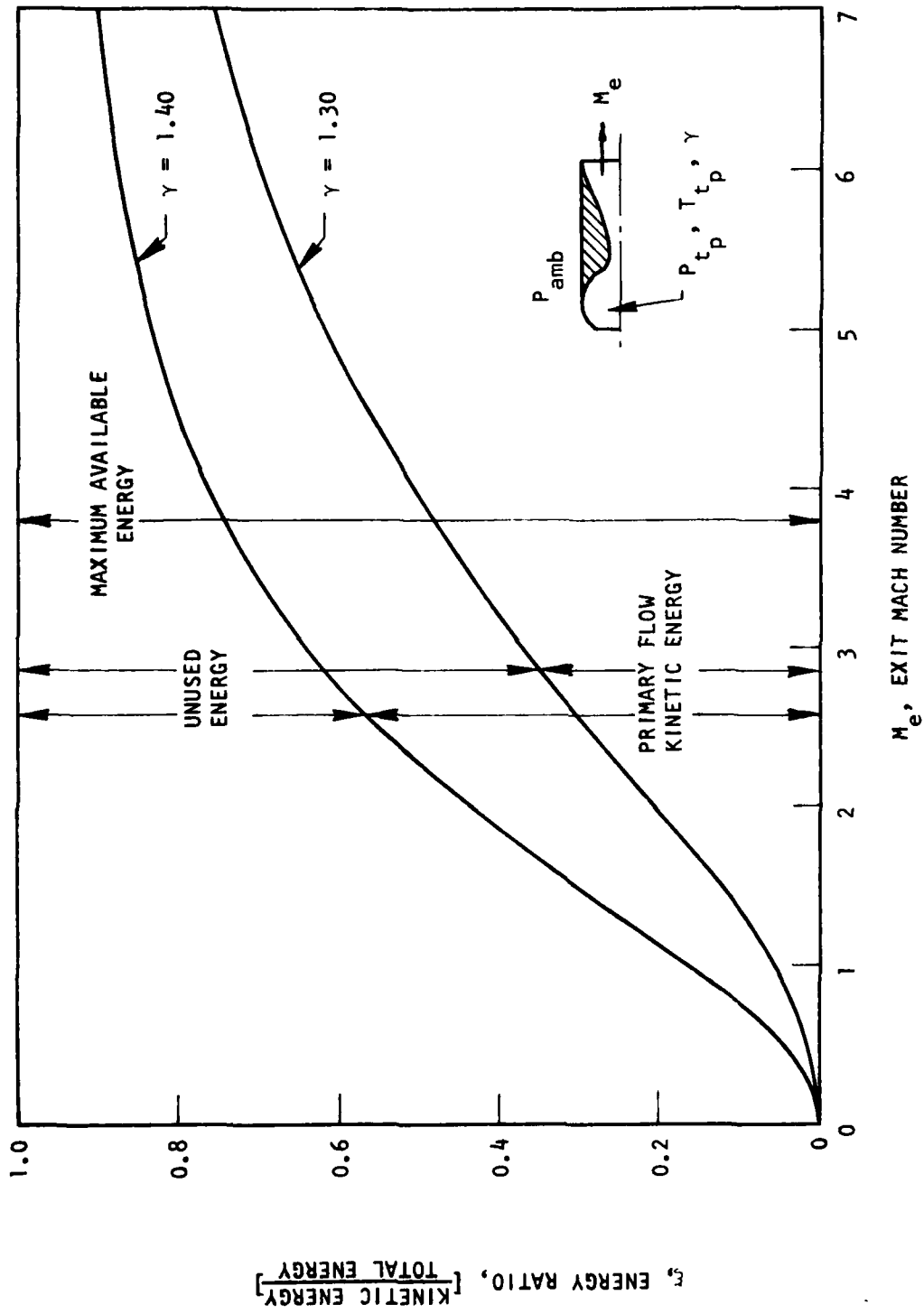


FIGURE 7. TOTAL ENERGY CONVERSION COMPARISON.

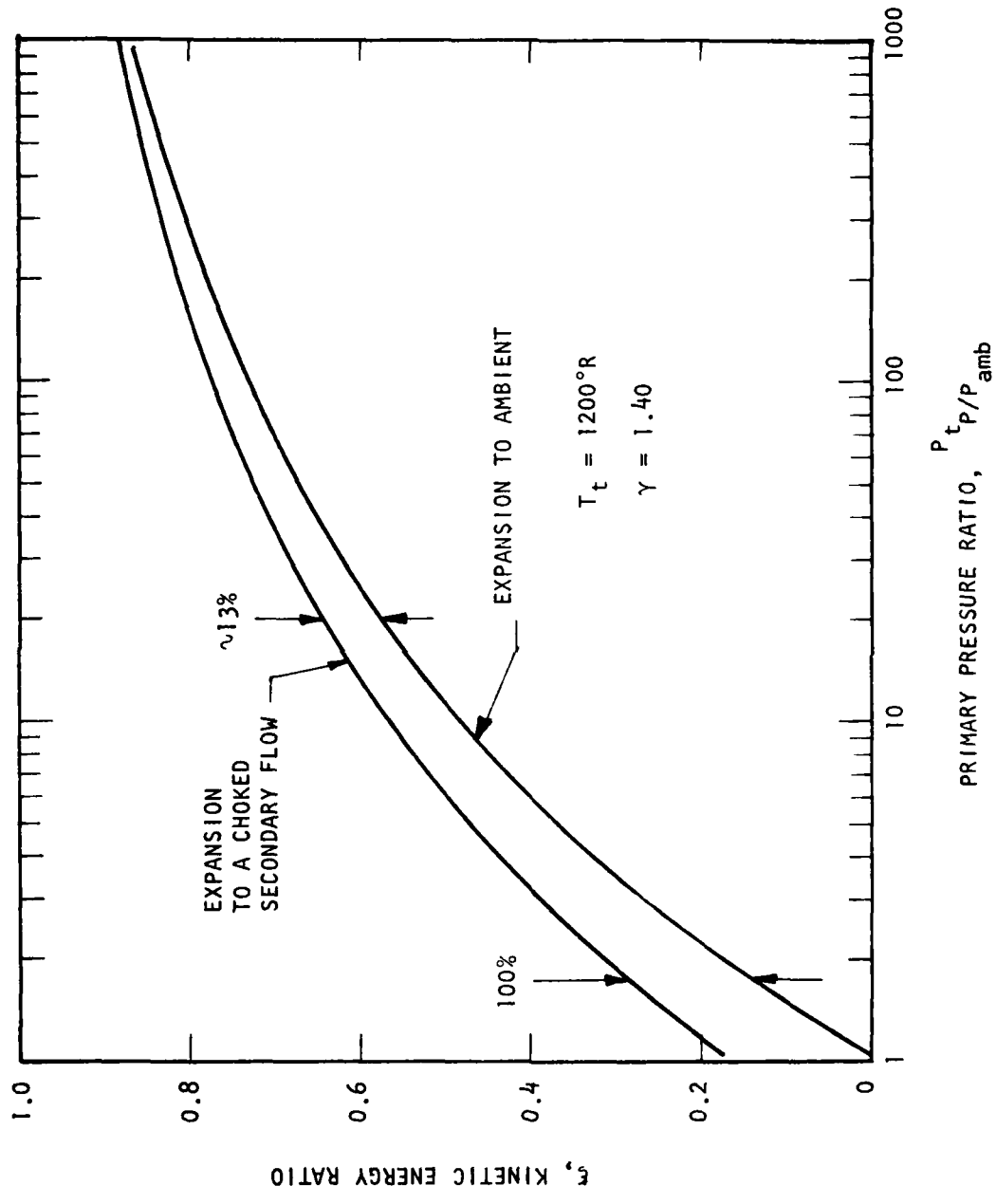


FIGURE 8. KINETIC ENERGY CONVERSION FOR PRIMARY NOZZLE FLOW WITH $\gamma = 1.40$.

As implied in the foregoing paragraphs, improvements in primary nozzle kinetic energy conversion may be achieved by shrouding the nozzle and inducing a secondary flow. The physical enclosure of the primary nozzle enables secondary flow to be induced, lowering the primary nozzle static back pressure below ambient due to local (secondary) velocity effects. The boundary condition for the maximum thrust per throat area parameter of the primary nozzle is consequently changed. Even though the nozzle exit pressure is less than ambient, the primary flow still senses this as an "ambient" condition. Lower exit static pressures permit a greater energy conversion from state to kinetic energy for the primary flow. The system can still achieve exhaust to ambient conditions at the shroud exit through the mixing process of the primary and secondary flows. The thrust performance of a shrouded primary is determined by the exhausting mixed flow properties; however, the primary nozzle is operating at a higher level of energy conversion. Examples of the improvement in primary flow energy conversion for the case where the secondary flow reaches sonic conditions at the primary nozzle exit plane are given, in Figures 8 and 9, for specific heat ratios, γ , of 1.4 and 1.13, respectively. For both gases at a nozzle stagnation to ambient pressure ratio near 1.80, the primary kinetic energy ratio, ξ , at the nozzle exit for expansion to the reduced static pressure caused by secondary flow choking is twice the value for an isolated primary expanding to ambient static pressure. An increase in primary pressure ratio decreases the maximum achievable gain in kinetic energy conversion since it represents a condition closer to the theoretical "vacuum" case for either value of γ . At a pressure ratio of 20, the maximum gain in performance is approximately 14% for both $\gamma = 1.4$ and $\gamma = 1.13$ over the baseline isolated nozzle.

It is important to note here that the improvement shown in thrust performance is due to the kinetic energy conversion of the total available energy of the primary nozzle alone. For an ejector with a primary nozzle and nozzle and shroud combination where the initial secondary total energy state is the same as that ambient state to which the mixed flow exhausts, no greater improvement in thrust performance is possible. The maximum static augmentation ratio achievable for an ejector can thus be expressed as $\phi_{\max} = 1.0/\sqrt{\xi}$, which is related to the primary stagnation to ambient pressure ratio as shown in Figure 10.

In order to illustrate the foregoing formulation for ϕ_{\max} , the results of numerous experimental investigations were examined. These results include steady

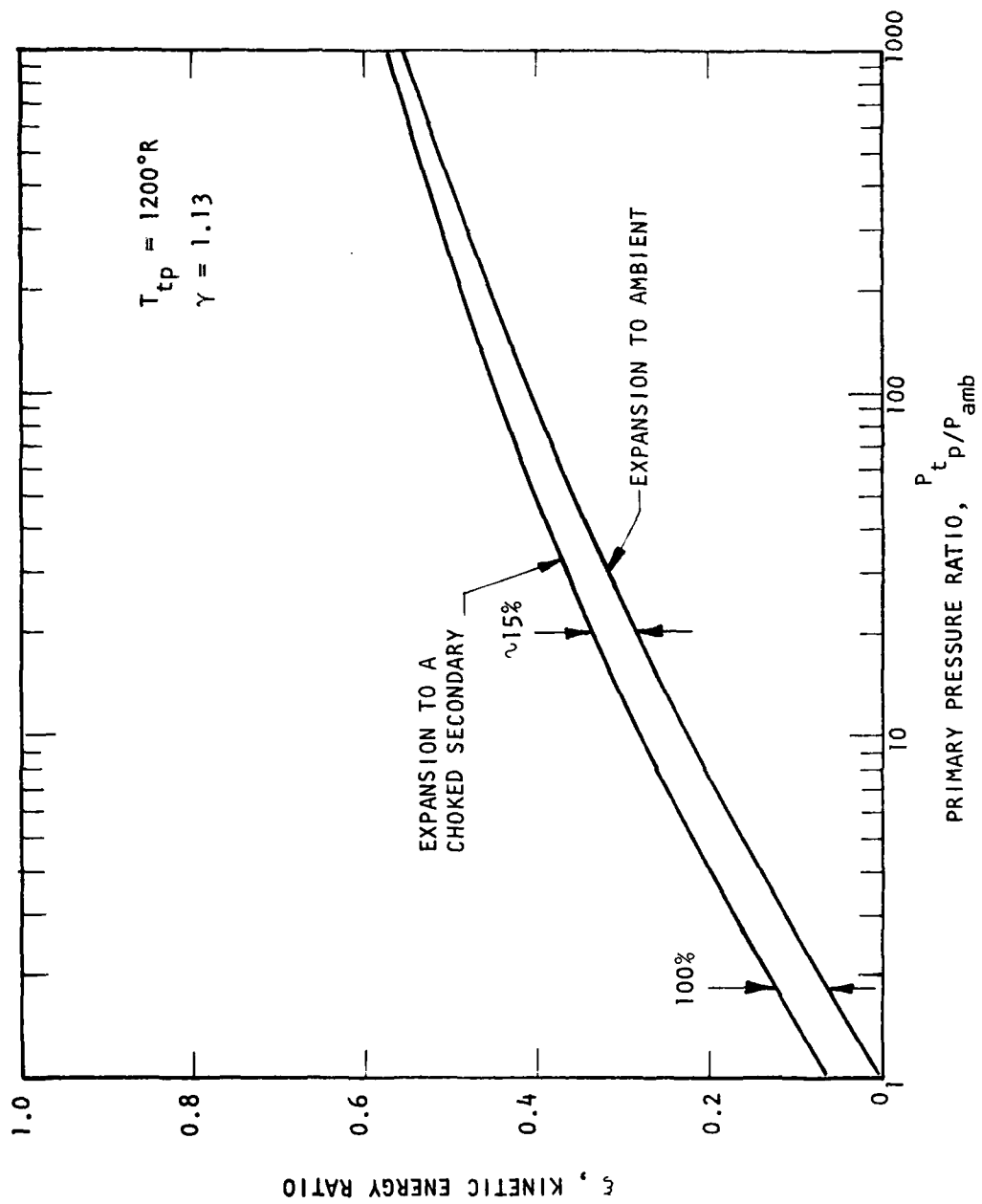


FIGURE 9. KINETIC ENERGY CONVERSION FOR PRIMARY NOZZLE FLOW WITH $\gamma = 1.13$.

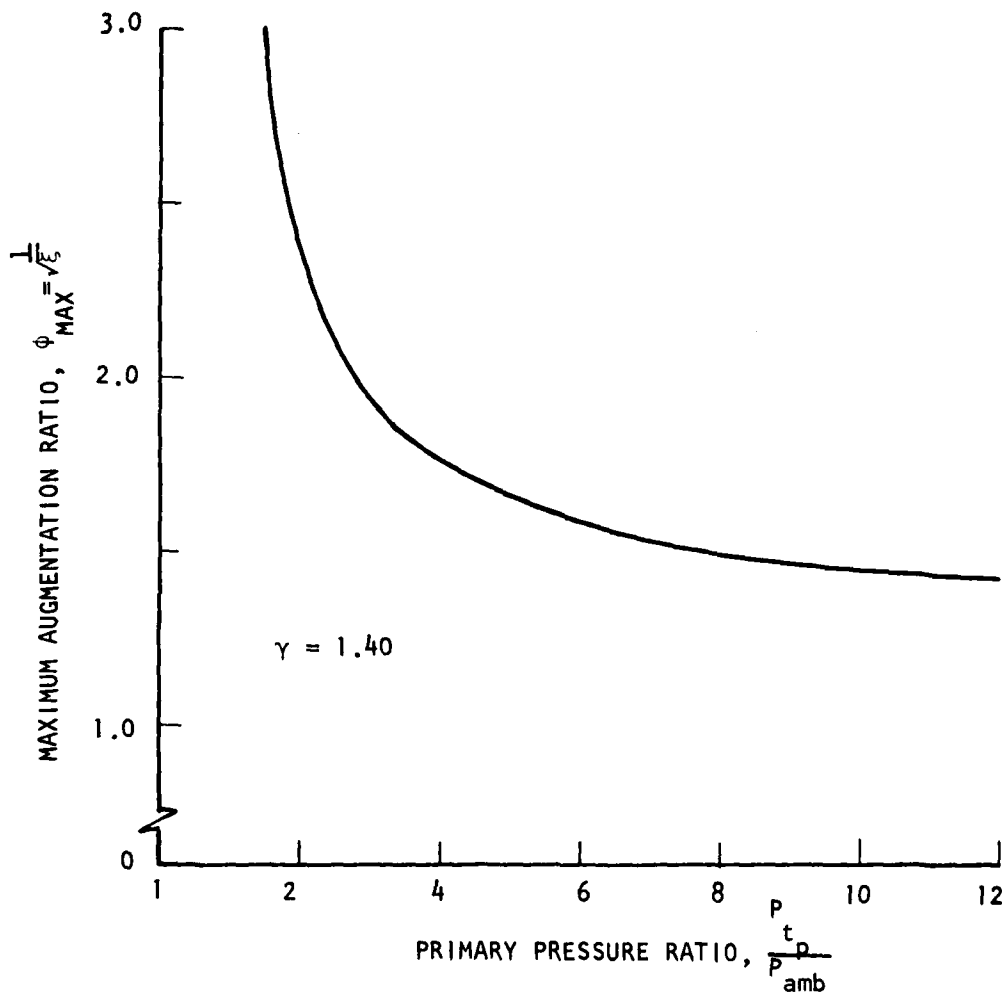


FIGURE 10. THRUST AUGMENTATION RATIO AS A FUNCTION OF PRIMARY FLOW KINETIC ENERGY CONVERSION RATIO, ξ .

state devices with mass flow ratios up to values of $\beta = 30$ and area ratios, A_e/A_p' , as high as 400, as well as non-steady augmentors and devices utilizing various forms of flow control - hypermixing and Coanda nozzles, BLC diffusers, etc. Figure 11 shows the results of this examination. In general, as indicated in Figure 11, the best results of all data available approached a limiting value of $\sim .9 \phi_{MAX}$ for all primary pressure ratios, independent of other initial or configuration parameters.

2.2 FUNDAMENTALS OF INDIVIDUAL PHYSICAL PROCESSES

Although the state of the art of ejector augmentor technology is such that an integrated understanding of the fundamental physics of the flows is currently not available, it is nevertheless possible to piece together isolated parts of the puzzle to form an almost coherent picture. Many of these parts are provided from experimental results for ejector pumps. Others come from well-known inlet, diffuser, or nozzle results for such varied phenomena as boundary layer growth and separation, supersonic plume/shock patterns, shear interactions between co-flowing streams, etc. While each individual physical phenomenon may be significant to the design and performance of an ejector augmentor, the nature of the device is such that the interaction between primary and secondary flows provides the key whereby the importance of the associated phenomena can be determined. The interaction phenomenon itself, however, is but poorly understood, and the relationships and importance of various types of transfer mechanisms are but ill-defined. Although this state of understanding is at first discouraging, it is not unlike other areas of propulsion technology, such as turbulent combustion: from a pragmatic point of view it works, from a scientific point of view it needs to be better understood to make it work better.

In the following section, the fundamental mechanisms of energy and momentum transfer between fluids, as currently understood in their relationship to ejector augmentor flow interactions, are discussed. In Section 2.3, the influence of these phenomena on associated component performance is considered, and in Section 2.4, a brief summary of the current understanding of the fundamental physics of ejector augmentor flows is presented.

2.2.1 The Interaction Phenomenon

As pointed out above, the "interaction phenomenon" is in reality an amalgam of various types of fluid transfer mechanisms. In a general formulation of these

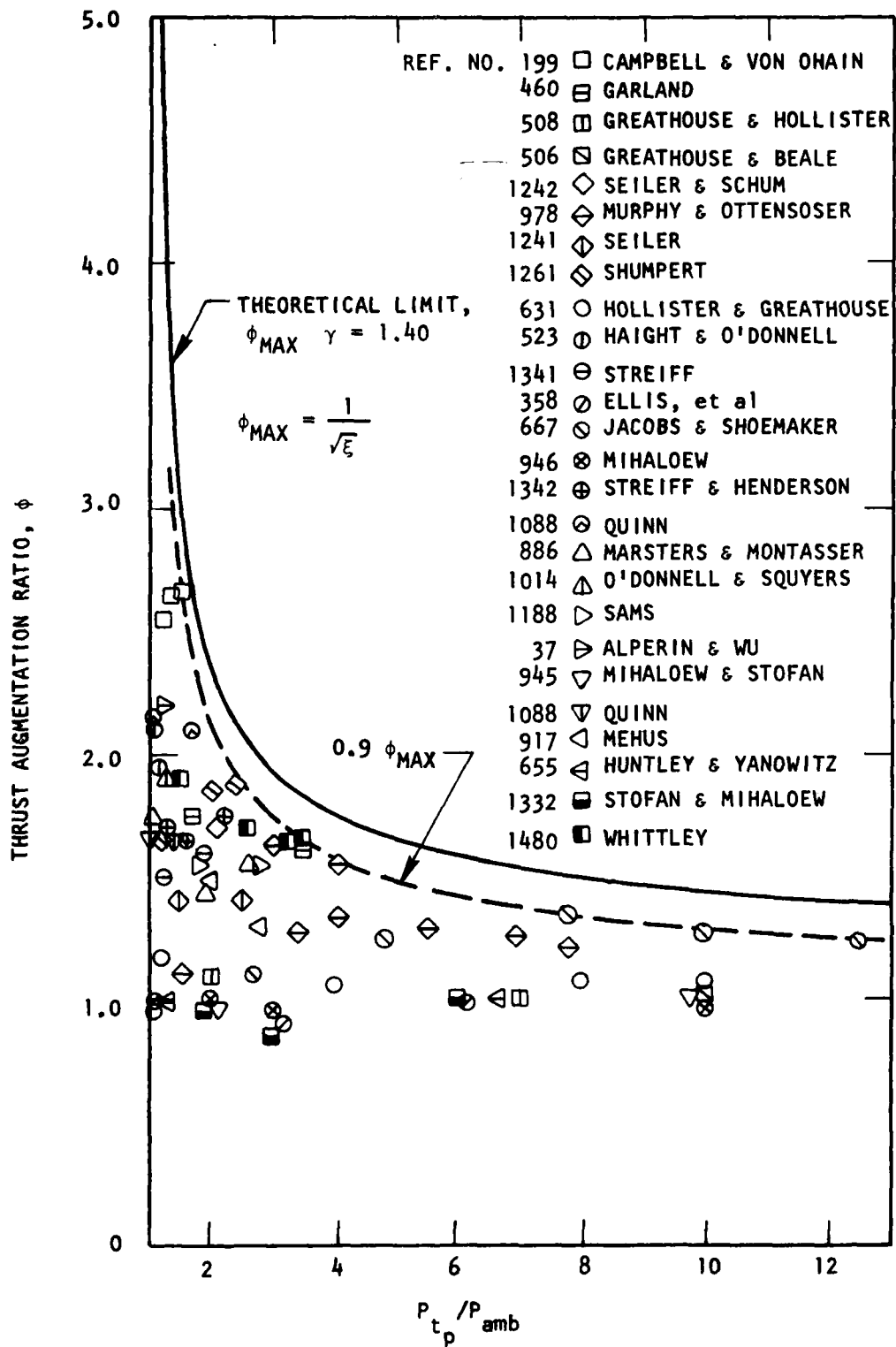


FIGURE 11. EJECTOR THRUST AUGMENTATION RELATIVE TO COMPLETE PRIMARY JET ENERGY CONVERSION.

mechanisms as given for instance by references 900 and 1511, exchange of momentum between flows may be defined in terms of (1) the (non-viscous) pressure forces acting on a fluid element per unit volume, and (2) the viscous forces acting on a fluid element per unit volume. Thus, for the x-direction, ignoring body forces (i.e., gravity, inertial and electromagnetic forces), the momentum equation may be written with the help of the continuity equation as:

$$\rho \frac{\partial v_x}{\partial t} + \rho v_x \left(\frac{\partial v_x}{\partial x} + \frac{\partial v_y}{\partial y} + \frac{\partial v_z}{\partial z} \right) = - \frac{\partial p}{\partial x} + \left(\frac{\partial \tau_{xx}}{\partial x} + \frac{\partial \tau_{xy}}{\partial y} + \frac{\partial \tau_{xz}}{\partial z} \right) \quad (22)$$

where the general stress tensor, τ_{ij} , has been separated into viscous and non-viscous terms as:

$$\tau_{ik} = -p\delta_{ik} + \tau_{ik} \quad (23)$$

and δ_{ik} is the Kronecker delta. The first term on the left hand side of (22) represents a rate of increase of momentum due to non-steady conditions, and the second term the rate of momentum increase due to convection. The first term on the right hand side represents a (equivalent) non-viscous pressure force acting on a fluid element, and the second set of terms give the rate of momentum gain due to viscous transfer. All terms are per unit volume. The basic momentum transfer mechanisms are thus seen to be the pressure and viscous stresses, but these may be influenced by, or may even cause, a non-steady velocity.

The exchange of energy between two flows may also be described in a general sense by writing the energy balance for a fluid element. When this is done, the energy equation, again neglecting body terms, looks as follows:

$$\begin{aligned} \frac{\partial \rho h_t}{\partial t} + \left[\frac{\partial \rho}{\partial x} (v_x h_t) + \frac{\partial \rho}{\partial y} (v_y h_t) + \frac{\partial \rho}{\partial z} (v_z h_t) \right] \\ = \frac{\partial p}{\partial t} - \left[\left(\frac{\partial}{\partial x} q_x + \frac{\partial}{\partial y} q_y + \frac{\partial}{\partial z} q_z \right) \right] \\ + \left[\frac{\partial}{\partial x} (\tau_{xx} v_x + \tau_{xy} v_y + \tau_{xz} v_z) + \frac{\partial}{\partial y} (\tau_{yx} v_x + \tau_{yy} v_y + \tau_{yz} v_z) \right. \\ \left. + \frac{\partial}{\partial z} (\tau_{zx} v_x + \tau_{zy} v_y + \tau_{zz} v_z) \right] \end{aligned} \quad (24)$$

where h_t is the total enthalpy level per unit mass of the fluid element,

$$h_t = (v^2/2 + e + p/\rho) \quad (25)$$

e is the internal energy, and q is the heat flux vector which describes the quantity of heat which flows through the element per unit time through a unit area. The terms on the left hand side of equation (25) represent the rate of gain of energy per unit volume due to non-steady and convective effects, respectively. These terms, by virtue of equation (25), include work done by non-viscous pressure forces. The non-steady, non-viscous pressure term appears by itself on the right hand side of equation (24). The two bracket terms on the right hand side of equation (24) represent the rate of energy input to the fluid element per unit volume by conduction and the rate of work done by viscous forces on the element per unit volume, respectively. It is interesting to note that for two flows with unequal temperatures, the heat conduction terms must be included in any model of the energy transfer process.

From the foregoing, it can be seen that the interaction phenomenon is comprised of both steady and non-steady terms and that these are related to forces which can be expressed in terms of non-viscous pressures, compressive stresses (τ_{xx} , τ_{yy} , τ_{zz}), and shear stresses (τ_{xy} , etc.). Two distinct types of interaction can be formulated from the momentum and energy equations: Case (1): An interaction in which the non-viscous pressures predominate, and the viscous stress terms are negligible, and Case (2): An interaction where the viscous stress terms predominate.

Case (1) can be qualitatively likened to the momentum and energy exchange which occurs when a shock propagates into quiescent fluid in a shock tube. It is typified by non-steady boundary conditions as well as the non-steady character of the interaction. It can be shown¹⁰⁹³ that for weak compression waves of this type (i.e., a shock Mach number, M_s , approaching 1.0), the process is quite efficient; the pressure rise is proportional to $(M_s^2 - 1)$ while the entropy increase vanishes with $(M_s^2 - 1)^3$. This is a key factor to the apparent success of various non-steady flow devices such as Foa's rotary jet flow augmentor.⁴¹⁶

A qualitative picture of the Case (2) type of interaction can be gained by first considering the classical Rayleigh problem of a flat plate, initially at rest in a fluid which is also at rest. When the plate is set impulsively into motion in its own plane, viscous stress between the plate and the fluid, as well as between infinitesimal layers of the fluid itself, cause motion of the fluid which extends for some distance away from the plate. It can be shown that for

Rayleigh's problem a certain amount of vorticity is produced initially and spreads into the fluid. In the ejector augmentor, viscous stresses between the primary and secondary fluid boundaries similarly produce motion of the secondary fluid. Vorticity is also produced and a turbulent shear flow results at the boundaries. Existence of the turbulent fluctuations results in pronounced mixing, and while the boundary conditions for this kind of ejector flow are steady, hence the term "steady-state mixing", the interaction itself is necessarily non-steady. For some conditions, the vortical motion produced at the boundaries of primary and secondary flow may be intermittent or periodic in nature and result in a macroscopic engulfing of the secondary flow by the primary as shown by Brown's & Roshko's experiments.¹⁷⁶ When this occurs, the momentum and energy transfer becomes strongly influenced by the normal force (pressure and compressive stress) terms in equations (22) and (24).

The two cases described above represent extremes which have been used to describe non-steady and steady ejector augmentors. However, for both types of devices, the actual interaction must be some combination of these transfer mechanisms. Thus, in the analysis of the rotary jet augmentor,⁴¹² the flow model hypothesized included "mixing" following the initial interface pressure interaction. It was subsequently shown that the sequence of interface pressure and conventional mixing interaction significantly affects the performance of the device. That is, if mixing occurs first, the coherence of the primary jet is apparently lost and its ability to effectively transfer momentum and energy to the secondary flow through normal force pressures is degraded. The success of the hypermixing nozzles¹⁰⁹⁹ is probably due to a combination of maintenance of the primary jet coherence through the persistence of the vortical flow established by the nozzles, and the macroscopic engulfment by the vortices and the resulting increased influence of normal force terms, as described above.

Turbulent fluctuations in velocity or vorticity also produce effects on the microscopic or molecular level through coupling with fluctuations in the variables of state. One such phenomenon is the generation of sound as reported by Quinn.¹⁰⁸⁷ Generally, the sound field energy level will be small compared with the turbulent energy level, but the spontaneous generation of the sound may be associated with near-optimal interaction conditions and has been observed to occur in supersonic ejector pumps when the terminal shock following the interaction finally becomes properly situated in the throat. Whether externally produced acoustical vibration can beneficially influence the interaction phenomenon is still a matter of conjecture.

2.2.2 Associated Component Phenomena

The interaction between primary and secondary flows is necessarily the most important phenomenon which occurs in an ejector augmentor since without it, there would be no secondary flow induction and thus no thrust augmentation. However, other components of the device also play an important part in the achievement of high performance since they dictate how external boundary conditions are matched and also significantly influence the interaction itself. These components are: the secondary flow inlet, the primary flow nozzle, and the exhaust flow diffuser. The phenomena associated with these components are discussed below:

Secondary Inlet - The major phenomena of interest in the secondary inlet component are (1) the degree of secondary flow non-uniformity and (2) the boundary layer of the secondary flow as it enters the interaction zone. Because the interaction is, for "steady mixing" devices, so strongly influenced by the shear stress terms which are in turn a function of the velocity difference between the primary and secondary flows (although for turbulent flows this relationship is not defined), the secondary velocity as it first comes into contact with the primary - i.e., at the end of the secondary inlet - is an important parameter. The primary jet loses kinetic energy as it progresses through the secondary flow if it is initially at some oblique angle to the secondary flow direction. If an optimal primary/secondary velocity relationship exists for the interaction, then it is necessary to have a non-uniform secondary inlet velocity which maintains this relationship for decreasing primary jet velocities. Even if the primary jet is not issuing at an angle to the secondary flow, its influence as propagated outward by the interaction will tend to decrease, again pointing toward the desirability of a non-uniform secondary inlet velocity. Von Karman¹⁴⁴² showed that a non-uniform secondary velocity assumption would in fact yield higher theoretical values of thrust augmentation ratio through its effect on the formulation of the momentum equation.

The extent to which the interaction penetrates into the secondary flow also affects the maximum useful area of the secondary inlet at the beginning of the interaction zone, and the interaction mechanisms together with other component phenomena establish an optimum secondary flow average velocity or Mach number at this location. The geometry of the secondary inlet should thus be a function of these phenomena, but little theoretical or experimental work has been done to establish the required relationships.

The boundary layer buildup in the secondary inlet is also important, since it can continue to grow through the interaction or mixing section and even into

the diffuser. Boundary layer separation can destroy the efficiency of the interaction and/or the diffuser, resulting in major losses in thrust augmentation. On the other hand, for interactions which occur primarily due to turbulent viscous shear stresses, a secondary flow which is comprised entirely of ingested boundary layer (e.g., from the fuselage of an aircraft) can be energized through the interaction with the primary jet without regard to separation effects. Naturally, the device geometry would be significantly different for the latter case.

Primary Nozzle - Primary nozzle phenomena of major significance are the following: (1) the time-dependent characteristics of the primary jet, (2) the peripheral surface interaction area, (3) the Mach number of the primary jet at the beginning of the interaction zone, and (4) the angle of the primary jet relative to the incoming secondary flow.

The time-dependent nature of the primary flow affects the interaction as described previously in Section 2.2; however, the manner in which non-steady primary flows are generated can affect the performance of an ejector augmentor, since significant losses in flow energy may arise due to the generation technique. Even for steady flow primaries, nozzle losses should be avoided since they decrease the energy available to the interaction.

The peripheral surface area of the primary jet(s) can provide an increased contact or interface area to the secondary flow. The usual way of doing this (and one which has provided demonstrated performance improvements) is by the use of multiple primary nozzles. For example, for a single circular primary jet of area $A = \pi D^2/4$, the peripheral length which comes into contact with the secondary flow, where viscous stresses arise, is simply $P = \pi D$. Now assume that the jet is divided into four smaller circular jets, each of area A' , but with the same total area, $A = 4A'$ (and hence the same primary mass flow, energy, etc.). The diameter of each of the smaller jets will be $D' = \frac{D}{2}$, and the total peripheral contact length for the four jets is $4P' = 4\pi D' = 2\pi D$, twice that of the single jet. The interaction between primary and secondary fluids thus takes place over an extended boundary.

The Mach number of the primary jet may be subsonic or supersonic, depending on the primary flow stagnation conditions and the local primary nozzle exit static pressure. For a primary total pressure greater than or equal to the value required to choke the primary flow, the exit static Mach number is set by the exit to throat area ratio of the primary nozzle. This in turn sets the exit static pressure both for the primary flow and the secondary flow at the entrance to the interaction

zone, and thus the pressure level at which the interaction is initiated. For supersonic primary nozzle exhausts, the exhaust plume characteristics and shock structure are also significant. The plume shape may form a convergent flow "passage" between its boundary and the shroud wall which may result in choking of the secondary flow within the interaction region, and shocks within the primary plume can decrease the energy available for interaction with the secondary flow.

The angle at which the primary jet issues into the secondary flow relative to the secondary velocity determines the bulk or mean flow properties used in equations (22) and (24). This angle may be due to geometric alignment of the primary jet or to the characteristic primary plume boundary, or both. The primary jet angle also determines the extent to which the interaction penetrates into the secondary flow, as well as the efficiency of the interaction (For instance, a primary jet directed normal to the desired secondary flow direction would be highly inefficient). Depending upon the strength of the primary jet, the incidence angle may result in impingement on the shroud walls and a subsequent loss of momentum and energy available to transfer to the secondary flow.

Exhaust Flow Diffuser - The phenomena of major significance with regard to the exhaust flow diffuser are: (1) the satisfaction of external (ambient or local) boundary conditions, specifically exit static pressure, (2) boundary layer growth and possible separation, and (3) continuation of primary/secondary interactions within the diffuser.

For maximum ejector augmentor thrust with supersonic exhaust flow the diffuser exit static pressure should be equal to the ambient static pressure.⁹⁷⁸ For subsonic exhaust flow, the ambient static pressure imposes this boundary condition, except for certain situations such as the so-called "jet flap diffuser" which provides forced boundary conditions different from ambient at the exit. The static pressure gradient which can be accommodated through the diffuser establishes, because of these boundary conditions, the static pressure at the end of the interaction zone. For ejector augmentors in which the interaction takes place at constant static pressure ("constant pressure mixing"), the diffuser thus ideally establishes the static pressure at the entrance to the interaction zone, and thus the secondary flow Mach number (and for a specified secondary inlet area, the mass flow) at that location. Other types of interactions are similarly influenced, so that the static pressure gradient through the interaction will provide a match with the static pressure at the entrance to the diffuser. The diffuser thus ideally provides a powerful influence on the interaction itself, the mass flow entrainment, and thus the overall device performance.

In order to provide the foregoing effects, the diffuser must operate efficiently. Inefficient operation may arise, however, if boundary layer growth in the presence of the diffuser's adverse pressure gradient is too large, and separation occurs. If boundary layer separation does occur, the ejector thrust augmentation is severely degraded.

As with the other ejector components, the diffuser phenomena cannot really be separated from the interaction process. Continuation of the interaction within the diffuser can occur, and whether this is beneficial to the overall device performance depends on a variety of complex factors. From these, the question of whether an efficient interaction can be sustained in the presence of an adverse pressure gradient arises, and similarly, whether the primary jet coherence can be maintained for a sufficient length to enable interaction within the diffuser to take place. The answer to the latter, based on hypermixing nozzle experiments, is apparently yes. However, even for hypermixing nozzles many questions concerning the best combination of interaction zone length and diffuser length, the effects of initial primary stagnation conditions (which may set the total length required for the interaction), the effects of flow skewness and asymmetric diffusion, etc., remain unanswered. Efficient interaction continuing in the diffuser is desirable since it enables a shorter total length for the ejector augmentor, but it is currently not a well-validated phenomenon.

2.3 SUMMARY OF FUNDAMENTALS OF EJECTOR FLOWS

The ejector augmentor represents a complete propulsion system with processes directly analogous to the inlet compressor, combustor, turbine and nozzle of a turbojet engine. It has an inlet, the (secondary) flow undergoes compression and energy addition (by interaction with the primary), energy to drive the process is obtained through an expansion process (of the primary), and the flow is exhausted through a nozzle/diffuser to obtain thrust. In further analogy to the turbojet engine, proper matching of the ejector augmentor components is critical to achieving high performance. In the ejector, however, the compressor-combustor-turbine processes all take place at once in one highly complex process; the interaction phenomenon. Proper matching between these "components" necessitates an understanding of how the interaction phenomenon works. This understanding is currently limited to a general description of the interaction phenomenon as provided by the steady and non-steady forms of the conservation equations, which relate the momentum and energy transfer to normal, "interface", pressure forces and viscous stress forces. The manner in which these forces arise, in the interaction between two flows, is not well-understood, and their relative magnitudes can be described currently only through empirically determined flow models.

Out of relevant experiments and complementing the general theoretical descriptions of the interaction phenomenon, however, have come some qualitative insights which have enabled the formulation of improved ejector augmentors. One such example is the advent of the hypermixing nozzle, which produces a vortical flow structure that apparently enhances the normal pressure and stress force-exchange between the primary flow and enables the interaction to be continued in the diffuser section, thereby achieving improved performance in a more compact device.

3.0 THEORIES OF OVERALL DEVICE PERFORMANCE

3.1 GENERAL BACKGROUND

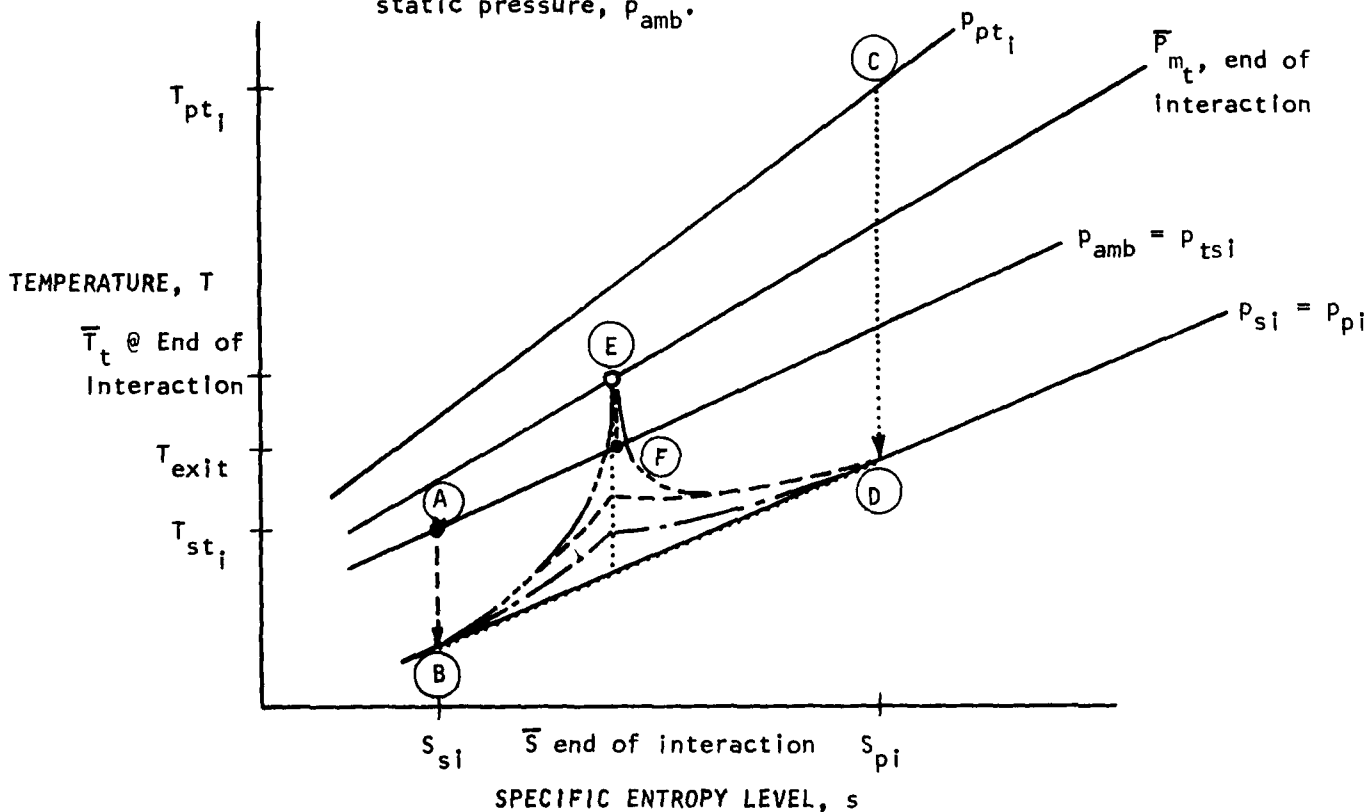
In the discussion of the fundamental physics of ejector flows in the preceding section, it was convenient to utilize the equations of motion written for a unit volume element in order to describe the interaction phenomena. Equations of this type can, of course, be utilized to determine the overall device performance through application of finite element techniques in which mass, momentum, and energy are conserved for discrete elements of the flow within the device. To do so requires phenomenological models for various terms of the equation; e.g., τ_{xy} must be defined as a function of μ and $\frac{dv}{dy}$. In this section, such an approach and other approaches which utilize specific phenomenological models to describe what happens within the ejector will be grouped under the category: "Physical Phenomena Approach." A second category of theories for overall device performance relies on application of the conservation of mass, momentum, and energy to the bulk flow properties, i.e., the conservation equations are applied between the upstream or interaction-entrance section and the interaction zone exit, with little regard for what takes place physically in between. Inlet and diffuser performance calculations are made on the basis of the resulting interaction entrance and exit conditions. Similar approaches may utilize loss factors or specify skewness conditions at the inlet or exit, etc., but these make little or no attempt to describe mathematically the mechanism whereby these conditions arise. This second category, including the approaches which introduce some corrective terms, such as friction losses, will be called: "Control Volume Approach" in this section.

In both types of approach, certain boundary conditions must be specified, such as: (1) interaction within a constant area section, (2) interaction which takes place at a constant static pressure, (3) whether the ejector has a diffuser, etc. In general, the control volume approach is considerably more constrained by the specification of boundary conditions since its chief feature of merit is in the simplicity of solution it provides, and complex boundary conditions negate this simplicity. On the other hand, the physical phenomena approach may suffer because of emphasis on a phenomenological model which has only minor bearing on the device performance, because of poor specification of the boundary conditions or unknown interaction effects.

In considering theoretical approaches to overall device performance, the question "What does ideal performance mean for an ejector augmentor?", frequently

PROCESSES ON THE T-s DIAGRAM:

- ① (A) to (B) is isentropic expansion of the secondary flow in the secondary inlet to static pressure p_{si} .
- ② (C) to (D) is isentropic expansion of the primary flow in the primary nozzle to a static pressure $p_{pi} = p_{si}$.
- ③ (B) & (D) to E is the "isentropic" interaction between the primary and secondary, in which the primary loses heat, $\Delta S_p < 0$.
- ④ (E) to (F) is the isentropic expansion of the flow to the exit static pressure, p_{amb} .



BY DEFINITION:
$$\frac{s_{pi} + \beta s_{si}}{(1 + \beta)} = \bar{s} \text{ end of interaction}$$

BY CONSERVATION OF ENERGY:
$$\frac{T_{pt} + \beta T_{st}}{(1 + \beta)} = \bar{T}_t \text{ end of interaction}$$

This establishes point (E) and the value of \bar{P}_{mt} at end of interaction for the ideal or isentropic process.

FIGURE 12. PROCESS DESCRIPTION FOR AN IDEAL EJECTOR AUGMENTOR

arises. It is possible to show on the basis of a temperature-entropy (T-s) diagram, such as that of Figure 12, and the conservation of energy, what an ideal, isentropic process would look like for an ejector augmentor. In Figure 12, it has been defined that the mass average specific entropy at the end of the interaction, \bar{s}_e , is equal to the mass averaged value for the two flows prior to the interaction. The boundary conditions and the nature of the interaction phenomena required to obtain this ideal process are not defined, and indeed it may be that they do not exist (although as mentioned earlier in Section 2.2, certain non-steady wave phenomena may approach this condition). In this regard, the ideal ejector augmentor is much like the ideal compressor or turbine. Some arguments have been proposed to the effect that the steady state "mixing" ejector cannot be even theoretically isentropic. These are usually based on the irreversibility of certain stress-related terms in the equations of motion (Equations (22) and (24) of Section 2.2).^{900,1511} However, they apply with equal validity to the "far-field" flow of conventional compressors and turbines -- i.e., that fluid which does not come into direct contact with the compressor or turbine blades. The degree of isentropicity or "ideal-ness", then, is intimately related to the nature of the interaction. It should also be noted that "ideal" control volume approaches which apparently do not consider the nature of the interaction may also result in a non-isentropic solution through specification of boundary conditions in the formulation of the momentum equation -- i.e., constant pressure or constant area "mixing". In general, although no explicit proof has yet been shown, it appears that for other initial and boundary conditions being equal, the constant pressure mixing formulation results in a lower value for the mass averaged entropy at the ejector exit than does the constant area condition. However, this does not imply that it is the optimum condition.

In the following Sections, 3.2 and 3.3, some of the specific formulations which have been developed for the two approaches "Control Volume" and "Physical Phenomena", respectively, will be described, and in Section 3.4, a brief summary will be provided of the state of the art for these theories of overall device performance.

3.2 CONTROL VOLUME APPROACH

The control volume approach is most easily described for a one-dimensional analysis, such as that of Keenan, Neumann and Lustwerk.⁶⁹⁸ For the simplest forms of such an analysis the primary nozzle and secondary inlet processes are assumed

to be isentropic, as is the exit diffuser process. The governing equations are then the bulk conservation equations (mass, momentum, and energy) for the interaction process, which is specified as either constant pressure or constant area mixing. Schematics of the corresponding ejector devices are shown in Figures 13 a&b. For the case of zero shear forces at the walls, primary and secondary fluids with the same values of molecular weight, specific heat at constant pressure, and ratio of specific heats the form of the continuity, momentum, and energy equations defining the mixing process for thermally and collisionally perfect fluids thus becomes, respectively:

$$\dot{m}_{s_i} + \dot{m}_{p_i} = \dot{m}_{T_e} \quad (26)$$

$$\dot{m}_{s_i} v_{s_i} + \dot{m}_{p_i} v_{p_i} + (P_{m_i} - P_{m_e}) A_e = \dot{m}_{T_e} v_e \quad (27)$$

$$\dot{m}_{s_i} \left(T_{s_i} + \frac{v_{s_i}^2}{2gJc_p} \right) + \dot{m}_{p_i} \left(T_{p_i} + \frac{v_{p_i}^2}{2gJc_p} \right) = \dot{m}_{T_e} \left(T_{m_e} + \frac{v_e^2}{2gJc_p} \right) \quad (28)$$

For known values of the initial stagnation properties, P_{ts} , T_{ts} , P_{tp} , and T_{tp} and the areas at the inlet to the mixing section, A_{s_i} and A_{p_i} , specification of the static pressure, P_{m_i} , at the entrance to the mixing section is equivalent to specifying the primary and secondary mass flows, \dot{m}_{p_i} and \dot{m}_{s_i} , and by equation (26) the total mass flow, \dot{m}_{T_e} . The perfect gas relation, written as $P = \frac{\dot{m}}{Av} RT$, provides the third equation necessary to solve equations (27) and (28) for v_e , T_{m_e} , and either A_e for the constant pressure mixing case, or P_{m_e} for the constant area mixing case.

Since the inlet and exit diffuser processes are assumed to be isentropic, the overall performance can be easily determined by rewriting the momentum equation across the total device. The augmentation ratio for expansion to ambient static pressure at the diffuser exit plane thus becomes:

$$\phi = \frac{\dot{m}_{T_e} (v_{\text{exit}} - v_o)}{\dot{m}_p (v_p' - v_o)} \quad (29)$$

where the denominator of equation (8) is the net thrust of the primary flow for ideal expansion to ambient static pressure, and the numerator is the total

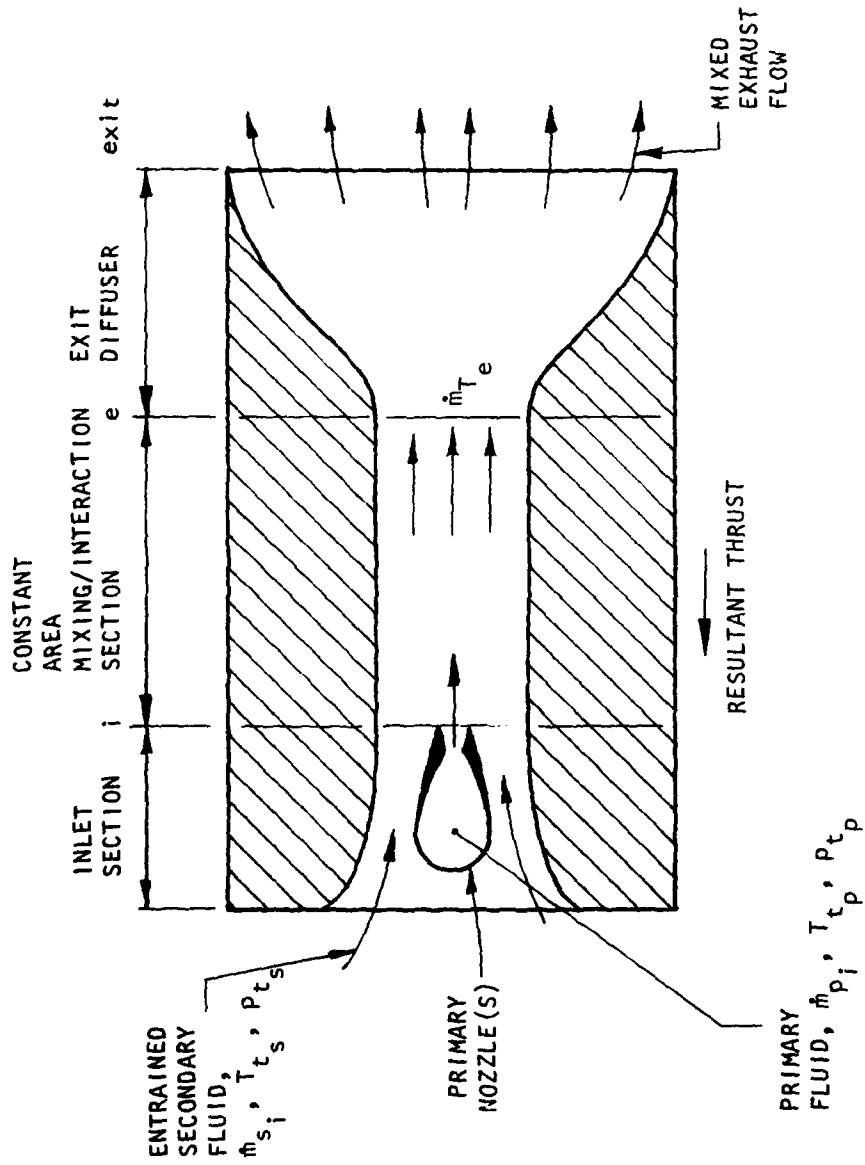


FIGURE 13a. CONSTANT AREA MIXING THRUST AUGMENTING EJECTOR SCHEMATIC

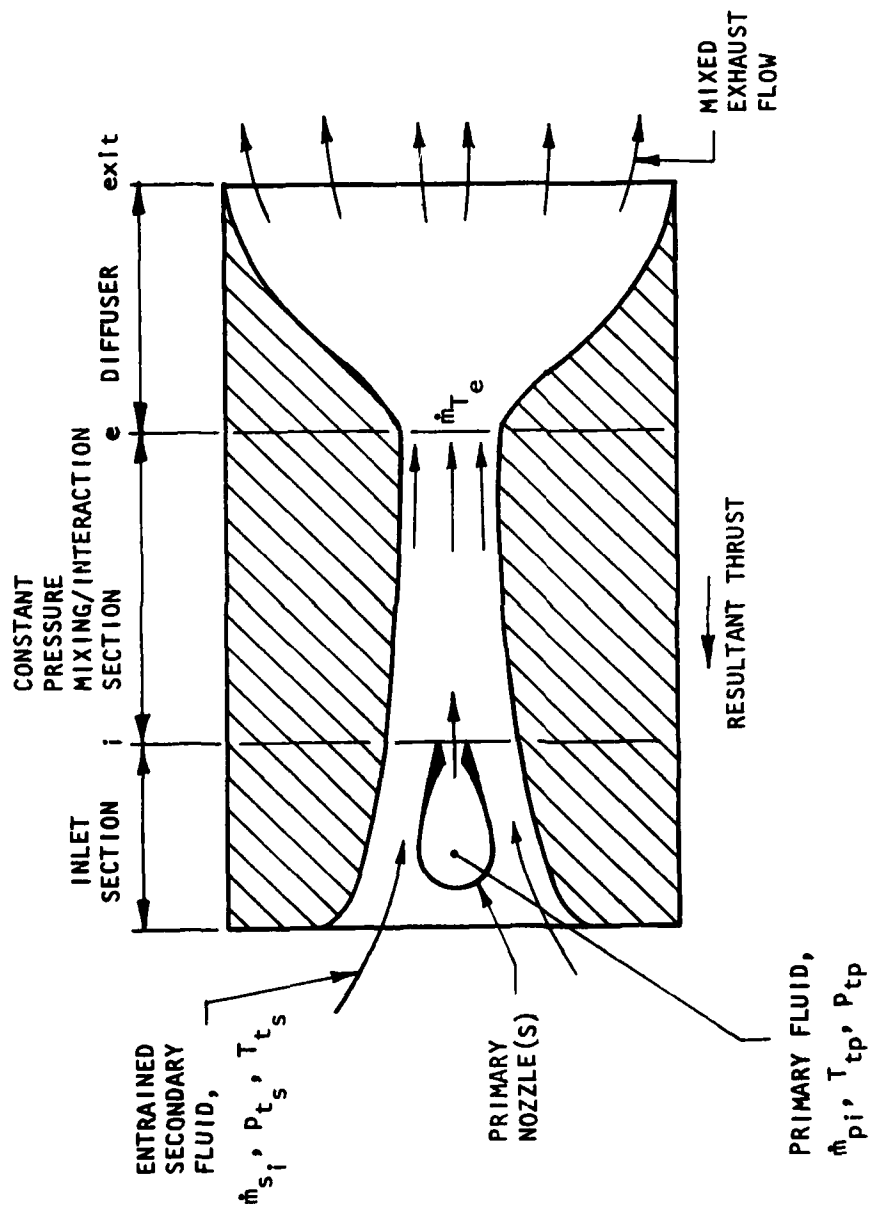


FIGURE 13b. CONSTANT PRESSURE MIXING THRUST AUGMENTING EJECTOR SCHEMATIC

ejector net thrust for expansion to ambient static pressure. The diffuser exit velocity, v_{exit} , is simply determined from the local isentropic relationships based on static to total property ratios at the end of the mixing section and the exit of the diffuser (e.g., T_{me}/T_{tme} and P_{amb}/P_{tme} , respectively).

Various techniques of correcting the predicted performance for the control volume approach have been applied. Among these, perhaps the simplest is that used by Keenan, Neumann and Lustwerk⁶⁹⁸ for constant pressure mixing devices. In this technique, the mass flow ratio, \dot{m}_s/\dot{m}_p , and the total pressure ratio, P_{tme}/P_{ts} , at the exit of the device are reduced by constant factors, i.e.:

$$\left[\frac{\dot{m}_s}{\dot{m}_p} \right]_{\text{corrected prediction}} = K \left(\frac{\dot{m}_s}{\dot{m}_p} \right)_{\text{control volume theory}} \quad (30)$$

and

$$\left[\frac{P_{tme}}{P_{ts}} \right]_{\text{corrected prediction}} = K \left(\frac{P_{tme}}{P_{ts}} \right)_{\text{control volume theory}} \quad (31)$$

where K is less than one. The performance can then be calculated for an exit velocity based on the corrected total pressure and the corrected exit mass flow. Performance so calculated is what would then be predicted for a device having the originally determined geometry.

More sophisticated correction techniques have been applied by others, notably Nagaraja, Hammond and Graetch,⁹⁸⁵ and Quinn.¹⁰⁹⁵ These techniques utilize corrective terms in the momentum equation to express various loss mechanisms affecting the performance. Thus, equation (27) might be expressed as:

$$\begin{aligned} \dot{m}_{s_i} \beta_{s_i} v_{s_i} + C_v \dot{m}_{p_i} v_{p_i} + (P_{m_i} - P_{m_e}) A_e - \tau \\ = \beta_e \dot{m}_{T_e} v_e \end{aligned} \quad (27a)$$

where β_{s_i} and β_e represent velocity skewness factors describing nonuniform velocity profiles for the secondary and mixed flow, respectively, C_v is the velocity coefficient for the primary nozzle, and τ represents a frictional force acting on the fluid at the wall. Generally, the correction terms are not applied to the continuity or energy equations, except indirectly through the

simultaneous solution of the equation set. The values used for the correction terms are empirically determined and are generally configuration dependent, and thus only applicable to geometrically similar devices. Little is known about scale effects on the correction term values.

3.3 PHYSICAL PHENOMENA APPROACH

Perhaps the best example of the physical phenomena approach is provided by the finite-difference flow model of Hedges and Hill.⁵⁶⁵ In this model, shown schematically in Figure 14, the interaction/mixing zone is characterized by several distinctive regions: (1) Secondary and primary fluid potential flow "core" regions, (2) Wall boundary layer and primary jet secondary shear layer regions, and (3) A downstream regime of developing flow.

The basic forms of the continuity, momentum and energy equations used in reference 199 are two-dimensional, steady, time-averaged, boundary layer types as follows:

$$\bar{\rho} \bar{u} \frac{\partial \bar{u}}{\partial x} - \bar{\rho} \bar{v} \frac{\partial \bar{u}}{\partial y} = \frac{-d\bar{p}}{dx} + \frac{1}{y^\alpha} \frac{\partial}{\partial y} \left[\bar{u} y^\alpha \frac{\partial \bar{u}}{\partial y} - \overline{u'(\rho v)'} y^\alpha \right] \quad (32)$$

$$\begin{aligned} \bar{\rho} \bar{u} \bar{c}_p \frac{\partial \bar{T}}{\partial x} + \bar{\rho} \bar{v} \bar{c}_p \frac{\partial \bar{T}}{\partial y} &= \bar{u} \frac{d\bar{p}}{dx} \\ &+ \frac{1}{y^\alpha} \frac{\partial}{\partial y} \left[y^\alpha \bar{k} \frac{\partial \bar{T}}{\partial y} - \bar{c}_p y^\alpha \overline{(\rho v)'T'} \right] \\ &+ \bar{u} \left(\frac{\partial \bar{u}}{\partial y} \right)^2 - \overline{(\rho v)'u'} \frac{\partial \bar{u}}{\partial y} \end{aligned} \quad (33)$$

$$\frac{\partial x^n}{\partial y} = \bar{\rho} \bar{u} y^\alpha \quad \text{and} \quad \frac{\partial \Psi^n}{\partial x} = -\bar{\rho} \bar{v} y^\alpha \quad (34)$$

where the bars denote time-averaged values, the primes denote instantaneous fluctuating components, $\overline{(\rho v)'u'}$ is the turbulent shear stress, τ , and $\overline{(\rho v)'T'}$ is the turbulent heat transfer, q_T . The constant α has a value of unity for axisymmetric flow and zero for plane, two-dimensional flow. Equations (34) are modified forms of von Mises Transformation¹⁶¹³ to convert the cross-stream variable into the stream function, Ψ , automatically satisfying continuity, and avoiding wall singularities through the use of values greater than one for the exponent, n .

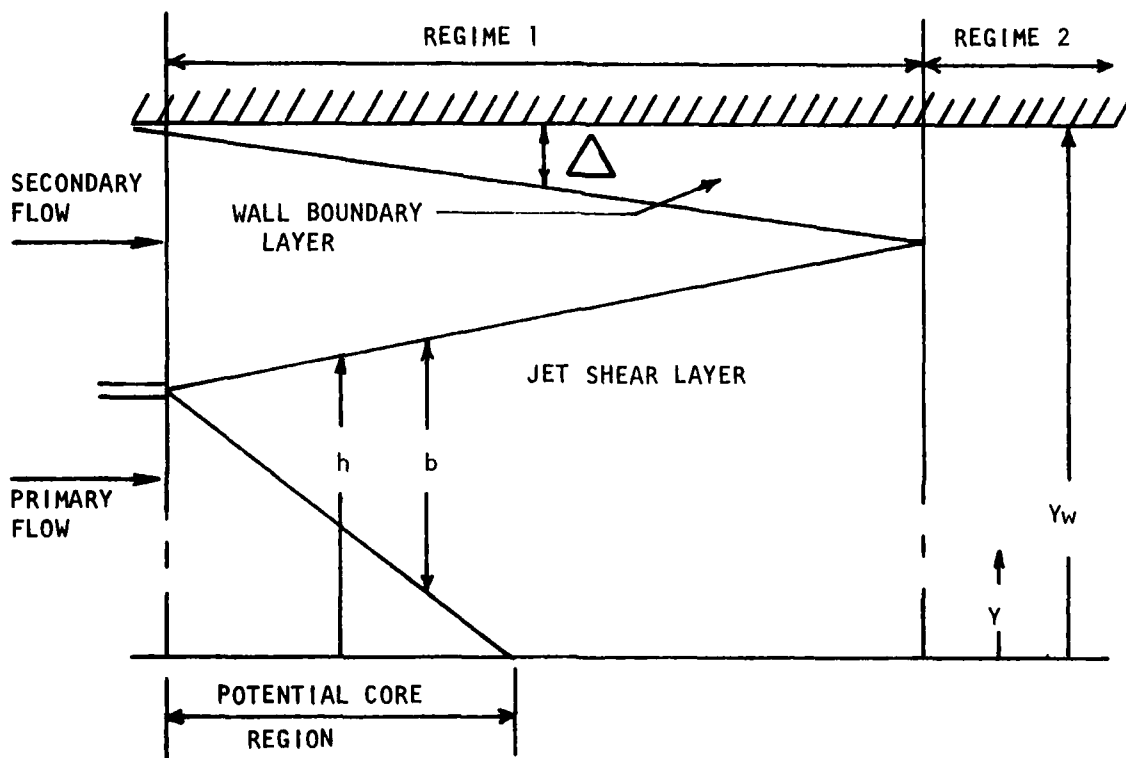


FIGURE 14. SCHEMATIC OF FINITE DIFFERENCE MODEL (FROM REFERENCE 565).

In order to obtain solutions of equations (32) and (33), transformed through use of equations (34), numerous auxiliary relationships and assumptions are required for the specific physical phenomena occurring in each of the flow regions. In particular, the following were used in reference 607:

- (1) The Prandtl assumption for the eddy momentum diffusivity, ϵ :

$$\epsilon = \ell_m^2 \frac{\partial \bar{u}}{\partial y} \quad (35)$$

- (2) An eddy viscosity model, which provides the turbulent shear stress and heat transfer relationships, respectively:

$$\tau_T = -\bar{\rho} \epsilon \frac{\partial u}{\partial y} = -(\bar{\rho} \nu)^T u' \quad (36)$$

and

$$q_T = \bar{\rho} \bar{c}_p \epsilon_H \frac{\partial \bar{T}}{\partial y} \quad (37)$$

- (3) The mixing length in the jet shear region, $(h-b) < y < h$, was assumed to be only a function of the shear layer width:

$$\ell_m = \kappa_0 [\text{local jet shear layer width}] \quad (38)$$

where h , b and y are as shown in Figure 14. κ_0 is a jet mixing length coefficient which varies with fluid compressibility.

- (4) The mixing length in the wall boundary layer region was taken to be a function of the following types:

$$\ell_m = C_1 (y_w - y) \quad \text{for } 0 < y_w - y \leq A \quad (39)$$

and

$$\ell_m = C_2 \delta \quad \text{for } A < y_w - y \leq \delta \quad (40)$$

where C_1 and C_2 are empirically derived constants, δ is the local wall boundary layer thickness, and A is defined by that point at which the viscosity model predicts a larger value of ℓ_m than $(C_2 \delta)$.

- (5) In the downstream developing flow region (Regime 2 in Figure 14), the mixing length was deduced to have the following characterization:

$$\ell_m = C_1 (y_w - y), \quad \text{for } (y_w - y) < \frac{\kappa_2 D C}{C_1} \quad (41)$$

and

$$l_m = \kappa_2 y_w D_c, \text{ for } (y_w - y) \geq \frac{\kappa_2 D_c}{C_1} \quad (42)$$

where κ_2 is the downstream mixing length coefficient and D_c is a correction factor characterizing the effect of compressibility on κ as a function of the local mean Mach number. Hedges and Hill⁵⁶⁶ note that this mixing length distribution differs significantly from that for fully developed incompressible pipe flow.

- (6) A turbulent Prandtl number of 0.9 was assumed throughout the flow, the molecular Prandtl number and specific heat were assumed constant, and Sutherland's formula for viscosity was used:

$$\mu = \bar{\mu} + \mu_o \left(\frac{\bar{T}}{T_o}\right)^{3/2} \left[\frac{T_o + C_3}{\bar{T} + C_3}\right] \quad (43)$$

The foregoing relationships (35-43) enable the modified (by equations (34)) forms of the conservation equations (32) and (33) to be formulated as finite-difference approximations which can be solved iteratively for individual grids or "elements" within the flow. The solution technique requires the following additional specifications:

- (7) Values for all flow variables at the upstream flow boundary (See Figure 14).
- (8) Values of the initial velocity and temperature distributions, eddy viscosity, duct and nozzle inlet dimensions, and the type of fluids.
- (9) Boundary conditions, such as the following:

$$\psi = 0, \frac{\partial u}{\partial \psi} = 0, \text{ and } \frac{\partial T}{\partial \psi} = 0 \quad (44)$$

along the centerline, $y = 0$; and:

$$y = f(x), \quad (45)$$

$$u = 0, \frac{\partial \bar{T}}{\partial \psi} = 0, \text{ and } \psi = \text{constant} \quad (46)$$

along the wall.

- (10) An initial estimate for the pressure gradient, $-\frac{d\bar{p}}{dx}$, in the momentum equation.

Only one value of the pressure gradient will simultaneously satisfy the conservation equations and the specified wall geometry, $y = f(x)$. This initial

pressure gradient value is incremented until a set of solutions is found for elements of length Δx , from $y = 0$ to $y = y_w$. These solutions then form a new set of initial conditions with which to proceed, and the complete flow field is "marched out" until the entire device has been analyzed. The set of solutions corresponding to the final value of x can then be used to determine overall performance, for instance, by using $v_{\text{exit}} = \bar{v}_{\text{exit}} = \int_{v/y=0}^{y_w} dv$ in equation (29).

It can be appreciated from the foregoing that significant detail is required in the specification of the parameters characterizing the flow phenomena and the geometry. The type of flow phenomena which are important must be a priori assumed in order to establish the initial flow model and the appropriate forms of the conservation equations. Designs for a specific level of overall device performance can only be obtained through parametric solutions for specified geometries -- generally a lengthy procedure for finite-difference type solutions. An alternate approach, used by Tai,¹³⁶¹ to the design problem is to specify the wall static pressure distribution through the device and solve for the wall geometry.

As implied above, the value of the physical phenomena approach and the ability to accurately predict ejector augmentor performance are intimately tied to the flow model assumed. Alternate configurations, for instance, of the primary nozzles, as reported in the reference 1422 study, require additional or different assumptions and empirically-based models for specific phenomena -- e.g., the hypermixing nozzle "tilt" angle, the resulting secondary flow initial transverse velocity component, and the initial jet turbulence intensity in reference 1422.

3.4 SUMMARY OF APPROACHES TO THEORIES OF OVERALL DEVICE PERFORMANCE

The theories of overall device performance for ejector augmentors can be grouped in two broad categories: (1) The Control Volume Approach, and (2) The Physical Phenomena Approach, with some inevitable overlapping between these.

The Control Volume Approach treats the ejector essentially as a "black box" by satisfying the bulk conservation equations between the device entrance and exit. In doing so, it enables only an understanding of "gross" effects on device performance -- i.e., the trends of area ratio effects on augmentation, initial stagnation property effects on performance, etc. Theoretical predictions based

on the Control Volume Approach can be forced into better quantitative agreement with experiments by introducing corrective terms to characterize losses such as skin friction, flow skewness, etc. which may be causing the discrepancies between the basic theory and experiments, but these terms are almost always highly configuration-dependent. Because, in the Control Volume Approach, the physical phenomena which underlie these corrective terms are not modeled, the nature of the configuration-dependence cannot be determined. Thus, neither the magnitude of the corrections needed to adapt the theory to alternative designs, nor the configuration designs needed to improve device performance, can be established.

The Physical Phenomena Approach attempts to overcome the limitations inherent in the Control Volume Approach by establishing flow models for the specific physical phenomena of significance to the device performance. Two problems arise in doing this: (1) The complexity of the flow interactions which take place in an ejector device is such that it is difficult, if not impossible with current computer capabilities, to model all of the significant phenomena, assuming that a distinction between those of significance and those which are unimportant can be correctly made; and (2) The state of the art of fluid dynamics in general is such that flow models for those phenomena known to be significant must rely on (usually limited) empirical bases which may not be appropriate -- e.g., free jet turbulent mixing parameters for confined hypermixing jets in a duct. Nevertheless, the Physical Phenomena Approach is amenable to adaptation to alternate configurations, particularly when the configuration differences can be directly linked with modeling parameters which are either well known, or which have been shown to have little effect on performance.

Although theories abound in both categories, no "universal theory" of overall ejector augmentor performance has been developed from either the Control Volume or the Physical Phenomena Approach. Control Volume approaches suffer from a lack of specification of the physical phenomena which take place within the control volume used, while Physical Phenomena approaches suffer from a lack of the comprehensive data on ejector flows needed to establish universal models. If and when such data become available, however, it is likely that the Control Volume Approach with configuration-dependent corrections will be sufficient for accurate overall device performance predictions.

4.0 EJECTOR COMPONENT THEORY AND EXPERIMENT

As discussed in the preceding sections, the relationships needed to properly model the real flow phenomena in an ejector in three dimensions are highly complex and currently insoluble analytically. Changes to the ejector configuration may require additional new phenomena to be modeled. Several interdependent variables are involved in describing the initial flow conditions, such as flow stagnation properties, inlet area ratios, mass flow ratio, etc., and the efficiency with which the augmentation process is completed is determined by their values, which determine the ejector configuration: the specification of the geometric detail, and the gasdynamic relationships. The ejector can be described as consisting of four distinct components (see Figures 13a & b): (1) Primary Nozzle(s), (2) Inlet Section, (3) Interaction Section, and (4) Diffuser. Of major importance to the ejector performance are the interrelationships between geometric and gasdynamic properties. As described in Appendix A, the following aspects of system definition appear to be the most significant to steady state ejector augmentors:

- o Primary flow thermodynamic properties.
- o Primary ejector nozzle type, arrangement, and location.
- o Secondary flow thermodynamic properties.
- o Secondary to primary area ratio.
- o Inlet, secondary flow contour with relationship to ambient reservoir conditions.
- o Volume, geometry, and length of the mixing section.
- o Diffuser geometry: exit to entrance area ratio, surface contouring, and boundary layer control.
- o External gasdynamics in terms of ambient conditions at the diffuser exit plane and the freestream velocity.

Fundamentally, all augmenting ejectors consist of the aforementioned components. The exhaust plane of the primary nozzle is usually positioned within the inlet section. The primary flow from the nozzle exhausts into the shroud and achieves a jet exhaust static pressure less than the secondary total pressure. The secondary fluid surrounding the primary nozzle becomes the entrained fluid. The secondary fluid enters the ejector through a constrained area provided by the inlet and is induced in a direction substantially

parallel with the primary flow. Viscous or interface pressure interactions occur between the primary and secondary flows in the interaction or "mixing" section, and the process is assumed to be completed whenever a uniform total pressure, total temperature, and velocity flow is achieved. This combined flow then exhausts with a greater mass flow, and thus momentum flux, than the primary nozzle can achieve alone.

While these components may be analyzed individually, ejector system performance is determined by their interrelationships. The major concerns in an ejector augmentor are thus, generally, the resultant net thrust produced by the system relative to a prescribed amount of input (primary) power and the resulting system volume. Changes to the components may thus be required to optimize the overall ejector system rather than its individual parts, for the desired performance levels and particular design application.

In this section, available empirical results of previous investigations and some theoretical considerations are used to describe the state-of-the-art for each of the previously defined components, primary nozzle(s), secondary inlet, mixing section and diffuser, as separate devices, but operating in an ejector environment. The understanding of individual component operation and performance optimization in relationship with the other components is essential to the overall design of an efficient thrust augmentor. The components have been considered with respect to their geometric and operating parameters and compared to total ejector system performance parameters.

4.1 PRIMARY NOZZLES

In Phase I (See Appendix A), it was concluded that significant advances in the state-of-the-art of ejector augmentor performance appear to have been achieved in recent years through the use of non-steady primary flows. While these improvements are derived from their effects on the interaction process, in discussing the primary nozzle(s), it is relevant to describe both steady state results and non-steady results separately.

4.1.1 Steady Flow Primary Nozzles

The primary nozzles in high performance steady flow ejectors should exhibit certain characteristics. The primary nozzle component must efficiently produce thrust by itself (The maximum thrust performance of a pressurized nozzle was discussed in detail in Section 2.1). The primary flow must also entrain substantial amounts of secondary fluid within a prescribed

distance and in a streamwise sense. The primary nozzle component must, as other components, exhibit minimum energy dissipation during expulsion of primary air and entrainment of secondary air and subsequent mixing in order to produce maximum thrust augmentation (Peschke).¹⁰⁴⁵ A wide variety of nozzle shapes and placement relative to the secondary flow inlet has been investigated. A few of the configurations are illustrated schematically in Figure 15. Figure 16 compares the augmentation ratio results for these various types. The figure shows the maximum augmentation performance from numerous experiments for subsonic and supersonic primary nozzle flows for ejectors with and without diffusers. The results are shown for total system performance, ϕ , versus the geometric parameter of inlet area ratio for single and multiple primary flow source arrangements. Multiple primary nozzle arrangements achieve greater peak thrust augmentation than single primary nozzles for any given inlet area ratio. The multiple primary nozzle arrangements exhibit improved augmentation peak performance with increasing inlet area ratio, while single nozzles perform at near uniform peak levels. Multiple primary nozzles which entrain secondary fluid and mix simultaneously, such as the hypermixing and Coanda nozzles, exhibit the highest ejector thrust augmentation results. Similar conclusions for comparison of multiple and single primary nozzle arrangements were reached by Thronson,¹³⁸⁰ Garland,⁴⁶⁰ and Shumpert.¹²⁶³ These results have been represented in Figure 17 to demonstrate the effectiveness of the multiple nozzle configurations in terms of both augmentation ratio and length to width. The peak augmentation performance for both types of arrangements follows the same trend with length to width ratio; however, the multiple nozzles achieve much higher levels of augmentation performance. Since the results shown are for both subsonic and supersonic primary flow initial operating conditions, it appears that in general, to achieve high levels of augmentation performance, multiple array primary nozzles are desirable.

The primary nozzle system of an ejector may be required to operate at subsonic, sonic, or supersonic flow conditions, depending upon the application and operating parameters. It can also be required to operate efficiently for a variable range of total pressure and temperatures, for an envelope of thrust requirements. The effect of driving pressure upon the primary nozzle system's ability to entrain and mix secondary fluid and produce thrust is presented as a function of the ejector system performance in Figure 18, where ejector thrust augmentation ratio is shown as a function of primary nozzle pressure ratio. The

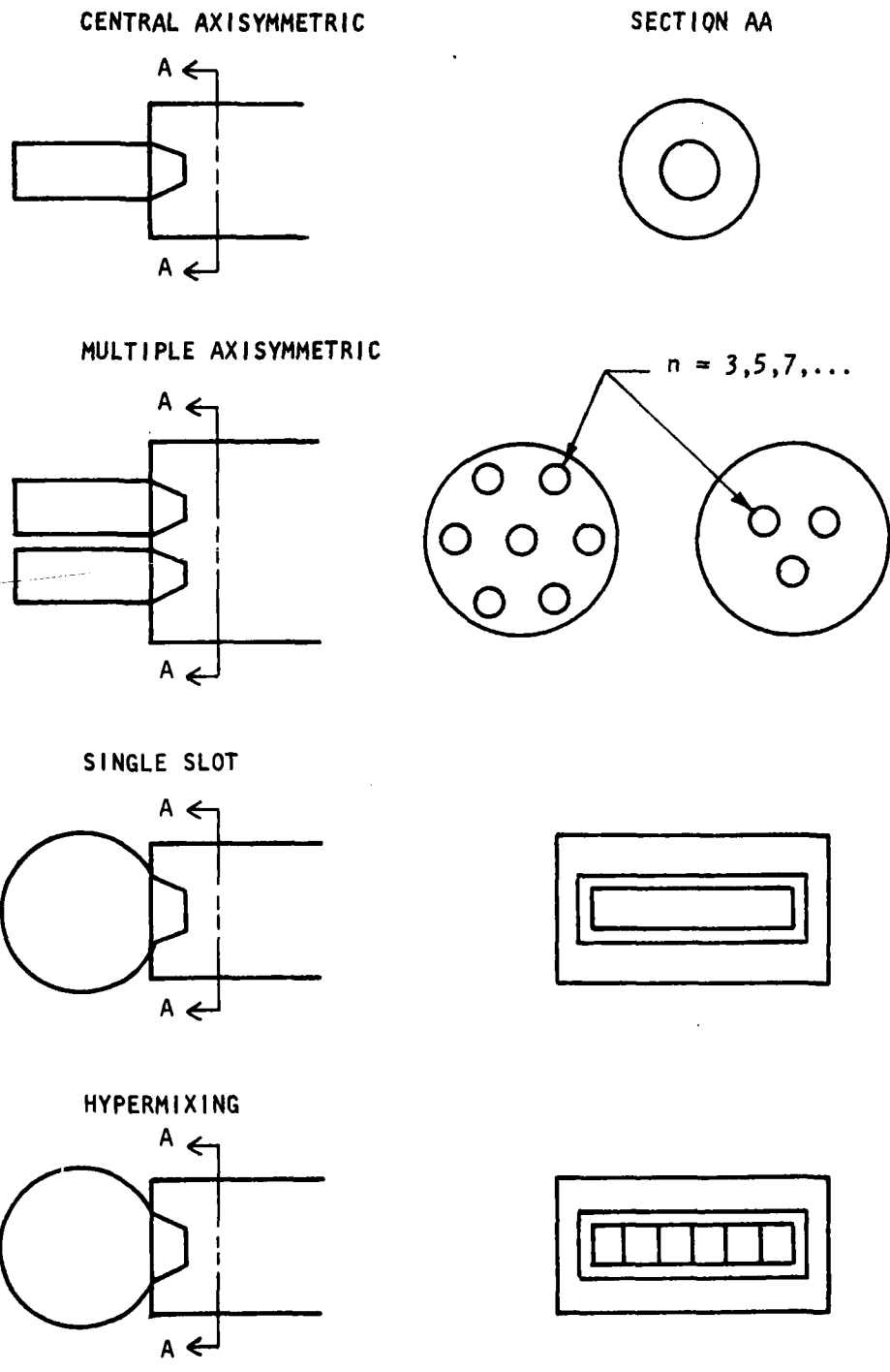
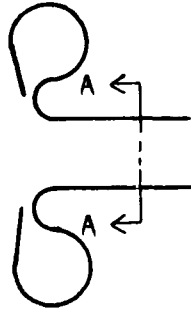
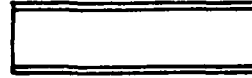


FIGURE 15. TYPES OF PRIMARY NOZZLES.

COANDA



SECTION AA



CRUCIFORM

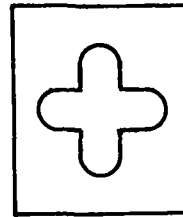
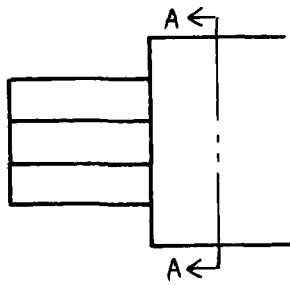


FIGURE 15. CONCLUDED.

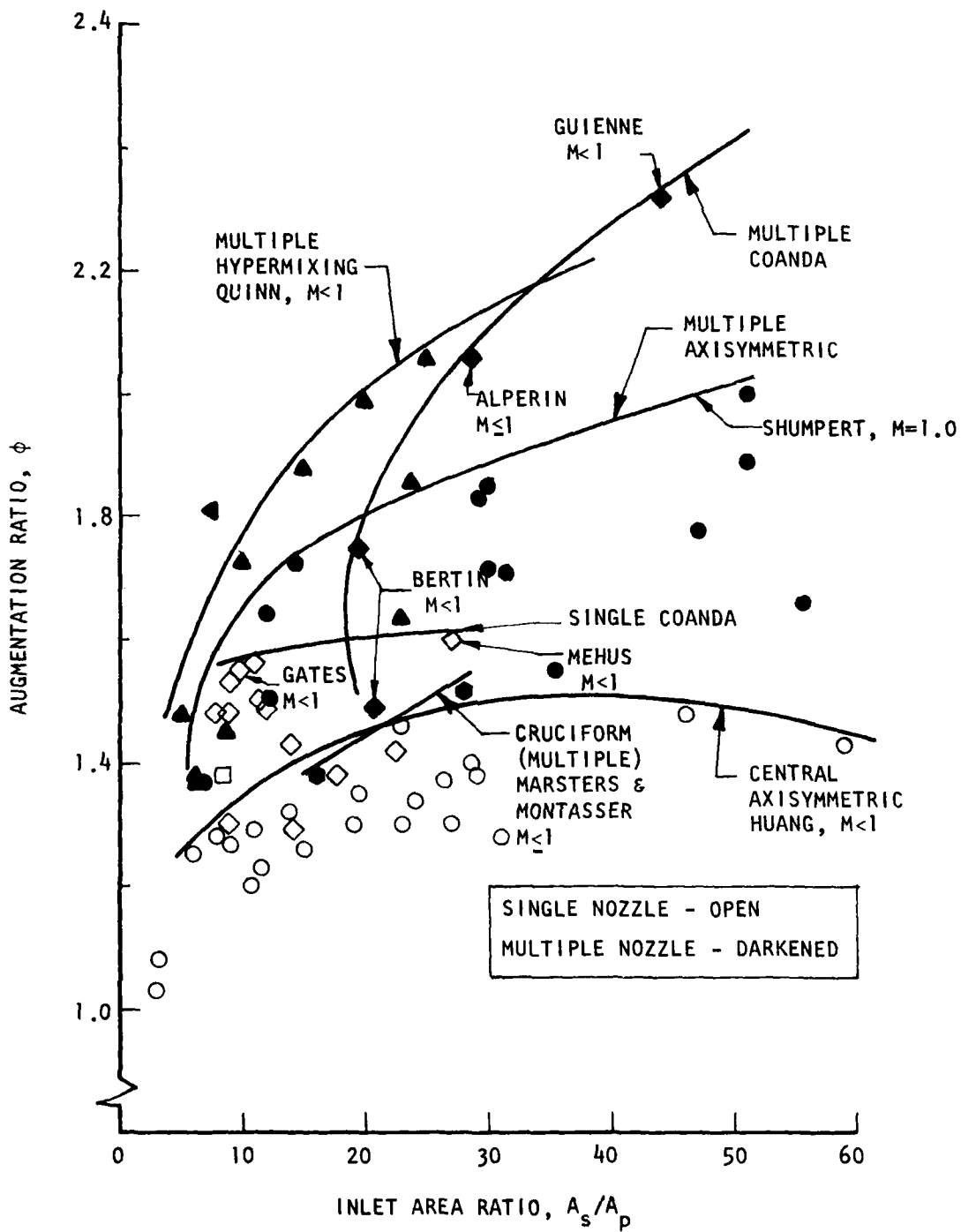


FIGURE 16. COMPARISON OF AUGMENTATION RATIO PERFORMANCE FOR SINGLE AND MULTIPLE NOZZLES AS A FUNCTION OF INLET AREA RATIO.

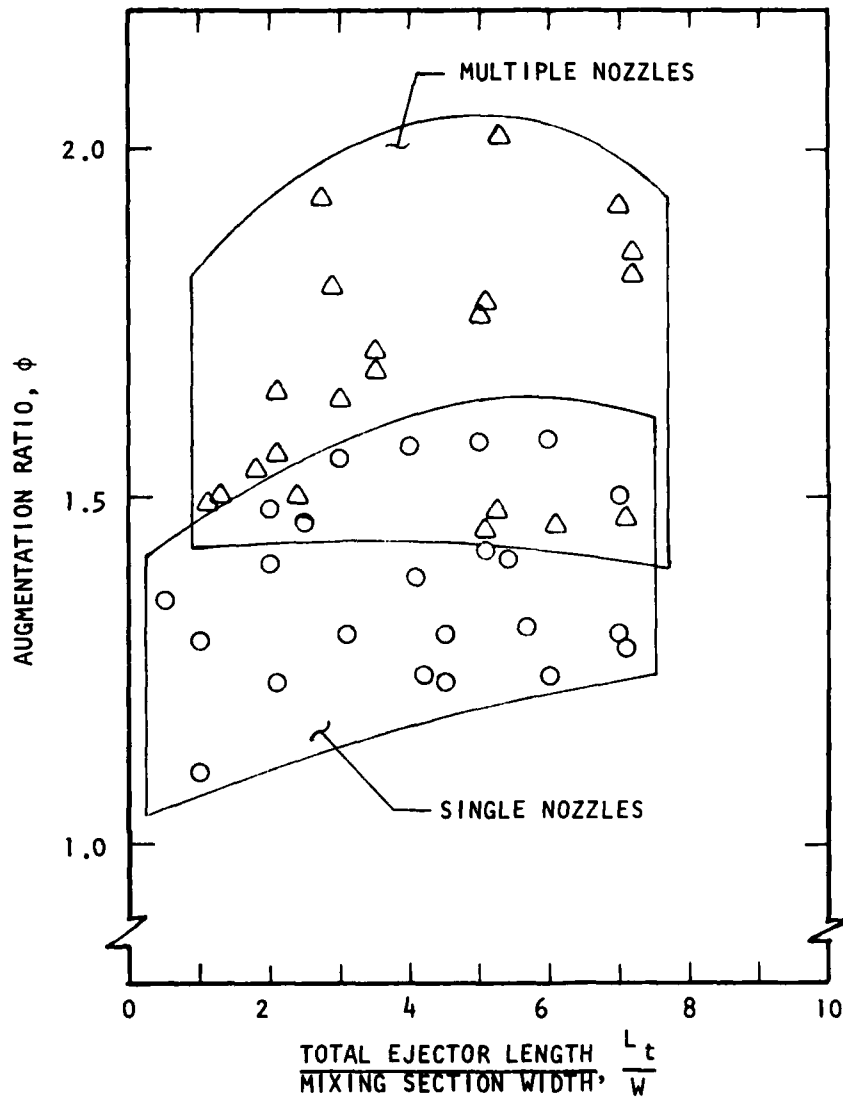


FIGURE 17. PERFORMANCE COMPARISON BETWEEN SINGLE AND MULTIPLE NOZZLES AS A FUNCTION OF EJECTOR LENGTH.

(Refer to Figure 11 for Data References)

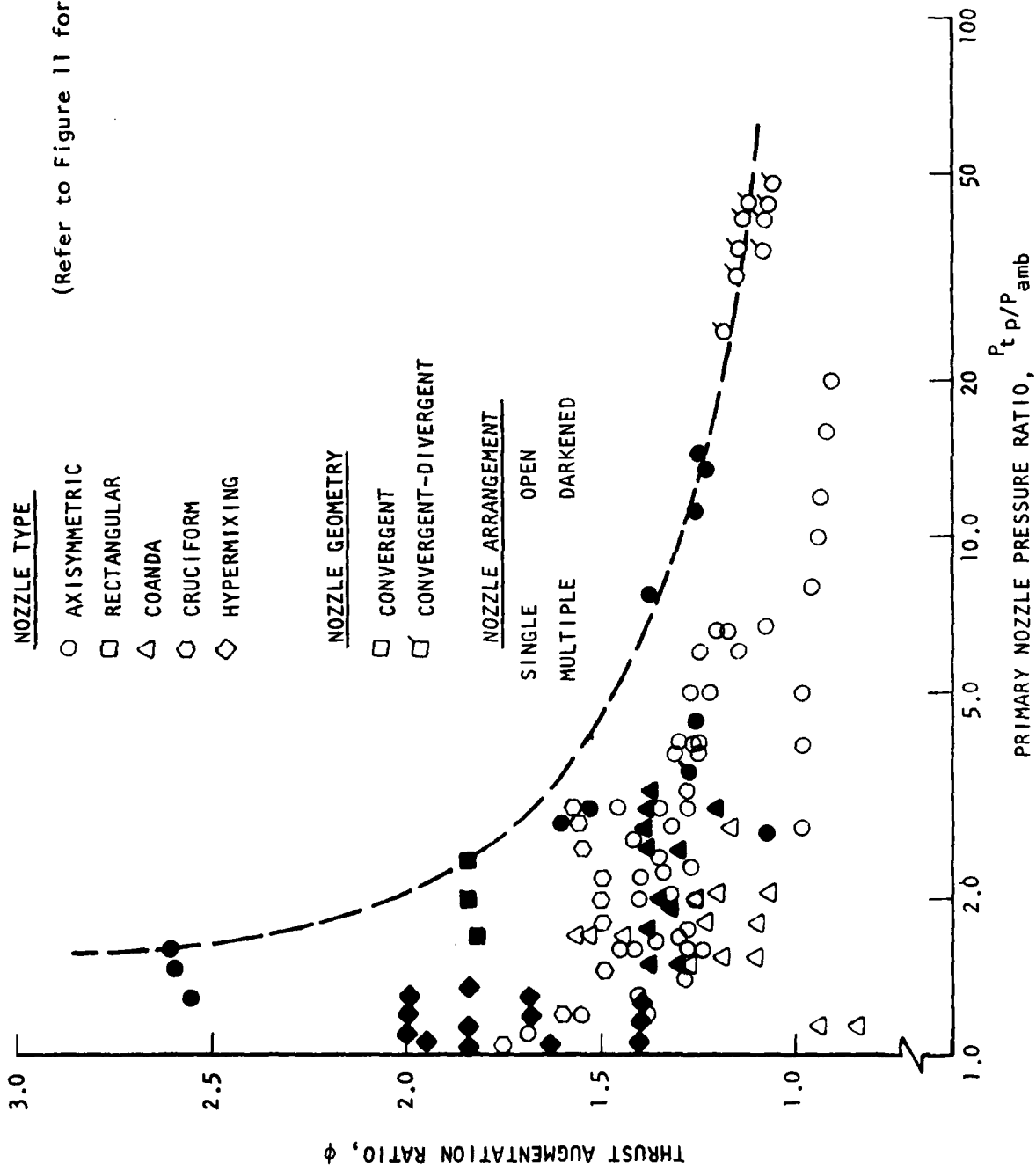


FIGURE 18. EFFECT OF PRIMARY NOZZLE PRESSURE RATIO AND NOZZLE CONFIGURATION ON EJECTOR PERFORMANCE.

overall trend shows a decrease in maximum augmentation ratio with increasing pressure ratio as indicated by the ϕ_{MAX} formulation of Section 2.1. However, it must be kept in mind that for a given geometric device, an optimum pressure ratio may exist. As shown in Figures 16 & 18, the greatest change in performance occurs in the pressure ratio range for which the primary nozzle flow is subsonic. Thereafter performance tends to level out, approaching one for high supersonic primary flows.

Individual tests in which the primary nozzle geometry remained fixed have shown that in the pressure ratio range from choked to supersonic flow thrust performance with varying pressure ratio can be maintained. Results of this type, for simple convergent and convergent-divergent primary nozzles, have been shown by Marsters and Montasser,⁸⁸⁶ and Jacobs and Shoemaker.⁶⁶⁷ The initial primary pressure ratio, when coupled with the geometry of the primary nozzle, generally dominates the performance of the primary nozzle system and the total ejector performance.

Definition of the effects of the primary nozzle flow total temperature is also important to understanding ejector performance. In the experimental results of Rabeneck, Shumpert, and Sutton,¹¹⁰¹ very little influence of the temperature ratio on thrust augmentation was found. Minimal effect on entrainment due to elevated primary temperatures was shown by Quinn,¹⁰⁸⁸ whose experiments complemented those done earlier by Reid¹¹²⁵ in an axisymmetric non-diffusing ejector. Armstrong⁶² also concluded on the basis of experimental results, that primary flow elevated temperature ratios have a small effect on ejector thrust. However, increasing the primary gas total temperature ratio does result in some decrease in thrust augmentation ratio. Examples of the change in magnitude of thrust augmentation are shown in Figure 19 for various levels of total pressure ratio. These results indicate the loss of thrust performance encountered and permit a comparison to the effects of increasing the primary total pressure ratio. It can be seen that the temperature effects become increasingly important to the performance, as the total pressure ratio increases.

The general trend between performance and temperature ratio is approximately linear. A 100 percent increase in temperature ratio results in approximately a 10 percent decrease in thrust augmentation, for other conditions held constant. It is important to note that in both the pressure and temperature ratios, Figure 19, that some test results showed that there was no influence on performance due to elevating the pressure or the temperature. These individual

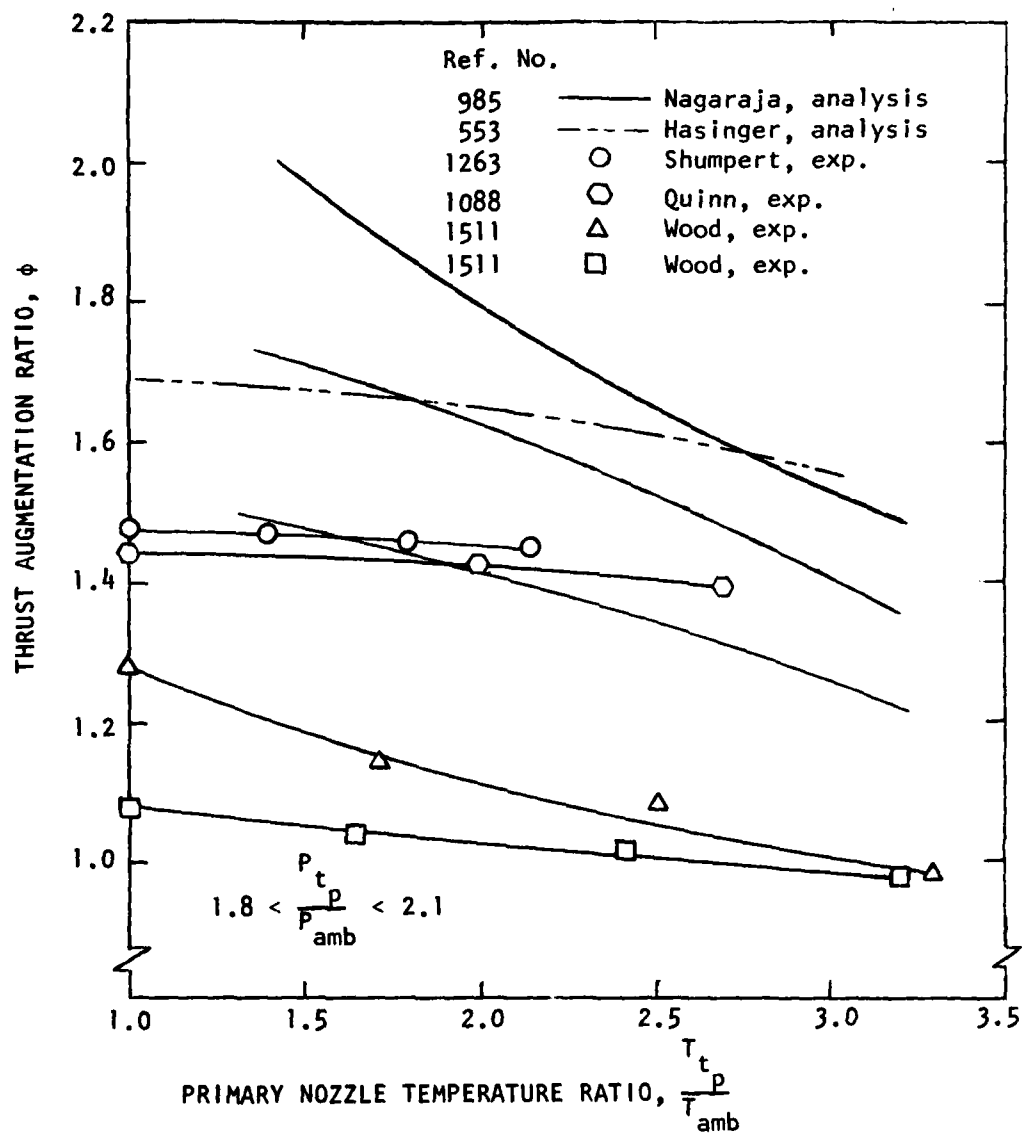


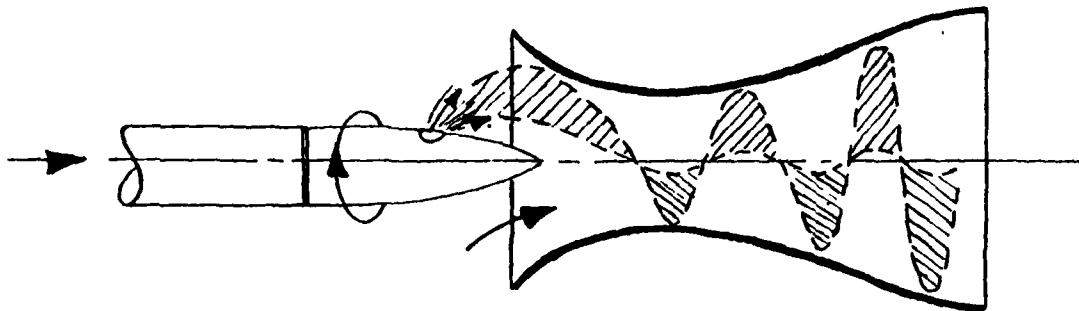
FIGURE 19. EFFECT OF PRIMARY NOZZLE TEMPERATURE RATIO ON AUGMENTATION RATIO

experimental results showed ejector absolute thrust performance that substantially did not decrease with increasing the pressure ratio, Quinn¹⁰⁸⁵ and Marsters and Montasser,⁸⁶⁶ and individual ejector augmentation ratios that did not significantly decline with increasing temperature; Rabaneck, Shumpert, and Sutton,¹¹⁰¹ and Quinn.¹⁰⁸⁸ Such examples of ejectors which do not explicitly follow the overall trends with pressure and temperature ratios probably represent non-optimal configurations. (Refer to the discussion of Figures 43-45 in Section 4.3)

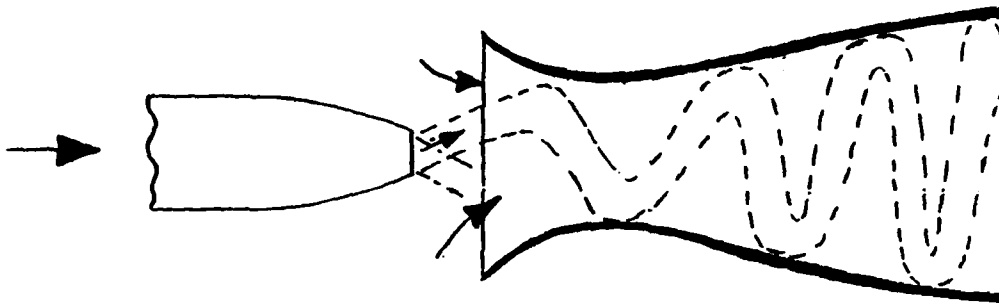
4.1.2 Non-Steady Primary Nozzles

The thrust augmentation of ejectors has been shown to be a direct function of the efficiency of energy transfer between the primary and secondary flows. Recent analysis and experimental results of Quinn,¹⁰⁹¹ Fancher,³⁷⁷ and Bevilacqua¹³³ showed for ejectors with hypermixing nozzles, used to enhance the transfer process, that thrust performance improved. An alternate technique to achieve efficient energy transfer between a primary jet and entrained fluid is the introduction of unsteadiness into the primary flow, Foa,^{412,418} Hohenemser,⁶²⁵ Hohenemser and Porter,⁶²⁸ and Viets.^{1419,1422} As discussed in Section 2.0, the fundamental benefit to be realized from a non-steady primary nozzle ejector when compared to a steady device is the phenomenon by which the energy is transferred. In a non-steady device, a contribution due to pressure-exchange is involved in addition to the conventional viscous shear mixing process. The primary advantage of a non-steady ejector is that efficient energy transfer can occur in a shorter distance than for a steady ejector.

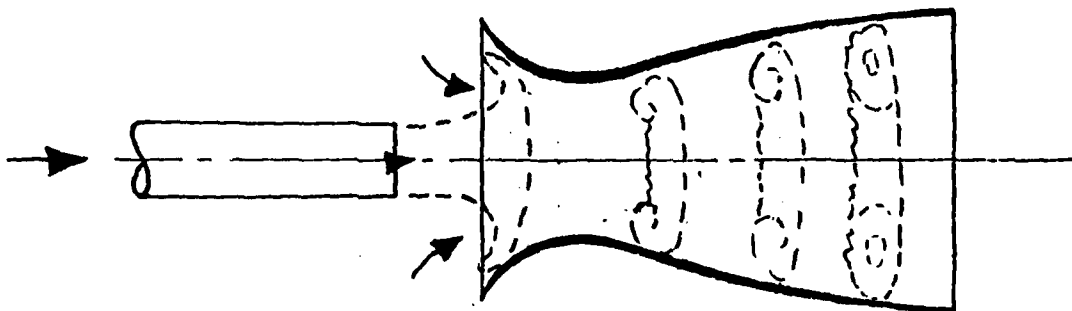
Numerous techniques for introducing non-steadiness into the primary flow have been proposed and tested successfully. Four basic mechanisms for non-steady primary flow injection are illustrated in Figures 20 and 21. Figure 22 illustrates the effect of energy transfer efficiency on static thrust augmentation as discussed by Foa in reference 416. The theoretical performance is represented by the solid lines from the analysis of Foa.⁴¹⁸ The performance of the ejector is shown to improve rapidly with increased energy transfer efficiency. The non-steady ejector results show improved performance over equivalent steady ejectors. For operation at the same transfer efficiency, the ejector performance is shown to be improved by ability to increase the inlet area ratio and entrain additional secondary fluid. Since the energy transfer mechanism for this type of interaction (see Section 2.0) involves no dissipation, the energy transfer efficiency is effectively 100%, and the attendant thrust augmentation for static operation is as shown in Figure 22, with $\eta_T = 1.0$. However, whenever account is taken of the losses incurred in the generation of the primary flow pulsations, the energy



(a) Crypto-Steady, or Spin-Jet, Ejector; (Foa)⁴¹⁸, (Hohenemser)⁶²⁵



(b) Ejector with Oscillating Primary Jet (Viets)¹⁴¹⁹



(c) One-Dimensional, or Pulse-Jet, Ejector (Curtet & Girard)²⁹⁵

FIGURE 20. TYPES OF NON-STEADY FLOW THRUST AUGMENTATION EJECTORS.

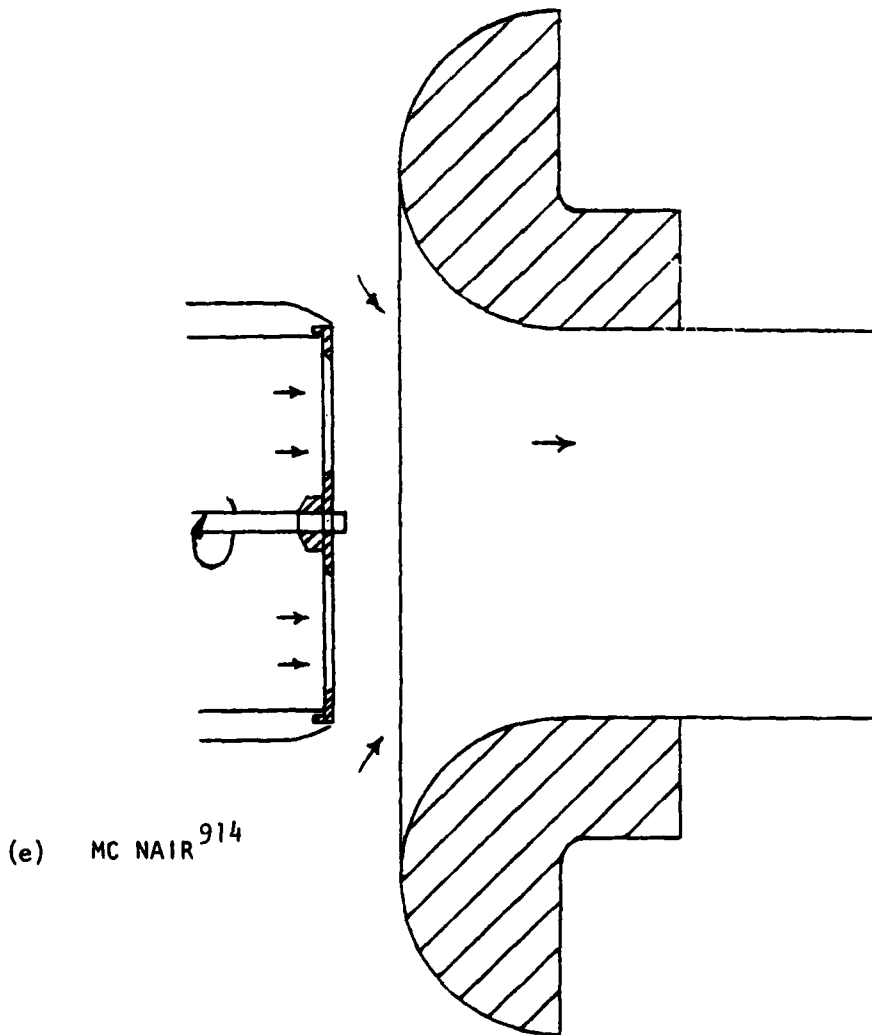
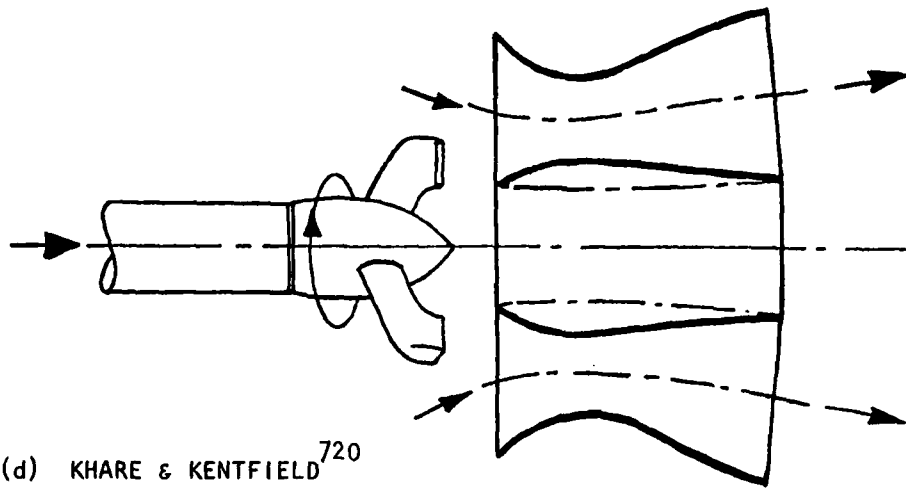
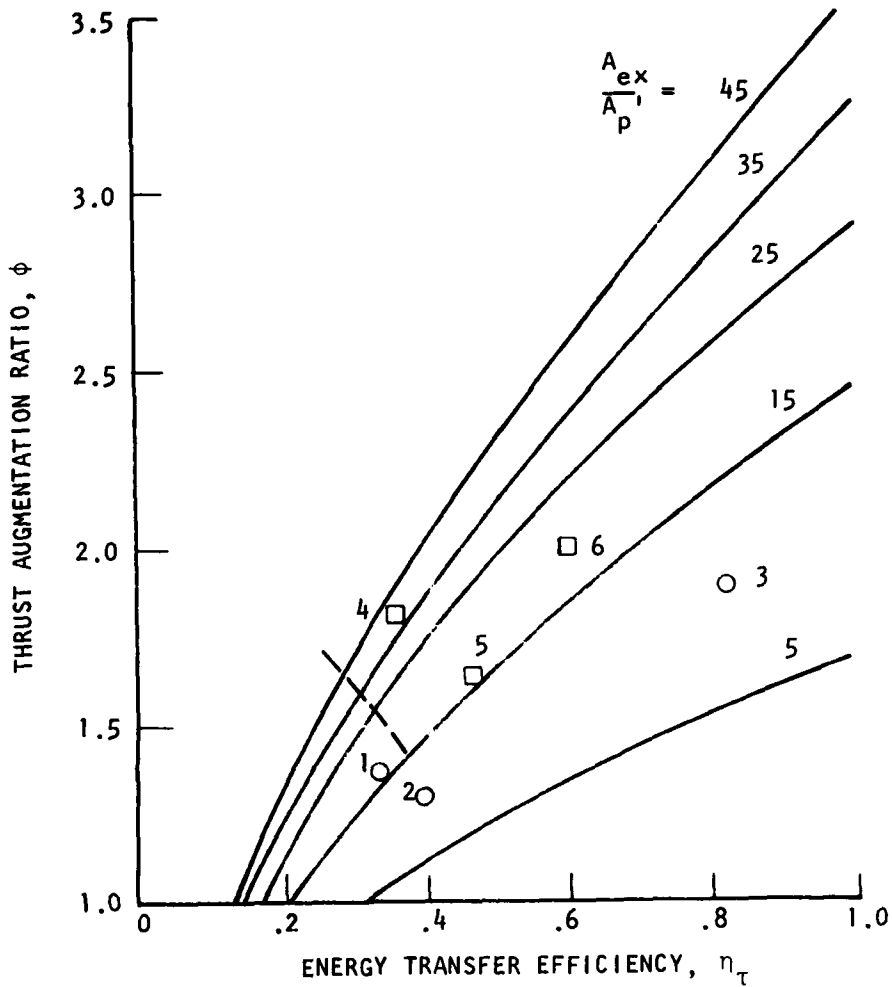


FIGURE 21. NON-STEADY PRIMARY EJECTORS.



--- Ideal Steady Flow Ejector, Von Karman

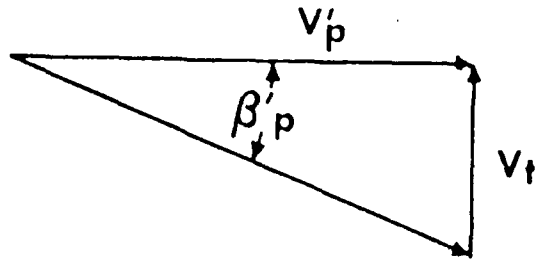
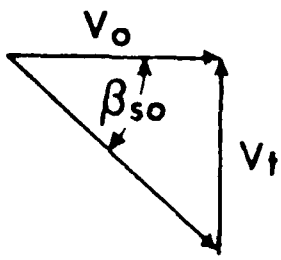
1. Steady-flow ejector, Hohenemser⁶²⁵
2. Steady-flow ejector, Morrisson⁹⁶⁹
3. Pulsating-flow ejector, Lockwood⁸³⁰
4. Rotary jet, air-air, Hohenmser⁶²⁵
5. Rotary jet, air-air, Hohenemser⁶²⁵
6. Rotary jet, water-water, Vennos¹⁴¹⁵

FIGURE 22. EFFECT OF ENERGY TRANSFER EFFICIENCY ON STATIC THRUST AUGMENTATION.

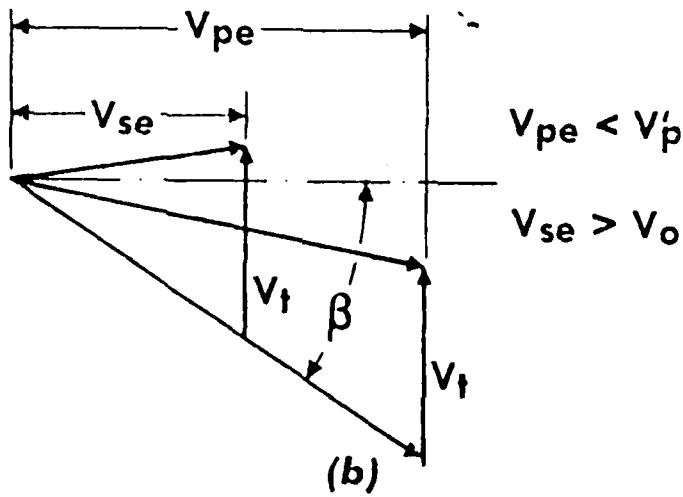
transfer efficiency of the pulsating-flow ejector is found to be lower than that of the conventional steady-flow ejector. At present, the rotary jet, of all nonsteady-flow augmentors, suffers least from the losses associated with the conversion to nonsteadiness. This is because the spiral flow pattern of the primary flow is achieved by ducting the primary flow, before interaction with the secondary flow, through a rotor that is driven by primary flow forces which have to overcome merely bearing and aerodynamic surface friction.

In a rotating reference system the flows have, before and after interaction, the velocities shown in Figure 23. In Reference 624 an analysis is presented that assumes two phases of flow interaction. The first phase is an isentropic interaction between the states (a) and (b) of Figure 23. This interaction amounts in a rotating reference system to a mutual deflection of the two flows into a common direction, whereby the axial component of the primary flow velocity is reduced and that of a secondary flow velocity increased. After the interaction, both flows have, in a lab-fixed reference system, opposite angular momentum. The axial kinetic energy of the two flows is reduced by the angular kinetic energy, which appears as a loss despite the isentropic interaction. In the second phase, the flow interaction is assumed to be completed by mixing, whereby the angular kinetic energies are dissipated and the angular momentum of the mixed flow is zero. The time-sequence of the two phases has been found to significantly affect the predicted performance. If the mixing occurs before the mutual deflection, the performance is lower. This agrees with experimental results in which it was found that circular nozzles are more effective than thin rectangular jets since the circular jet dissipates more slowly.

Tests providing a comparison with the analysis are also reported in Reference 624. They were conducted with a device shown in Figure 24. The mixing duct behind the dash line could be removed. The measured and predicted performance are compared in Figure 25. A number of different "spin angles", β_p , as defined in Figure 23, were used. The higher the spin angle, the faster the rotational speed of the rotor. Air of equal total temperature was used for primary and secondary flow. The exit to primary flow area ratio was $A_e/A_p' = 16$. The ratio of primary total pressure to ambient pressure was $P_{tp}/P_o = 2.8$. The ratio of the exit static pressure of the mixed flow to the inlet total pressure of the secondary flow, p_e/p_{ts} , is plotted vs. mass flow ratio, m_s/m_p , for various spin angles. Zero spin angle corresponds to a conventional steady flow ejector. The solid lines are from tests, and the dash lines are



(a)
BEFORE DEFLECTION



(b)
AFTER DEFLECTION

(REFERENCE 624)

FIGURE 23. ROTARY JET FLOW VELOCITY TRIANGLES.

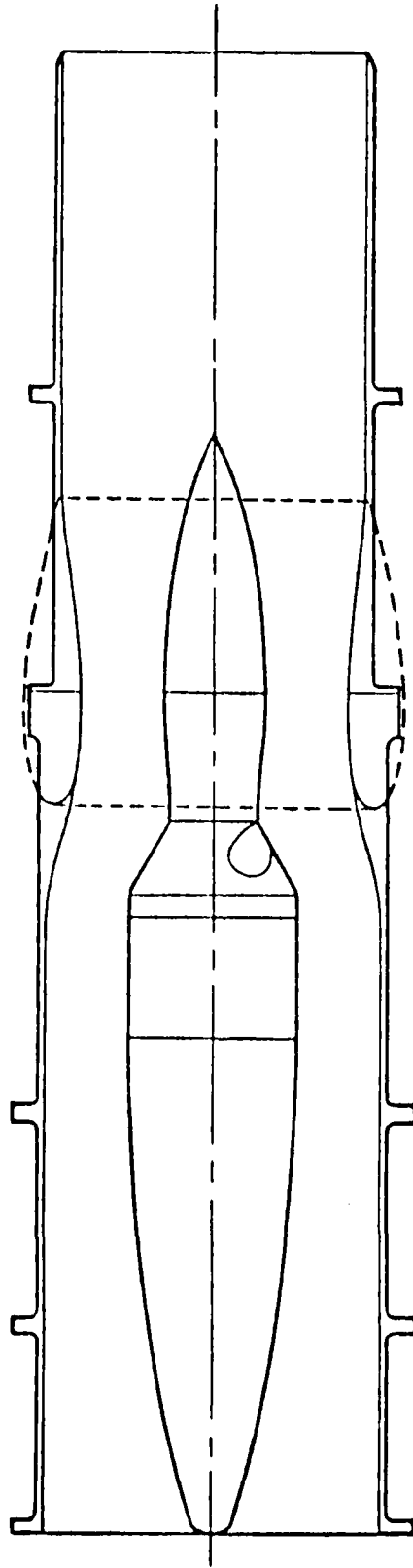


FIGURE 24. EXPERIMENTAL SET-UP FOR A ROTARY JET AUGMENTOR. (Reference 624)

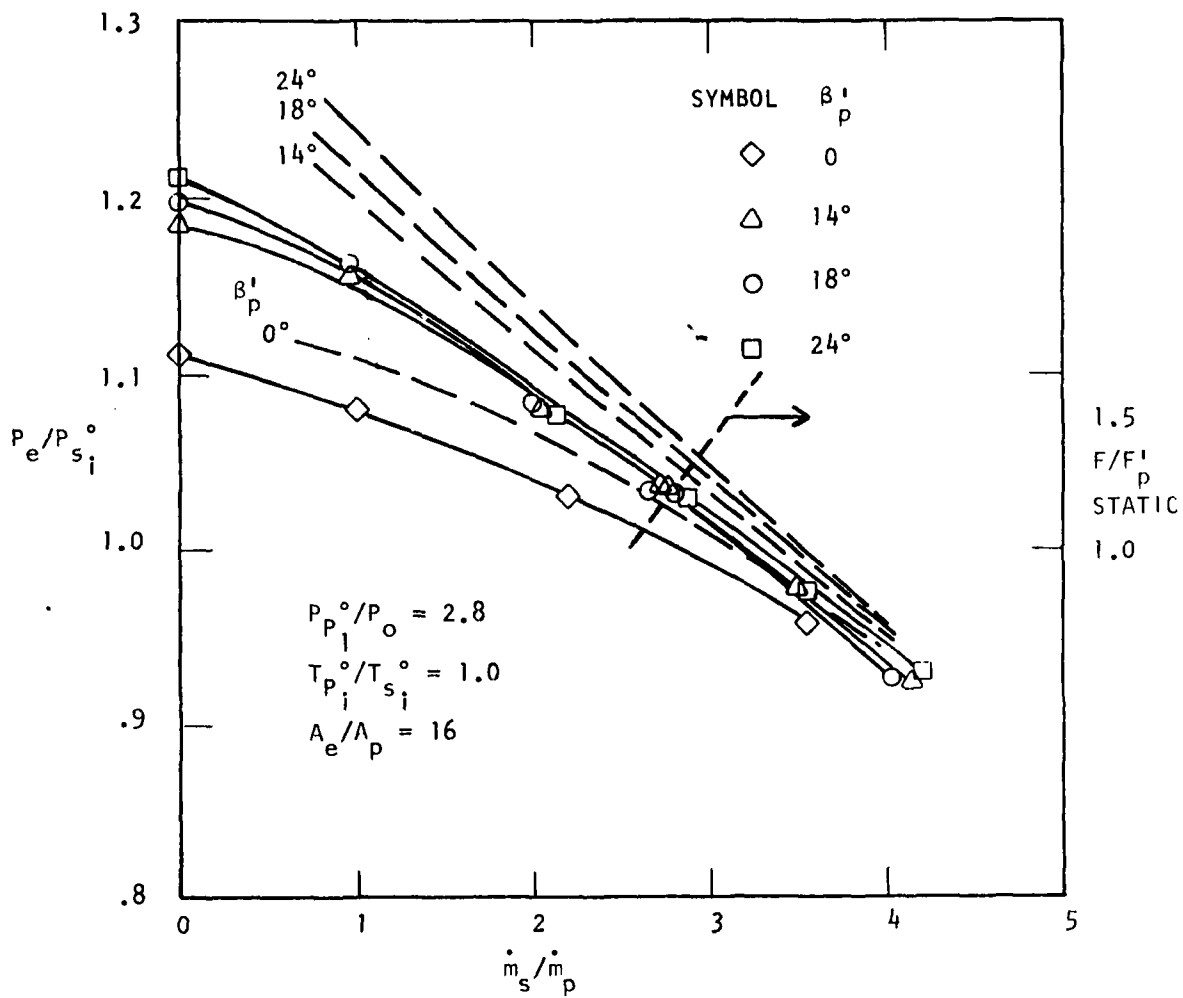


FIGURE 25. COMPARISON OF ANALYTICAL AND TEST RESULTS FOR A ROTARY JET AUGMENTOR. (REFERENCE 624)

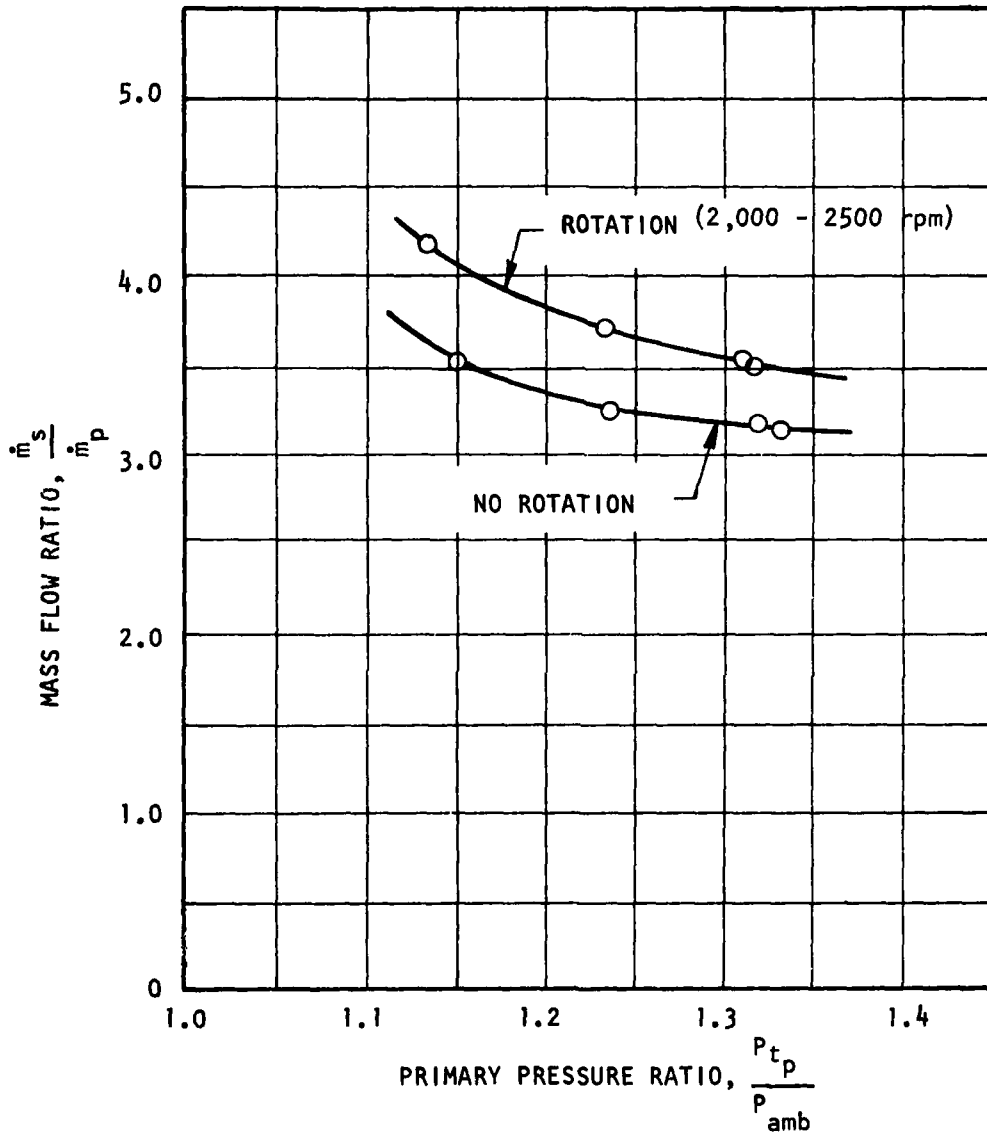
from the analysis. The improvement of the performance from primary flow rotation is about as predicted. However, both the rotary flow augmentor and the ejector have lower than predicted performance since wall friction, non-uniform flow, etc., were neglected in the analysis.

While the ejector needs the entire mixing length shown in Figure 24, the rotary flow augmentor needs only the short shroud indicated in Figure 24 by dash lines. For $P_e/P_{ts} = 1.0$, the measured thrust augmentation ratio for the ejector is 1.2 and for the rotary flow augmentor is 1.4. A diffuser behind the mixing section would have increased the static thrust augmentation. It was omitted in order not to superimpose two different effects. The analysis predicts for the rotary flow augmentor a thrust augmentation ratio of 1.6 (vs. measured 1.4), assuming 20 degrees spin angle.

It can be concluded from these results that in cases of equal density of primary and secondary flow (water-water, air-air of same temperature) and presumably also for a primary to secondary flow density ratio greater than one, a rotary flow augmentor with a spin angle of 10 to 20 degrees with a short shroud (length to diameter ratio of about one) is capable of substantially increased performance compared to a steady-flow ejector with its relatively longer mixing duct.

An alternate method of generating an unsteady primary flow is the multi-element fluidically controlled oscillating jet, described in Reference 1422. This technique was tested¹⁴²¹ in the low area ratio single channel rig, described in Reference 738, at the Aerospace Research Laboratories. Some results are shown in Figures 26 and 27. The performance of the oscillating nozzle in terms of thrust augmentation ratio ϕ as a function of diffuser area ratio, A_4/A_3 , is shown in Figure 27. The "flat" and "converged" notations refer to the end walls. In order to see the effect upon end wall separation, the end walls were converged in some of the tests which decreased the diffuser area ratio. There is significant scatter in the data, but the augmentation hardly exceeded 1.3. Comparing these results with those for a hypermixing nozzle in the same configuration, Figure 28, it is seen that the hypermixing nozzle performance is far superior.

Increased blockage of the oscillating jet, due to the feedback loops which interfere with the entrained flow, was simulated for the hypermixing nozzle configuration and was found to affect the performance by almost a tenth of a



(REFERENCE 914)

FIGURE 26. IMPROVEMENT IN AUGMENTOR ENTRAINMENT RATIO WITH NON-STEADY PRIMARY FLOW.

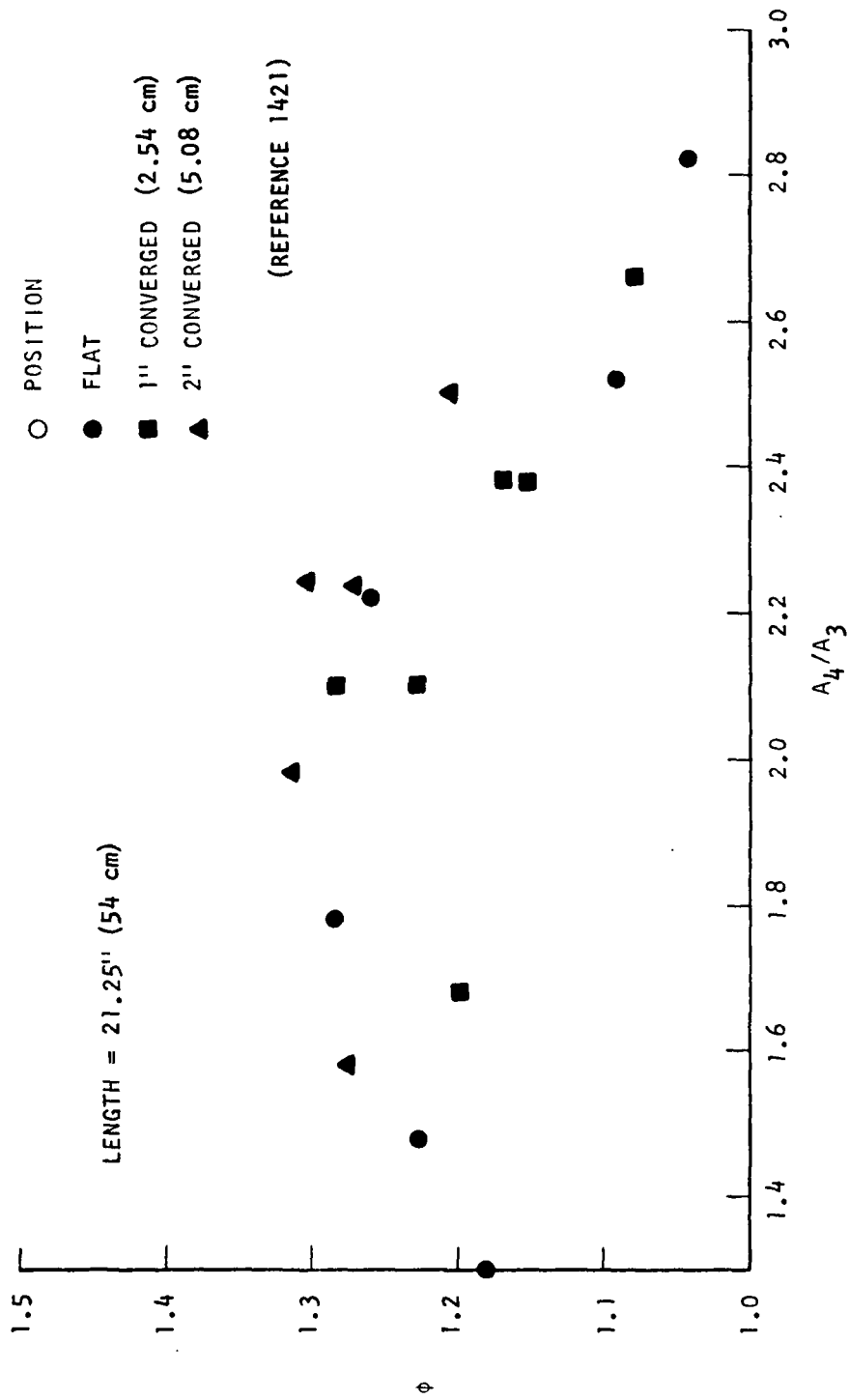


FIGURE 27. AUGMENTATION PERFORMANCE AS A FUNCTION OF DIFFUSER AREA RATIO EMPLOYING AN OSCILLATING FLOW NOZZLE.

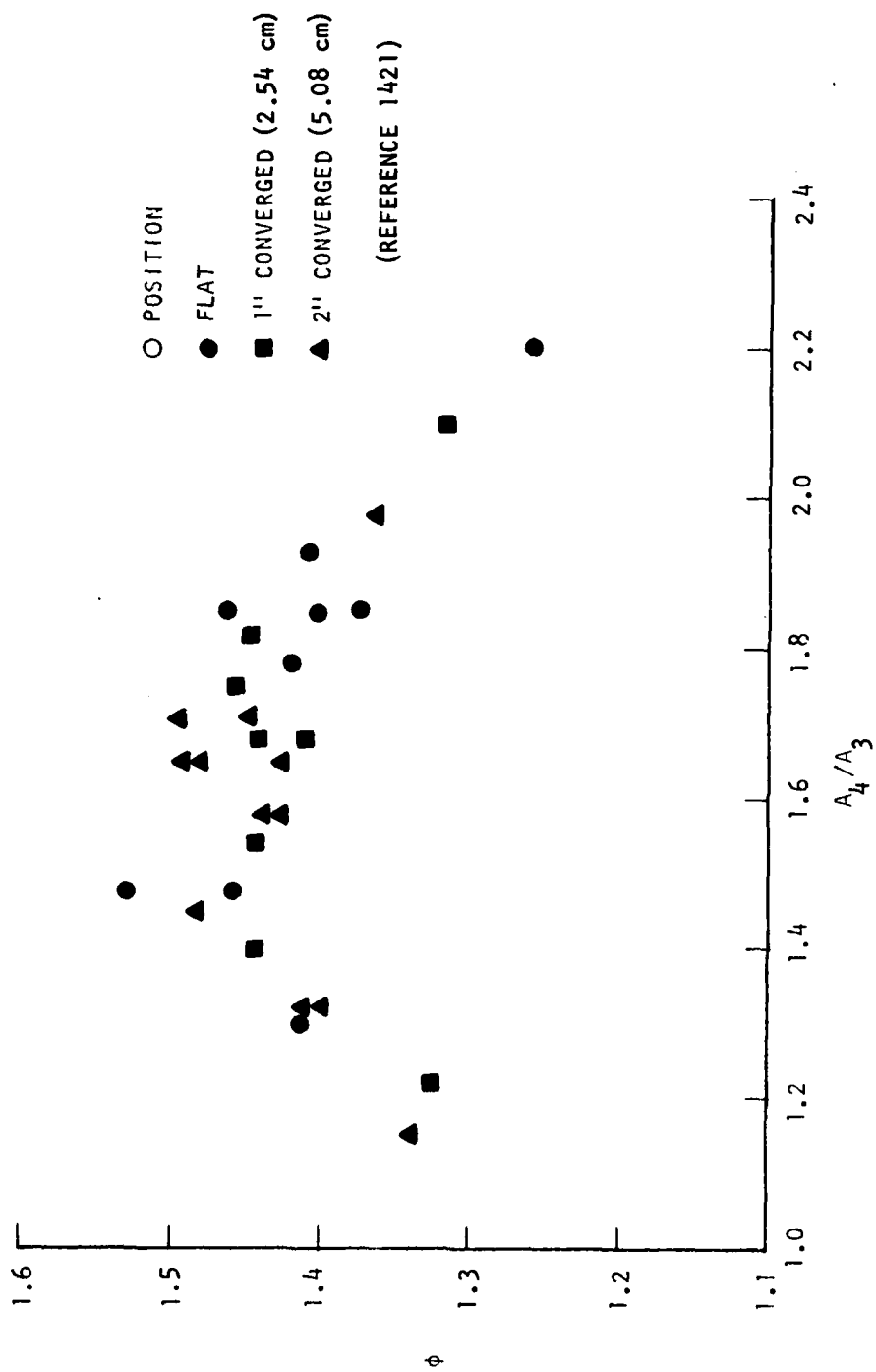


FIGURE 28. AUGMENTATION PERFORMANCE AS A FUNCTION OF DIFFUSER AREA RATIO EMPLOYING A HYPERMIXING FLOW NOZZLE

point in ϕ (Figure 29), but this does not satisfactorily explain the significantly greater than .10 difference between the steady and unsteady cases.

One penalty for use of this type of unsteady primary appears to be a reduction in the primary nozzle efficiency. Another penalty may be incurred for non-optimum frequencies, i.e., when the frequency of the oscillating jet is such as to allow less than a full cycle of the oscillation to exist in the ejector at any given time. Thus, the jet flow may exist in a quasi-steady state in spite of the fact that the price was paid in nozzle thrust efficiency. Finally, reduced performance may result from the fact that the pressure pulse moving down the nozzle is not sealed at the edges. That is, if the flow is to transfer energy through pressure the way a piston or shock tube does, then it may be necessary to have the wave move downstream coherently so that the pressure cannot "leak" around the edges of the jet.

As shown in the preceding figures, the impact of unsteady or pulsing primary flows on ejector performance is observed in the efficiency of the resulting non-steady interaction and ultimately in the total system thrust augmentation ratio. The results of Lockwood⁸³⁰ for a pulse-jet ejector augmentor (primary flow derived from a pulse-jet) are shown in Figure 30. With equal inlet area ratios, the unsteady flow ejector improved the peak augmentation ratio by 45 percent to 1.91, over the empirical results of Morrisson.⁹⁶⁹ In addition to improving the thrust augmentation, the non-steady ejector flow was mixed more quickly than the steady ejector. The peak augmentation ratio occurs at an augmentor length to diameter ratio of 1.5 for the unsteady flow ejector, similar to the results cited by Hohenemser previously, while the steady flow ejector required a mixing length four times as long to achieve its maximum augmentation ratio. The improvements in performance from Lockwood's results were from an ejector with a pulsed or intermittent primary flow in a non-diffusing ejector. Binder and Didelle¹⁴¹ also show improvements in thrust augmentation by utilizing a non-steady jet in diffusing and non-diffusing ejectors. Figures 31 and 32 show the results from steady and non-steady axisymmetric ejectors, with and without diffusers from Reference 141. A steady flow fluidically diverted and a pulsed primary jet were the source of the non-steadiness in the ejector configurations. For the non-diffusing ejectors, primary flow unsteadiness improved the thrust augmentation ratio at all total length to diameter ratios. In Figure 31, axisymmetric ejectors with single steady and pulsating jets are compared. At all mixing length to diameter

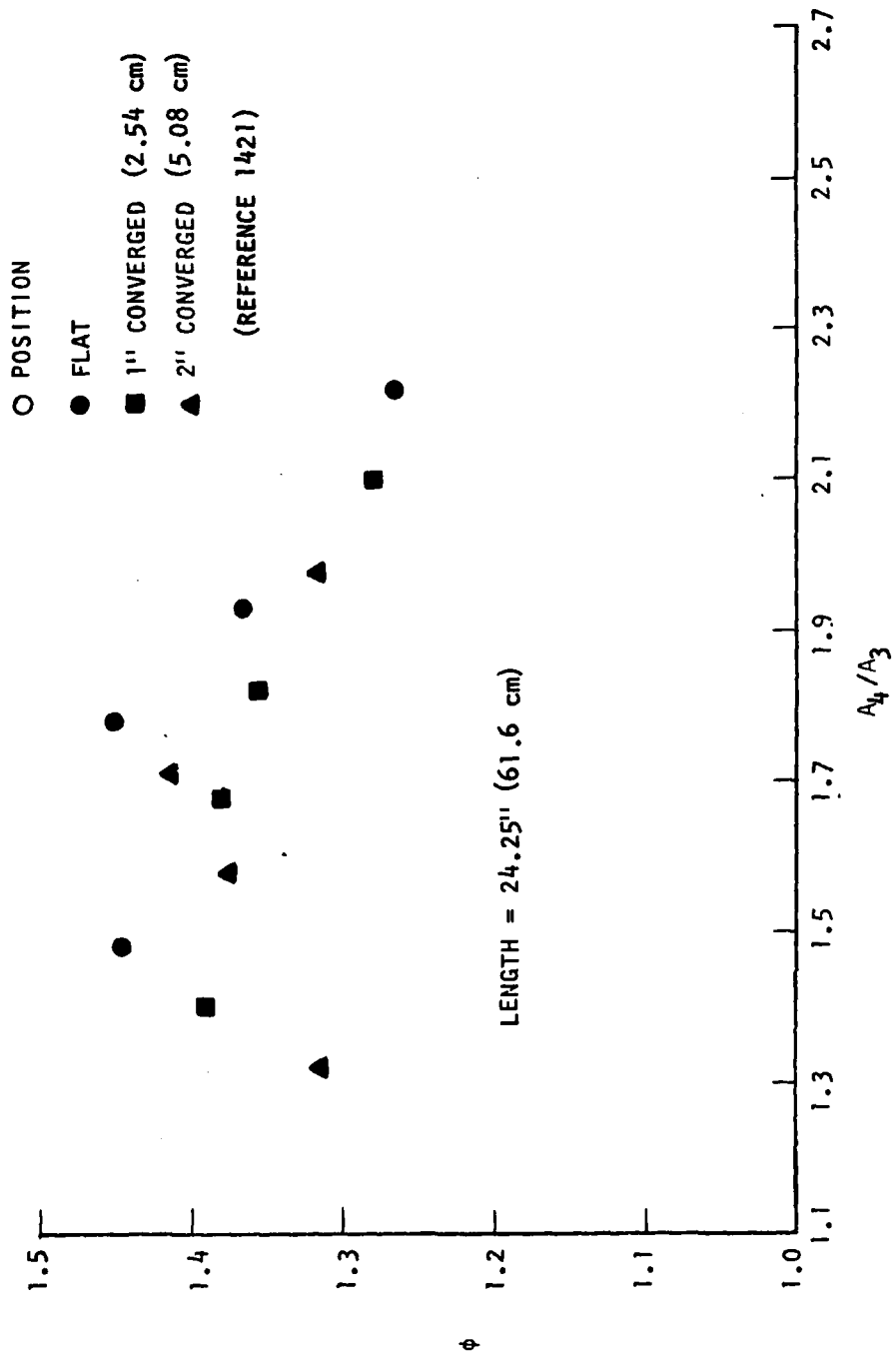


FIGURE 29. AUGMENTATION PERFORMANCE AS A FUNCTION OF DIFFUSER AREA RATIO EMPLOYING HYPERMIXING NOZZLE AND DIFFUSER BLOCKAGE.

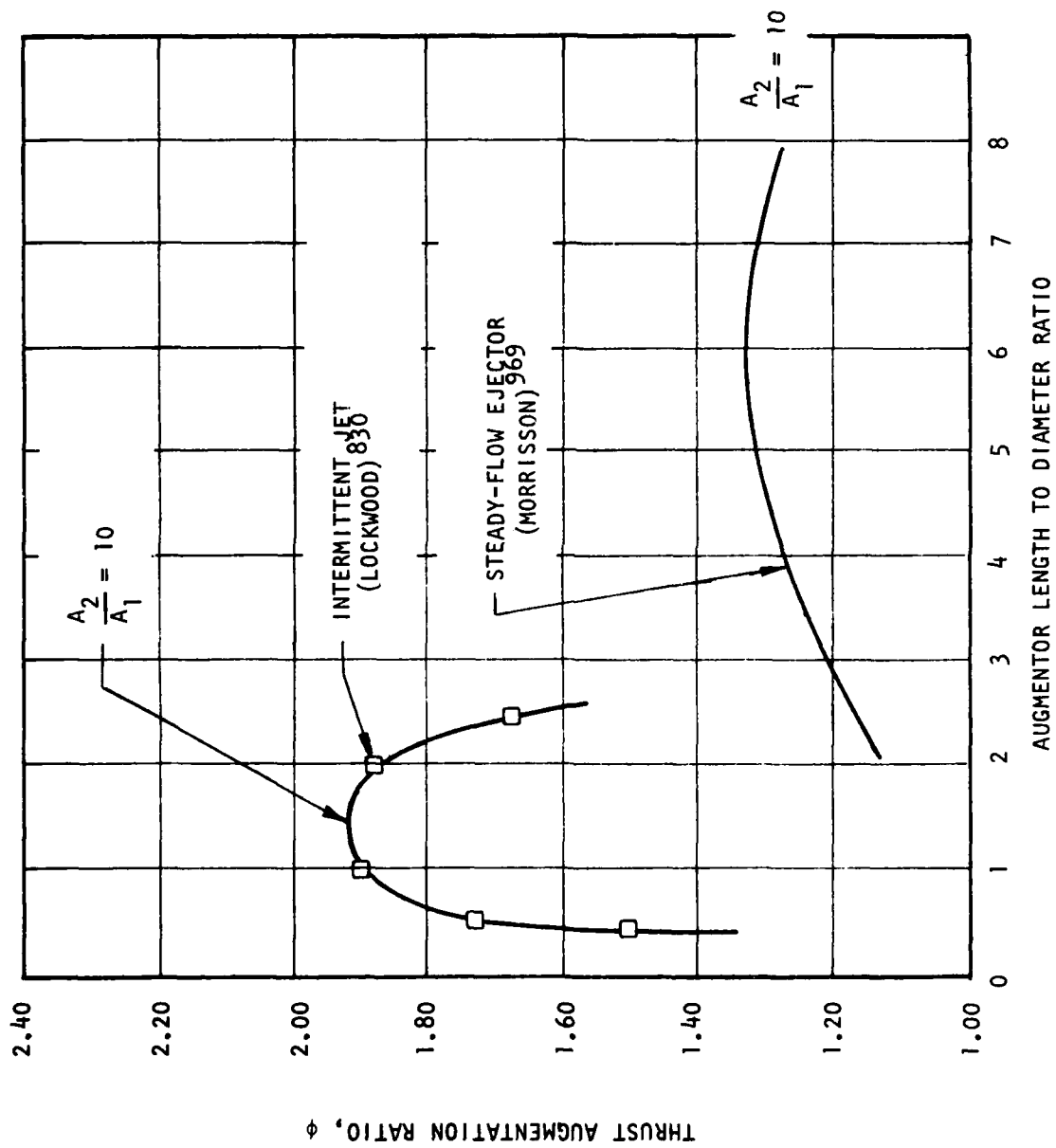
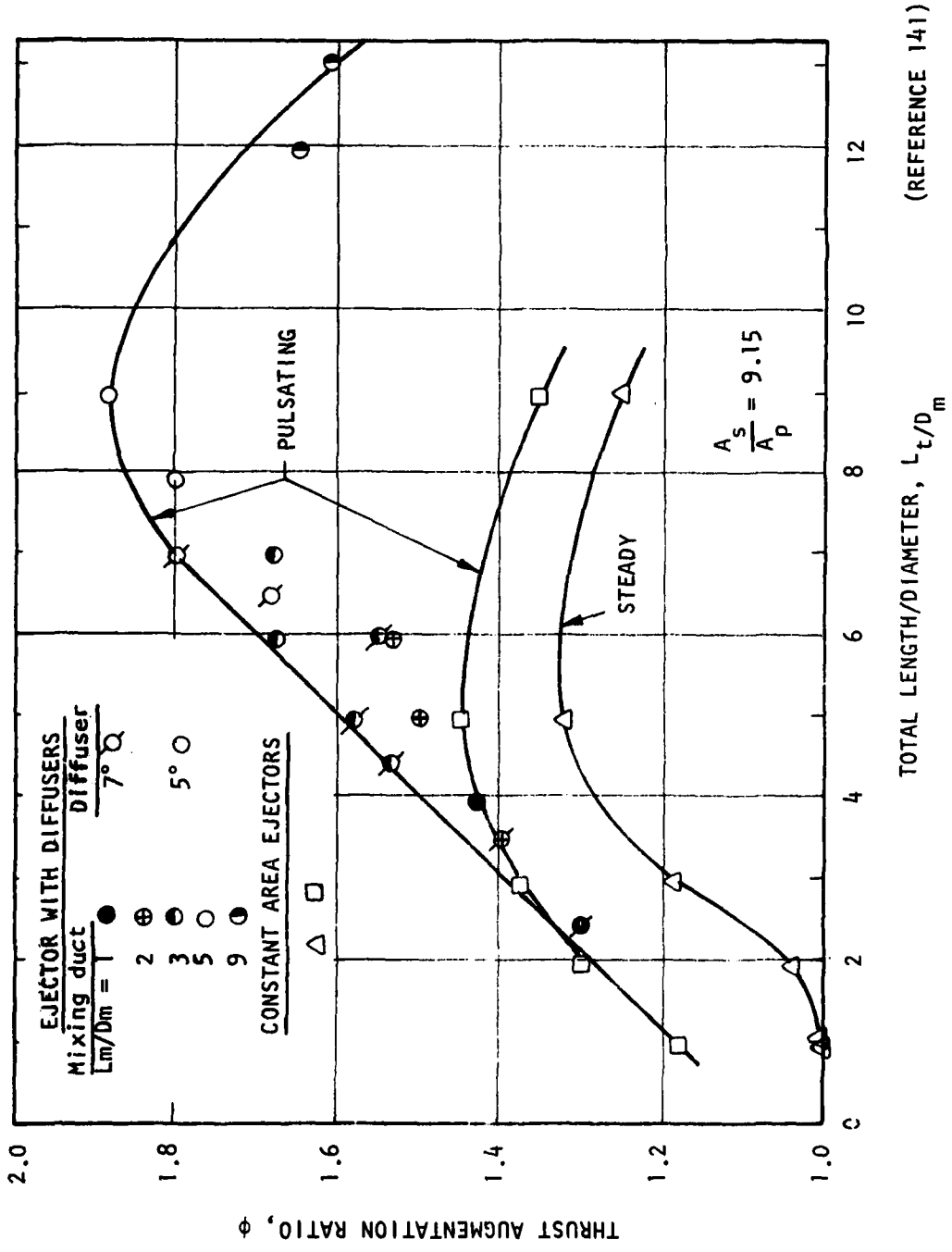
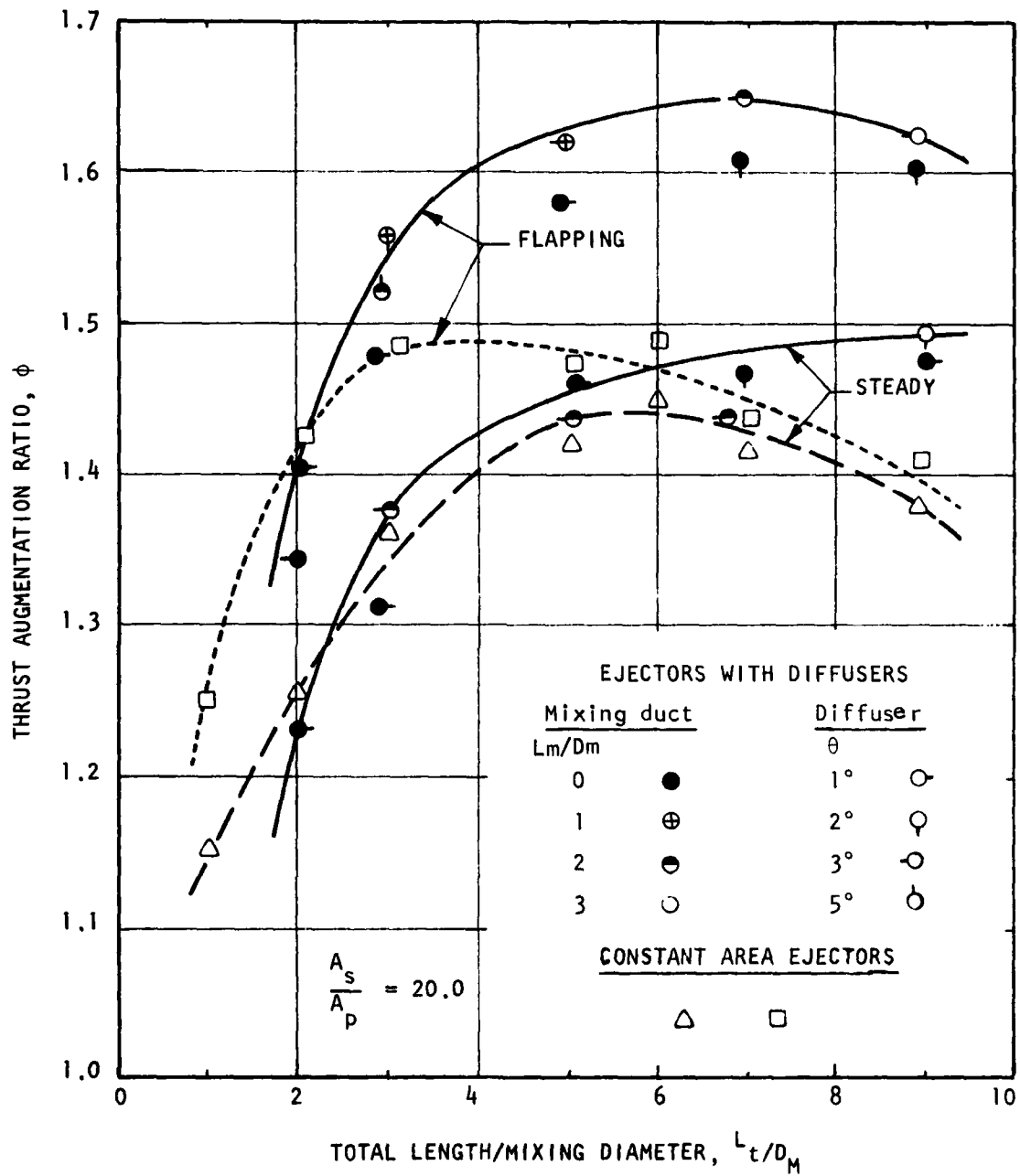


FIGURE 39. EFFECTS OF NON-STEADY PRIMARY FLOW FOR NON-DIFFUSING EJECTORS.



(REFERENCE 141)

FIGURE 31. AUGMENTATION PERFORMANCE AS A FUNCTION OF TOTAL LENGTH FOR STEADY AND PULSATING JET AXISYMMETRIC EJECTORS.



(REFERENCE 141)

FIGURE 32. AUGMENTATION PERFORMANCE AS A FUNCTION OF TOTAL LENGTH FOR STEADY AND FLAPPING JET 2-D EJECTORS.

ratios in non-diffusing ejectors, the pulsating ejector provided improved thrust performance. With the addition of a diffuser, the peak augmentation was greatly improved for the pulsing primary ejector. All the axisymmetric ejectors tested were at an inlet area ratio of 9.15. The pulsed primary ejector with a diffuser area of 2.89 achieved a peak augmentation ratio of 1.90.

Similar improvements in thrust performance for steady versus non-steady flows are shown in Figure 32 for two-dimensional ejectors. The unsteadiness of the primary in the 2-D ejectors was generated by a fluidically controlled flapping nozzle, similar to that of Viets. Improvements in augmentation ratio for the flapping primary nozzle ejectors were not as significant as those from the pulsed ejectors. Although the flapped flow ejectors were operated in a 2-D configuration and not an axisymmetric device, the results indicate that pulsing the primary is a more efficient technique for introducing unsteadiness to the ejector flow.

It is interesting to note that, in recent years, improvements in ejector augmentor performance have been obtained over what had appeared previously to be a limit of experimental results, as shown in Figure 33. The performance improvements indicated in Figure 33 are all for devices which either used non-steady primary flows, or some form of flow-control such as "jet flaps" or hypermixing nozzles.

4.2 SECONDARY INLET SECTION

The primary function of the ejector inlet section is to bring the secondary gas into the region of the primary nozzle exhaust with minimum losses. The inlet section geometry, with respect to the primary nozzle and mixing section geometries, determines the magnitude and flow quality (skewness) of the secondary fluid. In the following paragraphs, the performance of the ejector as a function of the inlet section will be presented for zero external flow velocity (static ambient) of the secondary fluid. Information gathered in Phase I of this study indicates that to achieve optimum inlet performance for an ejector in forward flight, a variable geometry configuration will be required (See Appendix B). This conclusion is well-founded in the fundamentals of flight propulsion-inlet design, and a majority of the vast amount of material available for designing inlets (for instance, in such books as the NAVWEPS Report 1488, Handbook of Supersonic Aerodynamics, Volume 6, Section 17, Ducts, Nozzles and Diffusers) is directly applicable.

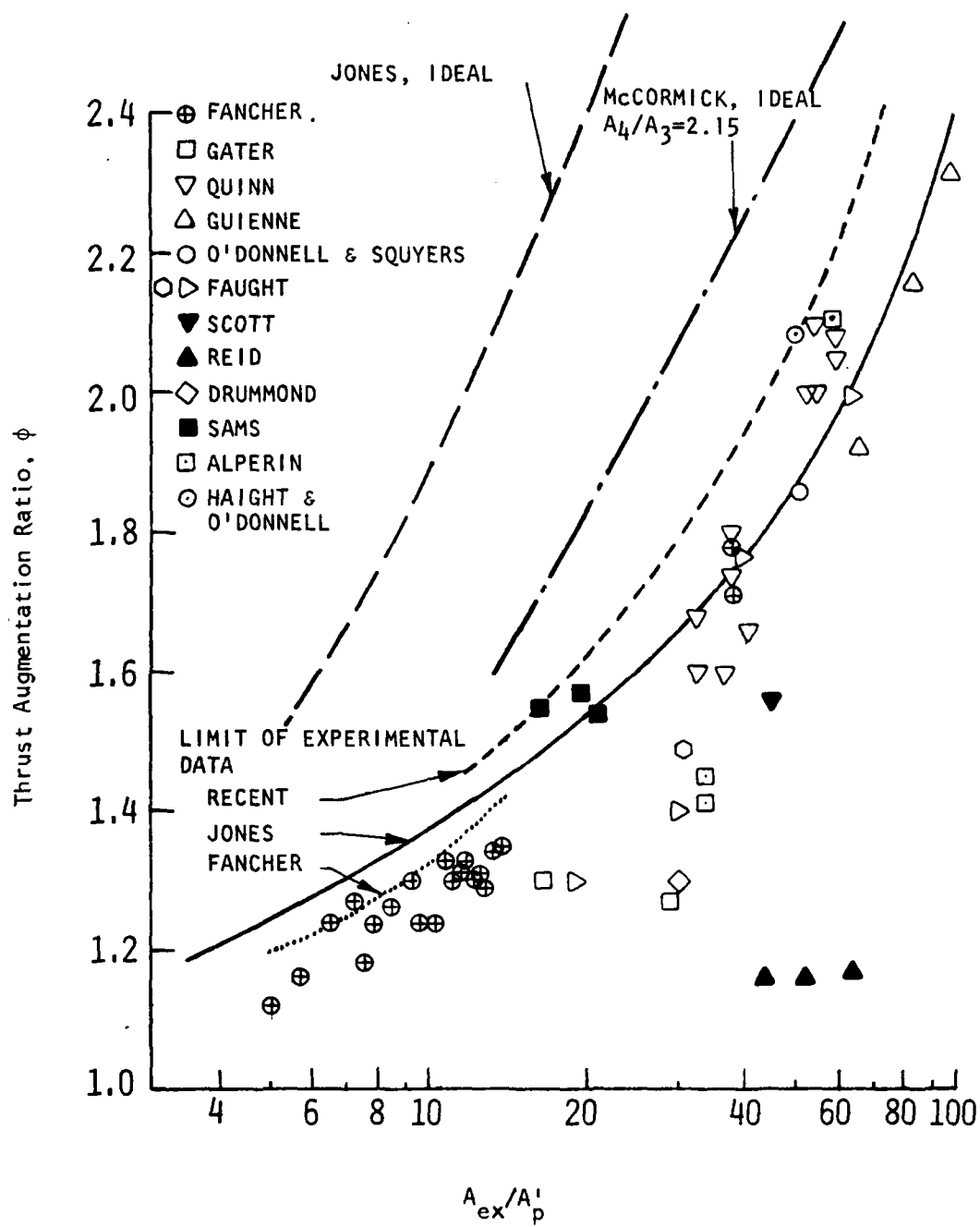
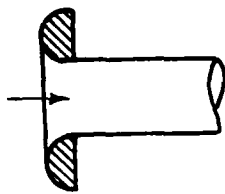


FIGURE 33. SUMMARY OF EJECTOR THRUST AUGMENTATION PERFORMANCE

Although a variety of inlet section shapes have been tested previously (see Figure 34), most of the previous experiments with ejectors have not used the inlet geometric shape as a major performance parameter. The relationship of the inlet area to the primary flow exhaust area, however, has been a significant parameter in many experiments. Figures 35 and 36 show the experimental results for ejector thrust augmentation as a function of inlet area with respect to the primary nozzle location. The inlet area ratio in these experiments was varied by simply displacing the location of the primary flow exhaust plane in a converging inlet section. The ejector configurations shown are for both diffusing and non-diffusing mixed flows. For both cases, the optimum performance occurs for X/W between 0.0 and 0.50. Thus, the primary nozzle should be located within the plane of the inlet for these configurations. The correct extent of the insertion is a function of the initial primary operating condition and the inlet/primary nozzle geometry. The data shown are for single convergent, primary nozzles exhausting into a constant area mixing section. The significant variations in augmentation results indicate that this parameter, x/w , is highly important and in general, should be used as an optimizing variable in experimental testing. Once a low loss inlet geometry has been defined, the variation of the inlet area ratio with other parameters held constant can improve thrust augmentation. Figure 37 shows the trend of increasing augmentation ratio with increasing inlet area ratio for fixed initial operating conditions. The trend is observable in thrusting ejector systems as long as a sufficient amount of primary flow energy is available to entrain the secondary fluid, and the proximity of the inlet wall is close enough to enclose the entrained gas. The free jet entrainment properties of the primary nozzle tend to dictate the maximum allowable distance of the inlet wall from the primary nozzle exit.

4.3 INTERACTION SECTION

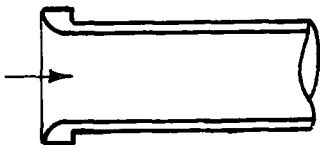
The major flow phenomenon with the greatest impact upon ejector performance is the interaction process. Most steady-state analyses assume that a sufficiently long interaction section is available to generate a uniform mixed flow profile. Several recent analytical and experimental efforts have been conducted to describe and understand the requirements for efficient complete mixing and the basic mechanisms of the mixing process; Kotwal, Reddy, and Kar,⁷⁶⁶ Spencer and Jones,¹³⁰¹ Quinn,¹⁰⁹³ Chriss and Harsha,²³² and Duvvurri, Raghunath, and Park.³³⁴ As stated in Section 3, a major assumption is that for a given configuration and operating parameters, the mixing process either occurs at (1) constant area, or (2) constant pressure boundary conditions. Opinions conflict as to which process



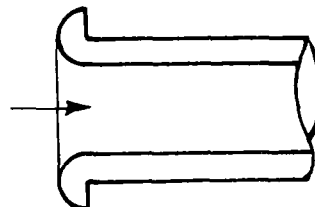
Bell Mouth



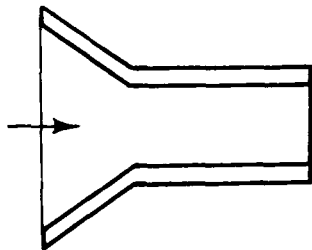
Half
Circular Arc
($r = d/8$)



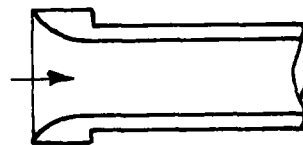
Half
Circular Arc
($r = d/4$)



Circular Arc
($r = d/2$)



Conical



Transitional

FIGURE 34. SCHEMATICS OF VARIOUS EXPERIMENTAL EJECTOR INLET SHAPES.

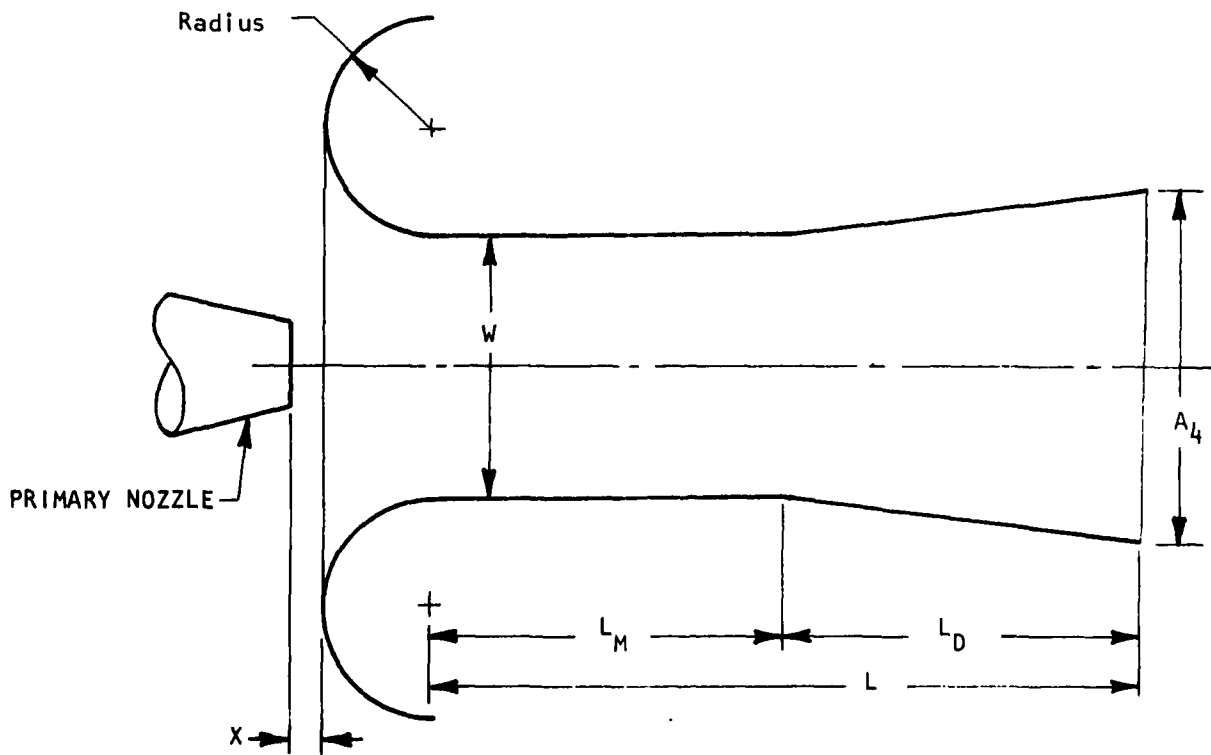
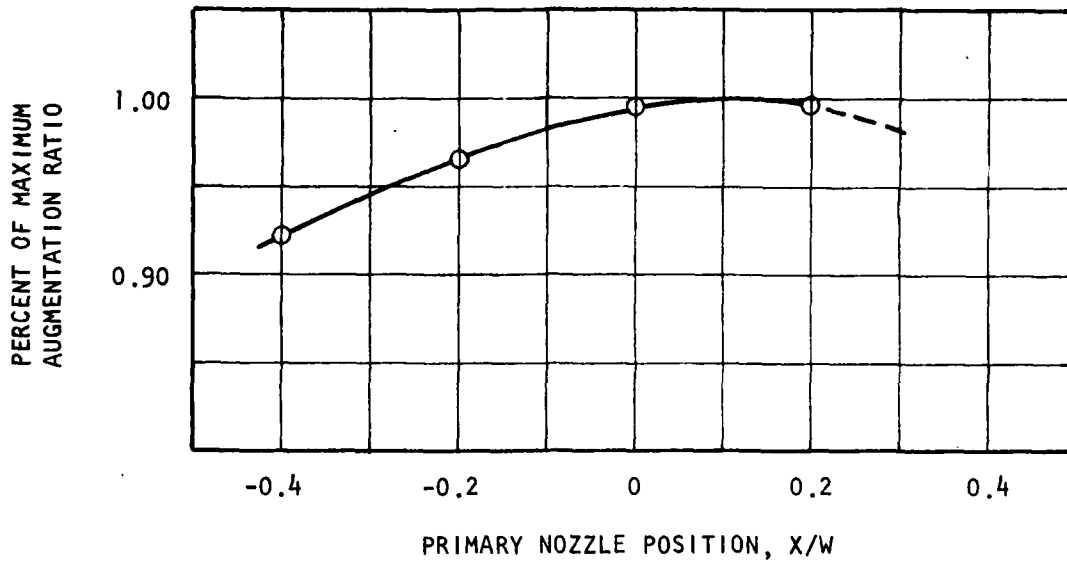
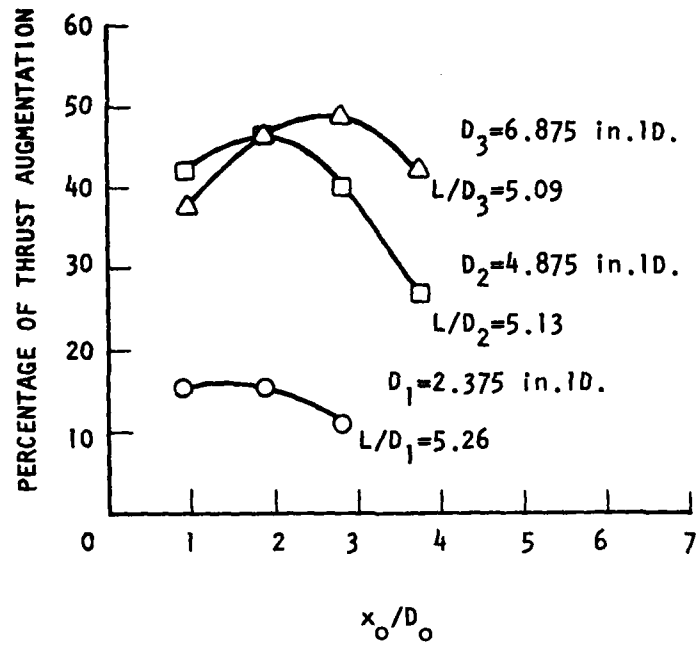


FIGURE 35. EFFECT OF PRIMARY NOZZLE POSITION ON RELATIVE THRUST AUGMENTATION RATIO FOR A 2-D EJECTOR.



AIR FLOW=1.07 lb_m/sec

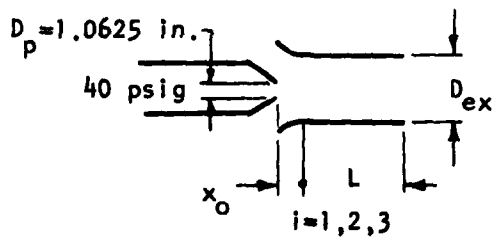


FIGURE 36. EFFECT OF PRIMARY NOZZLE POSITION ON RELATIVE THRUST AUGMENTATION RATIO FOR AN AXISYMMETRIC EJECTOR.

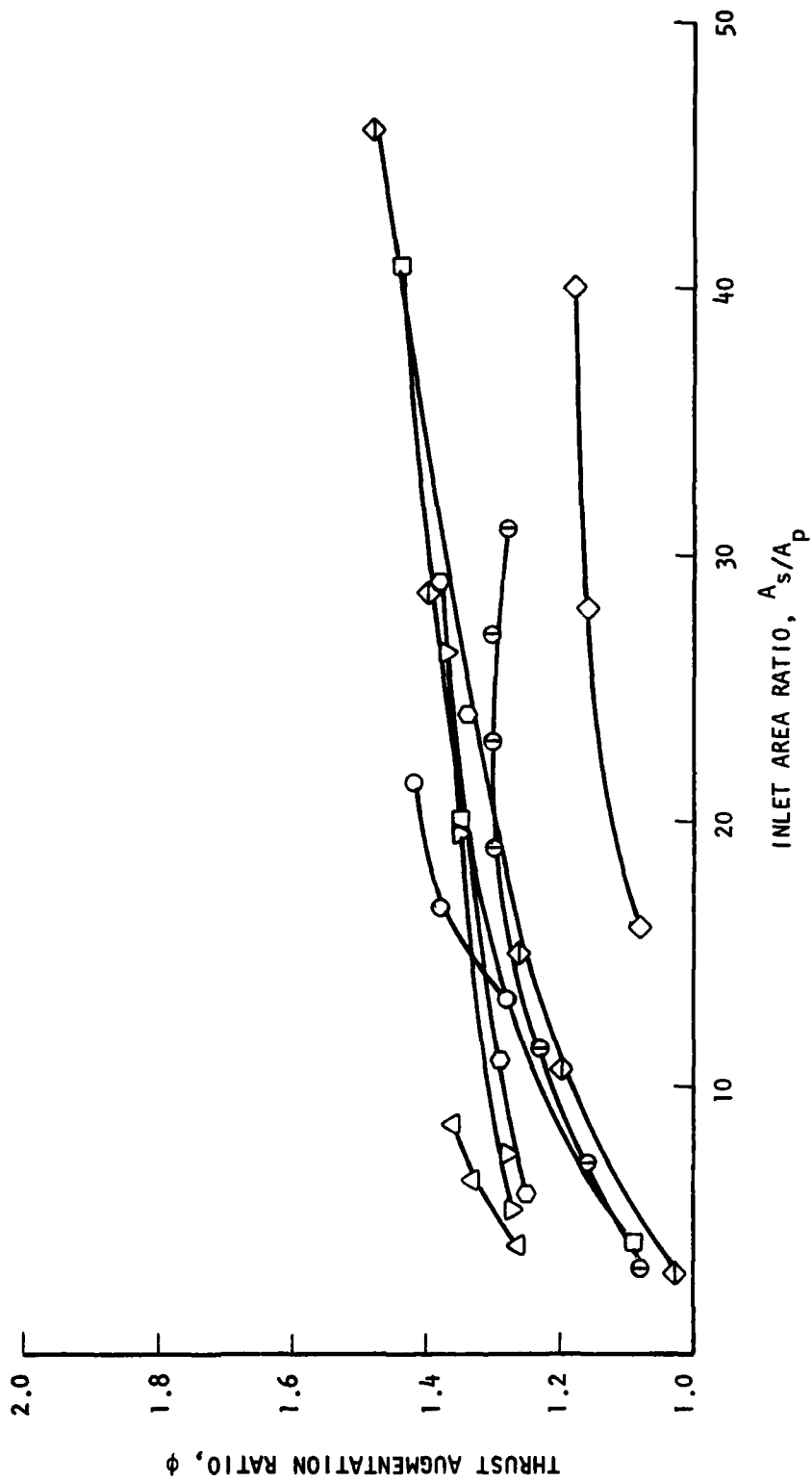


FIGURE 37. GENERAL TREND OF AUGMENTATION RATIO AS A FUNCTION OF INLET AREA RATIO.

is the most efficient. Empirical results have been obtained which show each process to be superior.

The primary and secondary flows enter the mixing section in the form of two distinct separate flows. These flows may possess the same gas characteristics but exhibit dissimilar flow parameters. Due to the presence of non-uniform flow properties, the separate flows interact through the phenomenon of turbulent mixing. A schematic of a typical mixing section process is shown in Figure 38. Although the figure illustrates the distribution of velocity in one plane, the actual mixing process, regardless of section geometry, is a three-dimensional process. Depending upon the initial flow parameters and the geometric boundaries of the mixing chamber, the mixing which occurs is a function of the mixing length available. In general, as the mixing section length of an ejector is increased from zero (a zero length mixing section may occur when all mixing takes place within the ejector diffuser) for either subsonic or supersonic primary nozzle flows, the performance of the ejector will improve. When the mixing process is nearly complete, if the mixing length is further increased, the skin friction effects begin to accumulate and become dominant. Further increases in length then degrade the augmentation performance. The optimum length varies with these two flow phenomena, and for non-diffusing flow, various investigations have determined the optimum ratio of L_2/D to be between 4 and 8. Multiple primary nozzle arrays will, in general, require a smaller ratio, while single primary nozzles require more mixing length. Other factors which influence the optimum ratio are the amount of entrained flow and whether the primary is subsonic or supersonic. From a microscopic viewpoint, it is probable that the length required for complete mixing is related to the mean free paths of the primary and secondary molecules, but to date, no explicit relationship of this type has been formulated. As discussed in Section 3.3, mixing length hypotheses have been used to predict the required mixing distance, but these, too, appear to be highly unreliable.

In considering microscopic vs. macroscopic mixing effects, it appears that large scale structure is more effective than small scale structure for mixing purposes. This is simply due to the difference in the rates of energy transfer accomplished by the small scale structure vs. the large scale. In the latter case, the primary flow can actually engulf and entrain rather large amounts of fluid, as shown by Roshko and Brown¹⁷⁶ for a mixing layer and Bevilaqua and

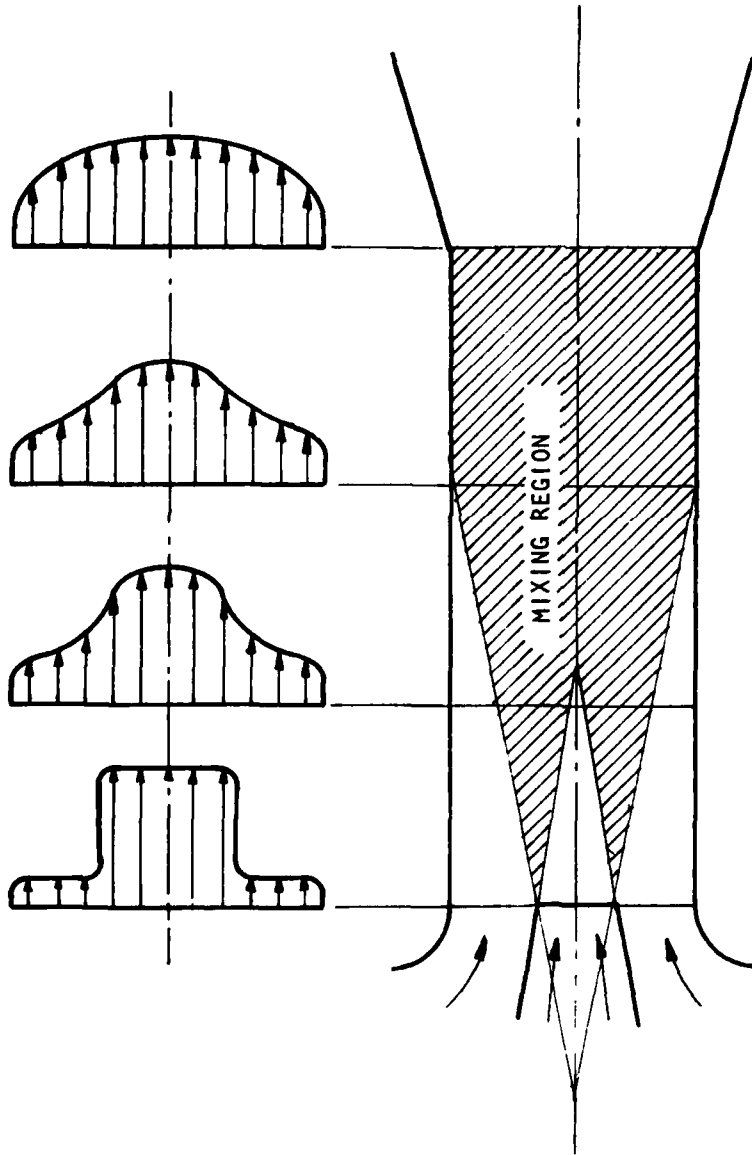


FIGURE 38. TYPICAL VELOCITY DISTRIBUTIONS IN AN EJECTOR MIXING CHAMBER

Lykoudis¹³⁶ for a turbulent wake. The relatively large entrained mass is rapidly accelerated by the entraining flow and assimilated.

Some of the traditional methods of large scale stimulation are boundary layer trips and vortex generators. More recently, streamwise vortices have been created in the jet case by inclining segments of the jet at an angle to other segments as in the hypermixing jet case, originated by Quinn.¹⁰⁸⁹ Time dependent flows have also been investigated in this regard and produce a transverse vortex structure by mechanical,^{142,414} acoustic,²⁷⁸ and fluidic¹⁴²² means. In the case of flows where the large scale structure of the flow is further enhanced by these special methods (e.g. hypermixing, vortex generators, unsteady flow), it is unlikely that the microscopic structure has any noticeable effect at all, since the flow is dominated by the macroscopic scale.

Comparison of the total ejector performance parameters, ϕ and β , enables a comparison of the efficiency of the mixing process for various devices. Using previous experimental efforts, the impact of the more critical mixing section geometric parameters upon ejector performance is described below.

As stated earlier, the mixing section geometry may be either decreasing area (approximately constant pressure), constant area, increasing area (i.e., diffusing), or combinations of the above geometries as illustrated in Figure 39. The mixing section length is usually normalized with respect to the characteristic width of the mixing chamber, L_M/D . The augmentation performance of several constant area mixing ejectors without diffusers is shown in Figure 40. By maintaining the ejector geometry and varying the mixing length, the influence of length on the mixing process can be determined. For all types of ejectors shown, with either subsonic or supersonic primary flow, the augmentation performance is shown to improve with mixing length to a maximum and decrease with further increases in length. The actual three-dimensional geometries of the mixing section can determine the efficiency of the mixing process. Basically, with the exit plane of the primary nozzle located at the onset of the mixing section, Cheng, Wang, and Chisel¹⁶¹³ show that there is an optimum position of the jet for given operating and geometric conditions. If the exit plane is too far from the proximity of the inlet, the secondary velocity is reduced and if the exit plane is too close, the secondary flow is constricted. Hasinger⁵⁵⁰ concurred that the actual geometric shape of the mixing section is an important parameter. Seiler's results¹²⁴¹ have shown that flow in a rectangular cross-section, due to "corner" effects, is less favorable for the mixing and transverse

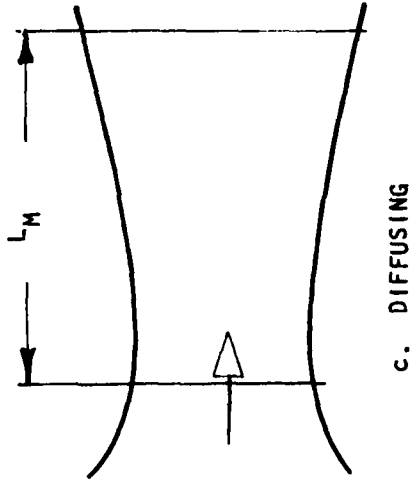
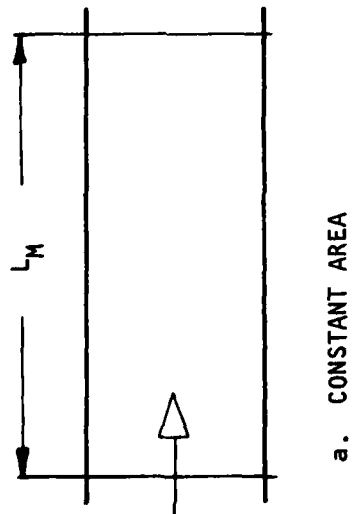
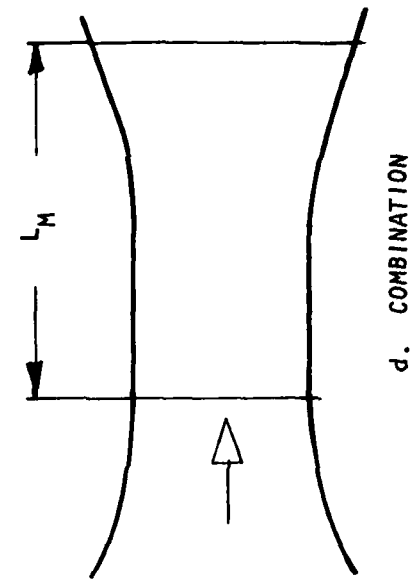
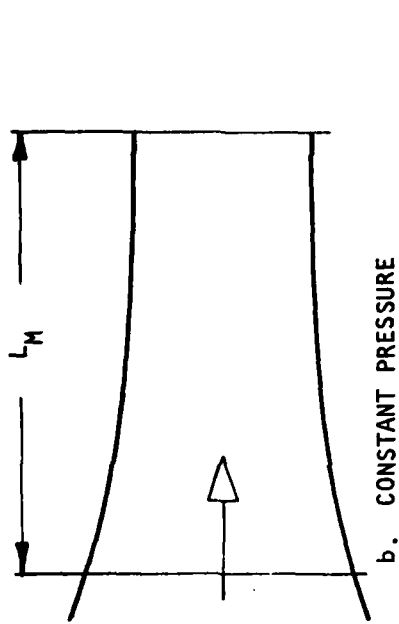


FIGURE 39. SCHEMATIC ILLUSTRATIONS OF BASIC MIXING SECTION SHAPES.

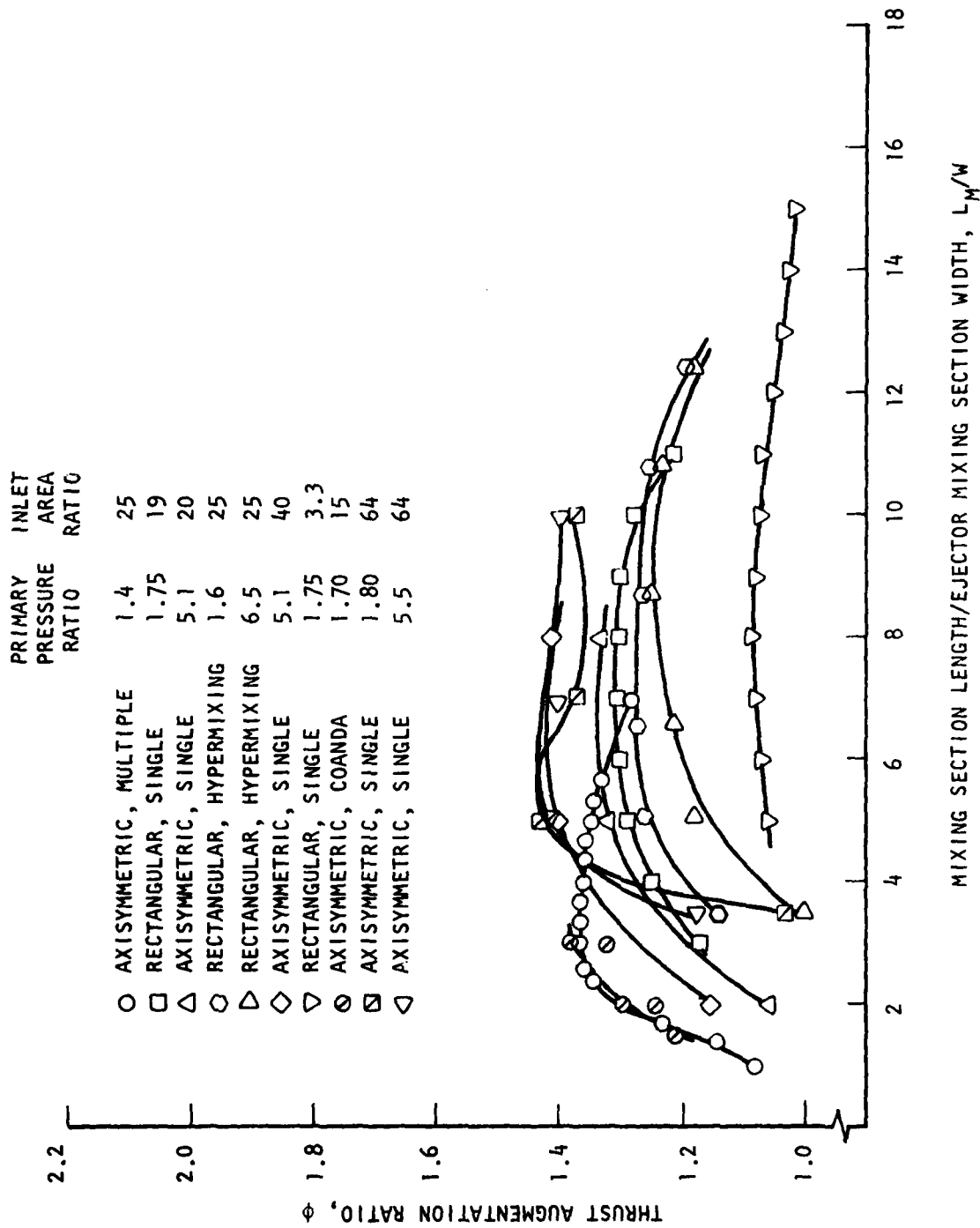


FIGURE 40. AUGMENTATION PERFORMANCE OF CONSTANT AREA MIXING EJECTORS WITHOUT DIFFUSERS.

flow than a circular section of an equivalent cross-sectional area. Given a sufficient length, the mixing process will be completed, after which, as mentioned previously, the internal viscous losses start to dominate the thrust performance. Mixing is completed in a shorter distance whenever multiple primary nozzles are used, and, as indicated in Figure 39d, may continue to take place in the diffuser section.

The mixing process has been shown by Von Karman¹⁴⁴² and Jones⁶⁸⁰ to be enhanced whenever flow skewness in the secondary is increased, by imparting flow skewness in the primary flow as shown by Jones,⁶⁸⁰ Fancher,³⁷⁷ Quinn,¹⁰⁹¹ Bevilaqua,^{133,137} and Salter,¹¹⁸¹ and by the use of hypermixing primary nozzles as discussed earlier. Jones⁶⁸⁰ indicated that a tradeoff between inlet flow skewness and diffuser area ratio exists and that maximum increase in augmentation ratio cannot be obtained simultaneously from both mechanisms.

The parameter of the mixing section which has the greatest impact on thrust augmentation ratio is the ratio of the mixing section length to section width, L_M/D . The results of experiments where this parameter has been investigated are consistent. For a subsonic secondary/supersonic primary flow in an axisymmetric mixing section, Morrisson⁹⁶⁹ has shown that, in the absence of a diffuser, the maximum augmentation ratio occurs for an L_M/D of approximately 6. For a subsonic two-dimensional slot nozzle configuration with no diffuser, Drummond and Gould have shown the maximum augmentation ratio also occurs around 6. McClintock and Hood⁹⁰⁰ show for a multiple subsonic primary array that the optimum L_M/D ratio is about 4.

Quinn¹⁰⁹⁰ shows that as the pressure ratio of a supersonic nozzle is increased, primary Mach number increases, and the optimum L_M/D ratio increases from approximately 5 to 10 in a non-diffusing ejector. This same trend in a non-diffusing supersonic primary ejector was shown by DeLeo and Rose³¹¹ where the optimum L_M/D ratio went from 6 to 8 for increasing the primary pressure ratio from 4 to 12.

Keenan and Neumann⁶⁹⁷ have shown for a simple supersonic ejector consisting of a primary nozzle and a cylindrical mixing tube with a rounded inlet, that constant area mixing is better than constant pressure mixing except for inlet area ratios less than 10. Below 10 some combination of the two gives the best results, e.g., a short constant pressure mixing length preceding a constant area mixing section. Hasinger,⁵⁵³ on the other hand, has stated that with a supersonic conical axisymmetric central nozzle, in contrast to a constant area mixing process, the

performance of the ejector improved with a tapered or nearly constant pressure mixing section, independent of area ratio. However, the general conclusion reached by Hasinger⁵⁵² was based on experimental results for devices with area ratios in the range cited by Keenan and Neumann. Constant pressure mixing thus appears to be more efficient for supersonic nozzles whenever the inlet area ratio is less than 10, or small secondary mass flows exist. The results of Chow and Yeh²³¹ indicate that the entrainment performance of a supersonic central nozzle ejector is better, at an inlet area ratio of 2.0, for a parabolic divergent shroud, compared with a constant area mixing section. This improvement in performance was consistent for increasing secondary to primary pressure ratios. For an annular subsonic primary nozzle, Spiegelberg,¹³⁰⁴ using a scaled model, and Gates and Cochran,⁴⁶⁴ for full scale test results, showed that a diffusing mixing section generated greater thrust augmentation ratios than constant area mixing. It is interesting to note as Payne did in the Phase I study (Appendix B) "that all of the successful ejectors shown in handbooks such as Mark's,⁸⁷⁸ have a characteristic necking down of the mixing chamber." No obvious explanation is available for such drastic disparities in experimental findings regarding the best mixing shape.

Inherent to the mixing process is the relationship of the secondary to primary mass flows, or entrainment ratio, β . The final mixed flow average values of flow properties, pressure, and temperature, and thus the mixing efficiency, are a direct function of β . Figure 41 illustrates the relationships of mixing length to entrainment ratio. Once a specified level of entrainment has been achieved by the primary nozzles and inlet section, then the mixing length required to maintain the flow is set. Beyond this minimum required length, additional mixing will not improve the entrained flow properties of the ejector or the augmentation performance. The fact that an upper limit to the augmentation ratio as a function of the entrainment ratio, β , appears to exist, may be noted in Figure 42. The upper curve in Figure 43 shows Heiser's result $\phi_{MAX} \leq \sqrt{1+\beta}$. The lower curve in the figure represents a limit-line for current state-of-the-art results and can be approximated by $\phi_{MAX} \text{ EXP}^{-L(M)} = (1+\beta)^{\gamma-1/\gamma}$. Relationships shown in Figure 42 between ϕ and β appear to be closely associated with the efficiency of the mixing process. Plots of ϕ vs. β for lines of various mixed flow entropy levels are shown in Figures 43-45 for various levels of initial pressure and temperature ratios. It is interesting to note, as shown on these plots, that by going to a larger device with higher entrainment, higher augmentation ratios may be obtained even though the mixed flow entropy level increases.

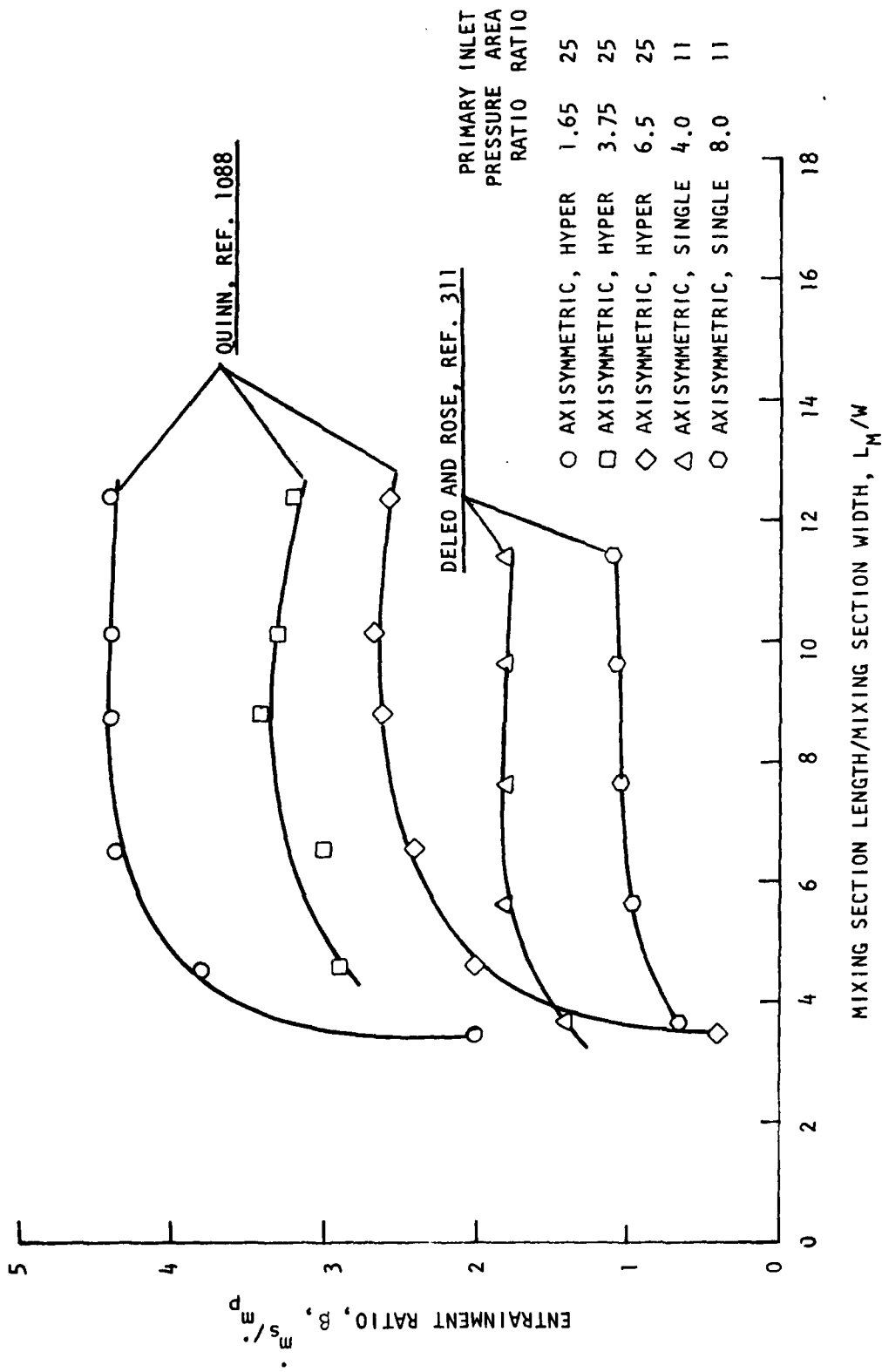


FIGURE 41. ENTRAINMENT RATIO, β_s , AS A FUNCTION OF MIXING SECTION LENGTH TO WIDTH RATIO.

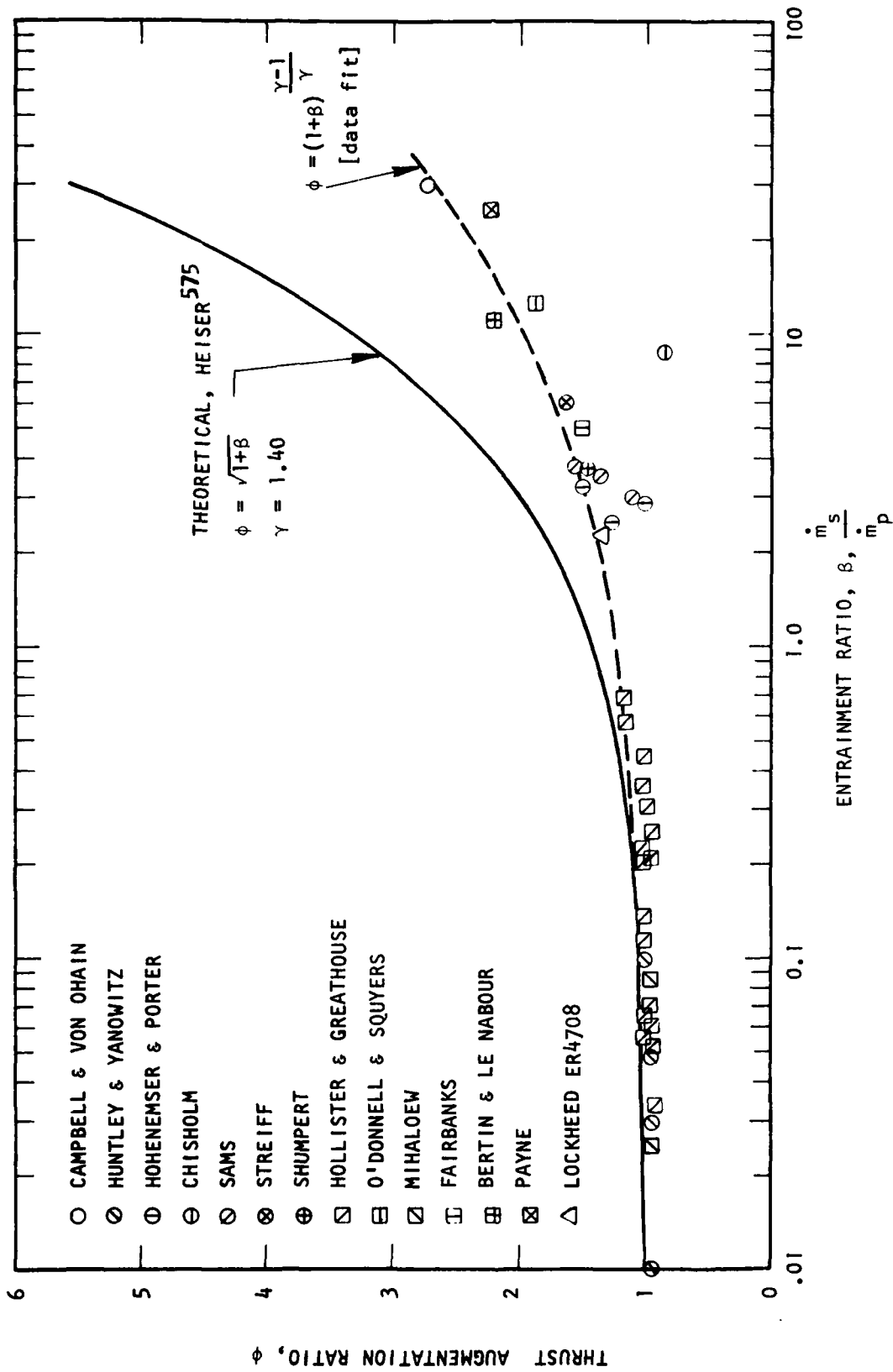


FIGURE 42. THEORETICAL AND EMPIRICAL LIMITS OF EJECTOR PERFORMANCE.

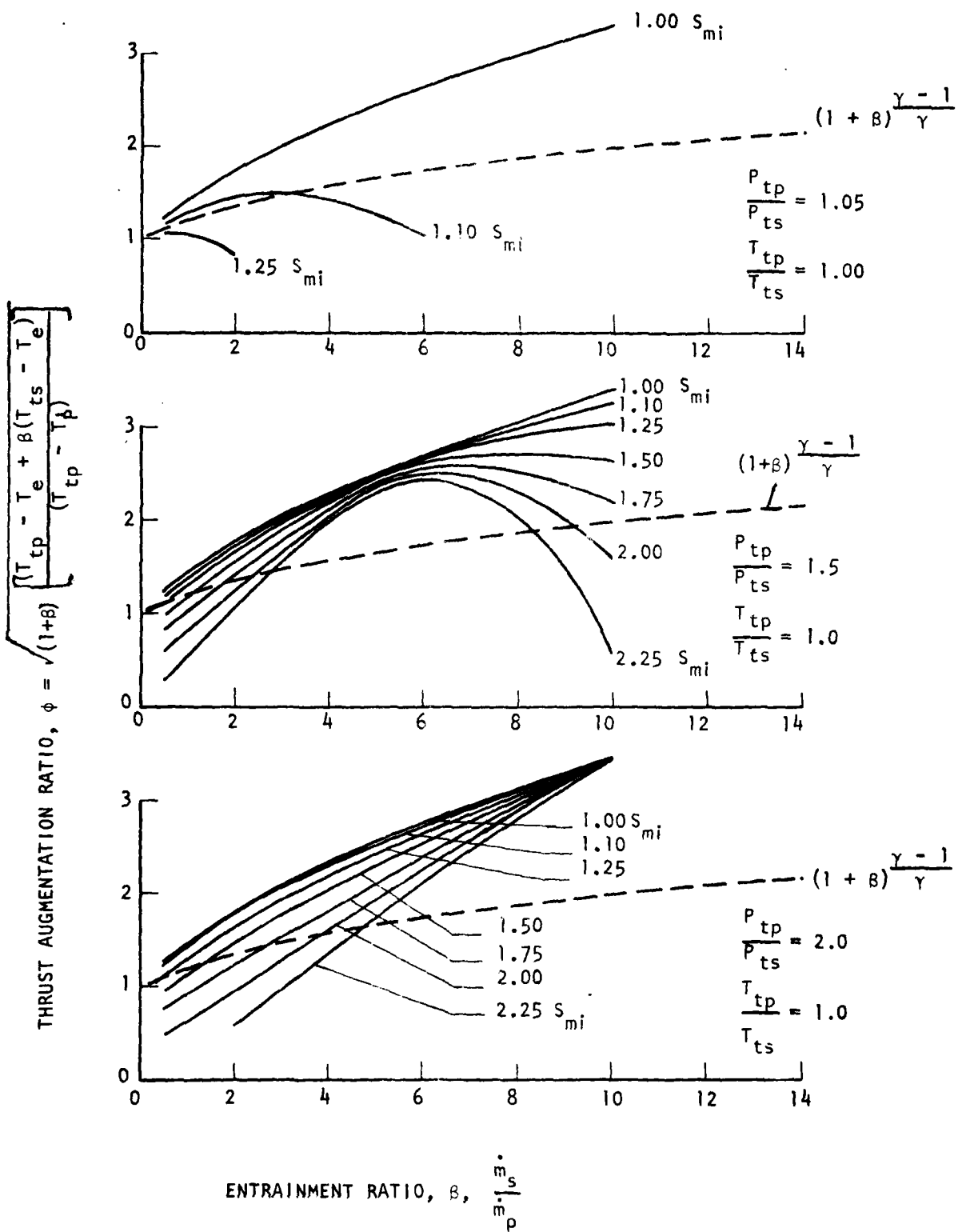


FIGURE 43. EFFECTS OF MIXED FLOW ENTROPY INCREASES FOR AN AUGMENTOR WITH AN INITIAL PRESSURE RATIO $P_{tp}/P_{ts} = 1.05$.

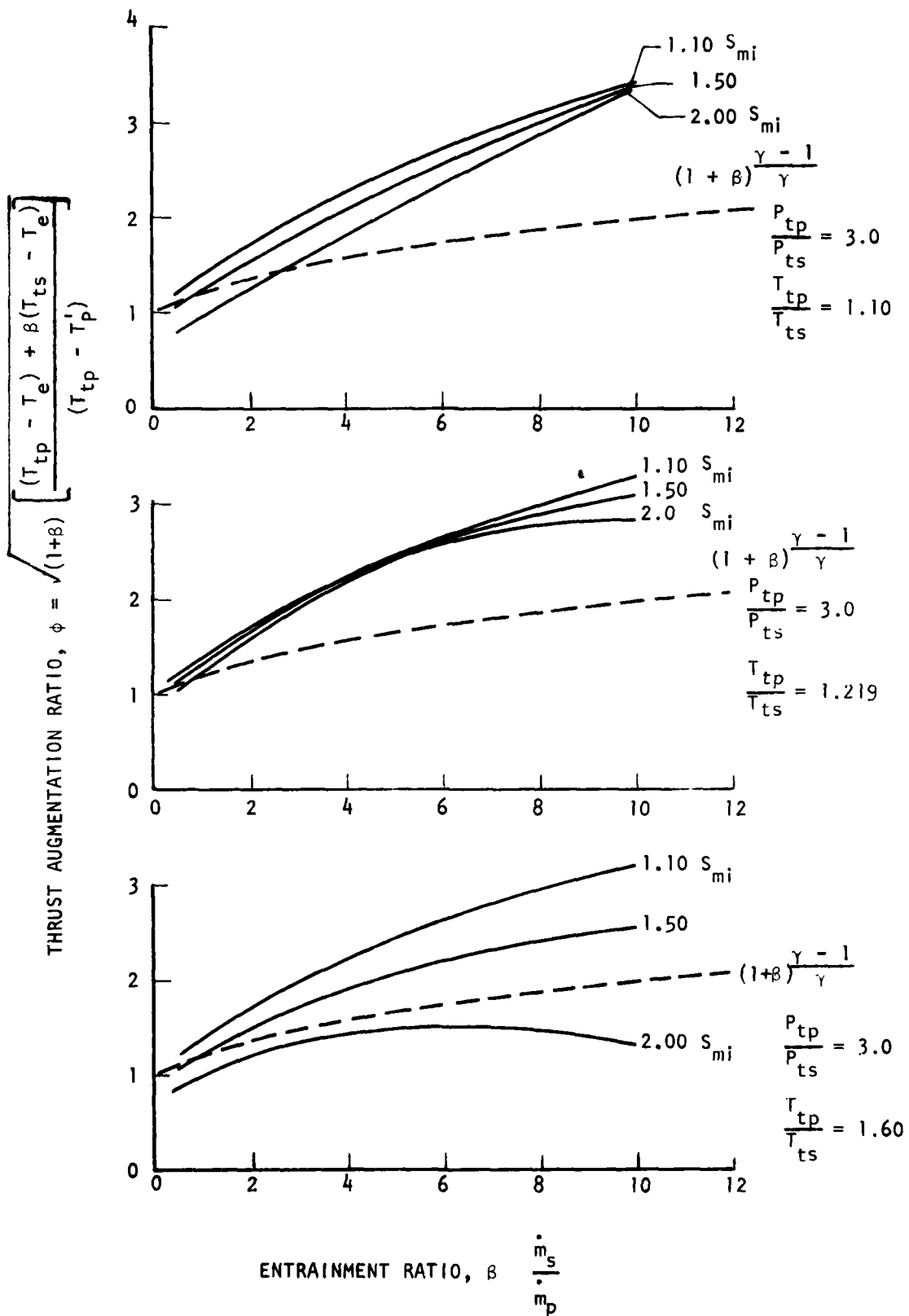


FIGURE 44. EFFECTS OF MIXED FLOW ENTROPY INCREASES FOR AN AUGMENTOR WITH AN INITIAL PRESSURE RATIO $T_{tp}/T_{ts} = 1.10$.

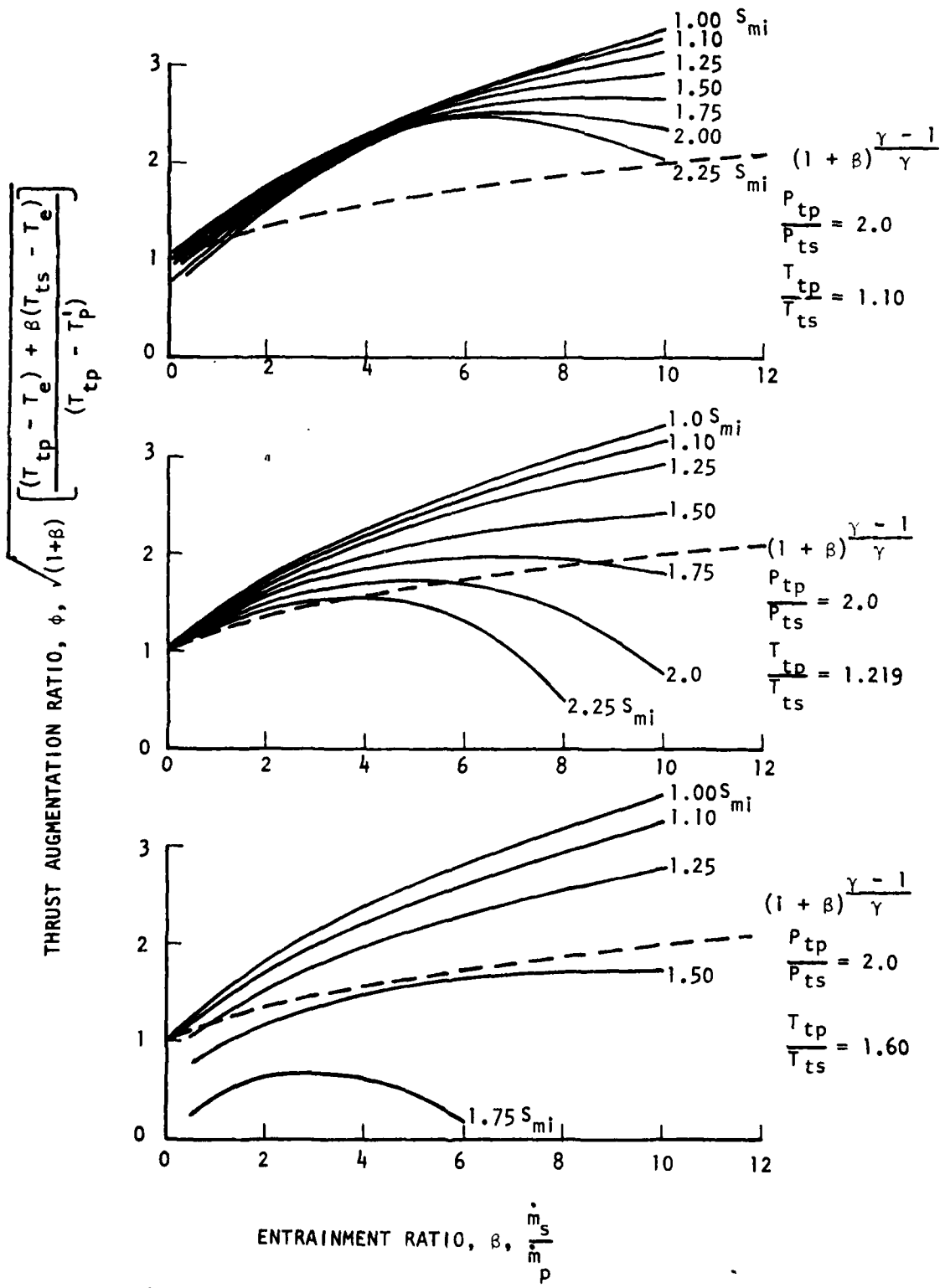


FIGURE 45. EFFECTS OF MIXED FLOW ENTROPY INCREASES FOR AN AUGMENTOR WITH AN INITIAL TEMPERATURE RATIO $T_{tp}/T_{ts} = 1.10$.

4.4 DIFFUSER SECTION

An efficient diffuser is a necessary requirement to achieve high levels of thrust augmentation in an ejector. The primary purpose of the diffuser section in a subsonic mixed flow ejector is to provide a mechanism for matching the ambient pressure boundary condition at the exit plane and maintaining an optimum mixing plane static pressure at a value less than ambient. Typical ejector diffuser configurations are illustrated in Figure 46. For supersonic mixed flow ejectors, Shapiro has shown that maximum thrust is achieved whenever the diffuser provides an exhaust flow static pressure equal to ambient pressure.

While the primary purpose is to match the ambient boundary conditions, ejector thrust augmentor diffuser sections also enhance the mass flow entrainment, by reducing the inlet static pressure, and thus increase augmentation performance. Experimental results, which investigated the impact of the diffuser design, illustrate the importance of the diffuser. By keeping all other operating parameters fixed and varying the diffuser area ratio, exit to entrance area, empirical results shown by Shumpert,¹²⁶³ McClintock and Hood,⁹⁰⁰ Bevilaqua,¹³⁷ and others illustrate that ejector performance for a specific configuration can be maximized by the diffuser configuration. In these results, the thrust augmentation is improved with increasing diffuser area ratio to a point of maximum performance, beyond which increasing the area ratio decreases the augmentation performance. The eventual loss in thrust performance is a direct result of high area ratio diffuser losses caused by partial or full wall boundary layer separation.

The performance of diffuser sections, and thus the total ejector, can be further improved by controlling the diffuser exit plane boundary conditions. By altering the manner in which the diffuser core flow achieves or matches the exit boundary conditions, improvements in thrust may be achieved. One method of achieving such improvements is through the use of the so-called jet flap diffuser which utilizes a containing jet stream to enable the core flow to achieve the ambient conditions downstream of the geometric exit plane as discussed by Alperin and Marlotte.³⁶ The jet flap diffuser is analogous to the jet flap wing, in that it is intended to prevent flow separation, provide a favorable pressure distribution near and at the trailing edge of the flap, and shorten the diffuser length for a given diffuser area ratio. The jet flap thus effectively provides a diffuser area ratio somewhat larger than the geometric area ratio represented by the diffuser hardware.

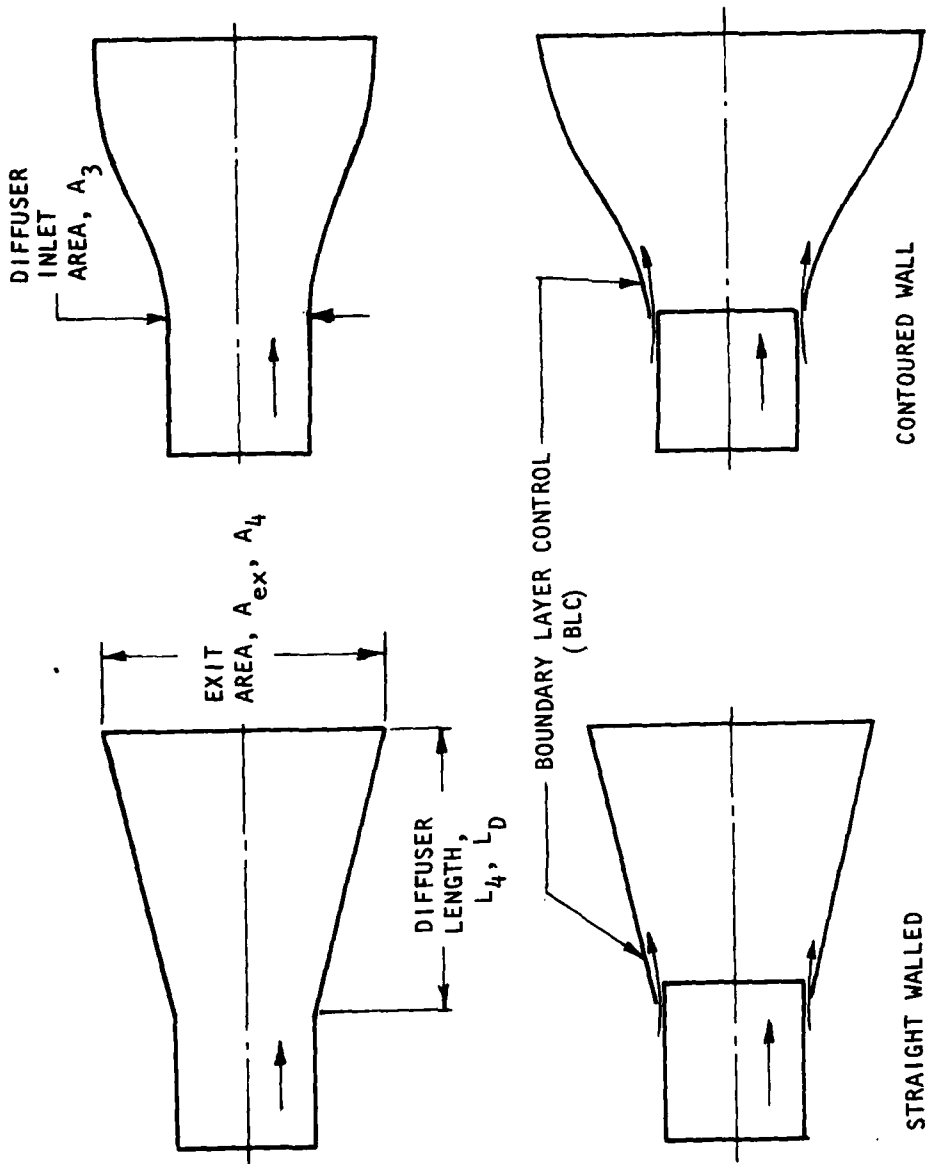


FIGURE 46. TYPICAL EJECTOR DIFFUSER CONFIGURATIONS.

For an ideal diffusion process, high diffuser area ratios (>2.50) generate large thrust augmentation ratios because their high pressure gradients allow low mixing inlet static pressures and large entrainment ratios. However, for most practical diffusers, with an area ratio greater than 2.0, the additional thrust increase resulting from higher area ratios is diminished and then dominated by viscous flow losses. Overall, with an efficient diffusion process following the mixing section, the thrust of the ejector will be increased, but for most ejector applications, the limiting diffuser area ratio is around 2.50.

The impact of a diffuser section is shown in Figure 47. For a fixed ejector configuration consisting of equivalent primary nozzle, inlet, and mixing sections, the addition of a diffuser improves the thrust augmentation ratio attainable. The improvement is shown to exist for the entire range of pressure ratios. A system penalty that can be attributed to the diffuser section is an incremental increase in ejector volume. However, an ejector which includes a diffuser, with the same volume as a non-diffusing ejector, will (or can) produce a greater thrust augmentation. A diffuser with a variable exit area allows for the modulation of system thrust for constant primary and secondary operating conditions.

While the thrust performance improvements achievable with the addition of a diffuser section are a direct result of increased secondary flow entrainment, the entrainment is also a function of the inlet area ratio and primary exit static pressure. Thus, proper coupling of the inlet area ratio, with the diffuser area ratio is necessary to achieve maximum thrust performance. The relationship between the diffuser and the inlet section is shown in Figure 48. Thrust augmentation for fixed operating conditions is improved as the inlet area ratio is increased for constant diffuser area ratio. For a given inlet area ratio the diffuser area ratio can be adjusted to achieve maximum performance. Figure 49 shows the results of optimizing ejector performance with the diffuser area ratio. The figure also illustrates the trend of greater levels of augmentation obtainable with increasing inlet area ratio. For each configuration the diffuser area ratio must be varied to maximize the entrained flow and thus the augmentation ratio.

The limiting factors on diffuser area ratio and total ejector performance are flow separation and skin friction of the internal flow. Flow separation occurs in the diffuser section whenever the diffuser boundary layer is unable to negotiate the adverse pressure gradient along the solid walls. Diffuser separation has a very strong influence on ejector performance. Significant separation very rapidly causes a reduction in augmentation, due to the fact that a separated

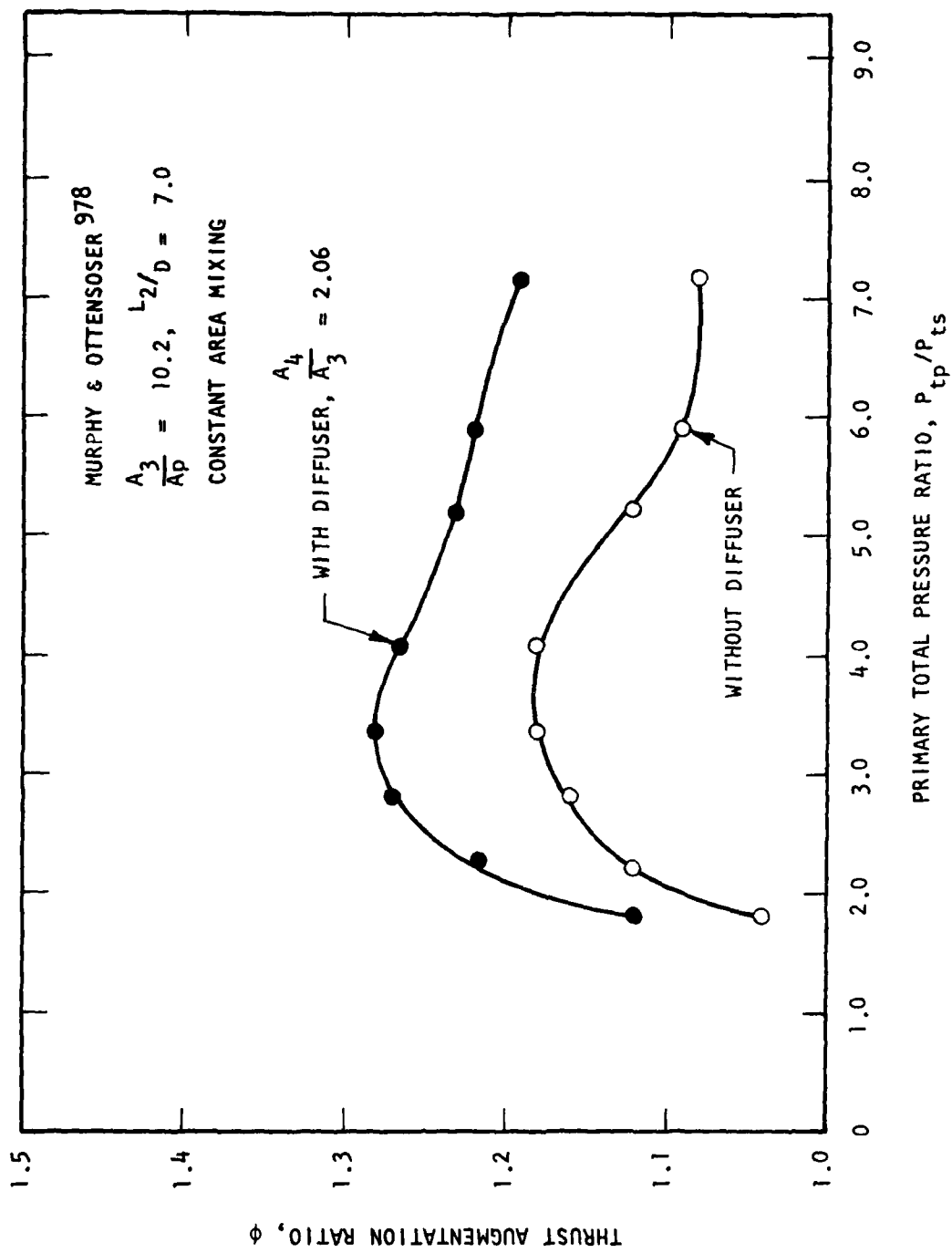


FIGURE 47. INFLUENCE OF A DIFFUSER ON EJECTOR AUGMENTATION RATIO AS A FUNCTION OF PRIMARY TOTAL PRESSURE RATIO

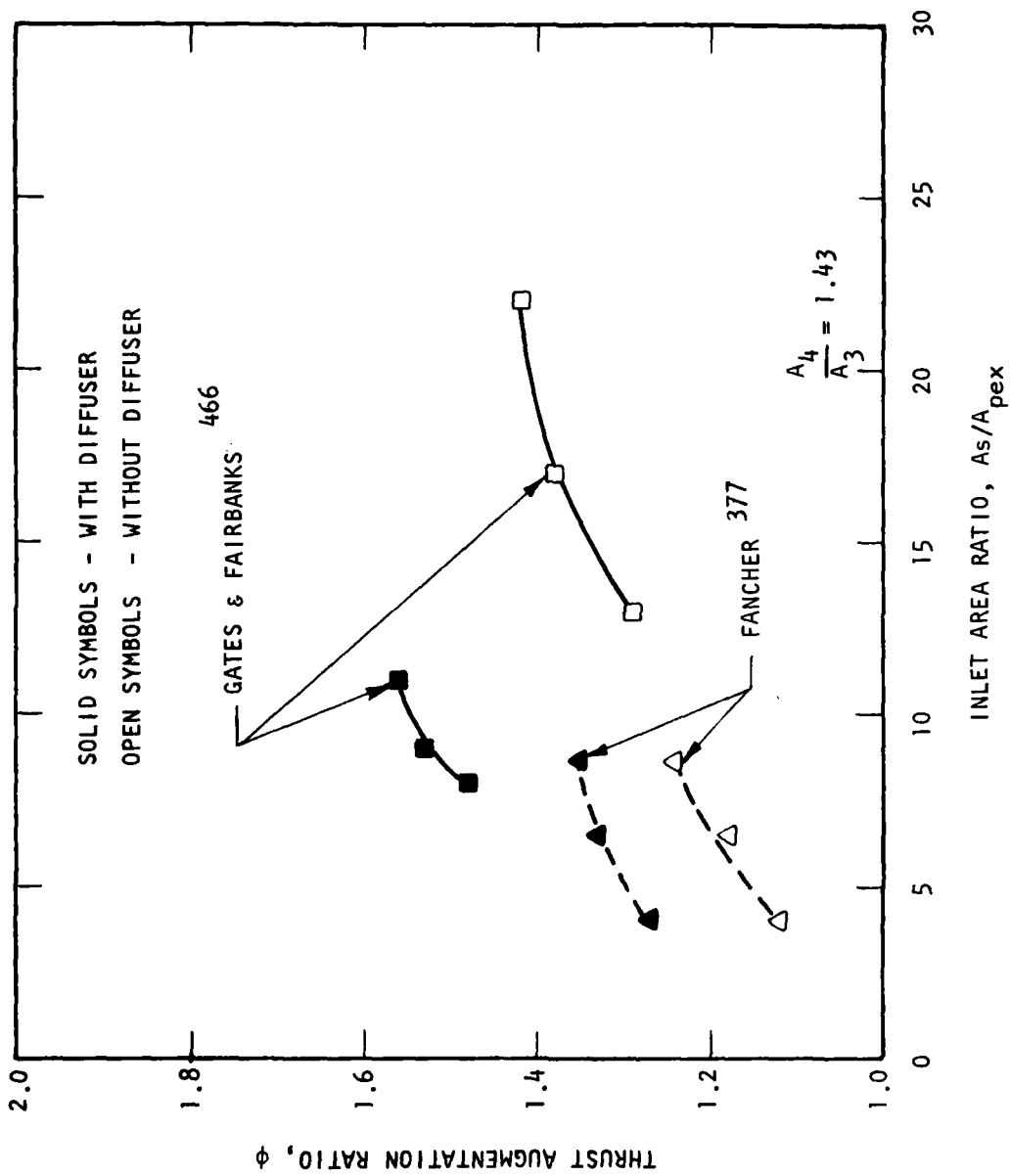


FIGURE 48. EFFECT ON AUGMENTATION RATIO OF THE RELATIONSHIP BETWEEN DIFFUSER AREA RATIO AND INLET AREA RATIO.

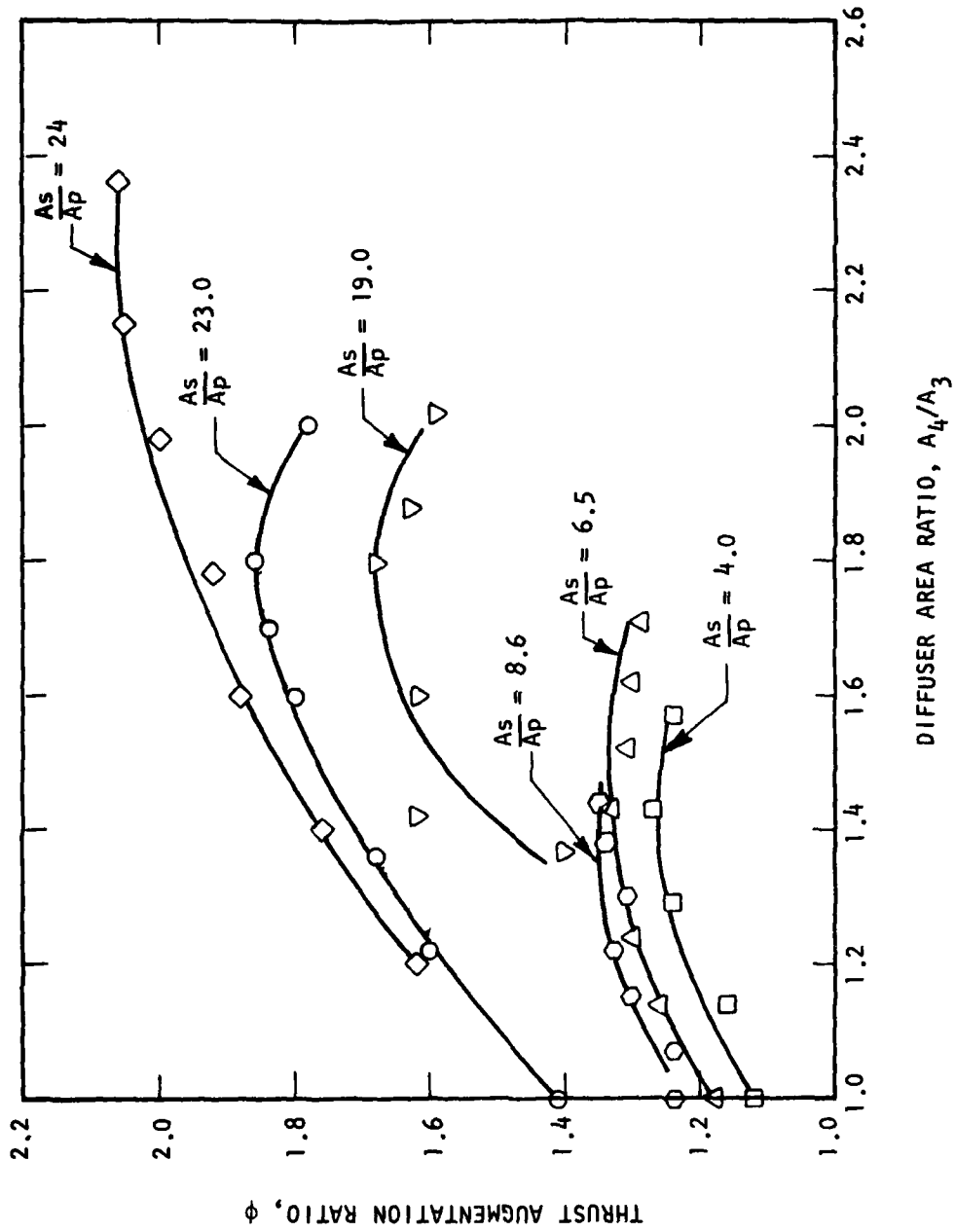


FIGURE 49. RESULTS FOR EJECTOR PERFORMANCE OPTIMIZATION THROUGH DIFFUSER AREA RATIO VARIATIONS.

diffuser can support only a reduced pressure ratio through it. This in turn causes an increase in the pressure within the ejector (since the downstream pressure is fixed at the ambient value), a reduction in entrained flow, and thus, a reduced augmentation. Figure 50 shows the impact of diffuser flow separation on thrust augmentation ratio and the influence of skin friction losses. As may be seen in the figure, the results are for ejectors with constant diffuser area ratio. As the diffuser wall half angle, θ , is increased while maintaining the diffuser area ratio, the result is to reduce the diffuser length, L_D . Thrust augmentation is improved as the angle is increased due to the reduction in diffuser length and corresponding reduction in wall skin friction. Whenever the length of the wall is reduced significantly, the diffuser wall boundary layer must negotiate too severe an adverse pressure gradient and subsequently separates from the solid boundary.

The effect of diffuser wall separation, as shown in Figure 50, can be catastrophic to the ejector performance. The geometric shape of the diffuser can also influence the location and extent of flow separation. If the diffuser is axisymmetric, the separation zone is generally localized. For two and three dimensional diffusers where the diffuser wall geometry is not consistent throughout, separation tends to occur on the non-diffusing or end walls, as discussed by Porter and Squyers.⁶¹⁴ Finite span ejector diffuser end walls tend to separate first because they are normally regions of limited flow control which must undergo the same pressure gradients as the diffusing walls.

By current theory, separation is likely to be more of a problem in model scale testing than in larger scale prototype testing, due to the fact that the Reynolds number of the model scale is generally below that of the prototype. This means that the inertial forces are smaller relative to the viscous forces, which produce the separation, than they are at the larger scale. However, the apparent situation may change if a Reynolds number for the two geometries is based on a characteristic mixing length scale, rather than a geometric characteristic.

Theoretically, increasing the diffuser area ratio, by increasing the diffuser wall length to maintain the diffuser half angle, can generate high levels of thrust performance. However, empirical results with long wall diffusers show that skin friction losses are increased and tend to diminish the gain due to increased area ratios. The major drawback to gradual sloping high area ratio diffusers (>2.0) is the increased volume of the section. High performance, high

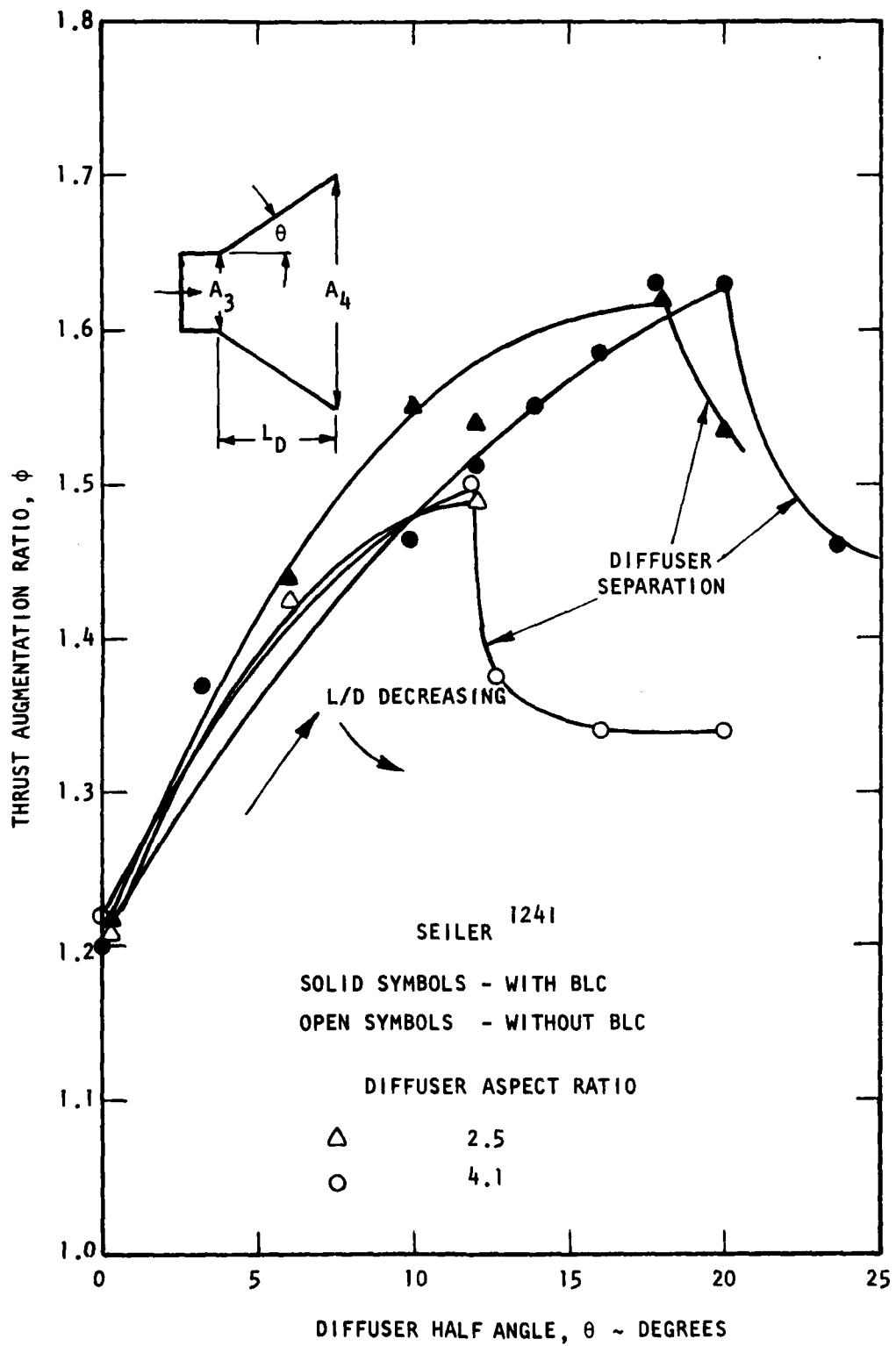


FIGURE 50. IMPACT OF DIFFUSER FLOW SEPARATION ON EJECTOR PERFORMANCE.

area ratio ejectors with long diffusers have been built and successfully tested (Quinn).¹⁰⁸⁵ Even though these ejectors were capable of producing high augmentation ratios ($\phi = 2.10$) the volume of the diffuser section would be prohibitive in an aircraft-constrained configuration. Separation can also be delayed by appropriate energization of the boundary layer, which is accomplished by various methods including suction, blowing and vortex generation. The suction method withdraws the low energy fluid near the wall, whereas the blowing accelerates the fluid in that region. The vortex generators cause some momentum from the external flow to be brought into the boundary layer. Traditionally, these have been streamwise vortex generators, as successfully applied by Brown, Nawrocki and Paley¹⁷² to an inlet diffuser. A lateral vortex structure (with axes perpendicular to the flow direction) has been proposed for diffusers by Stull, Curran and Velkoff^{1343,1344} and for aircraft wings by Quinn.¹⁰⁸⁴ The former involves a ribbed diffuser while in the latter case, the vortex structure is caused by a tunable cavity. Thus, to achieve rapid, efficient diffusion of the ejector mixed flow in compact lengths, diffusers should incorporate passive methods, such as contoured walls, and/or active methods (e.g., blowing) of boundary layer control. The works of Alperin and Marlotte,³⁶ Haight and O'Donnell,⁵²⁴ Sellar and Schum,¹²⁴² and O'Donnell and Squyers¹⁰¹⁴ show that thrust augmentation can be improved by employing the passive and active methods of flow control in diffuser sections. Also, the empirical results show that desirable levels of thrust augmentation can be maintained while significantly compacting the diffuser section by applying a combination of active and passive BLC techniques.

Some generic ejector diffuser configurations were illustrated previously in Figure 47. The correct contouring of the diffuser walls and proper amounts of boundary layer control improve ejector thrust augmentation performance. For a length constrained ejector configuration, the energization of the incoming diffuser boundary layer can allow the diffuser to operate more efficiently and at higher area ratios. Figure 51 presents the empirical results from two separate ejector tests with different methods of primary injection and BLC. Both ejector configurations had a diffuser length to mixing width ratio of 1.2. For the straight wall diffusers with no boundary layer control techniques, the optimum diffuser area ratios were 1.5 and 1.7, respectively. From the results of Sellar and Schum,¹²⁴² the augmentation ratio was increased over the entire area ratio range tested by approximately 12% by controlling the diffuser boundary layer with Coanda jets. The results of O'Donnell and Squyers¹⁰¹⁴ show that

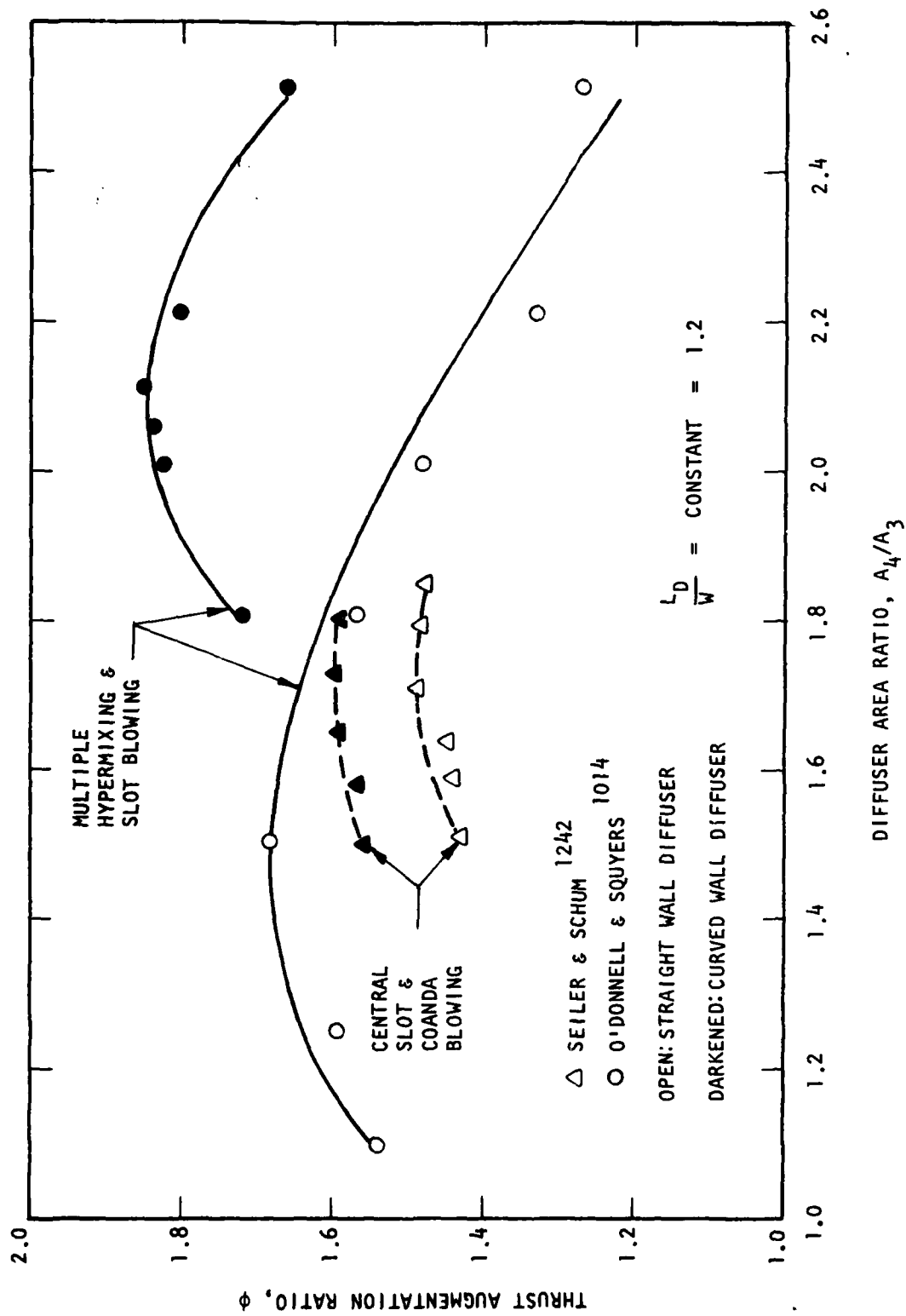
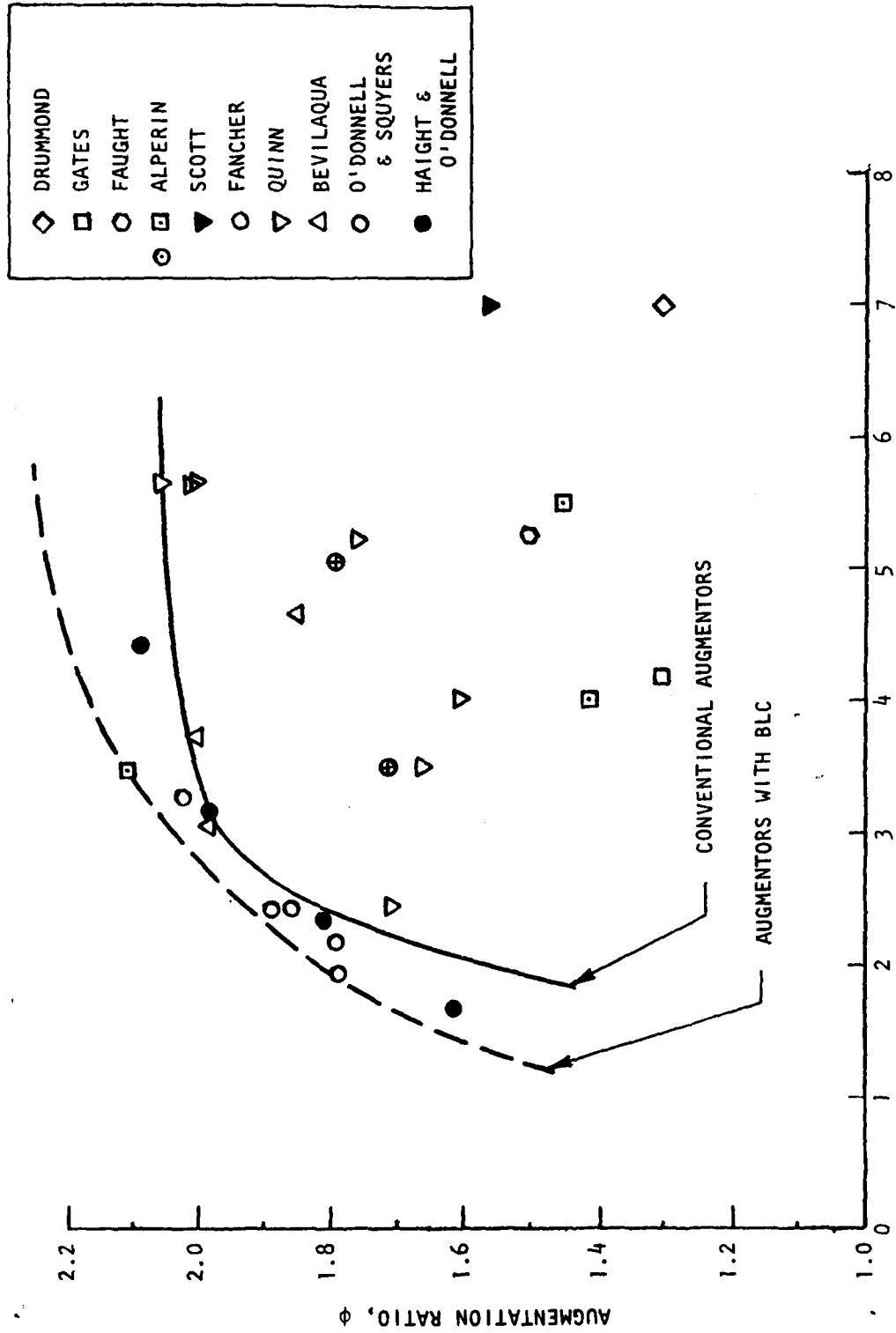


FIGURE 51. EFFECTS OF DIFFERENT PRIMARY INJECTION AND BOUNDARY LAYER CONTROL TECHNIQUES ON EJECOR PERFORMANCE AS A FUNCTION OF DIFFUSER AREA RATIO.

contouring in conjunction with slot blowing BLC also increased the peak augmentation ratio by 12% and allowed the diffuser to operate at a higher area ratio in the same length. In both cases, the injection flow of the BLC jet was considered in the calculation of the augmentation ratio. Because the diffuser boundary layer normally operates in an adverse pressure gradient region, contouring of the solid walls and blowing jet flow control provide the potential for improved total ejector performance. The improvements obtained by BLC can be considered in terms of increased augmentation ratio at a specified total length/diameter for the device or improvements in compactness as measured by L_t/W at a specified augmentation ratio, as shown in Figure 52.

4.5 EXTERNAL FLOW AND FORWARD VELOCITY EFFECTS

The thermodynamic state of the secondary fluid, which surrounds the total ejector, has a significant influence on the ejector system performance. While in static ejector operation, i.e., zero external flow velocity, the thermodynamic properties of the surrounding fluid are such that the total and static values are equal, as the velocity of the ejector device is increased above zero, the secondary fluid stagnation properties increase over the ambient static values and begin interacting with the ejector performance. At finite forward velocities, the static pressure of the flow around the shroud may affect the ejector exit boundary conditions. The increased secondary total pressure, as a result of forward velocity, may also result in an increased mixed flow pressure, for a constant primary pressure. As a result of forward velocity, the ejector can thus produce higher levels of gross thrust, as shown by Streiff, Ashby, and Krishnamoorthy.¹³⁴¹ Figure 53 shows the performance of a thrust augmenting ejector as a function of forward velocity as determined by Streiff and Henderson.¹³⁴² As shown in the figure, the gross thrust of the ejector increased with increasing velocity for fixed geometry and operating conditions. The discrepancies between the predicted gross thrust performance and actual data can be attributed to increased inlet losses. The ejector configurations in the cases shown were optimized under static conditions beforehand. There have apparently been no attempts to optimize ejector geometry for forward flight conditions, although the need has been recognized, for instance, by von Ohain, who responded to the Phase I questionnaire (see Appendix A) as follows: "While for 'hover' (or approximately static conditions) a large ratio \dot{m}_s/\dot{m}_p is desirable, for flight conditions, the ratio \dot{m}_s/\dot{m}_p should decrease with increasing flight speed. Correspondingly, the ratio of inlet area to primary throat area should decrease with increasing flight speed."¹¹ 1619



$$L_c/W = \frac{L_0 + L_1 + L_2 + L_3 + L_4}{W}$$

FIGURE 52. EJECTOR AUGMENTOR COMPACTNESS LIMITS.

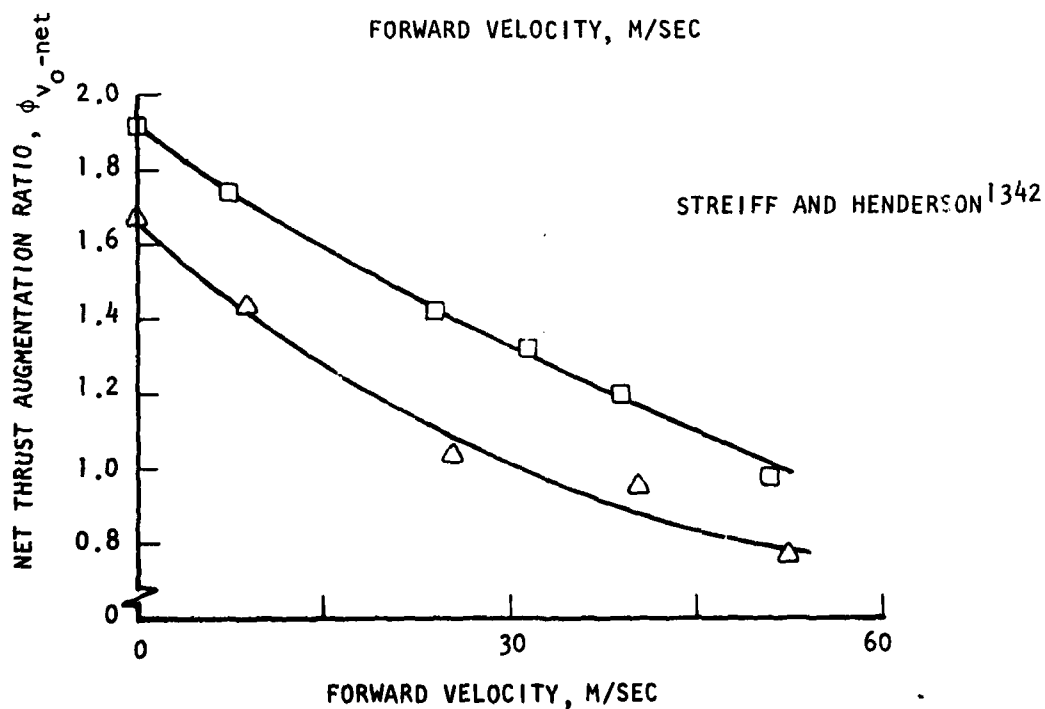
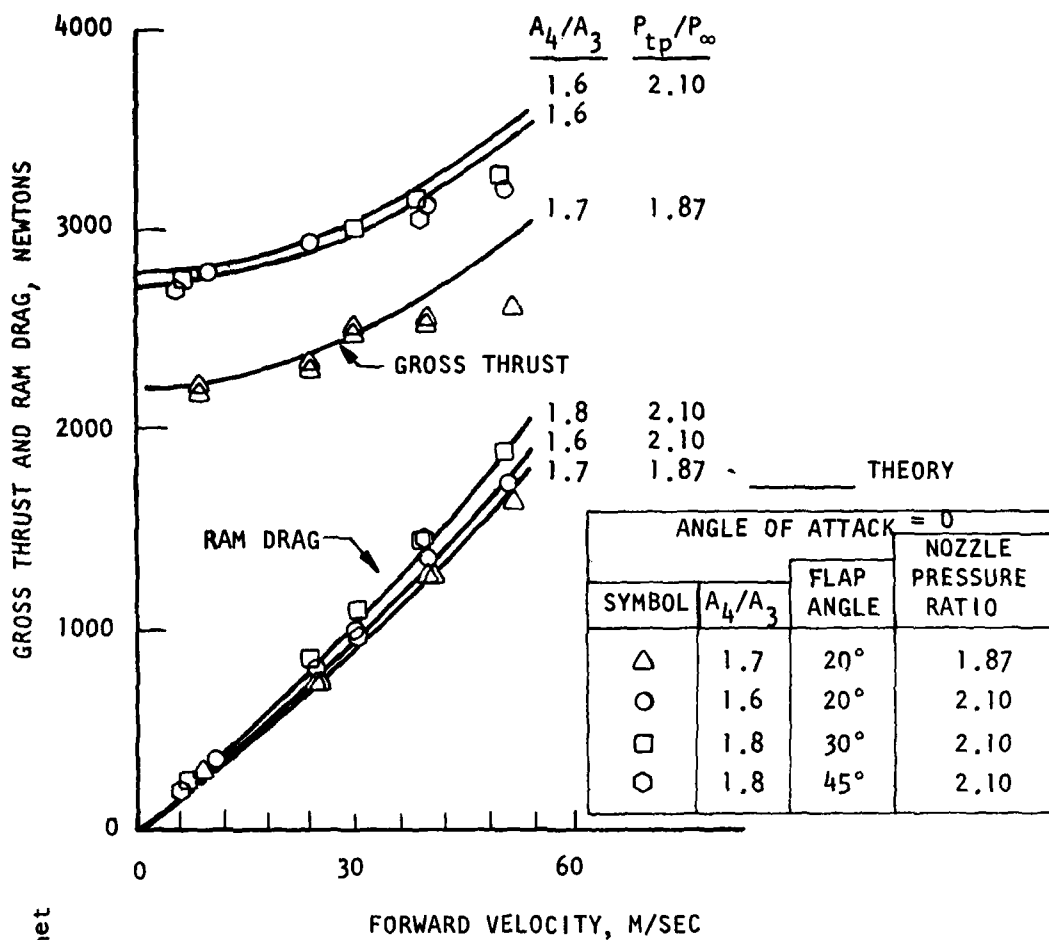


FIGURE 53. EFFECTS OF FORWARD VELOCITY ON EJECTOR THRUST LEVELS AND NET AUGMENTATION RATIO.

"Geometrically, the best inlet configuration for hover (static) would be a wide 'bell mouth' or very thick inlet lip while for flight conditions, the curvature radius of the inlet lip should decrease with increasing flight speed (in close analogy to the inlet of a gas turbine engine).¹¹ 1619

"The exit diffuser area ratio A_4/A_3 should decrease with increasing flight speed. The desired thrust augmentation ratio and correspondingly the ratio of secondary to primary mass flow increases from Case I to IV, as shown below:

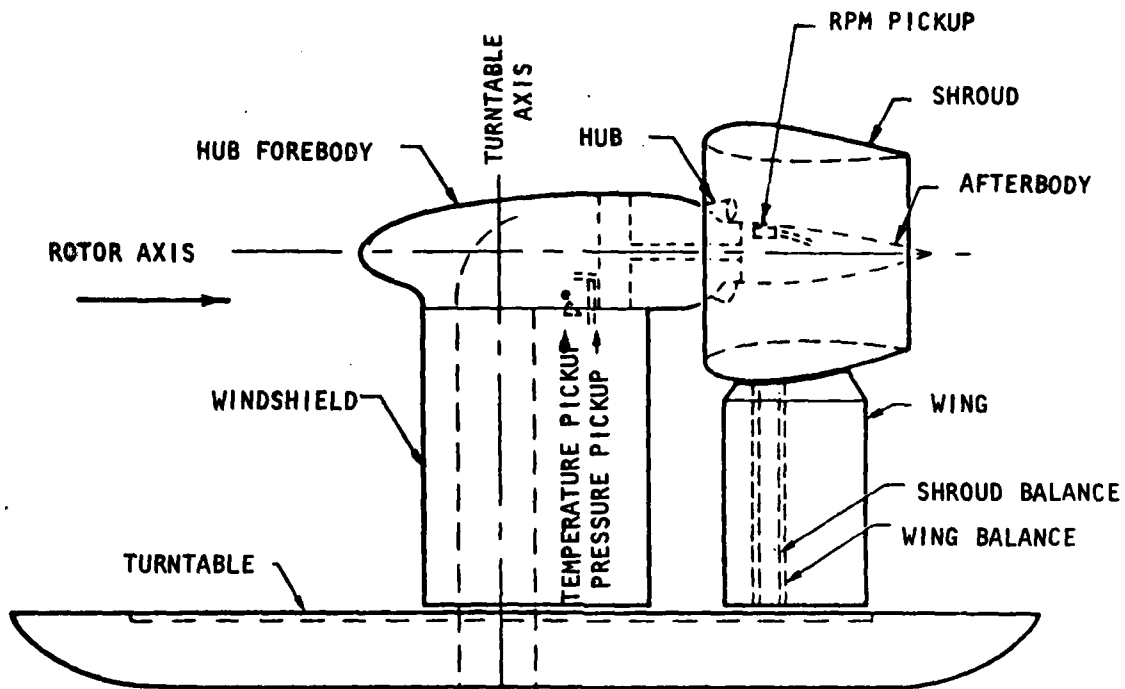
TABLE 1. FLIGHT VEHICLE AUGMENTATION RATIOS

	Supersonic Cruise Vehicle	Subsonic Cruise Vehicle
	I	II
STOL	Jet Flap or Augmented Flap	Jet Flap or Augmented Flap
	$\phi \sim 1.2$	$\phi \sim 1.4$
	III	IV
VTOL		
	$\phi \sim 1.5$	$\phi \sim 2$

"A totally different situation exists when vehicle boundary layer is used as secondary air for an ejector in flight. Very intriguing possibilities and configurations are conceivable. These conditions were discussed in a very preliminary way in Reference 178.¹¹1619

For fixed configurations, the greatest impact on the ejector thrust performance is due to the ejector ram drag term. Figure 53 shows that the ram drag of the ejector increases with forward velocity at a greater rate than the gross thrust. The penalty of the ram drag component is to reduce the net thrust, $F_{net} = F_g - F_{ram}$, of the ejector configuration. For constant operating conditions, the thrust augmentation ratio of the ejector decreases almost linearly with forward velocity. Similar performance degradation results for forward velocities are shown in Figure 54 for a rotary-jet non-steady flow augmentor.

For variable geometry ejectors, as suggested by von Ohain, above, it may be possible to maintain the net thrust with increasing velocity since decreasing the inlet area ratio will degrade the magnitude of the ram drag momentum component while slightly decreasing the gross thrust term. The alternate method suggested by von Ohain for decreasing the effects of forward velocity, through use of the boundary layer for the secondary flow, may be achievable through proper shielding of the ejector inlet. The paper of Hill and Marsters⁶⁰⁷ showed that for a thrust augmentor in forward flight, augmentation performance greater than 1.0 can be maintained for a fixed configuration with inlet shielding, to high levels of



SAMS 1188

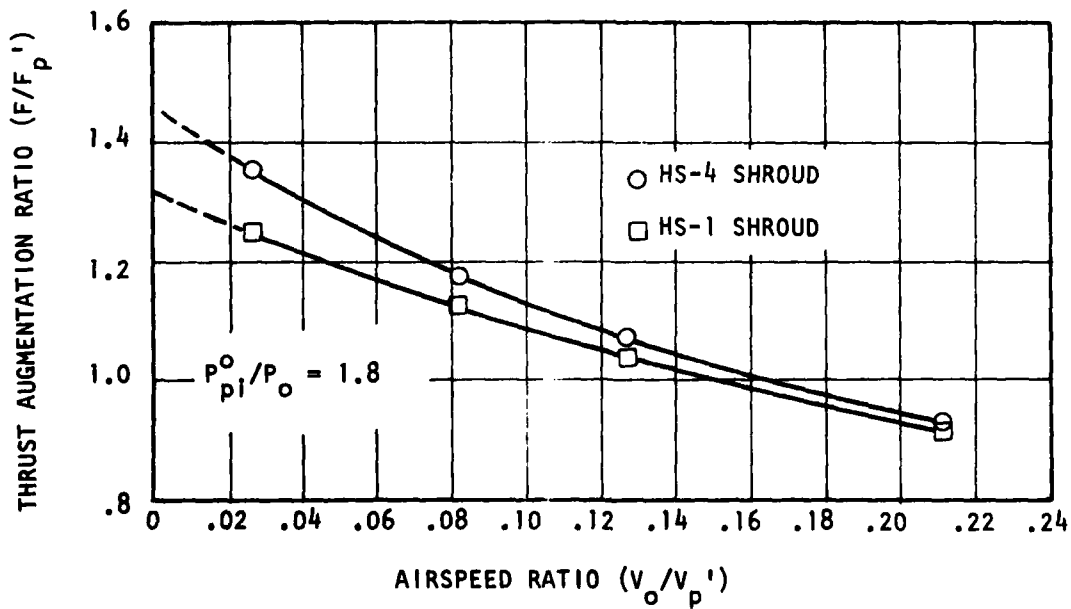
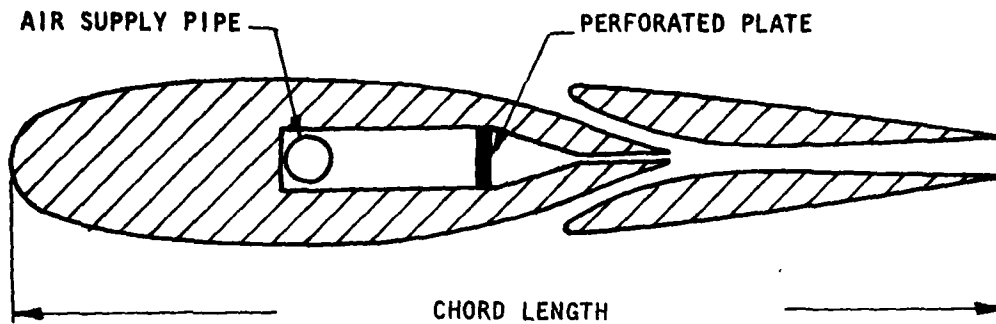


FIGURE 54. FORWARD VELOCITY EFFECTS ON ROTARY JET THRUST AUGMENTATION PERFORMANCE.

forward velocity. In this case, shown in Figure 55, the primary nozzle section acted as a shield for the inlet section, and the boundary layer of the upstream device constituted a significant portion of the secondary flow. The augmentation results shown are from DeHavilland Aircraft of Canada wind tunnel tests and exhibit the diminished influence due to a reduction in ram drag.

The interaction of an ejector with the wing aerodynamic performance has been considered analytically by Chan, Woolard, and Lopez^{216,1513,843} and experimentally by Clark²⁴⁵ for ejector wing configurations which look as shown in the schematic of Figure 56. The analytical models used to represent this type of ejector wing have generally made use of linearized potential flow solutions, such as vortex lattice methods, for the airfoil characteristics and incompressible, constant area, control volume approaches for the ejector characteristics. The solutions are "patched" together by representing the ejector secondary inflow as a sink on the airfoil, with a suction flow coefficient corresponding to the theoretical ejector secondary mass flow characteristics, and by using the predicted ejector mixed flow exit conditions to specify a jet-flap momentum coefficient at the airfoil's trailing edge.

Use of the ejector for configurations of this type provides two advantages. The thrust of the system is increased over that which could be obtained from the primary jet alone, and the lift is enhanced over that of a pure jet-flap wing, due to the increased flow over the wing from entrainment by the ejector. This latter effect is shown in Figure 57 from Woolard's calculations. Clark²⁴⁵ demonstrated experimentally that these effects are real, as shown in Figure 58.



THRUST AUGMENTOR
Wind Tunnel Data Reference 460

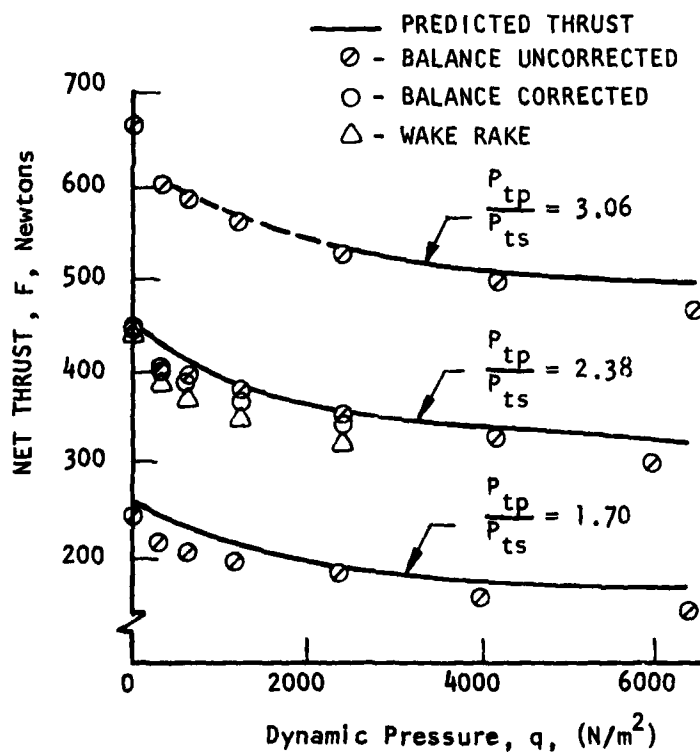
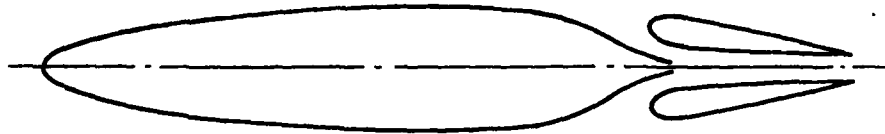


FIGURE 55. THRUST RESULTS FOR A SHIELDED INLET EJECTOR AUGMENTOR.

(a) CONVENTIONAL OR CRUISE FLIGHT CONFIGURATION OF THE EJECTOR BLOWN LIFT/CRUISE FLAP CONCEPT



(b) TYPICAL HIGH LIFT CONFIGURATION

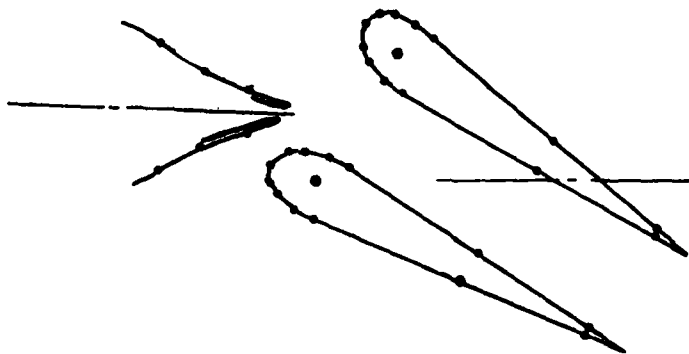


FIGURE 56. ALTERNATE CONFIGURATIONS OF THE EJECTOR BLOWN LIFT/CRUISE FLAP CONCEPT (FROM CLARK 245)

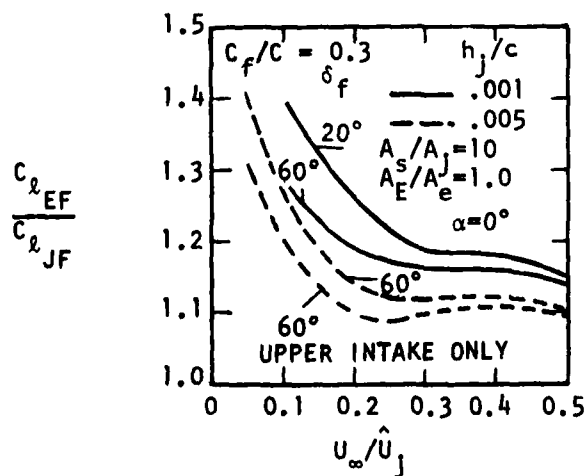


FIGURE 57. RELATIVE LIFT PERFORMANCE OF EJECTOR-FLAPPED AND JET-AUGMENTED-FLAPPED WINGS (FROM WOOLARD 1513)

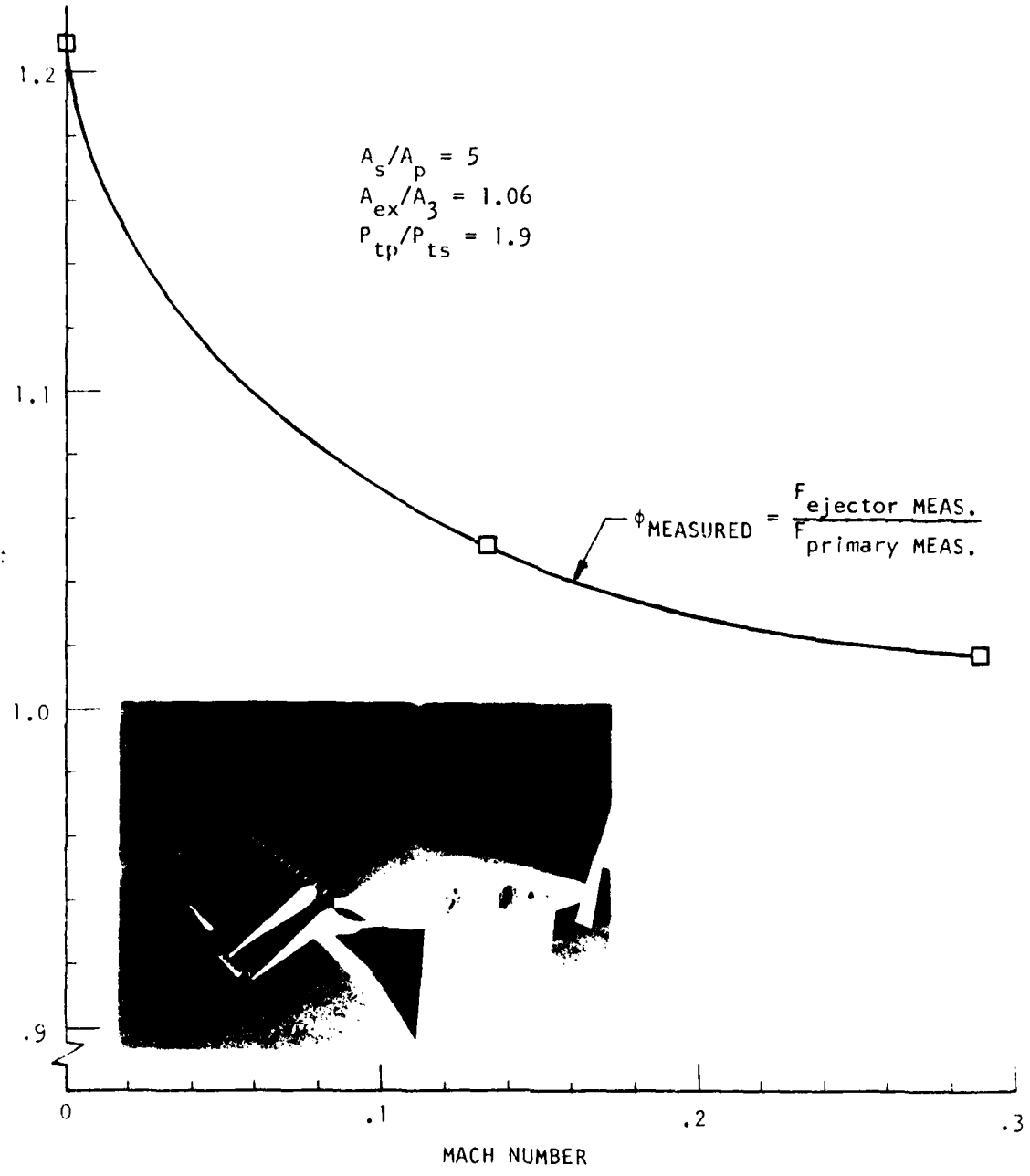


FIGURE 58. MEASURED THRUST AUGMENTATION CHARACTERISTICS (FROM CLARK 245)

5.0 EJECTOR AUGMENTOR FLIGHT SYSTEMS

In recent years, several attempts have been made to transition from laboratory experiments to full scale ejector augmentor flight systems. These attempts have, in general, been based on the following considerations:

- o Vertical or Short Takeoff or Landing (V/STOL) requirements.
- o Experimental ejector augmentor laboratory results indicating thrust augmentation ratios greater than about 1.4, for $(A_{\max}/A_p)'s < 20$ and $(L_{\max}/D)'s < 5$.
- o The apparent capability to configure ejectors to conform to structural and geometric requirements of specific aircraft without affecting performance.
- o Predictions of systems benefits for ejector augmentor flight systems, based on laboratory experiments.

5.1 GENERAL CONFIGURATION DESCRIPTION

Four significantly different configurations are represented in these recent attempts to produce viable ejector augmentor flight systems. These are: (1) the Lockheed Hummingbird, XV-4A, (2) the DeHavilland Buffalo, XC-8A, (3) The Rockwell International XFV-12A, and (4) the Ball-Bartoe JW-1 Augmentor Wing. The aircraft and schematic representations of the ejector configurations are illustrated in Figures 59-62. The XV-4A and the XFV-12A were designed for vertical takeoff and landing capability, while the Buffalo and Ball-Bartoe aircraft were designed for short takeoff and landing without vertical capability. It appears significant that the VTOL aircraft have not been considered successful, while the STOL aircraft have. The following sections contain discussions of each of these systems in relationship to the fundamental and component performance discussed earlier.

5.2 XV-4A VTOL CONFIGURATION

The XV-4A, shown in Figure 59, was a research aircraft. The primary purpose of the XV-4A program was to determine the feasibility of jet ejector augmentor application to VTOL. While the feasibility was demonstrated, due to the fact that only 93 percent of the predicted vertical lift was achieved

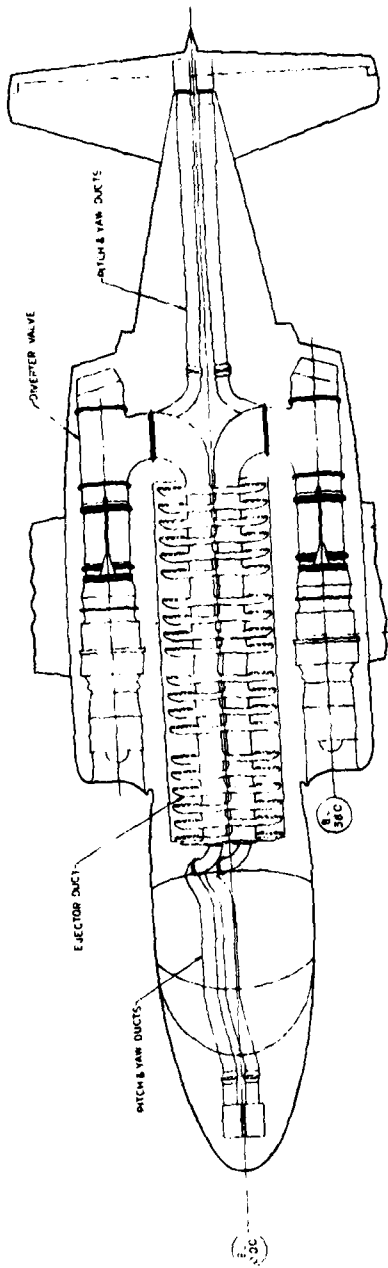
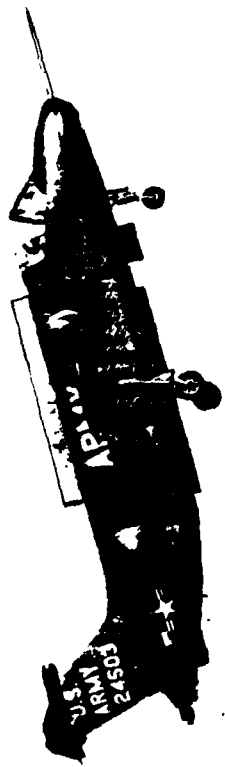


FIGURE 59. LOCKHEED/U.S. ARMY XV-4A EJECTOR AUGMENTOR AIRCRAFT.



EJECTOR SYSTEM

FIGURE 60. ROCKWELL/U.S. NAVY XFV -12A EJECTOR AUGMENTOR AIRCRAFT.

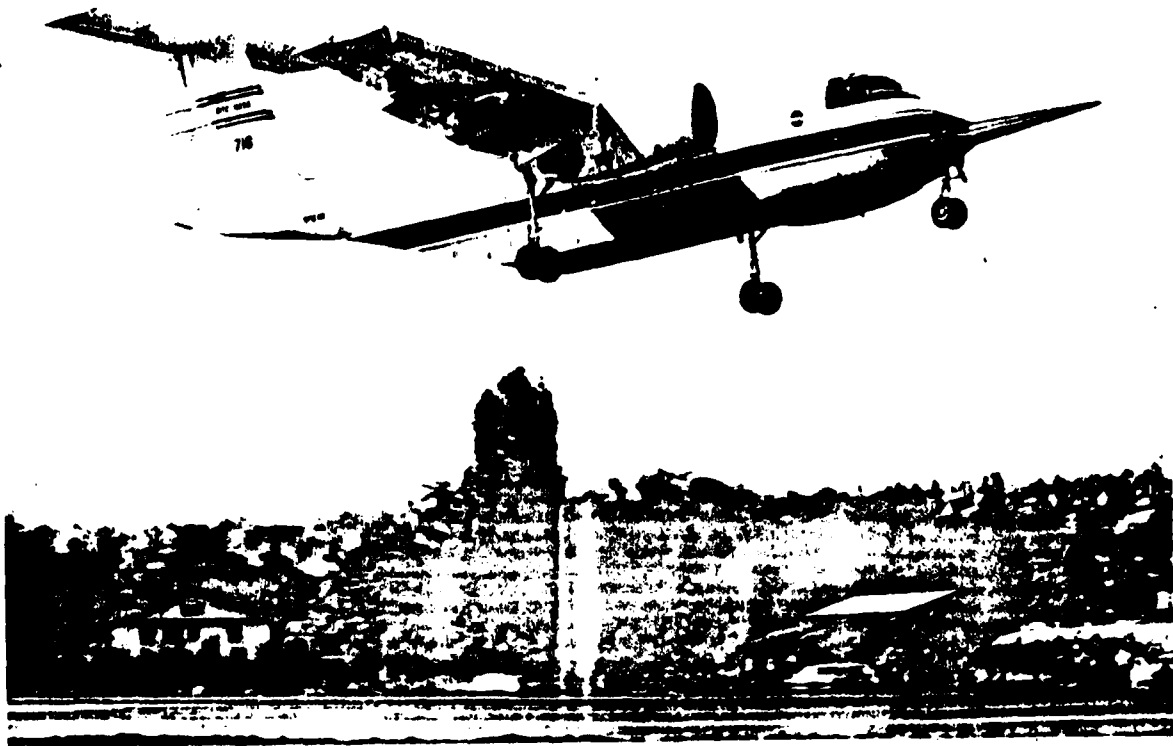


FIGURE 61. NASA/DITC XC-8A STOL CONFIGURATION.

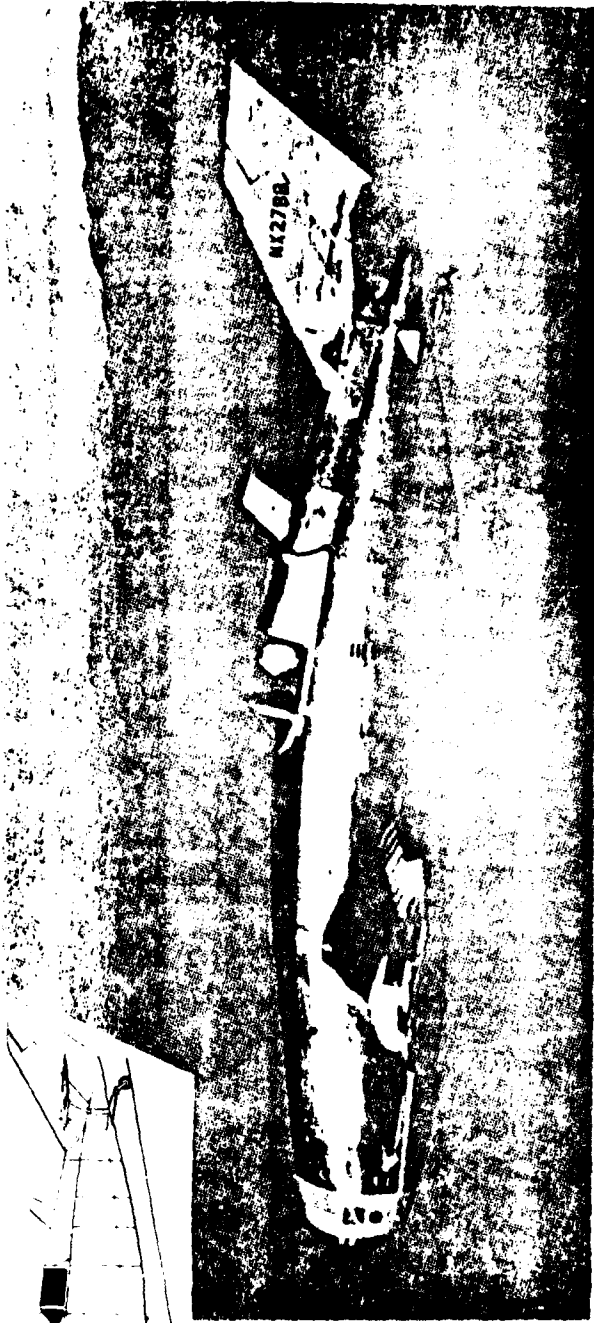
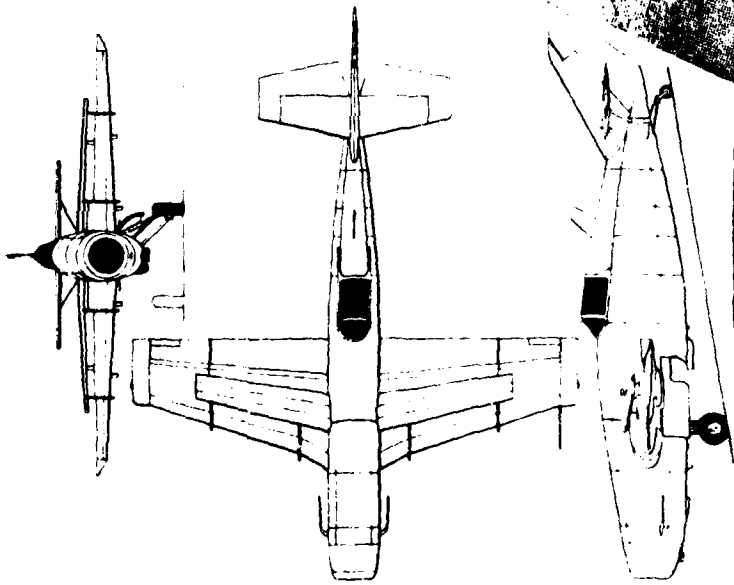


FIGURE 62. BALL-BARTOE/UNIVERSITY OF TENNESSEE JW-1 AUGMENTOR WING AIRCRAFT.

In the flight vehicle, the ejector augmentor propulsion system was not considered competitive with other VTOL propulsion system concepts. The ejector augmentor propulsion system consisted of two banks of four ejector bays each, on each side of the fuselage (see Figure 63). A thrust/takeoff gross weight of 1.16 was the design goal for the XV-4A, requiring an ejector augmentation ratio of ~ 1.4 based on the primary flow thrust capability at the ejector nozzles. The best ejector configuration which was flight tested only achieved $\phi = 1.3$, resulting in a 7 percent deficiency in required vertical lift.

The research program included the following phases, which have been summarized from the reference 1000 report.

- o Small Scale Wind Tunnel Model Tests - A .18 scale ejector powered model was used to determine aerodynamic characteristics for the actual airplane. The ejector area ratio was slightly different from that of the flight vehicle (14.5 vs. 13.6), and the primary total pressure and mass flow were significantly different, in order to achieve the correct value of scaled thrust for the same scaled exit area.
- o Flight Test Program - Prior to the free hover flights, two tethered hovering flights were successfully conducted. During the flight test program of 151 flights, 82 hover tests were flown. In general, only marginal vertical lift was achieved, even following installation of an improved ejector manifold design. "Because of the limited vertical thrust, the aircraft usually settled back to the runway one or more times (leap frogged) as it gained forward speed."¹⁰⁰⁰ At a forward speed of about 20 or 30 knots, reingestion and suckdown effects were sufficiently reduced that some excess power was available for climb and acceleration.
- o Lift Improvement Program - Sixteen different ejector configurations consisting of variations in the ejector manifold design, ejector inlet, ejector exit arrangement, and the ejector bay splitters were tested in a program conducted to improve the augmentor performance. The program was not completed until after the flight tests had been concluded, and while a maximum augmentation ratio of 1.48 was achieved, it was with a configuration which could not be installed on the XV-4A aircraft. The configuration which provided the best flight performance achieved an augmentation ratio of 1.3 during this program.

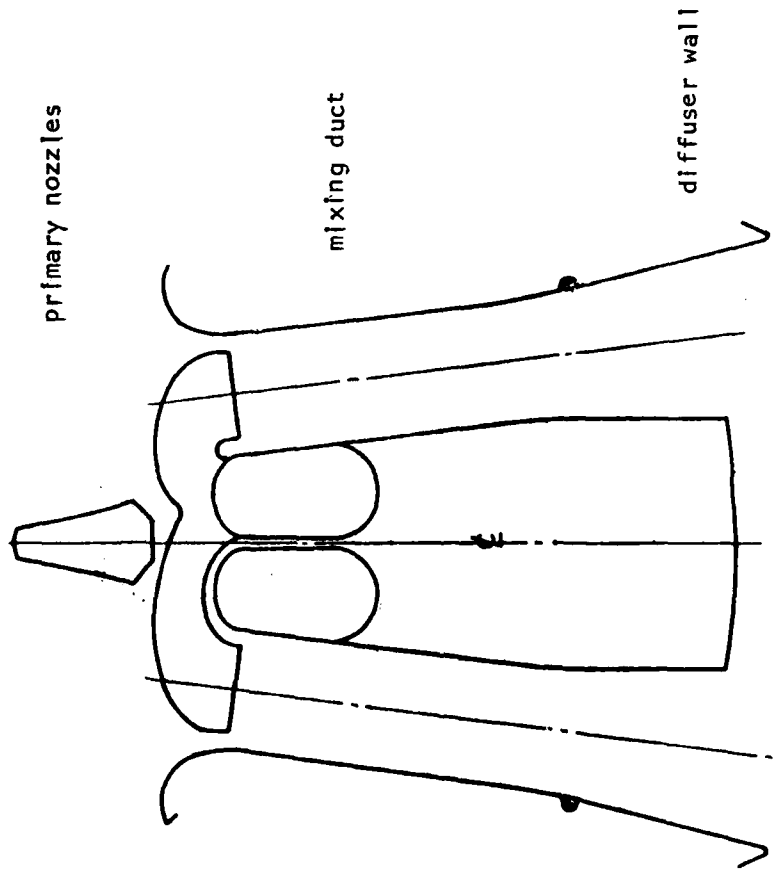
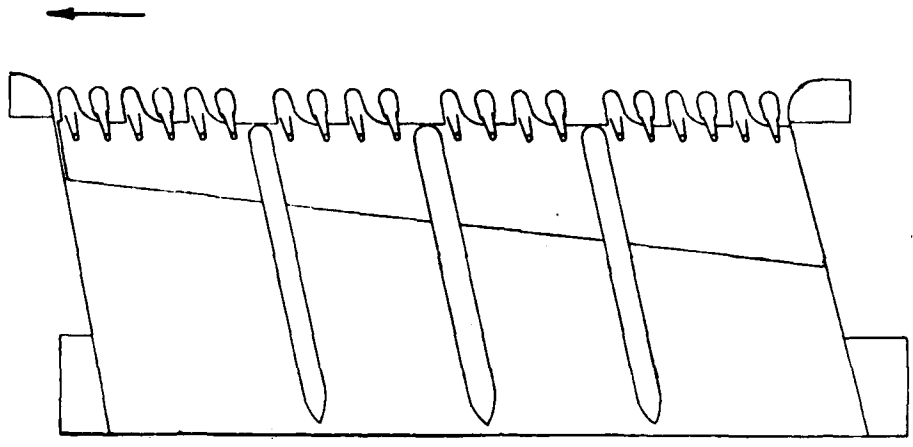


FIGURE 63. XV-4A EJECTOR BANK SCHEMATIC

- o Full Scale Wind Tunnel Tests - Flight tests had also been completed before full scale wind tunnel tests of one of the research aircraft were conducted in the NASA-Ames 40 x 80 foot wind tunnel. The full scale wind tunnel test data indicated less static lift capability than that observed during the flight tests and, in general, did not agree well with either small-scale wind tunnel or flight test results for the VTOL operation.

5.3 XFV-12A VTOL CONFIGURATION

The XFV-12A represents the first attempt at prototype development of an ejector augmentor VTOL fighter/attack aircraft. As shown in Figure 60, the XFV-12A is a Thrust Augmentor Wing (TAW) concept having a full-span ejector-flap system on each wing and canard.¹⁶¹⁶ This concept is intended to integrate the propulsion, lift, and control into a single system with the ejector providing all the VTOL thrust, and by its location in the lifting surfaces, enhancing the lift through supercirculation effects during transition flight. Control is provided by differential modulation of the ejector-diffuser flaps to provide both thrust vectoring and thrust modulation.¹⁶¹⁷ Because of proprietary aspects of the design, as well as some classified engine characteristics, data on the XFV-12A development program are somewhat lacking. Currently, however, the XFV-12A prototype cannot be described as a success for ejector augmentors. The design goal values of thrust augmentation ratio, 1.51 for the wing ejectors and 1.31 for the canard ejectors, were not met in the prototype tether tests conducted at NASA-Langley Research Center. The actual augmentation achieved in these tests fell far short (1.15 for the wings and 1.0 for the canards) of these goals.⁸⁴³

The development program, which was described briefly in the reference ⁸⁴³ workshop, included the following phases of ejector development:

- o Conceptual/Scaled Experimental Development - Small scale model testing was accomplished for the augmentor section and for the "swept" augmentor required to conform to the wing geometry. Tests of various primary nozzle types; hypermixing, cruciform, etc., were also conducted. In addition, a two-thirds scale model of the XFV-12A, which was fully blown using compressed air, was tested in the Rockwell International Company wind tunnel.¹⁶¹⁸ While results of these tests

have not been published in the open literature, it is known that they were successful enough to warrant proceeding with the next phase of development.

- o Full Scale Whirl-Rig Tests - A complete flight wing and canard with diffuser flaps were mounted on a rotary test rig to evaluate augmentor performance at speeds up to ~45 Knots. The design P&WA-F401 engine with a special thrust deflector was incorporated into the rig to provide the primary gas flow.¹⁶¹⁶ The whirl rig results apparently achieved the goal values of augmentation ratio, 1.5 for the wing and 1.3 for the canard, the former occurring at a diffuser flap angle of ~17° and the latter at an angle of ~12°.
- o Full Scale Tethered Hover Tests - The NASA-Langley Research Center Lunar Lander gantry was used for tethered testing of the prototype aircraft in the hover mode. Although a full size mockup had been built first to permit a careful study of the integration of the propulsion system into the aircraft, there is reason to believe that the actual prototype installation differed significantly from the full scale test hardware. For this and/or other reasons the prototype tethered hover tests were not successful, achieving a maximum augmentation ratio of only 1.15 for the wing and no augmentation (1.0) for the canard. After significant early successes in proof and ground testing of various other types and subsystems not discussed here, as well as of the ejector augmentor, the lack of success for the XFV-12A tether tests is currently not completely explained. The current status of the program is not available.

5.4 NASA/DITC XC-8A STOL CONFIGURATION

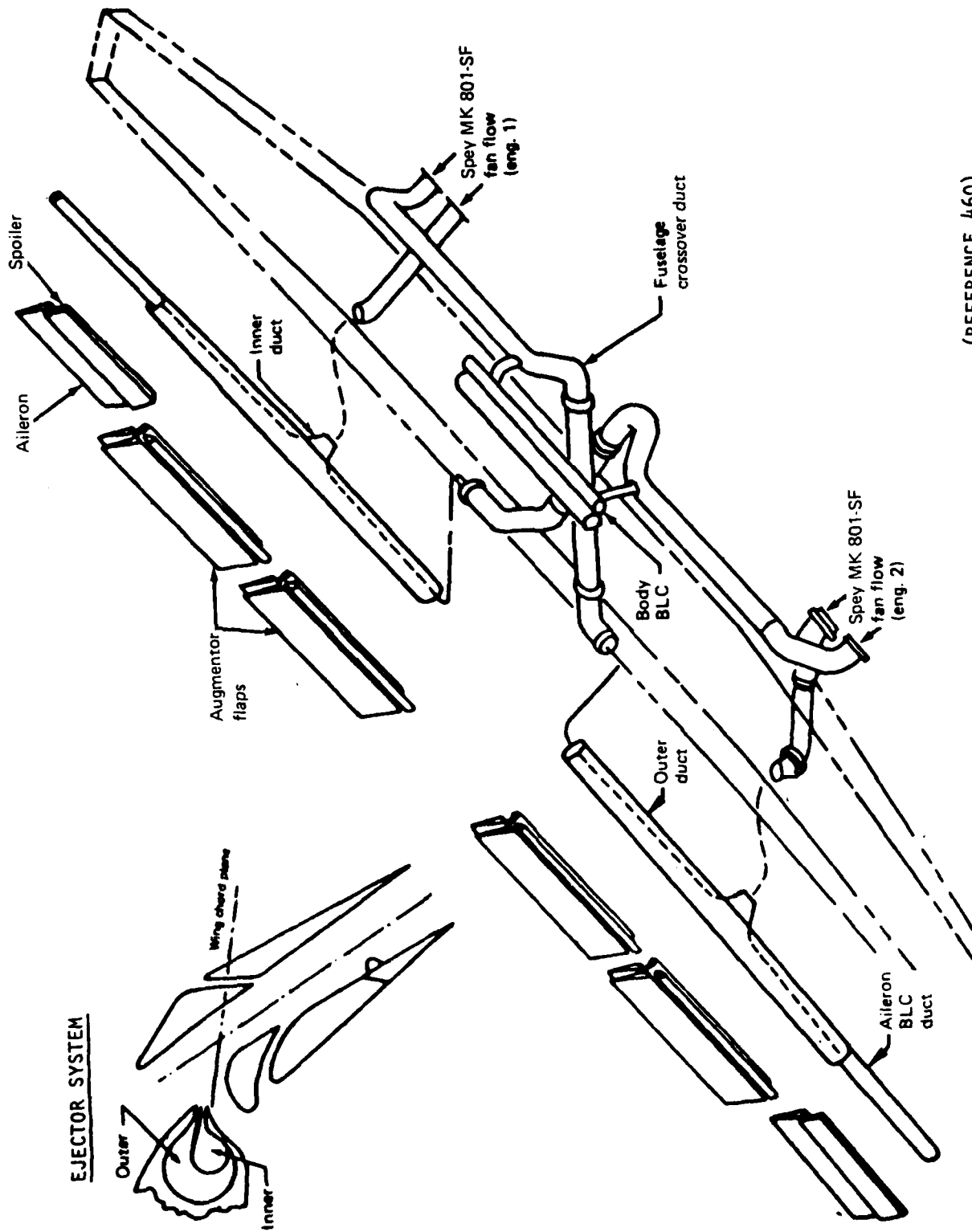
In cooperation with the Canadian government, as represented by the Department of Industry, Trade, and Commerce (DITC), NASA has worked with both DeHavilland Aircraft of Canada, Ltd. and The Boeing Company to modify a C-8A Buffalo utility transport aircraft, shown in Figure 61, to serve as an augmentor wing STOL research aircraft.¹⁶¹⁶ An ejector augmentor-flap system consisting of four equal spanwise sections, two on each wing, was added to the C-8A. The ejectors were designed to use only the fan air from the Rolls-Royce Spey MK-801 Split Flow turbofan engines, which were specially

modified to accommodate this. Augmentor "chokes" were designed to control the lift of the ejector-flap system by restricting the fan air outflow area.

The XC-8A has a significantly reduced designed stalling speed over the original C-8A, 41 Kts (76 Km/h) vs. 66 Kts (122.5 Km/h), and an improved designed STOL takeoff distance-to-height barrier approximately 77 percent that of the unmodified aircraft. The maximum cruising speed has been reduced, however, due to modifications for takeoff, climb and descent, and landing research rather than for cruise -- e.g., landing gear could not be retracted.

The following phases have comprised the ejector augmentor research program to date; however, it is still on-going, primarily in the research areas of avionics/handling qualities and noise abatement.

- o Large-Scale Augmentor-Wing Model - Large scale tests of a 42 foot span swept augmentor model were also conducted on an outside thrust facility and in the NASA-Ames 40 x 80 foot wind tunnel.⁴⁶⁰ The augmentor used a horizontal slot nozzle with a ventilated Coanda surface as shown in Figure 64. The augmentation ratio achieved in the wind tunnel tests for a similar straight wing was about 1.24, compared with 1.32 in previous laboratory tests. The swept wing tests, due to different nozzle efficiencies and duct losses, resulted in a reduction in augmentation ratio to $\phi = 1.17$. Outdoor tests at Ames were used primarily for checkout purposes of overall characteristics rather than investigations of ejector augmentor performance.
- o Augmentor Flap Model Tests - A .7 scale model of the augmentor flap system was built and tested at a Boeing facility prior to the actual modifications to the C-8A.^{460,540} While the model was similar to a previously tested wind tunnel model, it differed significantly by the use of a shorter flap chord and the addition of turning vanes within the nozzles. These design changes were made in order to adapt the design to the full scale configuration. Variations in augmentor throat spacing, inlet (area) door opening, lift dump angle, diffuser exit angle, flap deflection angle, and Coanda flap position were investigated. While the test results indicated an augmentation ratio in the desired range of 1.35 to 1.40 based on the measured nozzle-alone thrust, the augmentation ratio based on the fan air isentropic



(REFERENCE 460)

FIGURE 64. AIR DISTRIBUTION SYSTEM FOR THE NASA XC-8A STOL AIRCRAFT.

nozzle thrust was only ~1.26. The major factors contributing to this appeared to be nozzle and duct losses. As shown in the accompanying table (Table 2), a total thrust loss of ~12 percent was ascribed to such systems losses.

o Research Aircraft Flight Tests

The flight test program investigated the flight range from minimum airspeed, ~50 Kts, to design dive speed, ~180 Kts. Angles of attack up to 24° and bank angles exceeding 45° were flown. The objectives of the program were to "prove the augmentor wing concept with respect to aerodynamics, performance and handling qualities and to contribute to the development of jet STOL transport design and operating criteria."¹⁶¹⁵ In the first flight test program, reported in reference 1615, it was concluded that the flight envelope was sufficiently explored, and performance was close enough to predicted characteristics that the aircraft could be cleared for an extended flight test program.

The Modified C-8A is still flying and being used for research, primarily as indicated previously in the areas of handling qualities and noise abatement.

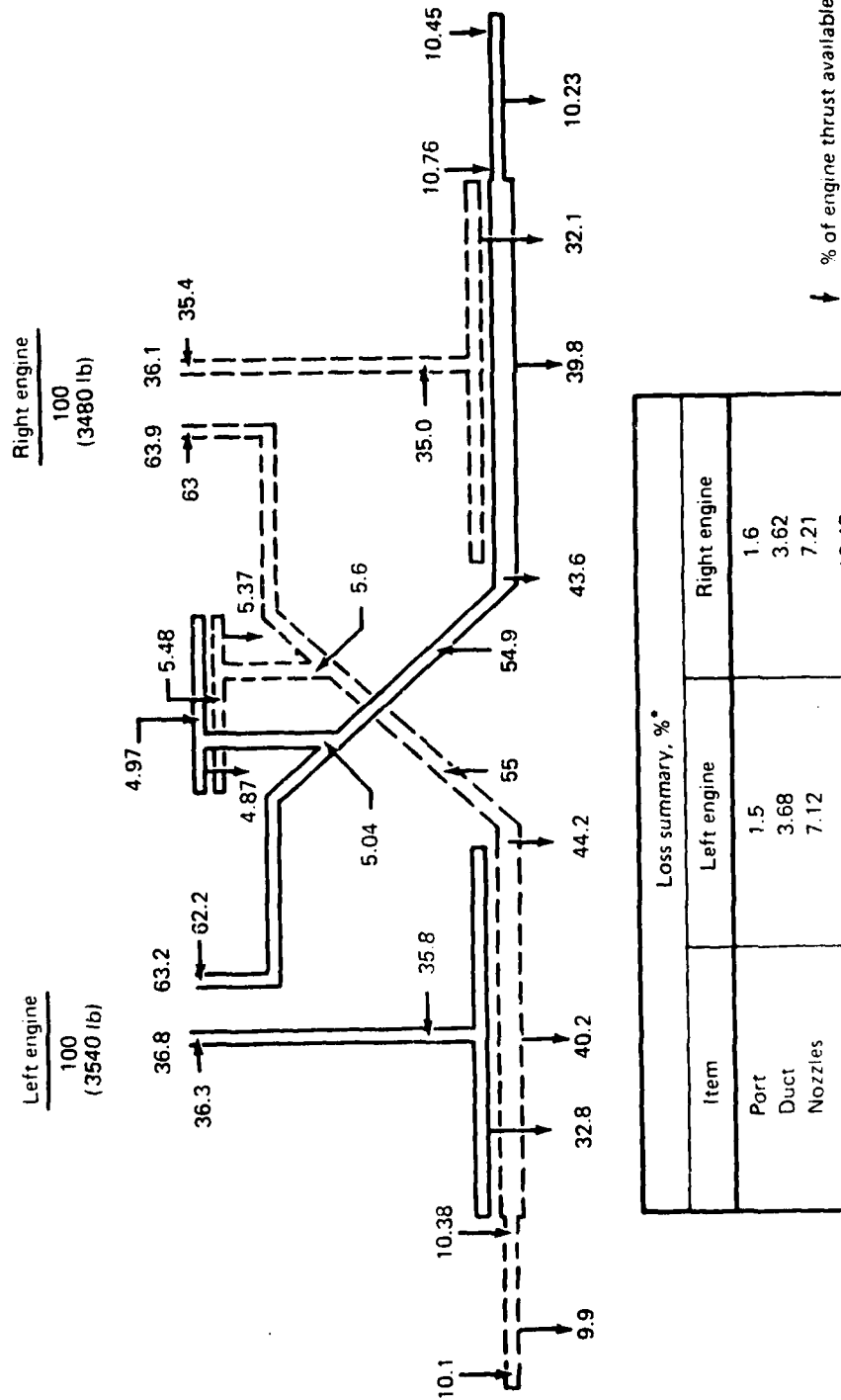
5.5 BALL-BARTOE, JW-1, AUGMENTOR WING AIRCRAFT

The Ball-Bartoe Jet Wing aircraft was designed and built during the period of 1973-1976. The first flight of the aircraft was completed in July of 1977. The configuration shown in Figure 62 was a flying testbed for the evaluation of the ejector augmented wing lift and thrust.

The aircraft uses a single Pratt and Whitney Aircraft of Canada JT15D-1 turbofan engine for propulsion. Both the bypass air and core flow exhaust are employed in the augmentor wing concept. With this propulsive lift system, the aircraft was aimed at demonstrating a slow-flight capability with application to short takeoff and landing operations.

In the jet wing concept, the hot core gases and the cold bypass air from the engine are both ducted, separately, to exhaust over the wing. The exhausting gases act as the primary ejector flows and provide propulsive force, as well as augmenting wing lift with super circulation effects.

TABLE 2. NASA XC-8A AIR DISTRIBUTION SYSTEM WITH TYPICAL THRUST LOSSES (MEDIUM POWER SETTING).



Some of the general aircraft characteristics and performance data available are:

- o To provide necessary contours for the exit nozzles; the wing leading edges have three different thicknesses.
- o Jet efflux from the turbofan engine is directed along the wing leading edge and discharged through rectangular slots for approximately 70% of the span.
- o A short-chord, augmentor shroud, wing extends over two-thirds of the wing span upper surface, over the engine gas exhaust slots.
- o The hot gases are ejected through nozzles adjacent to the fuselage, with an exit area of 40 square inches, and provide 35% of the propulsive thrust,
- o The cold bypass air is ducted and split into three flows before being turned 90° inside the ducts and exhausted outboard of the hot gas exits.
- o The bypass air contributes 65% of the propulsive thrust and generates a super circulation over the wing.
- o Aerodynamic fences separate the three sections of the wing.
- o A large trailing-edge flap system is deployable to a maximum of 52° and is located downstream of the exhaust gases.
- o The flap system rotates around a true radius to generate a Coanda effect and increase lift.
- o Some of the demonstrated flight parameters are:

Minimum Control Speed (Will not stall)	35 Kts	(65 Km/h)
Maximum Level Speed	350 Kts	(650 Km/h)
Ejector System Augmentation Ratio (Estimated)	1.17	

Recently, the jet wing aircraft and associated patents were obtained by the University of Tennessee for further flight research. Due to the private ownership of the aircraft, explicit performance characteristics of the ejector propulsive system are unavailable, and only limited information is presented in the open literature.

5.6 FLIGHT SYSTEM PERFORMANCE COMPARISONS

A comparison of the published or estimated augmentation ratio performance for the systems discussed in Sections 5.2-5.5 has been made in an attempt to discern possible causes for the generally reduced performance of these systems. As can be seen in Figures 65 and 66, critical performance parameters such as entrainment ratio, β , and exit to primary area ratio, A_4/A_p , were within ranges which should have enabled achievement of the desired augmentation ratios. In all cases, however, these desired values were not achieved. One parameter, the mixing length to diameter, may have contributed to this. Shown in Figure 67 is the augmentation ratio vs. L_M/D for each of the systems, which was not in the desirable range. Some of the systems relied upon predicted continuation of mixing within the diffuser section. However, this method of achieving short, high performance augmentors, which does not appear to be well-established in the available data examined, apparently failed to be realized by these systems. This is perhaps the most outstanding discrepancy between predicted performance/geometry and actual performance for these systems.

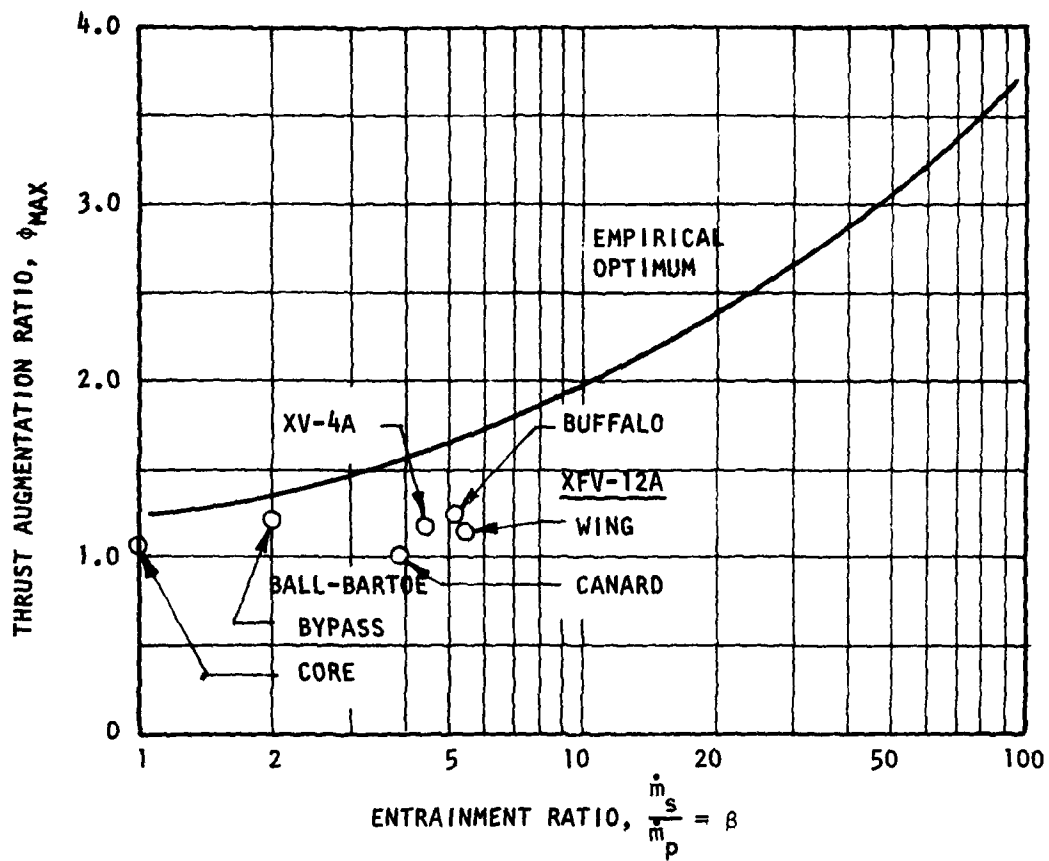


FIGURE 65. COMPARISON OF EJECTOR FLIGHT SYSTEMS ENTRAINMENT-AUGMENTATION PERFORMANCE.

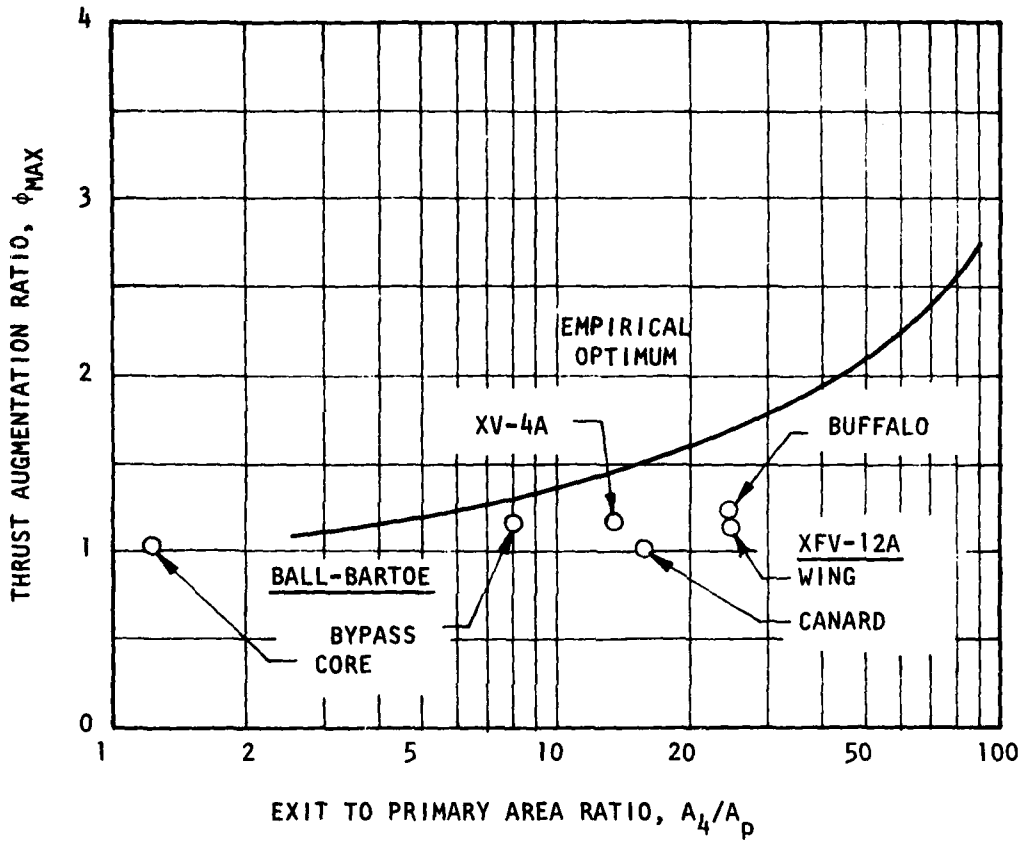


FIGURE 66. COMPARISON OF EJECTOR FLIGHT SYSTEMS OVERALL PERFORMANCE FOR TOTAL EXIT TO PRIMARY AREA RATIO.

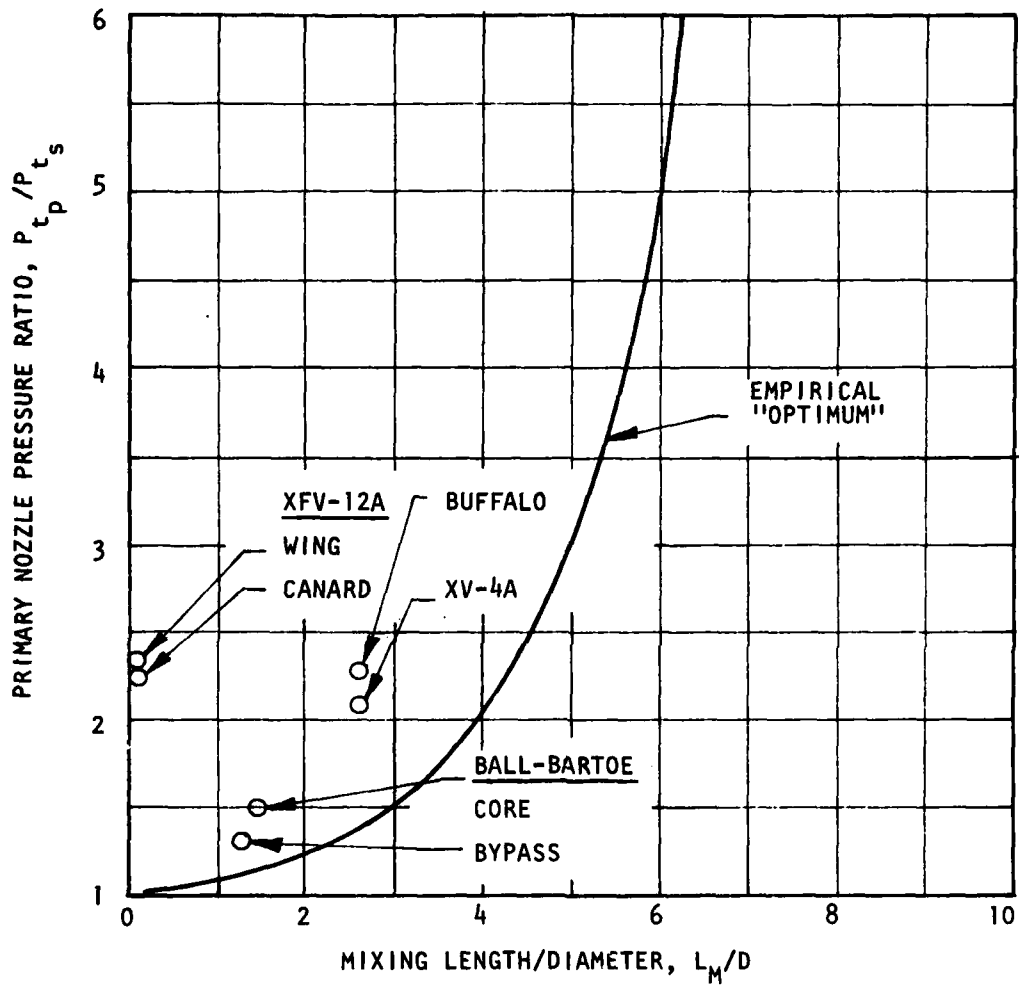


FIGURE 67. COMPARISON OF EJECTOR FLIGHT SYSTEMS ACTUAL MIXING LENGTHS (WITH LOSSES) OF OPTIMUM LENGTHS.

6.0 CONCLUSIONS AND RECOMMENDATIONS

In the following subsections, conclusions and recommendations are made which emphasize both the well-known and the poorly understood areas of ejector augmentor technology.

6.1 GENERAL CONCLUSIONS

There exist no fundamental results, either theoretical or experimental, which indicate that ejector augmentors cannot provide the basis for significant improvements in propulsion system performance. On the contrary, results abound from both theoretical and experimental investigations which indicate that significant aero propulsion system benefits can be gained through the use of ejector augmentors. The resounding fact, however, is that no major benefits have been shown when attempts were made to actually utilize ejector augmentors in full-scale flight system applications. The conclusion which must be drawn from these observations is not that the ejector augmentor won't work in flight system applications, but rather, that the state of the art of ejector technology is still deficient with regard to an understanding of how to make it work.

While advances in ejector augmentor technology have been rather sporadic over the past 50 years, a comparison of trends in the limits of experimental results for overall performance indicates that some significant advances have occurred recently. These are primarily in the areas of improved interaction performance (hypermixing, non-steady devices, etc.) and in the diffuser performance (jet flap diffuser, active diffusion control, etc.). Still, the interaction phenomenon and its interactive influence on other component performance need to be better understood, as do a variety of phenomena associated with the individual components.

In the following subsections, some specific conclusions and recommendations are made concerning both the areas of ejector augmentor technology where results are in substantial agreement and where information is lacking. Recommendations regarding the latter areas are further elaborated upon in Appendix C through an outline of needed research and development programs.

6.2 CONCLUSIONS AND RECOMMENDATIONS BASED ON THEORETICAL CONSIDERATIONS

- o An ejector augmentor can more efficiently utilize the total energy of the primary flow than can an optimum primary propulsive nozzle. The total primary flow energy provides the basis for the formulation of a

maximum augmentation ratio, which can be related to the primary to secondary stagnation pressure ratio.

- o For a steady flow ejector, the mixing process is the most critical phenomenon with regard to ejector augmentor performance. Generally, constant pressure mixing is better than constant area mixing for secondary inlet to primary exit ratios of 10 or less, whereas constant area mixing is better at higher area ratios. Fundamental studies to define correlation parameters to relate initial stagnation and geometric conditions to the energy transfer mechanisms should be made. Particular emphasis should be placed on the investigation of constant pressure interaction devices for thrust augmentation.
- o Inlet flow velocity and pressure non-uniformity can result in improvements in augmentation ratio. Systematic studies to define these effects experimentally are needed -- particularly for forward flight conditions.
- o The efficiency of the interaction or energy transfer process from primary to secondary flow can be improved through the use of "interface pressure forces" (normal vs. shear stresses in fluid interfaces), and these arise when unsteady primary jets are used. Concepts for generating efficient non-steady primary flows need to be investigated, and methods of characterizing non-steady flow interactions should be defined and implemented.
- o Diffuser operation is critical to achieving high augmentation ratios.
- o Boundary layer control and wall contouring afford means of achieving and maintaining proper diffuser operation. Systematic experiments need to be made to define the optimum geometry and diffuser jet conditions for control of the diffuser exit static pressure. Methods of non-steady BLC also need to be investigated.
- o Purely analytical methods of designing ejector augmentors capable of a specified level of actual performance do not exist.
- o Current computational techniques for predicting static and dynamic ejector thrust performance must incorporate variable component losses to predict realistic performance. Fundamental studies to define a comprehensive set of design data need to be performed.

6.3 CONCLUSIONS AND RECOMMENDATIONS BASED ON EXPERIMENTAL RESULTS

- o The primary to secondary stagnation pressure ratio is the most significant parameter in determining or predicting the level of thrust augmentation possible.
- o For a given stagnation pressure ratio, the effect of primary to secondary stagnation temperature ratio on augmentation ratio appears to be nearly linear, showing approximately a 10% drop in augmentation ratio for each 100% increase in temperature ratio. The initial level (at a temperature ratio of one) varies, however, with the device design. Future R&D efforts need to be concentrated toward understanding and achieving high performance designs compatible with stagnation pressure and temperature levels appropriate to current jet engine exhaust conditions.
- o While systematic investigation of the effects of secondary inlet flow velocity or pressure non-uniformities has apparently not been made, results showing the effect of primary nozzle exit position relative to fixed inlet walls (Coanda, multiple nozzles, etc.) appear to support theoretical conclusions regarding advantageous effects of non-uniform secondary flows.
- o Multiple nozzle primary flow devices can achieve higher performance than single nozzle configurations. System trade studies on the effects of increased primary nozzle loss factors versus improved total device performance for multiple nozzles are needed.
- o Non-steady primary flow devices can achieve higher augmentation ratios than steady flow devices for the same area ratios and length dimensions. Control of the exit static pressure and the diffuser flow for non-steady devices needs to be investigated.
- o For flow property and other geometric conditions fixed, an optimum mixing length exists. The ability to continue the interaction in the diffuser, for high pressure ratio ejectors, needs additional experimental validation.
- o Boundary layer control and wall contouring are required to achieve short, high area ratio diffusers. These techniques also need additional validation for high pressure ratio and high temperature ratio devices.

6.4 CONCLUSIONS AND RECOMMENDATIONS ARISING FROM FLIGHT SYSTEMS RESULTS

- o Full scale aircraft using ejector augmentors which were intended to have VTOL capability have not been considered successful, whereas aircraft designed only for STOL capability have achieved at least moderate success. Additional systems design studies of ejector augmentor systems emphasizing STOL-only capabilities should be made.
- o Of the four flight systems discussed, the two achieving moderate success utilized split engine exhausts, where most of the thrust augmentation was obtained with ejectors utilizing only the fan airflow. In the two systems which were unsuccessful, all of the engine exhaust was used as the ejector primary flow. The effects of the basic jet engine configuration and design parameters on the engine plus ejector augmentor propulsion system performance should be analyzed parametrically to establish ejector-compatible engine designs.
- o In at least three of the flight systems investigated, laboratory tests ranging from small to full scale were conducted, and desired levels of augmentation ratio were achieved. However, due to various reasons all of which in some ways reflect lack of full understanding of the component performance as well as of the significance of the ejector/airframe integration issues, none of the full scale installations achieved viable performance levels. A systematic scale-effects study, including installation effects, is mandatory if ejector-augmentors are ever to achieve their potential for flight system application.

6.5 GENERAL RECOMMENDATIONS

While a voluminous amount of work has been performed in the area of thrust augmenting ejectors in this century -- as evidenced in the Phase I study and the Bibliography, Part II, of this report -- no systematic, long-range, research and development program leading to high performance ejector augmentors capable of viable systems applications has ever been defined. It appears that to accomplish such a definition a governmental interagency panel, acting as an Ejector Technology Research and Development directorate, should be established.

In this manner, research and development programs, both privately funded and funded by the various governmental agencies could have not only common goals, but a synergistic interaction/communication which would minimize false starts and duplication of efforts, while maximizing the cost effectiveness and reduction of risk associated with the technology growth.

APPENDIX A - SUMMARY OF PHASE I EFFORT

The primary objective of Phase I of this program, "A Summary/Overview of Ejector Theory and Performance," was the assimilation of existing knowledge and data pertaining to ejectors of all types, into a usable guide. Secondary objectives included: (a) The determination of relationships between theoretical and experimental performance, (b) The determination of the most appropriate (most viable) areas of application for ejectors, and (c) The definition of required areas of continuing ejector research and development. These objectives were addressed for a single category (Category I) of ejectors (Single Phase, Single Fluid, and Steady State), with further emphasis on thrust augmenting devices. In addition, certain tasks relevant to the overall program objectives were accomplished: (a) The initiation of an extensive collection of ejector reports and references for all types of ejectors, (b) The initiation of a useful technical exchange with numerous organizations and individuals which are, or have been, involved with ejector research and development, (c) The definition of usable categories of ejector systems, and (d) The establishment of a baseline procedure, which was applied for comparison purposes to the Category I ejectors. In the following sections of this Appendix A, results of these Phase I activities, which are relevant to the total study of the theory and performance of ejector augmentors, are summarized.

A-1 Literature Search, Consultation, and Review

Literature Search and Review

An intensive literature search was conducted, and an information form requesting reports and references on ejectors was sent to 300 organizations in industry, education, and government. From the resulting information, an extensive bibliography of over 1500 references on ejector work in a wide variety of areas, both fundamental and applied, was compiled. Subsequently, during Phase II, the Bibliography was further expanded by an additional 300 references. Following the compilation of the bibliography, the reports were categorized according to their basic content, as follows:

1. Basic Operating State - The basic operating state of the fluid interactions discussed in each report was described as either (a) Single Phase, Single Fluid, such as an air primary exhausting to an air secondary fluid; (b) Single Phase, Dual Fluid, such as a helium primary exhausting into an air secondary fluid; (c) Dual Phase, Single Fluid, such as a steam primary exhausting into a water secondary fluid; or (d) Dual Phase, Dual Fluid, such as an air primary exhausting into a water secondary fluid. In addition, the operating state was further designated as either Steady State, or *Crypto and Non-Steady*, these states being applied to describe the primary flow at the entrance to the energy transfer section rather than the total flow at the exit.

2. Primary Subject - The primary subjects covered by each report were identified according to the following areas: (a) Augmentors--those reports which discussed uses of ejectors to increase thrust or reduce drag, (b) Bibliographies--those reports which were chiefly lists of ejector reports, with minimal or no discussion of ejector technology, (c) Coanda--those reports which dealt with the use of the Coanda effect in ejectors or as a fundamental flow phenomenon, (d) Cooling Systems--those reports which discussed the use of ejectors to provide a low temperature source of air or other fluid through their mixing or pumping action, (e) Diffusers--those reports which included discussions on the importance and performance of diffusers and nozzles coupled with ejector interactions, (f) Engine Simulation--reports discussing the use of ejectors to simulate or enable engine testing, (g) Fundamental--those reports which described fundamental flow phenomena, whose understanding may be critical to ejector performance, (h) General--those reports which provided general discussions of ejector theory, performance, and/or applications, such as textbooks, (i) Liquid Injectors--reports on the use of ejector devices to achieve improved pumping or mixing for special purposes such as fuel injection, (j) Mixers--reports describing the mixing phenomena or the use of ejectors for special mixing purposes (see (i)), (k) Noise suppression--reports discussing the use of ejectors to reduce the noise level of exhaust jets, (l) Pumps--those reports describing the use of ejectors for increasing the total pressure

or energy level of the secondary fluid, without necessarily discussing the use of the increased fluid energy (as opposed to thrust augmenting devices), (m) Unknown--those reports whose content could not be deduced from their titles, and were not obtained for review, (n) V/STOL Aircraft -- those reports which particularly discussed the use of ejectors to provide additional thrust for vertical (V) or short takeoff or landing (STOL), (o) Wing/Lift--Reports describing the use and performance of ejector-type interactions to augment conventional wing aerodynamics, including the use of boundary layer control, super circulation and jet flaps, and (p) Wind Tunnels--those reports discussing the use of ejectors for wind tunnel applications.

3. Type of Treatise - The primary types of discussions contained in each report were also categorized as follows: (a) Applications--Those reports which discuss specific applications of ejectors and the benefits to be gained by ejector usage for these applications, (b) Experimental--those reports which contain relevant test data on ejector performance, whether of a fundamental or overall performance nature, and (c) Theoretical--those reports which contribute to either the theoretical understanding of ejector phenomena, or the theoretical prediction of ejector performance, or both.

Categorization into the foregoing areas was accomplished through review of available reports and abstracts and by inference from report titles when they were not available for review. While the latter procedure is not rigorous, it provides an additional first culling into the areas of interest. The results of the categorization were considered, in order to gain insight into the historical trends in ejector research and development, for three key areas: (a) Fundamental research, (b) Augmentors, and (c) Pumps. The results are shown in Figures A-1 - A-3 in terms of the number of reports published in each area by year.

Consultation and Review

Approximately 300 requests for information, in the form shown as Figure A-4, were sent to various individuals and organizations in education, industry, and government who were believed to be or to have been engaged in use, research, or development of ejectors. While only a relatively small percentage, 15%, of these requests resulted in detailed responses, the

FUNDAMENTAL PHENOMENA

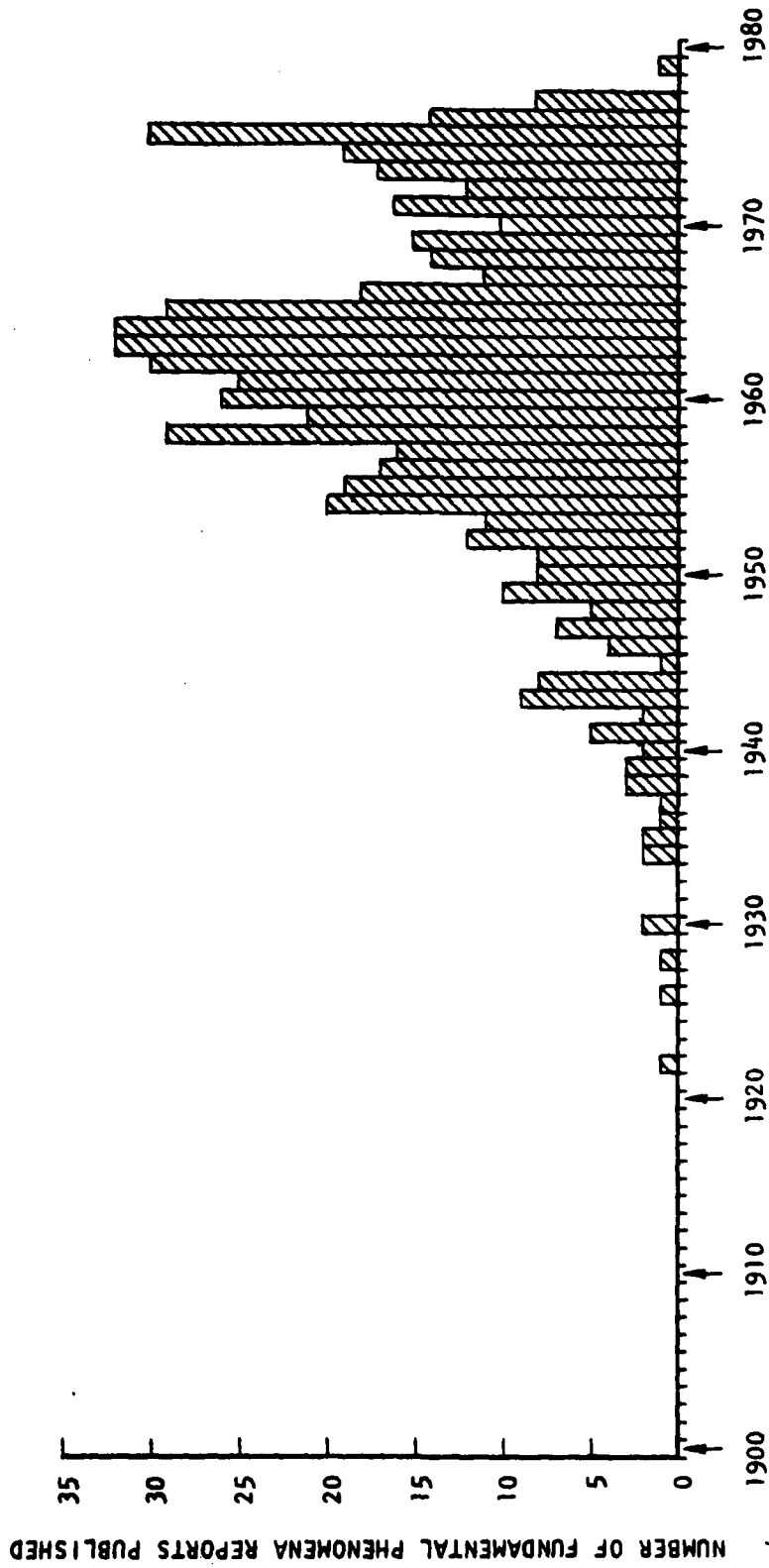


FIGURE A-1 CHRONOLOGICAL SUMMARY OF REPORTS ON FUNDAMENTAL EJECTOR PHENOMENA

AUGMENTORS

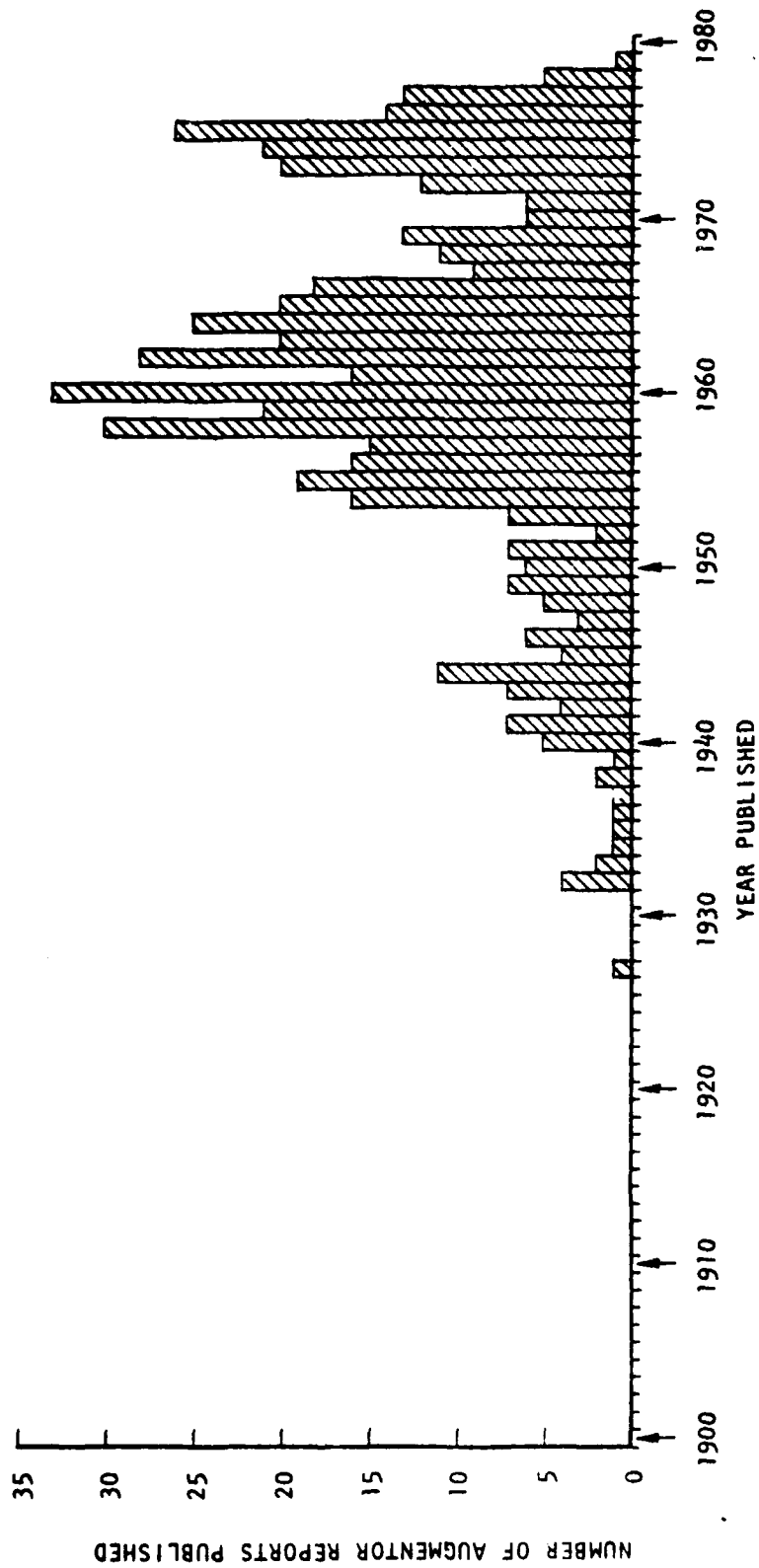


FIGURE A-2 CHRONOLOGICAL SUMMARY OF PUBLISHED REPORTS ON EJECTOR AUGMENTORS

PUMPS

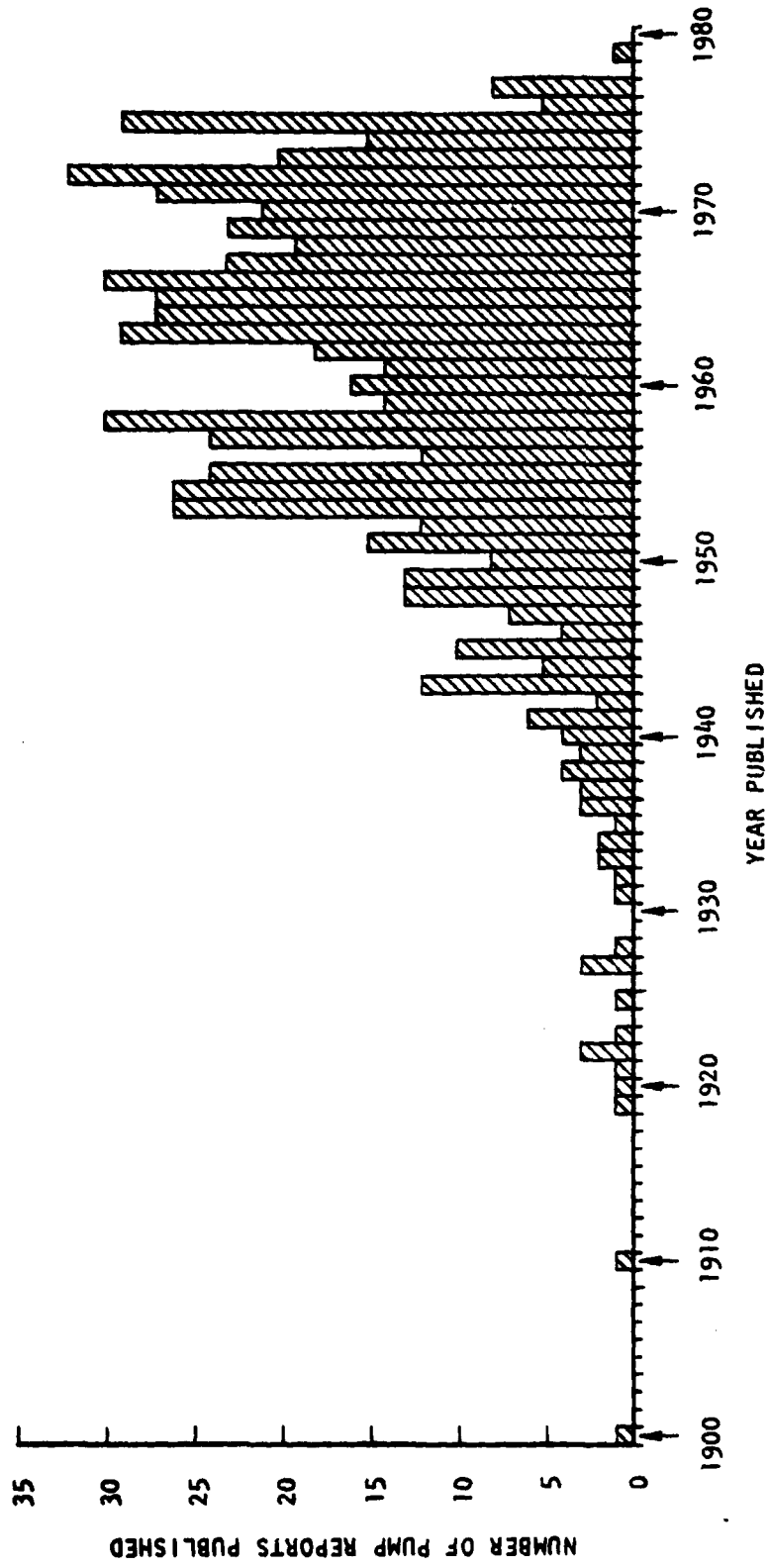


FIGURE A-3 CHRONOLOGICAL SUMMARY OF PUBLISHED REPORTS ON EJECTOR PUMPS

EJECTOR SUMMARY/OVERVIEW

ORGANIZATION NAME _____

1. Is your organization currently active in ejector work? Yes No

If so, what types? Thrust Augmentor Pump Mixer

Other (Specify) _____

2. Has it been active in the past? Yes No

If so, what types? Augmentor Pump Mixer Other _____

What years?

3. What are or were the specific applications of your organization's ejector activities?

<u>Application</u>	<u>Level of Performance Required:</u>	<u>Geometric Constraints To Be Met:</u>	<u>Other Constraints (Noise, Etc.)</u>
--------------------	---------------------------------------	---	--

Augmentors for a.

b.

c.

Pumps for a.

b.

c.

Other (specify)

4. Were the required performance levels: Not Met Deficit ___% Met

Exceeded Margin ___%

FIGURE A-4 EJECTOR SUMMARY/OVERVIEW INFORMATION FORM.

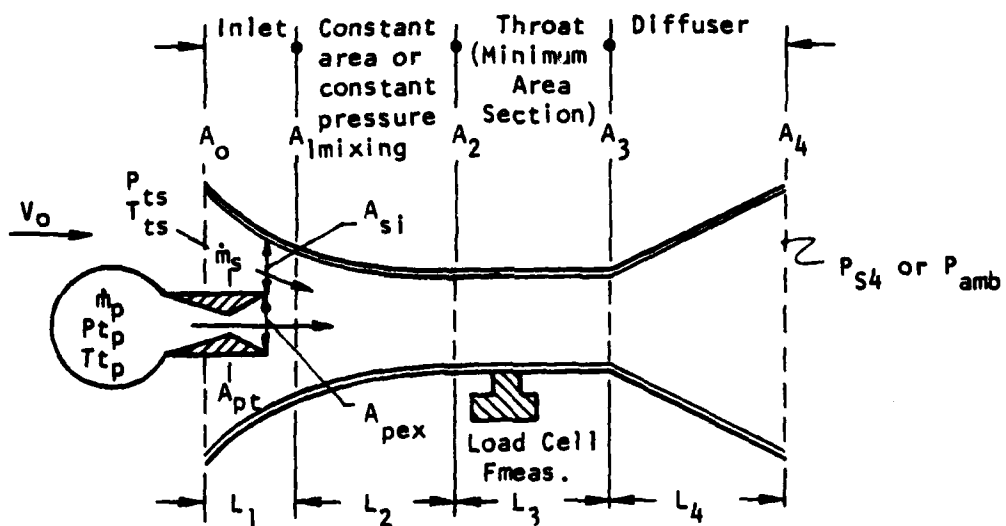


FIGURE A-4. EJECTOR SUMMARY/OVERVIEW INFORMATION FORM (CONTINUED)

replies which were received were quite informative. Summarization of the responses is included in the discussions in the following subsections of this appendix, and a general synopsis is provided below:

(a) A wide variety of ejector applications was evident from the responses. In general, the performance levels required were met or exceeded.

(b) The resulting list of foremost current experts was surprisingly short, relatively uniform, and generally limited to recent investigators. By inference with regard to the last point, it might be concluded that ejector technology is believed to have advanced beyond the state of some of the earlier noteworthy investigators.

(c) Definitions of basic performance parameters were extremely diverse, while maintaining enough similarity to create confusion in comparison of results.

(d) A wide variety of parameters was considered to be important in specifying ejector performance. Almost all responses included some area ratio and some length dimension, but only one response cited the ejector volume as important.

(e) With few exceptions, the individual who responded to the request for information indicated that an effort of this type is needed.

Following a review of the current literature and the answers to question No. 6 of the request for information (see Figure A-4), approximately 25 individuals were contacted regarding important questions concerning ejector technology. The following is a listing of those individuals contacted:

Dr. M. Alperin
Flight Dynamics Research Corp.
Van Nuys, California

Dr. Paul M. Bevilaqua
Rockwell International Corp.
Columbus, Ohio

Dr. Triumalesa Duvvuri
Duvvuri Research Associates
Chula Vista, California

Dr. J. Fabri
Office National d'Etudes
et de Recherches Aeronautique
Paris, France

Dr. Joseph Foa
School of Engineering
and Applied Science
George Washington University
Washington, D. C.

Dr. Kenneth A. Green
Naval Air Development Center
Warminster, Pennsylvania

Mr. P. Guenne
Societe Bertin & Cie
Paris, France

Dr. S. Hasinger
Wright-Patterson AFB
Dayton, Ohio

Dr. K. H. Hohenemser
Washington University
Department of Mechanical Engineering,
Sever Institute of Technology
St. Louis, Missouri

Dr. Kentfield
University of Calgary
Alberta, Canada

Mr. David Koenig
NASA Ames Research Center
Moffett Field, California

Mr. Lewis A. Maroti
Dynatech Research and
Development Company
Cambridge, Massachusetts

Dr. David Migdal
Grumman Aerospace Corp.
Bethpage, New York

Dr. K. S. Nagaraja
U. S. Air Force
Department of Defense
Wright-Patterson AFB
Dayton, Ohio

Dr. Peter Payne
Payne, Inc.
Annapolis, Maryland

Dr. Maximilian F. Platzer
Naval Post Graduate School
Monterey, California

Dr. M. R. Seiler
Rockwell International
Columbus Aircraft Division
Columbus, Ohio

Dr. Frank D. Stull
U. S. Air Force
Department of Defense
Wright-Patterson AFB/APL
Dayton, Ohio

Dr. Helmut T. Uebelhack
Dornier System
Friedrichshafen
GERMANY

Dr. Hermann Viets
Wright State University
Dayton, Ohio

Dr. Hans J. P. Von Ohain
Chief Scientist
U. S. Air Force
Department of Defense
Wright-Patterson AFB
Dayton, Ohio

Dr. Brian Quinn
Air Force Office of
Scientific Research

Dr. James Wilson
Air Force Office of
Scientific Research

Mr. Henry Woolard
Air Force Flight
Dynamics Laboratory

The questions which were addressed covered the topics listed below:

V/STOL Ejector Augmentors
Coanda Effect Ejectors
Ejector-Diffusers
Supersonic Ejector Augmentors

The specific questions in each of the foregoing topic areas are listed below. The discussions provided by those who responded to these questions have been incorporated into the main text of the Phase II technical report.

V/STOL EJECTOR AUGMENTORS

1. What is the importance of scale effects in developing a full-scale aircraft ejector system on the basis of small scale tests? Are inlet and nozzle separation effects significantly dependent on scale?
2. What is the most effective method of energy transfer? Does mixing on the microscopic level affect the optimum design geometry? Are large or small scale eddies most effective for mixing? What types of analytical or experimental programs are needed to understand the mixing phenomena? (How well is it currently understood?)
3. Can acoustic interactions be used to enhance mixing and alleviate temperature degradation effects?
4. What tradeoffs, in a practical sense, are required for ejectors designed for an aircraft application?
5. What are the major considerations to be made in matching an aircraft engine and ejector design for optimal performance?
6. What geometric or primary flow conditions or variations are required to maintain a high augmentation ratio in forward flight?
7. What are the similarities between augmentors in forward flight and ejector compressors or pumps?
8. What is the most meaningful definition of thrust augmentation ratio for a V/STOL aircraft application, and why? What is the most meaningful geometric compactness parameter, and why?
9. Complete utilization of the energy in a primary jet is not realized, even for the theoretical ideal expansion to ambient. How does the maximum ideal augmentation total thrust compare with a hypothetical complete utilization of the primary jet energy for thrust in a single nozzle? How do the propulsive efficiencies compare for the ideal and real cases? What is the relationship between energy transfer fraction and augmentation ratio? How does this compare with a tip turbine driven fan?

COANDA EFFECT EJECTORS

1. What is the main theoretical advantage which can be obtained in ejector performance by the use of the Coanda effect? How does the theoretical advantage hold up in practice?
2. What practical limitations arise when applying the Coanda effect to an ejector design?
3. What geometric or initial flow conditions could be varied to enable a Coanda effect ejector to maintain performance under varying ambient conditions (cross wind, reduced pressure, etc.)?
4. What part does mixing and/or entrainment play in the efficiency of the Coanda effect?

EJECTOR-DIFFUSERS

1. How significant are separation effects in ejector diffusers? How is separation affected by scale in model and prototype testing? How is it affected by the flow conditions--subsonic, low pressure vs. supersonic, high pressure primary jets?
2. What are the theoretical considerations for the jet flap diffuser work, and what wall radius of curvature is required?
3. How important is mixing in an ejector-diffuser to the augmentation and compactness?
4. Can augmentation be related to the total primary jet diffusion area ratio, rather than some combination of mixing and diffuser area ratios? If so, how?

CRYPTO & NON-STEADY AUGMENTORS

1. How do the theoretical maximum augmentation ratios for steady flow and non-steady flow augmentors compare? Why is viscous energy transfer less (or more, if it is) efficient than direct impact energy transfer?
2. What are the practical limitations of crypto and non-steady augmentors, in terms of valving, aircraft integration, rotational speeds, noise, etc.?

3. How do the actual augmentation ratios compare between non-steady and steady flow augmentors?

4. What pulse frequency limits exist due to choking phenomena?

SUPERSONIC EJECTOR AUGMENTORS

1. How can the primary jet influence a supersonic secondary flow? What limits the maximum mass flow ratio?

2. What type of inlet is most suitable for a supersonic augmentor, i.e., internal compression with normal shock at the ejector entrance vs. external compression with subsonic secondary flow at the ejector entrance?

3. How does the efficiency of a supersonic ejector augmentor compare with the efficiency of a turbofan operating at supersonic speeds?

4. Is it feasible to attempt to utilize non-steady augmentors at supersonic flight conditions? (See question 4 on Non-Steady Augmentors.)

A-2 Definition of Application Areas for Ejector Augmentors

In the area of thrust augmentation, the ejector energy transfer phenomenon has been applied, or proposed for application, to the following problems:

- (1) V/STOL aircraft thrust
- (2) Underwater vehicle thrust
- (3) Vehicle Base drag reduction
- (4) Ramjet Thrust
- (5) Fighter and Transport Aircraft thrust (Horizontal Flight)
- (6) Reaction Control thrust
- (7) Helicopter Blade tip jet drive

Within the area of thrust augmenting ejectors, there is thus represented an almost overwhelming complexity of problems ranging from geometric "packaging" to fundamental flow phenomena. A brief consideration of the specific areas of thrust augmentation application provides some insight into the uniqueness of each:

V/STOL aircraft thrust - The primary requirement is for short mixing lengths, capable of being fitted into a wing or fuselage.

Underwater vehicle thrust - Dual phase flow performance (steam-water) may be the most significant difference for this augmentor application.

Vehicle base drag reduction - The requirement for a significantly higher mixing plane static pressure makes this application unique.

Ramjet thrust - Operation at supersonic Mach numbers can result in a supersonic-supersonic (depending on the secondary flow inlet configuration) energy transfer mode.

Fighter and Transport aircraft thrust - Performance over a wide range of secondary inlet forward velocities, up to high subsonic Mach numbers, poses a serious problem to fixed geometry/fixed primary flow ejectors.

Reaction Control Thrust - Possibly intermittent operation coupled with high velocity primary flows and extreme volume requirements result in a different set of problems.

Helicopter Blade tip jet drive - This application presents a unique problem, since in forward flight, the ejector is presented with a non-steady secondary flow as the blade alternately advances and retreats.

While the differences in these applications may be at first discouraging, certain similarities with other applications tend to provide a more optimistic outlook. For instance, steam-water pumps are well-proven devices with a long history of useful application. The techniques which enable the steam-water pump to work effectively may be equally valid for underwater vehicle thrust augmentation. Similarly, the unsteadiness of the secondary flow in a helicopter blade tip jet drive application may prove to be an asset if the primary flow is correspondingly non-steady. Similarities of this type have been examined in greater detail in the Formulation of Comparison Bases (Section A-3) and the Identification of Significant Operating Parameters (Section A-4) for both theory and experiment.

A-3 Formulation of Comparison Bases

In the past it has been the practice to restrict comparisons of ejector performance to areas of specific application. Few comparisons cut across these lines, so that the relationships between, for example, ejector augmentors and ejector pumps can not be easily ascertained. Although to a lesser degree, this practice is also predominant in discussions of ejector theory and design; where, for example, the analysis of an ejector pump for laser applications may differ so much from that for cooling system applications that the two seem to have little or no relationship. While the end use of the ejector is undoubtedly important to its analysis, design and performance, the basic concept of energy transfer from one stream to another is inherent in all applications. The fundamental differences and similarities between applications must thus be found in the definitions of the streams themselves and in the mechanisms of the energy transfer.

In this Formulation of Comparison Bases, then, the fundamental descriptions for ejectors of all types have been addressed. Three sets of baseline descriptions have emerged. All categories of ejectors may be placed within each set, and the resulting three-element code appears to uniquely describe ejectors with similar design, analysis and performance traits. Through the use of this categorization procedure, identification of significant operating parameters (described in the following subsection (A-4)) leads to additional insight into design and performances similarity. The sets which were defined are:

Primary/Secondary Stream Phase Relationships

Energy Transfer Property of Interest

Primary/Secondary Time-Dependence

These baseline areas for segregating ejectors are discussed briefly below:

Primary/Secondary Stream Phase Relationships

Classification of ejectors by phase relationship has occurred naturally in the past due to the difficulty in specifying a general analytical procedure for all types of phase relationships, as well as the fact that differences in phase relationships generally occur for what are on the

surface, completely unrelated applications. Table A-1 shows a matrix of the types of phase relationships between secondary and primary streams. Virtually all known applications of ejectors fall into one of the categories defined by this matrix. Also shown in Table A-1 are specific examples where these relationships have occurred in practice. The numbers in each square of the matrix refer to reports listed in the bibliography which are relevant to the phase relationship of the matrix square.

It is interesting to note that the matrix of Table A-1 makes no distinction between the use of single, dual, or multi-fluid ejectors, except in their phase relationships. That is, helium/air and air/air ejectors fall into the same baseline set (Gas/Gas) and as such, should be placed on the same design, analysis, and performance basis.

Energy Transfer Property of Interest

While two ejectors may have the same phase relationship, because of differences in their intended use, a comparison of their performance may seem irrelevant, if not impossible. Thus, the augmentation ratio of one air/air ejector has seemingly little bearing on, or relationship to, the pumping pressure ratio of another air/air ejector. In considering the fundamental differences between areas of ejector application, it appeared that the important aspect was the intent of the type of energy transfer. In this Phase I activity, a preliminary breakdown into four main areas of ejector application has thus been made on the basis of the Energy Transfer Property of Interest. Table A-2 shows examples of the four areas of application and the energy transfer properties which are primarily associated with each. It can be seen from this table that there is, in general, an overlap in the energy transfer properties associated with the various applications, although in each of the applications shown, one type of energy transfer is desired.

It is recognized that the matrix shown in Table A-2 is not complete at this time and that other transfer processes might be included (i.e., momentum and mass) in a base formulation, but from the results of this Phase I activity, the energy transfer appears to be the most consistent comparison base.

TABLE A-1 EXAMPLES OF PRIMARY/SECONDARY RELATIONSHIPS FOR EJECTORS.

PRIMARY

		PRIMARY				
		GAS	LIQUID	GAS/LIQUID	GAS/SOLID	LIQUID/SOLID
SECONDARY	GAS	Air/Air (920)	Water/Steam (461)	H ₂ O, O ₂ , N ₂ /Air (314)	Particle-Laden Air/Air (313)	NaCl, Water/Air (127)
	LIQUID	Air/LO ₂ or LN ₂ (410)	Gasoline/Gasoline (1488)	Saturated Steam/Water (689)	—	—
	GAS/LIQUID	Gas/LH ₂ , H ₂ , LO ₂ , O ₂ (410)	Salt Water/Steam, CO ₂ (155)	Vapor Fuel/vapor fuel (1417)	—	—
	GAS/SOLID	Air, Air/Fly-ash (1485)	Water/Air, Sand (356)	Air, Water/Air, Water Silt (567)	—	—
	LIQUID/SOLID	Air/Water, Coal (276)	Water/Mud Slurry (1591)	Air, Water/Water, Fish (484)	—	Liquid Metal/Liquid Metal (154)

I. SINGLE PHASE

II. DUAL PHASE

III. MULTI-PHASE

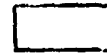


TABLE A-2 EJECTOR ENERGY TRANSFER PROPERTIES OF INTEREST

EJECTOR APPLICATION EXAMPLE	PRIMARY & SECONDARY TRANSFER PROPERTY			
	A. KINETIC	B. PRESSURE	C. THERMAL	D. ACOUSTIC
1. PUMPING	X	⊗		
2. THRUST AUGMENTATION	⊗	X		
3. NOISE SUPPRESSION	X			⊗
4. COOLING		X	⊗	

⊗ PRIMARY

X SECONDARY

TABLE A-3 EJECTOR PRIMARY/SECONDARY TIME-DEPENDENCE

		PRIMARY	
		STEADY	NON-STEADY
SECONDARY	STEADY	CONVENTIONAL EJECTOR (#1178)	ROTARY JET FLOW INDUCTOR (#384)
	NON-STEADY	HELICOPTER BLADE CONVENTIONAL EJECTOR JET TIP DRIVE (#585)	HELICOPTER BLADE ROTARY JET TIP DRIVE (#585)

Primary/Secondary Time-Dependence

While various mechanisms for energy transfer may be postulated, currently two mechanisms are predominant in the literature. These are: (a) Viscous mixing and (b) Direct Impact. Generally, all ejector-type devices have some combination of these two mechanisms present in their operation. Specification (a priori) of the extent of either transfer mechanism is, however, extremely difficult, if not impossible. However, because one (viscous) mixing is predominantly associated with a device which has steady-state operation, while the other is generally associated with devices which are non-steady in a lab-fixed reference system, the time-dependence feature has been used to form the reference base.

Table A-3 shows the basic matrix for this comparison base references reports in the Bibliography which discuss the various prime combinations which have been considered.

The matrices shown in Tables A-1 - A-3, which specify the operational characteristics of ejectors, must be combined to form specific Operational Categories. As part of this Phase I activity, which was restricted to Steady State, Single Phase, Single Fluid, the following Operational Categories have been tentatively defined (All are steady state, single phase):

Category I-A: SP, SS - Kinetic Energy Transport

Category I-B: SP, SS - Pressure Energy Transport

Category I-C: SP, SS - Thermal Energy Transport

Category I-D: SP, SS - Acoustic Energy Transport

A-4 Identification of Significant Operating Parameters

Because of the diversity of uses and types of ejectors, identification of significant operating parameters on the basis of available theory and experiment resulted in a somewhat different set of parameters for each operational category. The identification is further complicated by inconsistencies in parameters' definitions, even within a specific category, as well as a lack of uniformity in the nomenclature used for common parameters.

Despite the situation described above, certain parameters appear to be significant for virtually all types and categories of ejectors, and these may eventually provide the key whereby ejector technology will advance beyond its present "black art" state to a well-defined science.

Based on the available reports and personal recent responses, the significant operating parameters for ejectors have been grouped as follows:

- Static Properties
- Geometric Parameters
- Mean Flow Properties
- Performance Descriptors
- Loss Descriptors

An overview of the basic parameters of significance, as well as what appear to be especially important ratios in defining design or performance, is provided in this subsection as Tables A-4 - A-8 for each of the above groups. Also shown on these tables are the operational categories which were found to utilize given parameters in either design, analysis, or performance specification.

It can be seen from this latter cross-reference that certain parameters do tend to show up in almost all operational categories. These are:

Static Properties - Virtually all static properties are appropriate to all categories considered.

Geometric Parameters - The following geometric parameters and ratios appeared to be common to the four categories considered:

- (a) Ejector Exit Area, A_4
- (b) Number and type of primary nozzles, N
- (c) Mixing section length, L_2
- (d) Minimum width or diameter, W
- (e) Total displaced volume, v
- (f) Non-dimensional total length, L_t/W
- (g) Secondary to primary area ratio, $A_{s1}/A_{p_{ex}}$

TABLE A-4 SIGNIFICANT OPERATING PARAMETERS OF STATE

PROPERTY/PARAMETER		STATE PROPERTIES	USED IN OPERATIONAL CATEGORY*			
			I-A	I-B	I-C	I-D
1. Phase			X			X
2. Pressure			X	X	X	X
P_{tp}	primary fluid total pressure		X			X
P_{ts}	secondary fluid total pressure		X	X	X	X
P_{s1}	secondary fluid inlet static pressure		X	X	X	X
P_{s3}	mixed fluid minimum area pressure		X	X		X
P_{s4}, P_{amb}	exit static pressure		X			X
3. Temperature			X	X	X	X
T_{tp}	primary fluid total temperature		X			X
T_{ts}	secondary fluid total temperature		X	X	X	X
4. Density			X	X	X	X
ρ_p	primary fluid density		X			X
ρ_s	secondary fluid density		X	X	X	X
5. Specific Heat			X	X	X	X
$C_{p,p}, C_{v,p}$	primary fluid specific heat		X			X
$C_{p,s}, C_{v,s}$	secondary fluid specific heat		X	X	X	X
6. Molecular Weight			X	X	X	X
MW			X	X	X	X

(REFER TO FIGURE A-5 ON PAGE A-32)

Table A-4 (Continued)

STATE PROPERTY RATIOS		USED IN OPERATIONAL CATEGORY*			
PROPERTY/PARAMETER	DESCRIPTION	I-A	I-B	I-C	I-D
1. P_{t_p}/P_{t_s}	Primary to secondary total pressure ratio	X	X	X	X
2. T_{t_p}/T_{t_s}	Primary to secondary total temperature ratio	X	X	X	X
3. ρ_p/ρ_s	Primary to secondary density ratio	X	X	X	X
4. $P_{t_p}/P_{t_{si}}$	Primary nozzle pressure ratio	X	X	X	X
5. $\gamma_p = C_{p_p}/C_{v_p}$	Primary Flow Specific Heat Ratio	X	X	X	X
6. $\gamma_s = C_{p_s}/C_{v_s}$	Secondary Flow Specific Heat Ratio	X	X	X	X
7. C_{p_p}/C_{p_s}	Primary to secondary fluid specific heat ratio	X		X	
8. γ_p/γ_s	Ratio of Specific Heat Ratios of Primary to Secondary Fluid	X	X	X	X

TABLE A-5 SIGNIFICANT GEOMETRIC PARAMETERS

GEOMETRIC PARAMETERS		USED IN OPERATIONAL CATEGORY*			
PROPERTY/PARAMETER	DESCRIPTION	I-A	I-B	I-C	I-D
		1. Area	Primary nozzle exit area	X	X
Apex	Inlet area	X	X	X	
A ₀	Secondary flow area	X	X	X	
A _{5j}	Mixing area	X	X	X	
A ₁	Throat area				X
A ₂	Diffuser entrance area	X	X	X	
A ₃	Ejector exit area	X	X	X	
A ₄	Diffuser half angle	X	X	X	
2. θ	Number of primary nozzles	X	X	X	
3. N	Primary nozzle length	X	X	X	
4. Length	Inlet length	X	X	X	
	Mixing length	X	X	X	
	Throat (minimum area) length	X	X	X	
	Diffuser length	X	X	X	
	Minimum width or diameter	X	X	X	
	Total displaced volume	X	X	X	
5. W, D					
6. v					

TABLE A-5 (Continued)

GEOMETRIC PARAMETER RATIOS					
PROPERTY/PARAMETER	DESCRIPTION	USED IN OPERATIONAL CATEGORY#			
		I-A	I-B	I-C	I-D
7. Ratio					
$\frac{L_t}{W} = \frac{L_0+L_1+L_2+L_3+L_4}{W}$	Non-dimensional total length	X	X	X	X
$\frac{L_2+L_3+L_4}{W}$	Non-dimensional mixing and diffuser	X	X	X	
$\frac{A_4}{A_{pex}}$	Ejector exit area to primary exit ratio	X	X		
$\frac{A_{5i}}{A_{pex}}$	Secondary to primary area ratio	X	X	X	X
$\frac{A_4}{A_3}$	Diffuser area ratio	X	X	X	X

TABLE A-6 SIGNIFICANT MEAN FLOW OPERATING PARAMETERS

PROPERTY/PARAMETER		MEAN FLOW PROPERTIES				USED IN OPERATIONAL CATEGORY*			
		DESCRIPTION				I-A	I-B	I-C	I-D
1. Mach Number		Primary nozzle exit Mach number				X	X		X
M_{pex}		Secondary flow inlet Mach number				X	X		X
M_{si}		Forward flight Mach number				X	X		X
M_o		Primary mass flow rate				X	X	X	X
2. Mass Flow Rates		Secondary mass flow rate				X	X	X	X
\dot{m}_p, \dot{m}_p		MEAN FLOW PROPERTY RATIOS							
\dot{m}_s, \dot{m}_s		Primary to (average) inlet velocity ratio				X	X	X	
1. Ratio		Primary to secondary mass flow ratio				X	X	X	X
$\frac{V_p}{V_j}$		Primary to secondary Mach number ratio				X	X	X	X
$\frac{\dot{m}_s}{\dot{m}_p}$		Diffuser velocity ratio				X	X		X
$\frac{M_{pex}}{M_{si}}$		Velocity skewness factor [at either the inlet (i) or exit (4)]				X	X		X
2. Factor/Value									
$\frac{\bar{V}_4}{\bar{V}_3}$									
$\lambda = \frac{\int v^2 dA}{\bar{V}^2 A}$									

TABLE A-7 SIGNIFICANT PERFORMANCE DESCRIPTORS

PERFORMANCE DESCRIPTORS		USED IN OPERATIONAL CATEGORY*			
PROPERTY/PARAMETER	DESCRIPTION	I-A	I-B	I-C	I-D
$1. \phi = \frac{\text{measured ejector thrust}}{m_p V_{pisen}}$ $= \frac{\text{measured ejector thrust}}{\text{ideal nozzle thrust}}$ $= \frac{(m_p + m_s) V_4 - m_p V_{pex} - m_s V_s}{m_p V_{pex}}$ $= \frac{\text{measured ejector thrust}}{\text{measured primary jet thrust}}$	Thrust augmentation ratio (V_{pisen} = primary nozzle velocity expanded to ambient)	X			
$2. \mu = \frac{m_s}{m_p}$ $= \frac{m_s}{m_p} \sqrt{\frac{T_{ts}}{T_{tp}}}$ $= \frac{m_s}{m_p} \frac{P_{tp}}{P_{ts}} \sqrt{\frac{T_{ts}}{T_{tp}}}$ $= \frac{m_p + m_s}{m_p}$	Pumping ratio		X	X	
				X	
			X		
				X	
			X		

TABLE A-7 (CONTINUED)

PERFORMANCE DESCRIPTORS		USED IN OPERATIONAL CATEGORY#			
PROPERTY/PARAMETER	DESCRIPTION	I-A	I-B	I-C	I-D
<p>3. η_E</p> $= \frac{[\text{total energy}]_4}{[\text{total energy}]_{p_0} + [\text{total energy}]_{so}}$ $= \frac{1 - \phi_{meas}}{1 - \phi_{max \text{ theoretical}}}$ $= \frac{m_s (V_{s4}^2 - V_0^2)}{m_p (V_{pex}^2 - V_{p4}^2)}$ $= \frac{m_s}{m_p} \left[\frac{P_{s4} - P_{ts}}{P_{tp} - P_{s4}} \right]$	<p>Ejector efficiency</p> <p>(1)</p> <p>(2)</p> <p>(3)</p> <p>(4)</p>	X	X	X	X
<p>4. Pressure</p> $\frac{P_4 - P_{ts}}{P_{tp}}$ P_4/P_{ts}	<p>Dimensionless static pressure rise</p> <p>(1)</p> <p>(2)</p>	X	X	X	

TABLE A-8 SIGNIFICANT LOSS DESCRIPTORS

LOSS DESCRIPTORS		USED IN OPERATIONAL CATEGORY*			
PROPERTY/PARAMETER	DESCRIPTION	I-A	I-B	I-C	I-D
1. η_D $= \frac{P_{s4} - P_{s3}}{\frac{1}{2}(V_4^2 - V_3^2)}$ $= \frac{T_4 \text{isen} - T_3}{T_4 - T_3}$	Diffuser efficiency (1) (2)	X	X		X
2. η_{poly} $= \frac{\ln T_4 \text{isen} - \ln T_3}{\ln T_4 - \ln T_3}$	Polytropic Diffuser efficiency	X	X	X	X
3. $C_f L_t$ $\frac{C_f L_t}{2d}$	Skin friction loss coefficient	X	X	X	X
4. $\frac{P_{t3}}{P_{t2}}$	Total pressure ratio across shock (downstream/upstream)	X	X		

Mean Flow Properties - Mass flows, mass flow ratios, and the Mach number ratio were the common mean flow properties:

- (a) m_s, m_p , Secondary and Primary mass flows, respectively
- (b) m_s/m_p , Secondary to Primary mass flow ratio
- (c) $M_{p_{ex}}/M_{s_i}$, Primary to Secondary Mach Number

Performance Descriptors - Because of the disparity in the desired result of the ejector application between the various categories, only internal overall efficiencies appeared as common performance descriptors:

- (a) Total energy ratio, $\frac{E_{t_4}}{E_{t_p} + E_{t_s}}$
- (b) Kinetic energy transfer efficiency, $\frac{m_s (V_4^2 - V_o^2)}{m_p (V_{p_{ex}}^2 - V_4^2)}$

Loss Descriptors - Specific descriptors of internal losses which were common to all four categories were:

- (a) Polytropic diffuser efficiency, $\frac{\ln T_{4;SEN} - \ln T_3}{\ln T_4 - \ln T_3}$
- (b) Skin friction loss coefficient, $\frac{C_f L_t}{2d}$

A general schematic of an ejector configuration which shows the orientation of the significant geometric parameters is shown in Figure A-5.

A-5 Definition of Parametric Effects and Comparison of Available Theory and Performance

The definitions and comparisons presented herein have been restricted to Category I-A ejectors, with emphasis solely on thrust augmenting devices. In this subsection then, first, a somewhat general discussion is presented of the parametric effects of the significant geometric and operating parameters

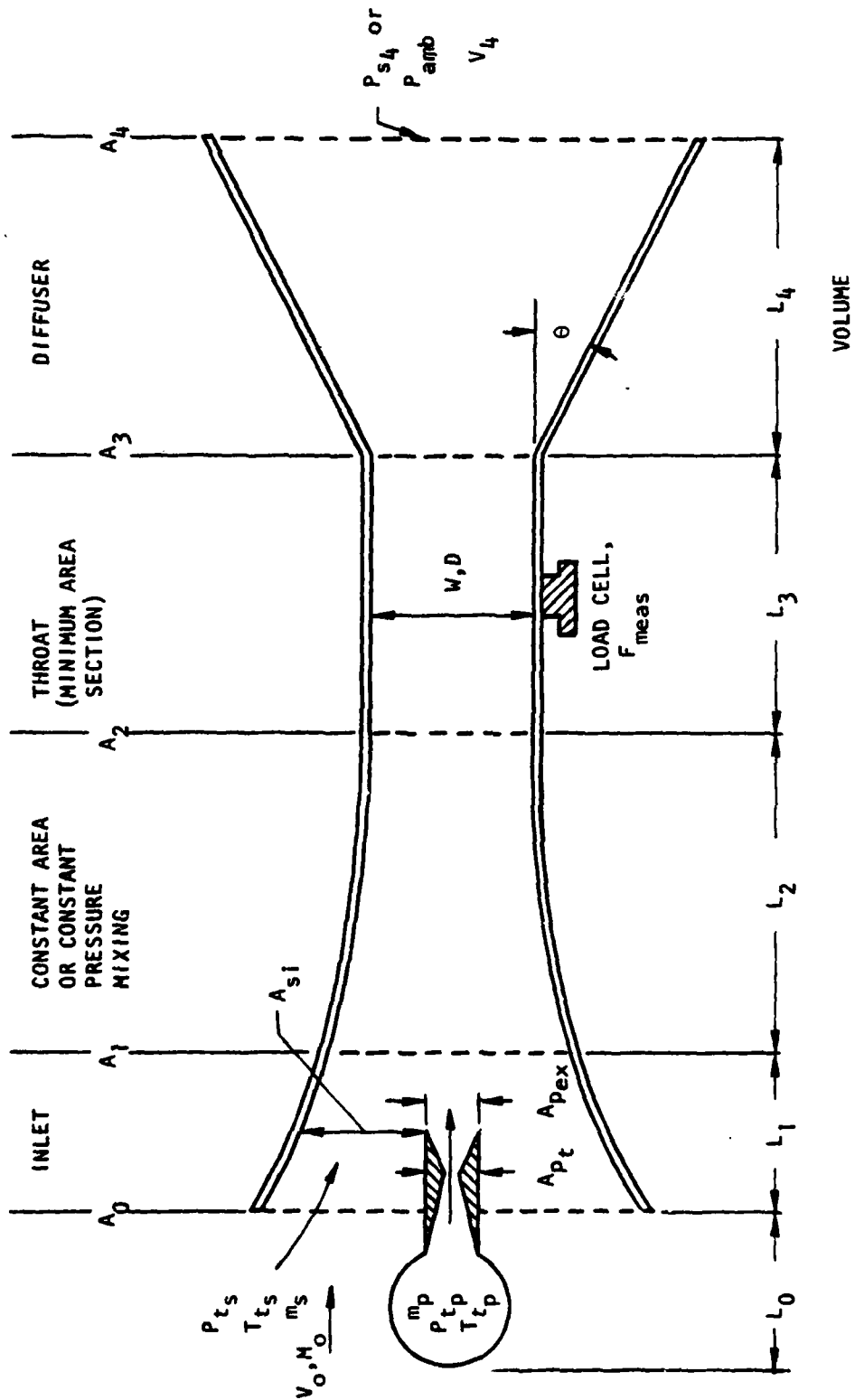


FIGURE A-5. EJECTOR SCHEMATIC

on ejector augmentor performance, and second, a rather broad comparison of theory and experimental performance on the basis of overall system parameters.

Ejector Augmentor Parametric Effects

The performance of thrust augmenting ejectors is generally agreed to be best measured by the thrust augmentation ratio, ϕ . However, as shown in Section A-2, there is not always agreement on the definition of this parameter. The major difference probably occurs in the variations in the definition of the primary normalizing thrust. Experimentally, the measured mass flow times the velocity for ideal expansion to ambient, \dot{m}_p measured V'_p , is used; in theoretical treatments, mass flow degradations due to a primary nozzle discharge coefficient less than one are generally not included. Variations from the theoretical primary nozzle exit static pressure are also common to experiments having operating parameters otherwise comparable to the theoretical treatments. These pressure differences result in differing primary exit velocities and thus, differences between the theoretical and experimental primary normalizing thrust. In this discussion of parametric effects, such variations have not been considered.

The other significant element of a discussion of theoretical and experimental parametric effects is that few theories or experiments have completely identical sets of significant geometric and operating parameters. Because of this, the comparisons presented in this subsection are generally only indicative of general trends of parameters and the correspondence of these trends to theoretical predictions.

Figures A-6 and A-7 show the effect of area ratios A_{s1}/A_p and A_4/A_3 and lengths L_2/W and L_4/W on augmentation ratio. Ideal augmentor performance increases monotonically with increasing A_{s1}/A_p and A_4/A_3 , but real fluid effects (mixing losses, skin friction, and separation) cause a falling off in performance at higher area ratios. As is shown in Figure A-6, augmentation ratio is very sensitive to diffuser efficiency (early studies showed no benefit in adding a diffuser to an augmentor, probably because the diffuser efficiency was poor). Efficient, high area ratio diffusers have been the goal of recent studies.

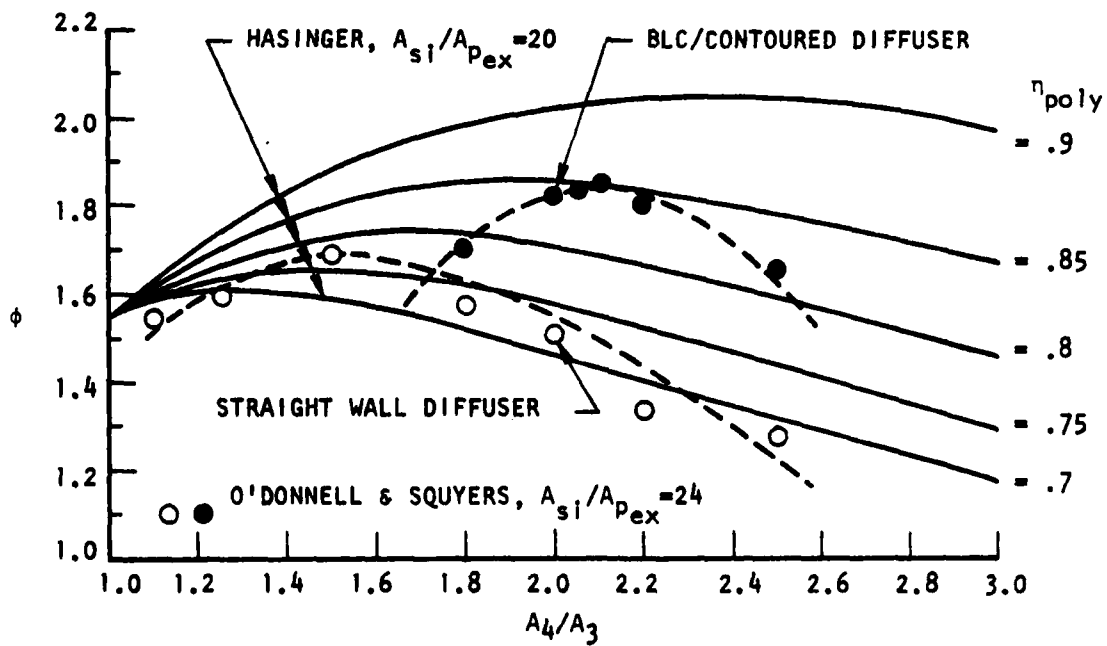
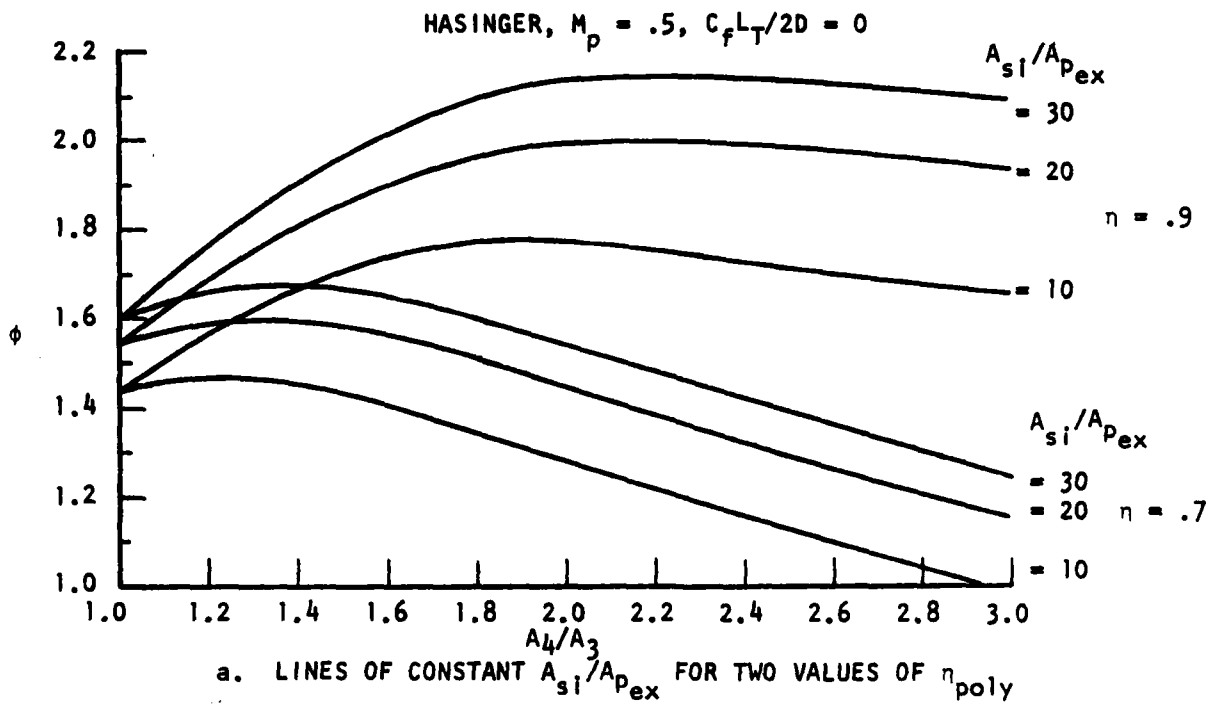


FIGURE A-6 EFFECT OF DIFFUSER AREA RATIO AND SECONDARY TO PRIMARY INLET AREA RATIO ON AUGMENTATION.

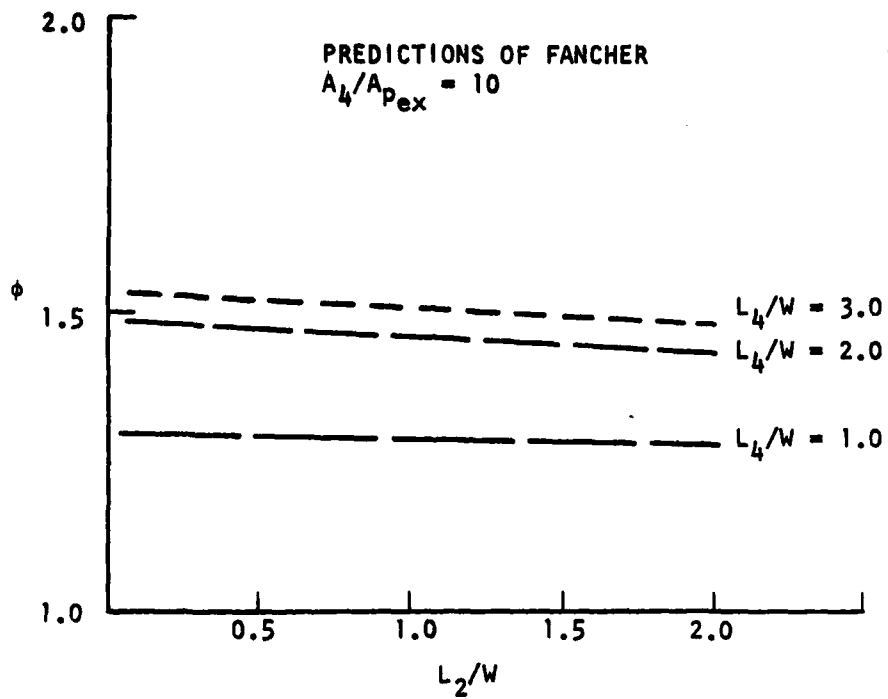
Overall length effects can be broken down into mixing length (L_2) effects and diffuser length (L_4) effects, which are presented in Figures A-7a&b. For compactness and minimum skin friction losses, both should be made as short as possible. Minimum mixing length is limited by the rate of momentum transfer (mixing), and minimum diffuser length is limited by diffusion rate (separation) criteria.

Figures A-8a,b&c present the general effects of variation in the state property ratios T_{tp}/T_{ts} , P_{tp}/P_{ts} , and ρ_p/ρ_s . As shown in Figure A-8a, the theoretical effect of variation in T_{tp}/T_{ts} on ϕ is slight, but some investigators have obtained experimental results indicative of a more rapid fall-off in ϕ at increased temperature ratios. The theoretical effect of increased pressure ratio, P_{tp}/P_{ts} , on the other hand, shows a greater fall-off of ϕ than that found experimentally, as shown in Figure A-8b.

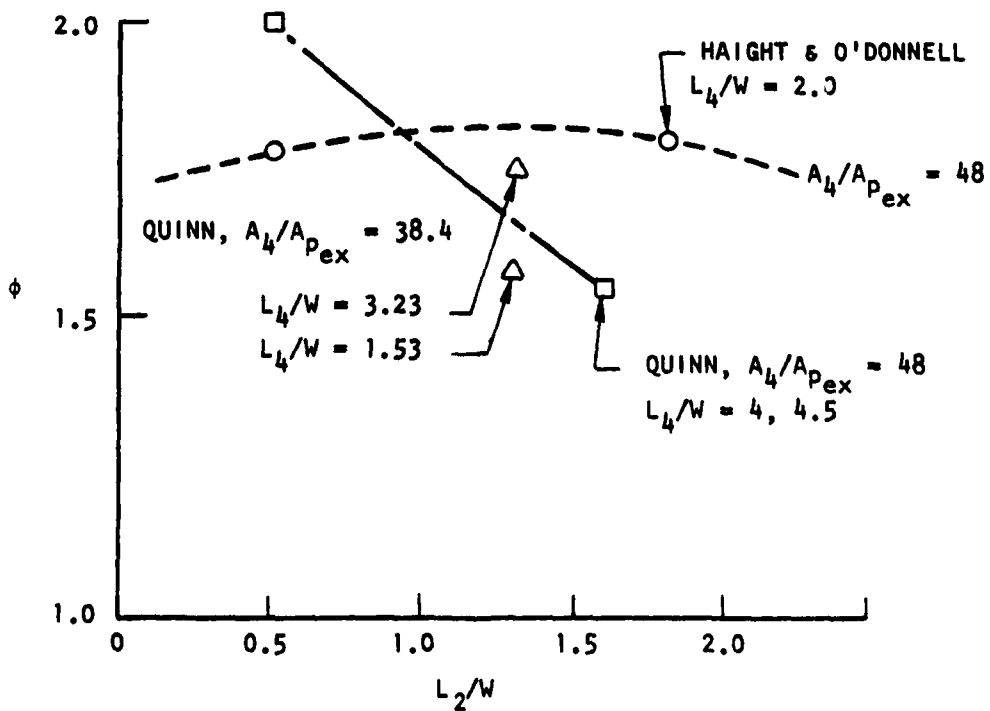
Increasing primary to secondary density ratio, ρ_p/ρ_s , at a constant mass flow ratio, m_s/m_p , theoretically provides a significant improvement in ϕ . However, the limited data available shows a contrary trend in performance, as shown in Figure A-8c. These experimental results may be misleading, however, since it was not possible to determine if other significant operating parameters had been held constant between the two data points shown.

The effects of mean flow properties M_p , M_o , and m_s/m_p are presented in Figures A-9a,b&c. In Figure A-9a, the theoretical effect of increasing primary Mach number, M_p , is shown to cause a gradual reduction in ϕ . This is in contrast to a slight increase for the experimental results shown in Figure A-9a, which can also be deduced from Figure A-8b.

Perhaps the most serious drawback to the use of ejector augmentors to increase aircraft thrust is the rapid degradation in augmentation ratio with increasing forward flight velocities. This is presented both theoretically and experimentally in Figure A-9b, where it may be observed that the two trends are in good agreement.

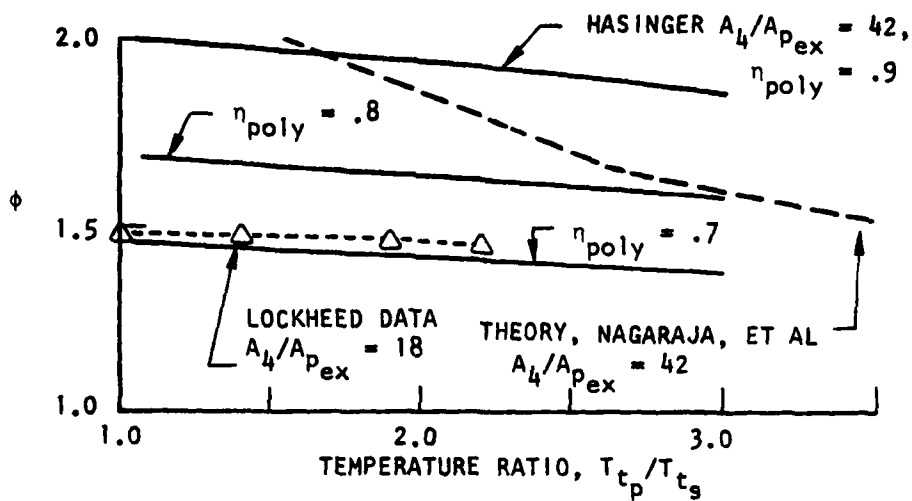


a. THEORETICAL EFFECTS

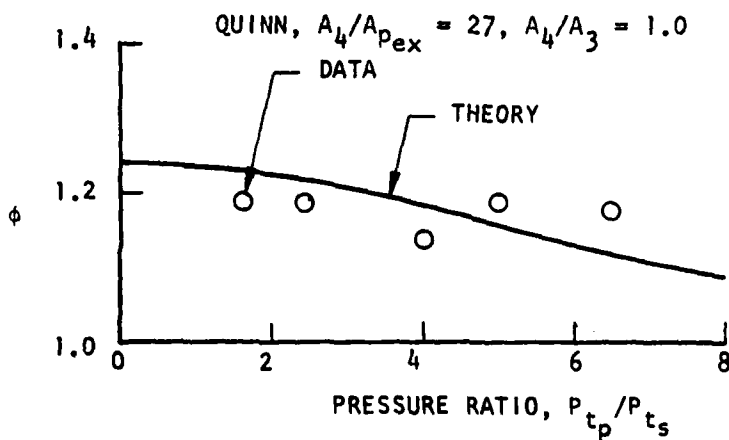


b. EXPERIMENTAL EFFECTS

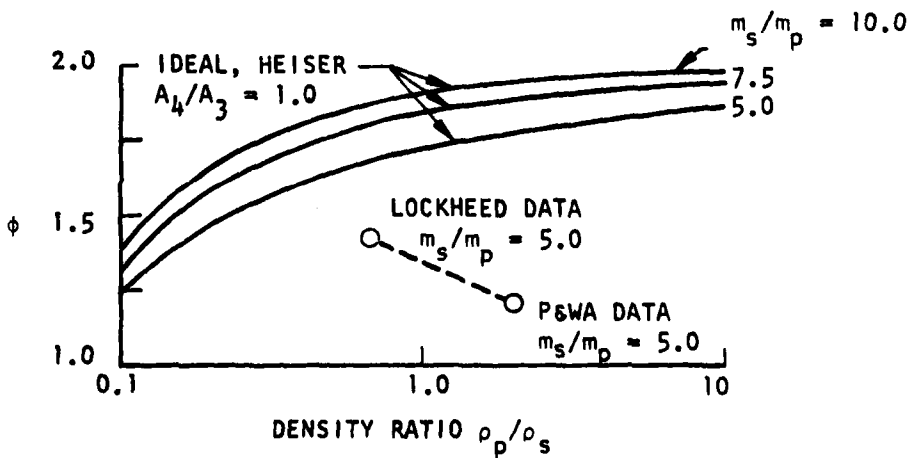
FIGURE A-7. MIXING LENGTH EFFECTS



a. EFFECTS OF TEMPERATURE RATIO, T_{tp}/T_{ts}

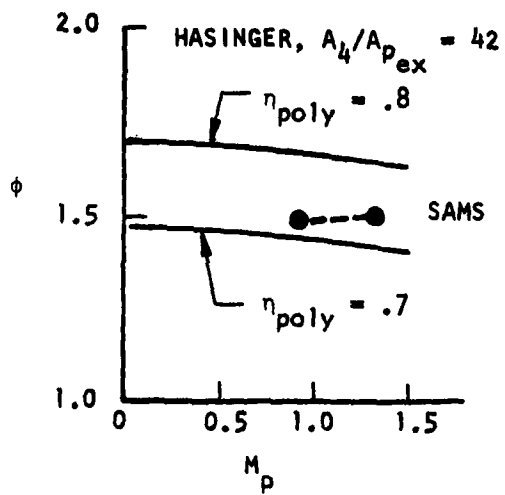


b. EFFECTS OF PRESSURE RATIO, P_{tp}/P_{ts}

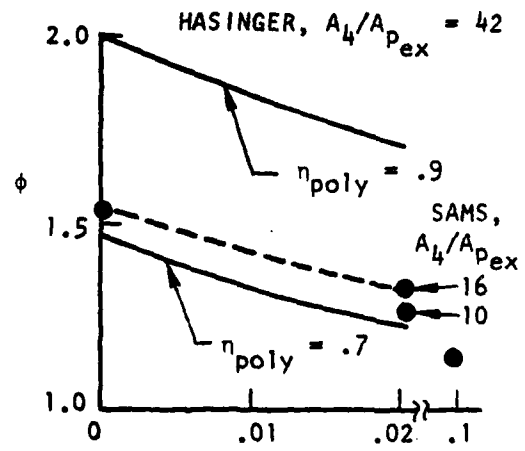


c. EFFECTS OF DENSITY RATIO, ρ_p/ρ_s

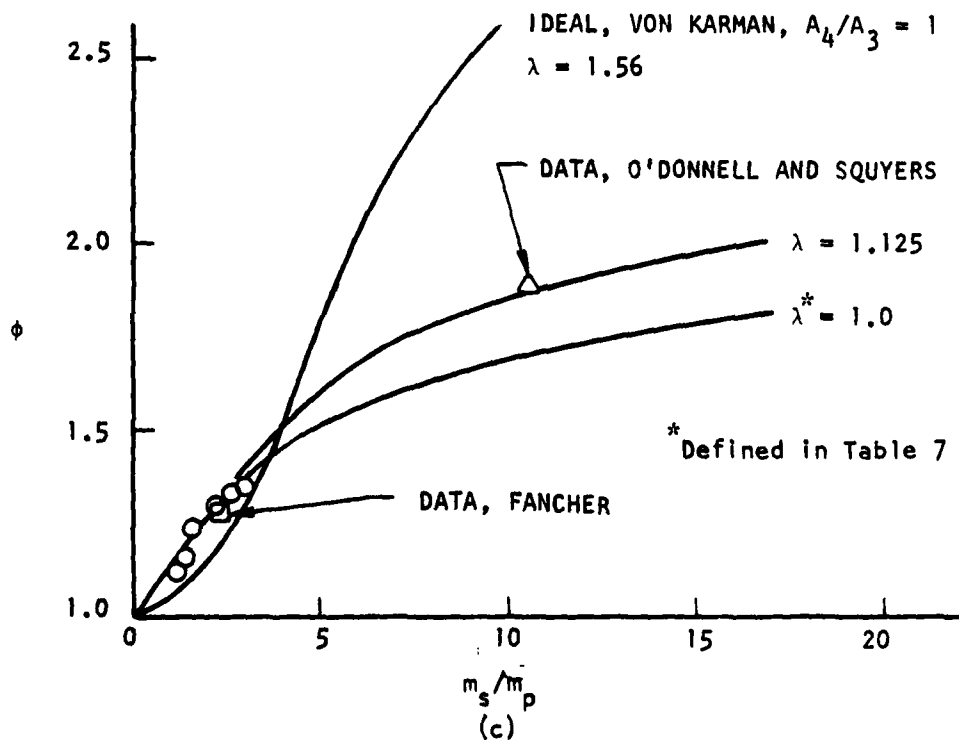
FIGURE A-8. STATE PROPERTY EFFECTS ON AUGMENTATION RATIO



(a)



(b)



(c)

FIGUREA-9. THE EFFECT OF MEAN FLOW PROPERTIES ON AUGMENTATION RATIO

Comparison of Available Theory and Experiment

In the preceding discussion, the effects of significant geometric and operating parameters on the thrust augmentation ratio, ϕ , were presented, both theoretical and as evidenced by experimental results. While these trends and effects are important to understanding and designing ejector augmentors for maximum performance, the almost limitless variety in which the significant geometric and operating parameters can be combined, as well as the difficulty in determining some of the parameters experimentally, gives rise to a need for a method of comparing total system performance, both between theory and experiment and between different experiments.

The most common (and significant) parameter for overall system performance comparisons has been the device exit area to primary exit arearatio, $A_4/A_{p_{ex}}$. Figure A-10 shows augmentation ratio vs. $A_4/A_{p_{ex}}$ from various sources. The apparent performance limit is probably related to efficiencies of the mixing momentum and energy transfer and the diffusion process. Both of these processes (mixing and diffusion) have optimum lengths, as shown previously, so that higher augmentation ratios are generally achieved at the expense of compactness. Apparently, these restrictions on mixing length and diffusion rate can be overcome by use of non-steady devices which achieve high performance through normal stress (pressure) momentum transfer, though some diffusion rate limits probably exist for such devices, also. The increase in the limit of experimental results from the work of Jones (639) to the present effort is indicative of advances in ejector state of the art, which may be attributable to non-steady primary flow characteristics. The success of the hypermixing nozzles (1019, 1021) may be due in part to the non-steady character of the primary vortex formation.

The trend toward improved performance through technology advances is also evidenced in Figure A-11, which presents augmentation ratio as a function of device total length to width ratio. Again, the use of special features such as non-steady primary flow, jet flap diffusers, and boundary layer control have resulted in significant advances in performance/compactness characteristics.

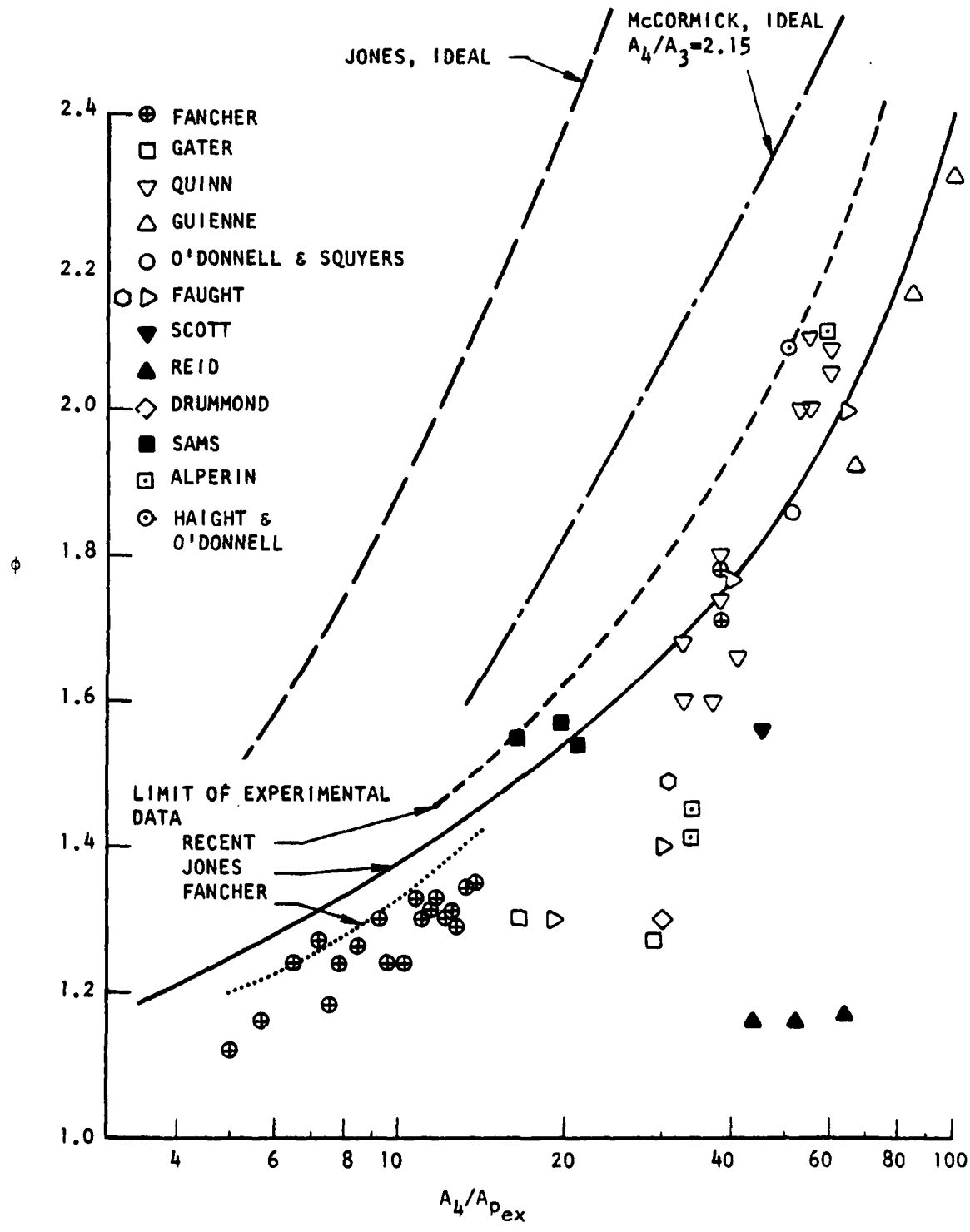


FIGURE A-10- AUGMENTATION RATIO VS. $A_4/A_{p_{ex}}$

- ◇ DRUMMOND
- GATES
- FAUGHT
- ⊠ ALPERIN
- ▼ SCOTT
- ⊕ FANCHER
- ▽ QUINN
- △ BEVILAQUA
- O'DONNELL & SQUYERS
- HAIGHT & O'DONNELL

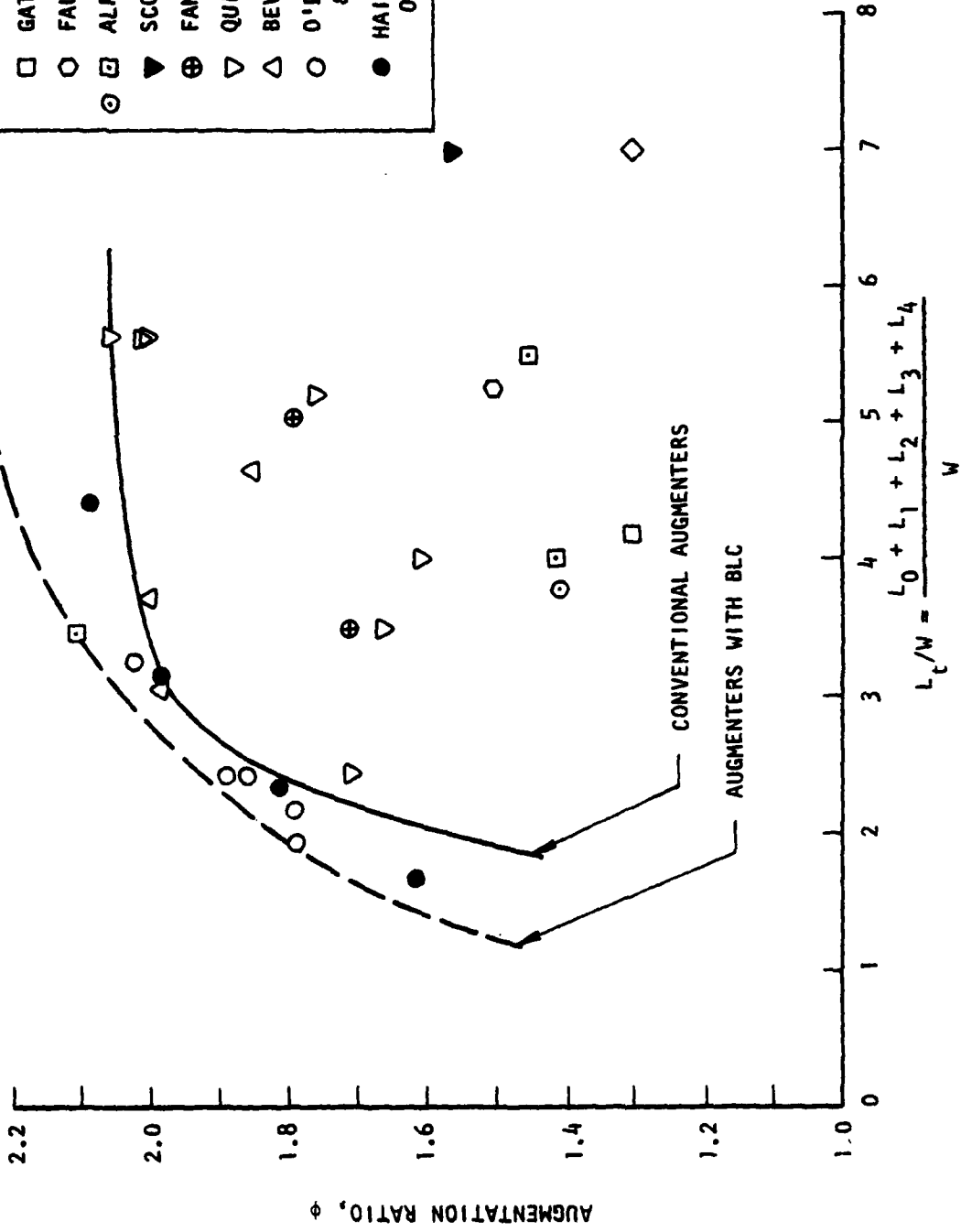


FIGURE A-11 AUGMENTATION RATIO VS. TOTAL LENGTH

A-6 Conclusions From Phase I Effort

The results of the Phase I effort on a "Summary/overview of Ejector Theory and Performance" led to the following preliminary conclusions:

General

A steadily increasing emphasis on the use of ejectors, as evidenced by the technical reports published each year, has been taking place this century.

The use of ejectors for pumping applications increased more steadily than for thrust augmenting applications, which underwent a more cyclic advance.

Stream phase relationships, the intended purpose of the energy transfer process, and the time-dependence of the initial flows were established as important criteria for categorizing ejector theory and applications.

Comparison of significant operating parameters shows similarities and corresponding relationships between ejectors used in different applications.

No unified theory appropriate to ejectors of all categories exists.

Category I

Experimental trends for ejector augmentors agree in a general sense with predicted effects, but the inability to adequately predict absolute values for significant loss factors limits the capability to predict the overall performance of a specified design.

Large discrepancies exist between ideal theoretical predictions and the (statistical) limits of available experimental results for ejector augmentors.

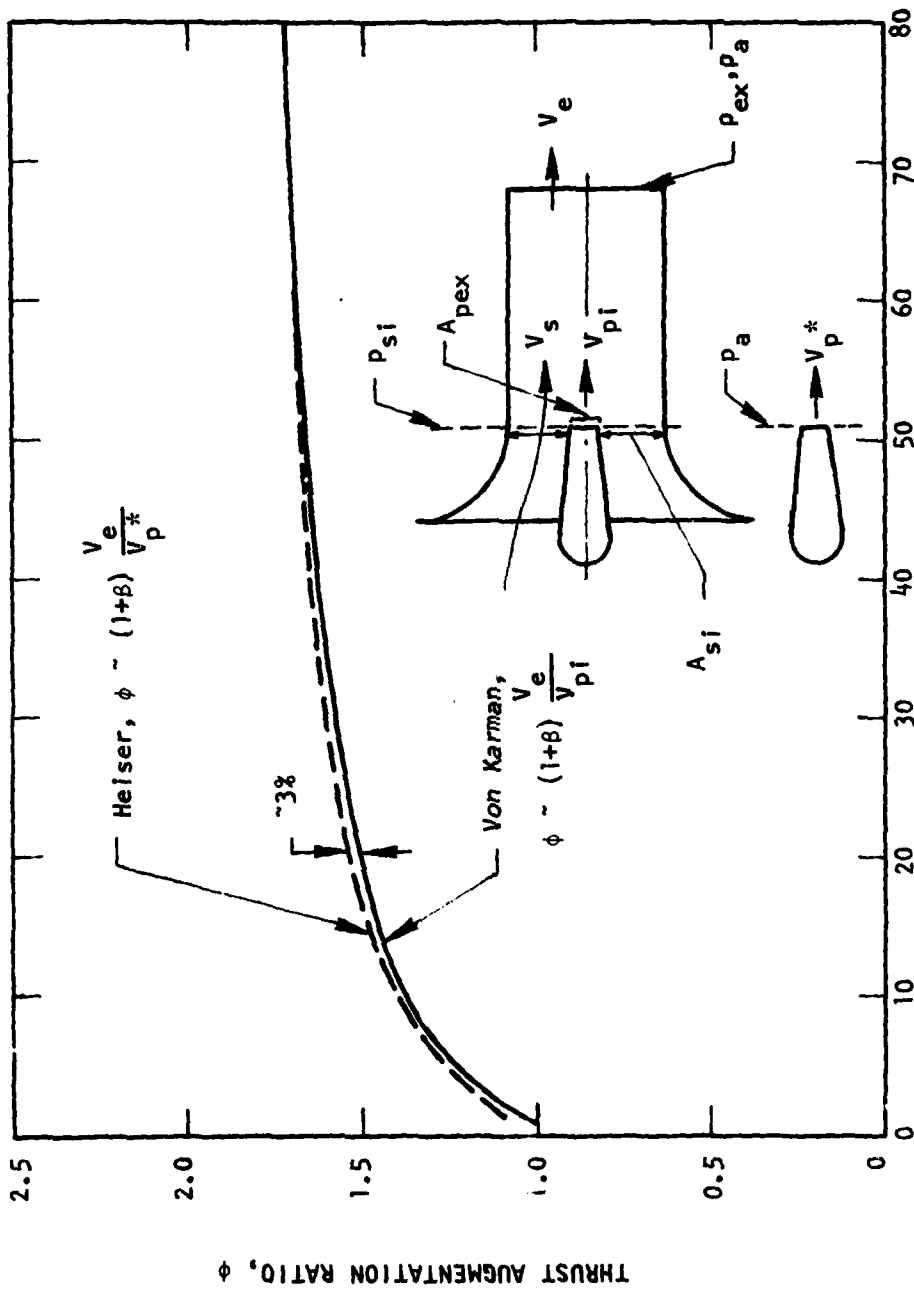
A comparison of trends in limits of experimental results for overall ejector augmentor performance indicates that significant advances have been made in recent years.

APPENDIX B

COMMENTS ON PREVIOUS THEORETICAL TREATMENTS

In discussing ejector augmentor technology, favorite treatises are frequently cited to prove or disprove points of dispute. Such questions as, "Didn't von Karman show that an ejector couldn't have an augmentation ratio greater than two?", or statements such as "Heiser proved that an ejector is never as good as a mechanical fan," may be encountered. Because simplifying assumptions are frequently made to facilitate solution of the equations defining ejector augmentor performance, care must be taken with such interpretations of existing theoretical results, particularly when the original purpose was for comparison with other types of propulsion devices for use in system applications. While it is not feasible to attempt to decipher all of the theoretical treatments which might be cited, in the following paragraphs, three well-known theoretical treatments, von Karman's,¹⁴⁴² Heiser's,⁵⁷⁵ and Jones'⁶⁸⁰ are discussed to illustrate the effects of the assumptions made.

In von Karman's famous Reissner Anniversary paper,¹⁴⁴² the significance of secondary flow non-uniformity at the entrance to the mixing section is discussed, with emphasis on its relevance to ejectors with "Coanda" primary nozzles. In the development of the comparison of the thrust augmentation ratio for devices with uniform and non-uniform secondary flow, von Karman arrived at a limiting value, $\phi = 2.0$, for the augmentation ratio for uniform secondary flows. Two simplifying assumptions in this treatment stand out as detracting from its general usefulness: (1) the thrust augmentation ratio is defined in terms of the primary thrust for expansion to the mixing plane static pressure, which is necessarily lower than the ambient (secondary driving) pressure. The mass flow and velocity of the primary for this condition, and thus the reference primary thrust, F'_p , used in the denominator of ϕ , are greater than for the maximum isolated primary nozzle for ideal expansion to ambient. The values of ϕ obtained as a function of area ratio and the limit value, $\phi_{MAX} = 2.0$, thus have no real meaning, since the actual thrust augmentation varies with primary pressure ratio. Figure B-1 compares the effect of using the primary velocity, V_{pi} , with the more standard augmentation ratio as defined by Eq. (B.8). As may be seen in the figure, the primary pressure ratio, P_t/P_{amb} , significantly affects the augmentation for fixed values of inlet area ratio, A_{si}/A_{pi} , corresponding to fixed values of the mixing entrance static pressure, P_{si} . The importance of this effect is perhaps better



INLET AREA RATIO, A_{si}/A_{pi}

FIGURE B-1 THEORETICAL NON-DIFFUSING EJECTOR PERFORMANCE.

realized by the fact that for fixed values of the primary stagnation conditions, P_{t_p} and T_{t_p} , the maximum absolute thrust of the ejector device increases faster with increasing area ratio than indicated by von Karman's curve of ϕ vs A_{s_i}/A_{p_i} . The fact that the expression for ϕ obtained by von Karman is independent of the primary and secondary stagnation conditions -- i.e., $\phi = \phi$ (area ratio only) -- has probably contributed to the erroneous conclusion made by some investigators that these conditions do not significantly affect ejector performance.

In addition to the foregoing, von Karman's limiting ϕ values have little bearing on actual ejector augmentor performance, since no effects of mixed flow diffusion were accounted for. In general, as discussed in Section 4.0 and shown by Quinn,¹⁰⁹³ Viets,¹⁴¹⁹ Fancher,³⁷⁷ Jones,⁶⁸⁰ McCormick,⁹⁰⁷ Hasinger,^{550,551,553} and others, addition of a diffuser to the ejector augmentor enables a reduction in mixing plane static pressure for a specified secondary to primary area ratio and a consequent increase in the mass flow ratio, \dot{m}_s/\dot{m}_p , and augmentation ratio, ϕ . Unfortunately, many of those who contributed to the extension of von Karman's simplified analysis also persisted in the definition of thrust augmentation referenced to the primary jet thrust for expansion to the mixing plane static pressure. While this allows straightforward relationships to be obtained for ϕ as a function of inlet and diffuser area ratio, it does not permit an understanding of what inlet and diffuser area ratios are required to maximize ϕ for specified primary and secondary stagnation conditions.

While the foregoing discussions appear to limit the usefulness of von Karman's contribution, it should be kept in mind what his purpose was: "...to show that the augmentation in the case of non-uniform (secondary pressure and velocity) distribution can be considerably larger than in the case of uniform distribution." Von Karman's comparative results serve this purpose quite completely and are unaffected by his choice of augmentation ratio definition or the lack of a diffuser.

In Heiser's extremely well-written paper, he reaches the conclusion that "compressibility can have no effect upon thrust augmentation for the conditions under which they (Equations demonstrating certain inequalities leading to the definition of a maximum thrust augmentation ratio) were derived." However, one

of the conditions is that entropy increases along the primary flow streamlines from the mixing section entrance plane to the augmentor exit. This condition is generally not met in typical ejector augmentors, since the increase in secondary fluid entropy, $ds_s \geq \frac{dQ_s}{T}$, is accompanied by a decrease in primary fluid entropy, which corresponds to cooling of the primary flow: $dQ_p = -dQ_s$. Thus, although the total system (secondary plus primary) entropy change is greater than or equal to zero, the inequality necessary to define the maximum augmentation ratio cannot be established for the compressible case. In particular, if the energy equation is written as

$$T_{p_i} + \frac{V_{p_i}^2}{2} + \beta \left(T_{s_i} + \frac{V_{s_i}^2}{2} \right) = (1 + \beta) \left(T_e + \frac{V_e^2}{2} \right) \quad (B.1)$$

and it is assumed that the system kinetic energy cannot increase, i.e.,

$$\frac{V_{p_i}^2}{2} + \beta \frac{V_{s_i}^2}{2} \geq (1 + \beta) \frac{V_e^2}{2} \quad (B.2)$$

then it follows from (B.1) that

$$T_{p_i} + \beta T_{s_i} \leq (1 + \beta) T_e \quad (B.3)$$

or

$$\frac{T_{p_i}/T_{s_i} + \beta}{1 + \beta} \leq T_e/T_{s_i} \quad (B.4)$$

It also follows, since for a secondary drawn from ambient static conditions,

$$T_{s_i} + \frac{V_{s_i}^2}{2} = T_a, \text{ that}$$

$$\frac{T_{p_i}/T_a + \beta}{1 + \beta} \leq T_e/T_a \quad (B.5)$$

Since for a supersonic primary flow, T_{p_i} is uniquely determined by the primary total temperature, T_{p_t} , and the primary Mach number (i.e., primary nozzle area ratio) at the mixing plane entrance, it is easy to see that $T_{p_i}/T_a < 1$ can be chosen, so that equation (B.5) allows the condition

$$T_e/T_a < 1.0 > \left(\frac{\beta + T_{p1}/T_a}{1 + \beta} \right)$$

or

$$\frac{\beta + T_{p1}/T_a}{1 + \beta} \leq T_e/T_a \leq 1.0 \quad (B.6)$$

to exist. It is this condition which negates the general conclusion by Heiser that compressibility does not affect the incompressible results.

This can also be seen by rewriting Eq.(B.1) in terms of the primary conditions for expansion to ambient: $T_{p_t} = T_a + V_p^{*2}/2$. Then it follows that (with $T_a = T_{s_1} + V_{s_1}^2/2$):

$$\frac{V_e^2}{V_p^{*2}} = [2(T_a - T_e) + \frac{1}{1 + \beta}] \quad (B.7)$$

and from the definition of static augmentation ratio,

$$\phi = (1 + \beta) \frac{V_e}{V_p^*} = \sqrt{2(T_a - T_e)(1 + \beta)^2 + (1 + \beta)} \quad (B.8)$$

Thus, for the compressible flow, if $T_e/T_a < 1.0$ (see Eq. (B.6)), $\phi > \sqrt{1 + \beta}$ is possible. In particular, as shown on the accompanying T-s diagram, Figure B-2, if the mixed exit flow is supersonic and overexpanded, the required conditions exist. Specifically, the ability to use a supersonic primary nozzle to set the mixing plane entrance static pressure (and primary temperature) independently of the secondary to primary area ratio results in the possibility of significantly different operating conditions for the compressible vs. incompressible cases.

In general, however, it is possible to show by use of the T-s diagram that whenever the initial relative entropy states of the primary and secondary flows are not equal, the theoretical relationship between ϕ and β is different from $\phi = \sqrt{1 + \beta}$. Figure B-3, which also shows an alternate form of Eq. (B.8), illustrates this point.

Jones, in two carefully constructed ejector discussions, concludes that "ejectors are inherently inferior to plain jets, size for size ..." and "For a given energy input, an ideal ejector is no more efficient than a plain jet, size for size ..." These conclusions are based on the comparison of a parameter for which they are valid, the (momentum/kinetic energy) = $\left(\frac{\dot{m} V_e}{1/2 \dot{m} V_e^2} \right)$ of a jet at its exit plane. Jones calls this parameter,

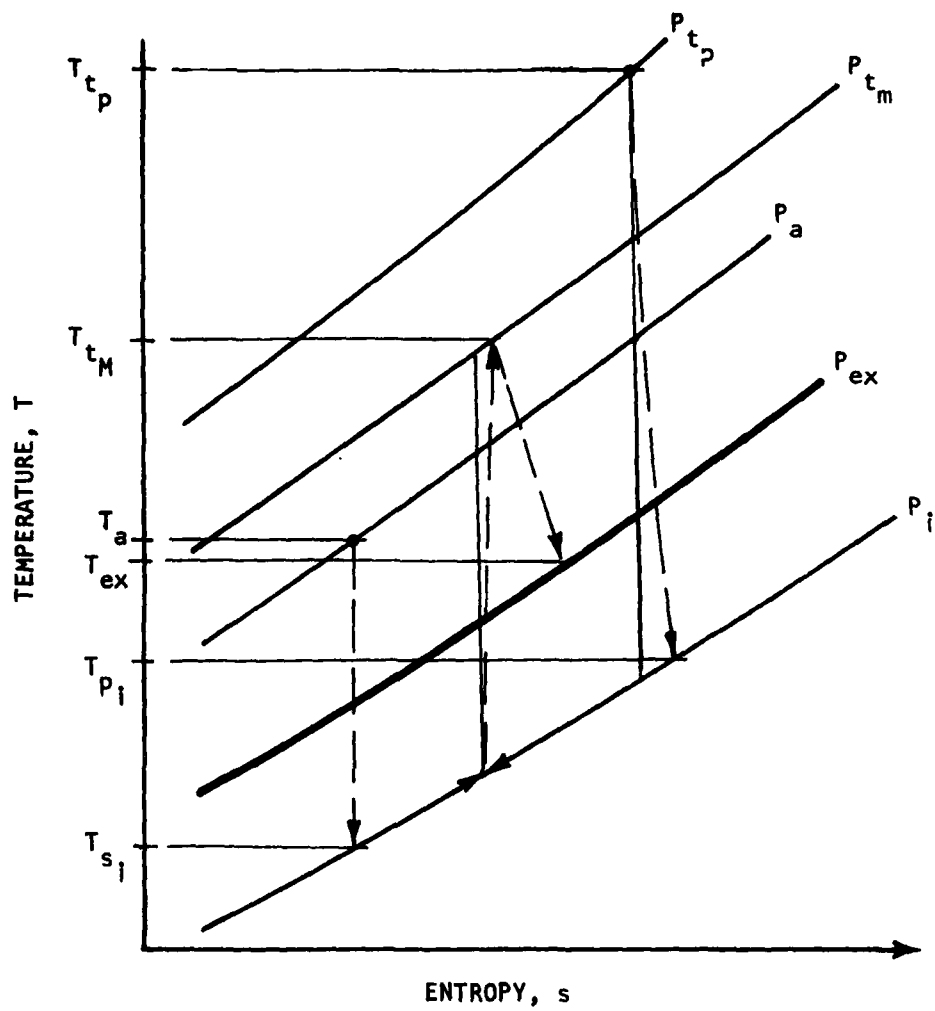


FIGURE B-2. TEMPERATURE-ENTROPY DIAGRAM FOR A SUPERSONIC MIXED FLOW AUGMENTOR (OVEREXPANDED, $P_{ex} < P_{amb}$)

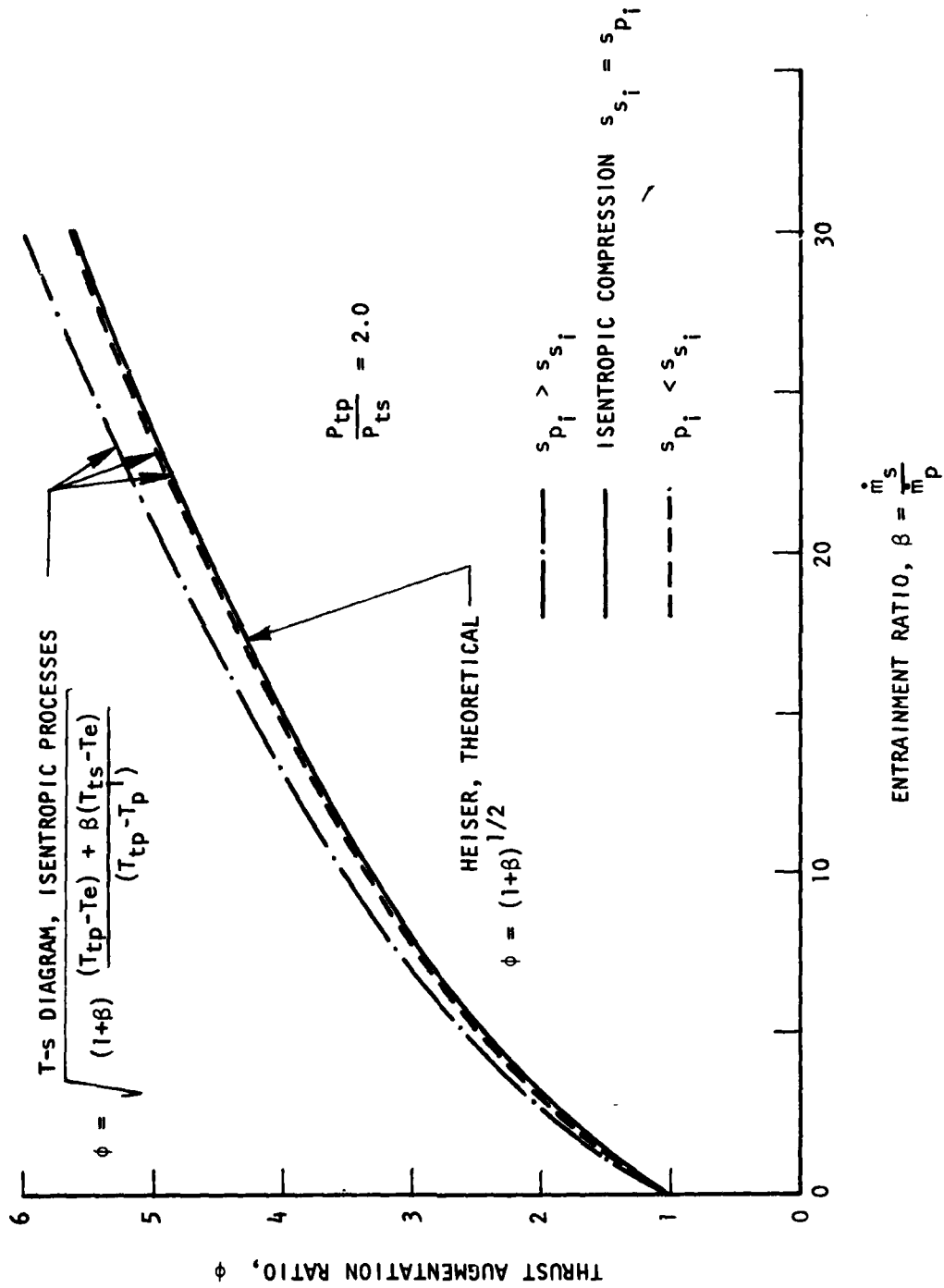


FIGURE B-3 EFFECTS OF RELATIVE INITIAL ENTROPY LEVELS ON THEORETICAL THRUST AUGMENTATION.

which is related to the propulsive efficiency, the specific thrust; and if the exit kinetic energy is assumed constant, the ratio of specific thrusts for two different jets is

$$\frac{J_2}{J_1} = \frac{V_1}{V_2} = \left(\frac{A_2}{A_1}\right)^{1/3} \quad (\text{B.9})$$

Thus, for two pure jets of the same exit kinetic energy, the one with the larger exit area will have the greater momentum/kinetic energy.

However, when thrust/airflow, F/w_a , specific fuel consumption, SFC, or thrust/exit area, F/A_{ex} , are considered as performance criteria, the jet with less momentum/kinetic energy has the higher performance. Thus, from Eq. (B.9), with constant kinetic energy,

$$\frac{F_2}{A_2} = \frac{F_1}{A_1} \left(\frac{A_1}{A_2}\right)^{2/3} \quad (\text{B.10})$$

showing that for $J_2/J_1 > 1$, $F_2/A_2 < F_1/A_1$.

Also,

$$\frac{F/w_a)_2}{F/w_a)_1} = \frac{V_2}{V_1} = \left(\frac{A_1}{A_2}\right)^{1/3} \quad (\text{B.11})$$

Equation (B.11) is the inverse of Eq. (B.9), showing that for $J_2/J_1 > 1$, $F/w_a)_2 < F/w_a)_1$ and since, for a fuel/air ratio, f/a ,

$$\text{SFC} = \frac{f/a}{F/w_a} \quad (\text{B.12})$$

for $F/w_a)_2 < F/w_a)_1$, SFC_2 is greater than SFC_1 , for the same specific energy input to the jets in terms of the fuel/air ratio, f/a . The comparison of an ejector with a pure jet having the same exit area, A_e , on the basis of momentum/exit kinetic energy thus does not appear to provide an adequate measure of performance. Rather, Jones' comparison on the basis of a pure jet which is powered by an energy source operating at the same "duty cycle" should be emphasized. Consider then a jet with fixed P_{tp} , T_{tp} , \dot{m}_p , and f/a , i.e., a fixed total energy, corresponding to some particular turbojet engine. It can be shown as discussed previously in Section 3, that for a choking pressure ratio,

P_t/P_a , the maximum thrust per area occurs for expansion to ambient static pressure. This is precisely the condition used to define the ejector augmentation ratio. Thus, since $F_{ej} = \phi F_1$,

$$\frac{F_{ej}}{A_1} > \frac{F_1}{A_1} \quad (B.13)$$

for $\phi > 1.0$. Also,

$$\frac{F_{ej}}{A_2} > \frac{F_1'}{A_2} \quad (B.14)$$

where F_1' is the thrust for expansion to the non-ideal area A_2 rather than A_1 -- i.e., further expansion of the pure jet to the area A_2 decreases the thrust/area -- i.e., $\frac{F_1'}{A_2} < \frac{F_1}{A_1}$. Equation (B.14) is appropriate to vehicles which may have a maximum body diameter greater than that for the pure jet exit area, A_1 , so that no penalty for the ejector area, A_2 , is added to the vehicle drag. It should be noted, however, that $F_{ej}/A_2 < F_1/A_1$, which is also generally true of a turbofan compared with its core engine.

If the thrust/airflow is based on the primary mass flow, then since $F_{ej} = \phi F_1$,

$$\frac{F/w_a}{\dot{m}_p}_{ej} = \frac{F_{ej}}{\dot{m}_p} > \frac{F_1}{\dot{m}_p} = \frac{F/w_a}{\dot{m}_p}_{jet} \quad (B.15)$$

and it follows that $SFC_{ej} < SFC_{jet}$.

The foregoing discussions have established the following important points, which appear to be frequently misinterpreted from the papers described:

- o Von Karman's maximum augmentation ratio of $\phi = 2.0$ is based on an incompressible analysis of a constant area device. Addition of a diffuser, as shown by many others, permits ϕ to be significantly greater than 2.0.

- o The limiting value of $\phi_{max} = \sqrt{1 + \beta}$ which Heiser derived for an incompressible flow cannot be established for realistic ejector conditions, with significant compressibility effects and heat transfer from the primary to the secondary.

o The momentum/exit kinetic energy, related to the propulsive efficiency, and used by Jones to compare an ejector with a pure jet having the same exit area, does not provide an adequate performance comparison between ejectors and other propulsion devices, such as turboejector or turbofan engines.

APPENDIX C

RECOMMENDED EJECTOR AUGMENTOR RESEARCH
AND DEVELOPMENT AREAS

Throughout this Summary/Overview of Ejector Augmentor Theory and Performance, it has been necessary to distinguish between what is known and what is unknown about the basic theory, performance, and design of ejector augmentors. In so doing, a multitude of research and development topics have appeared, which are needed to supplement and fill certain voids in the current ejector state of the art. In Table C-1, the most important of these topics are listed for three categories: (1) Fundamental Research, (2) Ejector Environment, and (3) Ejector (Systems) Development.

To more effectively establish the type of research and development activity which appears to be required on the basis of this Summary/Overview, a few high priority programs and their objectives have been further described below:

1. PROGRAM - Fundamental Interaction Phenomena in Ducted Flow
Objective - To define correlation parameters relating primary and secondary initial flow conditions and geometry to the flow interaction phenomena and to subsequent, mass-averaged, downstream conditions, and performance in an ejector device.
2. PROGRAM - Effective Energy Transfer Techniques and Measurements
Objective - To investigate the mechanisms of primary to secondary flow energy transfer and also, the transfer of kinetic energy to pressure energy within each flow regime. This would lead into simultaneous diffusion and entrainment processes.
3. PROGRAM - Energy Efficient Non-Steady Flow Augmentation
Objectives - The objectives of this program would encompass a wide range of flow problems as indicated below:
 - (1) Develop an Energy Efficient Non-steady Flow Generation Technique. Concepts for generating a non-steady primary jet with minimal energy and thrust loss of the primary nozzle would be proposed and compared in experimental investigations. Two prime candidates would be the "Fluidic Flip-Flop Nozzle" -- Viets¹⁴²² -- and the Rotary Jet -- Foa,⁴¹² Hohenemser & Porter.⁶²⁸
 - (2) Characterize Non-Steady Flow Interactions and Formulate Design Parameters. Parametric experimental investigations, including subsonic and supersonic primary jets, would be performed using the basic test apparatus from the fundamental flow interaction program, in conjunction with the best non-steady primary flow concepts obtained under the first objective of this program.

TABLE C-1 EJECTOR TECHNOLOGY RESEARCH AND DEVELOPMENT TOPICS

1.0 Fundamental Research Topics

- o Turbulent Mixing Phenomena
 - Parameters of Interest in Turbulent Mixing
 - Measurement Techniques and Accuracy
 - Compressibility Effects on Mixing
 - Variations of Flow Densities and Temperature
 - Pressure Fluctuations in Mixing Flows
 - Eddy Structure and Motion
- o Effective Energy Transfer Techniques and Measurement
 - Transfer of Kinetic to Pressure Energy
 - Effective Method of Primary to Secondary Energy Transfer
 - Interface Pressure versus Viscous Shearing Energy Transfer
 - Non-Steady Flow Interactions on Energy Transfer
- o Non-Steady Flow Influences
 - Energy Efficient Non-Steady Primary Jets
 - Fluidic Flip-Flop Nozzles
 - Acoustic Wave Interactions
 - 3-Dimensional Non-Steady Jets
 - Rotary Jet Flow Augmentors

2.0 Ejector Environment Research Topics

- o Supersonic-Subsonic/Supersonic Ejector Mixing Phenomena and Performance
- o Underwater Ejector Propulsion - Dual Phase Flows
- o External Flow Field Definitions and Configuration Dependence of Augmenting Ejectors
- o BLC-Jet Flap Diffuser/Favorable Backpressure Concept
- o Systematic Ejector Scale Effects Investigation
- o Ejector Propulsion Cycle Analysis - Turbofan versus Turboejector
- o Effects of Variable Ejector Geometry on Forward Flight Performance
- o "Porous" Wall Mixing Section Analysis
- o Component Flow Phenomena Analysis and Interactions

TABLE C-1 EJECTOR TECHNOLOGY RESEARCH AND DEVELOPMENT TOPICS (concluded)

3.0 Ejector Development Topics

- o Thrust Augmenting Ejector Aircraft Systems
- o Ejector Wing/Subsonic and Transonic Flight
- o Reaction Control Ejectors for V/STOL and Maneuvering Flight
- o Helicopter Blade Tip - Ejector Jet Drive

(3) Develop Non-Steady Boundary Layer Control Techniques. Exit and inlet flow fluctuations resulting from a non-steady primary would be investigated to determine their effects on and interactions with the boundary layer. Methods of controlling the boundary layer to prevent diffuser and inlet flow separation would be formulated and tested for a range of non-steady flow conditions.

4. PROGRAM - Investigation of Supersonic/Subsonic/Supersonic Augmentor Ejectors

Objective - Design and build a parametric configuration for the investigation of the feasibility of supersonic ejector exhaust operation and compare the performance gains for this type of thrust augmenting ejector system both statically and in forward flight.

5. PROGRAM - Systematic Scale Effects Investigation

Objective - To identify and determine the impact of scaling effects and laboratory-to-systems environment transition in developing full-scale aircraft ejector systems.

DISTRIBUTION LIST

Naval Air Development Center
Warminster, PA 18974
Attn: Mr. C. Mazza (Code 3015)
Attn: Mr. J. Cyrus (Code 3014)

Department of Defense
Under Secretary for Research &
Engineering (R&D)
The Pentagon
Washington, D.C. 20301
Attn: Mr. R. F. Siewert

Naval Ship Research & Development Center
Carderock, MD 20034
Attn: Code 1606

Naval Air Propulsion Test Center
Trenton, N.J. 08628
Attn: Mr. Eric Lister (Code PE4)

Naval Weapons Center
China Lake, CA 93555
Attn: Mr. B. Kowalsky (Code 3183)

Defense Documentation Center
Building #5
Cameron Station
Alexandria, VA 22314

General Dynamics
Convair Division
P.O. Box 80986
San Diego, CA 92138
Attn: Technical Library

Rockwell International
Science Center
P.O. Box 1085
Thousand Oaks, CA 91360
Attn: Dr. N. Malmuth

Col. G. F. Cudahy, (Code FG)
Air Force Wright Aeronautical Laboratories
Flight Dynamics Laboratory
Wright-Patterson AFB, OH 45433

Col. C. Simon, (Code CCN)
Air Force Wright Aeronautical Laboratories
Aero Propulsion Laboratory
Wright-Patterson AFB, OH 45433

Kettering Research Institute
University Of Dayton
Dayton, OH 45469
Attn: Mr. Maurice Lawson

Dr. M. Alperin
Technical Director
Flight Dynamics Research Corp.
15809 Stagg Street
Van Nuys, CA 91406

Dr. Paul Bevilaqua
Group Leader
Rockwell International Corp.
4300 E. Fifth Avenue
Columbus, OH 43216

Mr. R. Clark, (Code FXM)
Air Force Wright Aeronautical Laboratories
Aeromechanics Divison
Wright-Patterson AFB, OH 45433

Dr. Tirumalesa Duvvuri
Duvvuri Research Associates
641 Windsor Circle
Chula Vista, CA 92010

Dr. J. Fabri
Office National d'Etudes
et de Recherches Aeronautique
Paris, France

Dr. Joseph Foa
School of Engineering & Applied Science
George Washington University
Washington, D.C. 20052

Dr. Kenneth A. Green
Naval Air Development Center
Warminster, PA 18974

Mr. P. Guienne
Societe Bertin & Cie
B.P. n^o3
78370 Plaisir
FRANCE

Dr. S. Hasinger
Wright-Patterson AFB
Dayton, OH 45433

DISTRIBUTION LIST (CONTINUED)

Dr. K. H. Hohenemser
Washington University
Department of Mechanical Engineering
Sever Institute of Technology
Lindell & Skinker Blvd.
St. Louis, Missouri 63130

Mr. R. J. Jeffries, (Code FIMM)
Air Force Flight Dynamics Laboratory
Aeromechanics Division
Wright-Patterson AFB, OH 45433

Mr. David Koenig
M/S 247-1
NASA Ames Research Center
Moffett Field, CA 94035

Mr. Lewis A. Maroti
Dynatech Research and Development Co.
101 Erie St.
Cambridge, Mass. 02139

Dr. David Migdal
Grumman Aerospace Corp.
1111 Stewart Ave
Bethpage, N.Y. 11714

Dr. K. S. Nagarajah
Air Force Wright Aeronautical Laboratories
Flight Dynamics Laboratory
Wright-Patterson AFB
Dayton, OH 45433

Dr. Peter Payne
Payne, Inc.
1933 Lincoln Drive
Annapolis, Maryland 21401

Dr. Maximilian F. Platzler
Superintendent
Naval Post Graduate School
Monterey, CA 93940

Dr. M. R. Seiler
Rockwell International
Columbus Aircraft Division
4300 E. Fifth Street
P.O. Box 1259
Columbus, OH 43216

Dr. Frank D. Stull
Air Force Wright Aeronautical Laboratories
Aero Propulsion Laboratory
Wright-Patterson AFB/APL
Dayton, OH 45433

Dr. Helmut T. Uebelhack
Dornier System
Friedrichshafen
GERMANY

Dr. Hermann Viets
Wright State University
7751 Col. Glenn Hwy
Dayton, OH 45431

Dr. Hans J. P. Von Ohain
5598 Folkestone Drive
Dayton, OH 45459

Prof. G. F. Marsters
Mechanical Engineering Department
Queen's University
Kingston, Ontario
CANADA K7L 3N6

Dr. C. Padova
Aerodynamics Department
CALSPAN CORP
P. O. Box 235
Buffalo, N.Y. 14221

Dr. T. Yang
Mechanical Engineering Department
Clemson University
Clemson, S. C. 29631